Molecular Investigation of the MAST Kinase family in the mammalian CNS

by

Patrick Garland BSc

A thesis presented for the degree of

Doctor of Philosophy

of the

University of Southampton

in the

Faculty of Medicine, Health and Life Sciences

School of Biological Sciences

September 2007

UNIVERSITY OF SOUTHAMPTON

ABSTRACT

FACULTY OF MEDICINE, HEALTH AND LIFE SCIENCES

SCHOOL OF BIOLOGICAL SCIENCES

Doctor of Philosophy

Molecular Investigation of the MAST Kinase family in the mammalian CNS

by Patrick Garland

Scaffolding of proteins allows precise spatial and temporal control of cellular signalling. The MAST kinase family have evolved the ability to scaffold their own kinase activity using a PDZ, protein-protein interaction, domain. The capacity of both these domains to perform their respective function has been established within a variety of biological settings. Interestingly, one member of the MAST family, MAST4, has be shown to be upregulated within the brain following seizure-like activity , which suggest it may contribute to scaffolding and/or signalling within neurons following synaptic activity. To better understand this member of the MAST family, a molecular investigation of its expression and interacting proteins has been performed.

Expression analysis of the whole MAST family has been performed using reverse-transcriptase PCR (RT-PCR), northern blot analysis and *in situ* hybridisation. RT-PCR using cDNA derived from multiple mouse tissues has shown an overlapping expression pattern for MAST1, & 2, and a more distinct expression pattern for MAST3, 4 and MAST-like. MAST1-4 were expressed in brain. The expression of MAST1-4 in brain has been investigated using *in situ* hybridisation. Again, MAST1 & 2 have been shown to have an overlapping pattern, which is in the cortex, hippocampus and cerebellum. MAST3 is expressed more strongly in the hippocampus, and it also shows a more distinct expression in the striatum. MAST4 is expressed in both non-neuronal oligodendrocyte cells as well as hippocampal and cerebellar granule neurons. The activity-dependent expression of MAST4 in the dentate gyrus has also been confirmed.

The yeast-two hybrid system has been used to identify potential interacting proteins for MAST4. Although, MAST1 & 2 have been shown to interact with group I & II metabotropic glutamate receptors via their PDZ domains (mGluRs; Pilkington, BJ, PhD thesis), this has interaction does not appear to occur for MAST4.

MAST4 contain a noticeable extension of its C-terminus that is unique to this family member. This 'C-domain' does not contain any identifiable domains and may contribute a novel function to this family member, which supports the known PDZ and kinase domain. A yeast-two hybrid screen for interacting proteins using the C-domain has revealed a potential interaction with a family of transcription elongation factors, as well as other proteins know to be involved in elongation and/or splicing. These interactions have been confirmed using heterologous expression in HEK293 cells.

A model is proposed whereby MAST4 may contribute to transcription and/or alternative mRNA splicing following synaptic activity. Based on these studies, possible new routes have been opened up to investigate the molecular mechanisms underlying neural signalling and plasticity.

Contents

List of Figures

List of Tables

Acknowledgments

I would like to thank my supervisor Dr Vincent O'Connor for his help and support over the last four years.

I thank Dr Pim French for providing seized tissue, and giving helpful technical advice.

I would also like to thank everyone in lab 6095, past and present, for providing laughs as well as help. I would like to thank family and friends for keeping me in touch with the real world. In particularly, I would like to thank my mum for making sure I don't actually live in it…

And finally, I would like to thank my partner Jo, whose love, support and understanding over the last 4 years has made the whole process bearable.

Publications and presentations

Garland, P. French, P & O'Connor V. (2007). Expression of the MAST family of serine/threonine kinases (submitted).

Garland, P & O'Connor V. (2006). Characterising MAST4, an activity-regulated brain kinase. BioScience 2006, Glasgow.

Garland, P. French, P. O'Connor, V. (2004) Characterising the expression of the MAST family of serine/threonine kinases using in situ hybridization. Biochemical Society, Brighton.

Abbreviations

AA - Acetic anhydride
AC - adenylate cyclise
AD - activation domain
AKAP79/150 - A-kinase anchor protein 79/150
Amp - Ampicillin
AMPA - α-amino-3-hydroxy-5-methyl-4-isoazole
APS - ammonium persulphate
ARE - AU-rich elements
ATP - adenosine triphosphate
BDNF - brain derived neurotrophic factor
BSA - Bovine serum albumin
CaMKII - Ca^{2+}/calmodulin-dependent protein kinase II
CaMKIV - CaM kinase IV
cAMP - Cyclic adenosine 3' 5' monophosphate
CASK - calcium/calmodulin-dependent serine protein kinase
CaM - calmodulin
CaN - calcineurin
CBP - CREB binding protein
Cdk - cyclin-dependent kinase
cDNA - complementary deoxyribonucleic acid
CK2 - Casein kinase 2
CNS - central nervous system
CPE - cytoplasmic polyadenylation elements
CPEB - CPE-binding protein
CRE - Ca2+/cAMP responsive element
CREB - Ca^{2+}/cAMP responsive element binding protein
DAPC - dystrophin-associated protein complex
DAPI - 4'-6-Diamidino-2-phenylindole
DBD - DNA-binding domain
DBE - deubiquitination enzymes
DEPC - diethylpyrocarbonate
DIC - Differential interference contrast
DIG - digoxigenin
DMEM - Dulbecco's Modified Eagles Medium
DMSO - dimethyl sulfoxide
DNA - deoxyribonucleic acid
DNMT - DNA methyltransferases
DRE - downstream regulatory elements
DREAM - DRE antagonistic modulator
DTE - Dendritic Targeting Elements
ECL - enhanced chemiluminescence
ECM - extracellular matrix components
EDTA - Ethylenediaminetetraacetic acid
EGFP - enhance green fluorescent protein
ELL - eleven-nineteen lysine-rich leukaemia protein

EVH1 - Ena/VASP homology domain 1
EMS - electro-shock evoked maximal seizures
ER - endoplasmic reticulum
ERK - extracellular signal regulated kinase
FBS - Fetal Bovine Serum
FHA - forkhead-associated
GK - guanylate kinase
GKAP - guanylate kinase-associated protein
GluR - glutamate receptor
GRIP - glutamate receptor interacting protein
HAT - histone acetyltransferases
HEK293 - human embryonic kidney 293
HEPES - 2-[4-(2-hydroxyethyl)-1-piperazinyl]ethanesulfonic acid
HDAC - histone deacetylases
HRP - horseradish peroxidase
HUGO - Human Genome Organisation
IEG - immediate early gene
IKK - IκB kinase
IL - interleukin
ILK - integrin-linked kinase
IPTG - Isopropyl-β-D-thiogalactopyranoside
K ch - potassium channel
LATS - large tumour suppressor
LB - luria broth
LIF - cytokine leukaemia inhibitory factor
LPS - Lipopolysaccharide
LTD - long-term depression
LTP - long-term potentiation
MAST - microtubule associated serine-threonine kinase
MAGUK - membrane-associated guanylate kinase
mGluR - metabotropic glutamate receptor
MAPK - mitogen-activated protein kinase
MLL - mixed-lineage leukaemia 1
mRFP - monomeric red fluorescent protein
mRNA - messenger ribonucleic acid
MT - methyltransferase complex
NDR - nuclear Dbf2-related
NIPP1 - Nuclear inhibitor of PP1
NMDA - N-methyl-d-aspartate
NMJ - neuromuscular junctions
NFATc4 - nuclear factor of activated T-cells 4
NF-kB - nuclear factor-kB
NLS - nuclear localisation signals
NPC - neural progenitor cells
ORF - open reading frame
PACAP - pituitary adenylate cyclase activating polypeptide
PBS - phosphate buffered saline
PDK - phosphoinositide dependent kinase
PDZ - postsynaptic density 95/discs large/zona occludens
PFA - paraformaldehyde

PH - pleckstrin homology
PIK - phosphatidyl inositol 3-kinase
PLL - Poly-L-lysine
PIP - phosphatidylinositol phosphate
PICK1 - protein interacting with C kinase 1
PKA - cAMP-dependent protein kinase
PCR - polymerase chain reaction
PolII - RNA polymerase II
PP1 - protein phosphatase 1
PP2B - protein phosphatases 2B
PSD - postsynaptic density
PTEN - - phosphatase and tensin homolog
RNA - ribonucleic acid
RNAi - RNA interference
RNPS1 - RNA binding protein S1
ROCK - Rho-kinase
RT-PCR - reverse transcriptase polymerase chain reaction
SAP97 - synapse -associated protein 97
SAST170 - Syntrophin-Associated Serine/Threonine Kinase of 170kDa
SAST124 - Syntrophin-Associated Serine/Threonine Kinase of 124kDa
SDS - sodium dodecyl sulphate
SDS-PAGE - SDS-Polyacrylamide Gel Electrophoresis
SGZ - subgranular zone
SH3 - Src homology 3
Shank - SH3 and ankyrin repeat-containing protein
SKD3 - Suppressor of K+ transport defect 3
SNK - Serum inducible kinase
SPAR - Rap GTPase activating protein
SVZ - subventricular zone
SUMO - small ubiquitin-like modifier protein
SytXI - Synaptotagmin XI
TAE - Tris-acetate EDTA
TBS - Tris buffered saline
TdT - terminal transferase
TEA - Triethanolamine
TFP - target fusion primer
Tbr-1 - T-box element 1
TBS - Tris buffered saline
TEMED - N,N,N',N'-tetramethyl-ethylenediamine
TJ - tight junction
TNF - tumor necrosis factor
tPA - tissue plasminogen activator
TRAF6 - TNF receptor associated family
UPS - ubiquitin-proteasome system
UAPC - utrophin-associated protein complex
UTR - untranslated region
VGCC - voltage-gated calcium channel
Wdr5 - WD40 repeat domain 5
X-gal - 5-bromo-4-chloro-3-indolyl-β-D-galactopyranoside
xt-PDZ - extended PDZ

YENB - Yeast Extract Bacto Nutrient Broth
YTH - yeast-two hybrid
ZO-1 - zona-occludens 1
ZONAB - ZO-1-associated nucleic acid binding protein

Amino acids

A	Alanine	Ala
C	Cysteine	Cys
D	Aspartate	Asp
E	Glutamate	Glu
F	Phenylalanine	Phe
G	Glycine	Gly
H	Histidine	His
I	Isoleucine	Ile
K	Lysine	Lys
L	Leucine	Leu
M	Methionine	Met
N	Asparagine	Asn
P	Proline	Pro
Q	Glutamine	Gln
R	Arginine	Arg
S	Serine	Ser
T	Threonine	Thr
V	Valine	Val
W	Tryptophan	Trp
Y	Tyrosine	Tyr

Nucleotide bases

A	Adenosine
C	Cytosine
G	Guanine
T	Thymine
U	Uracil

Chapter 1 - Introduction

1.1. Understanding neural plasticity using systems, cellular and molecular neuroscience

Activity-dependent changes in the behaviour of neurons can be expressed at multiple levels, as illustrated in Figure 1.1. These levels can be studied using systems, cellular and molecular neuroscience.

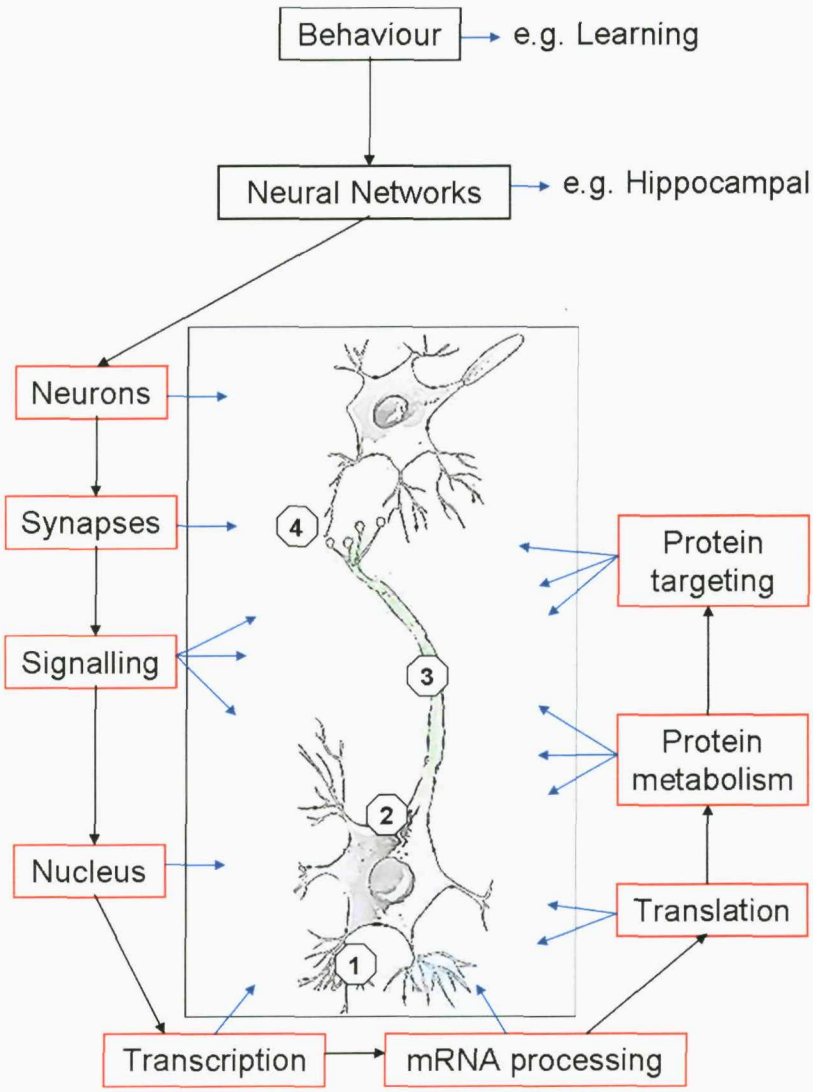

Figure 1.1. Levels between behaviour and events in the brain affected by neural plasticity. Behaviour, such as learning, is dependent on neural networks; for example the hippocampal network. The hippocampus contains neurons that consist of a cell body (2) that receives inputs via their dendrites (1) and sends an output via their axons (3), which forms synapses (4) with other neurons. Synapses can signal to the nucleus and affect transcription. Nascent transcripts, translation and protein processing can also be affected by synaptic activity; these events may subsequently modify the function of the neuron and/or its synapses. These changes can be studied at the systems, cellular and molecular levels by neuroscientists. Red boxes indicate a 'level' directly affected by neuronal activity.

Adaptive behaviour such as learning is dependent on specialised brain regions such as the hippocampus (Martin and Clark, 2007). As a principle site for learning and memory the hippocampus is a good model for discussing plasticity in the brain; therefore, an overview of this brain region will be given in section 1.1.2. Like the rest of the brain, the hippocampus contains neurons, which are the principle cells for the processing and storage of information. Neurons consist of a cell body that receives inputs via its dendrites and sends an output via its axon. Both the structure of neurons (structural plasticity) and the generation of new neurons (cellular plasticity or neurogenesis) will be discussed in sections 1.3 and 1.4., respectively.

At rest, neurons generate a potential electrical difference between their plasma membrane and the external milieu. Following stimulation, the controlled release of this membrane potential by voltage-gated ion channels allows the progression of an action potential from the dendrites to the opposing axon. The action potential causes release of neurotransmitter from the presynaptic membrane. The postsynaptic membrane contains receptors that are activated by neurotransmitters and can allow passage of ions or the activation of intracellular signalling cascades. Synaptic membranes also contain voltage-gated ion channels and cell adhesion molecules. These membrane-bound proteins are organised by 'scaffolding' proteins, which lie beneath the plasma membrane and consist of modular protein-protein interaction domains (Kim and Sheng, 2004). The molecular events within the synapse both support and are affected by plasticity; therefore, a selection of the multitude of proteins found within the postsynapse will be highlighted in section 1.2.1 to illustrated its functional organisation. Many of the proteins within the synapse are part of signalling complexes, which contain signalling molecules such as kinases and phosphatases (Kim and Sheng, 2004; Wong and Scott, 2004). Following synaptic activity, these complexes may promote changes in transcription by signalling to the nucleus . Therefore, both signalling to the nucleus and events within the nucleus (i.e. chromatin modification, transcription, mRNA processing) will be discussed in the context of neural plasticity in sections 1.2.2. & 1.2.3.

Following the processing of the nascent transcript it will be translated into its cognate protein. The translation of mRNA within the dendrites of neurons has emerged as a point of regulation following synaptic activity. Therefore, this will be discussed within section 1.2.4. Also, the processing of nascent proteins either by metabolism (proteolytic

cleavage and/or degradation) and/or targeting to specific sites within neurons will be discussed within the context of synaptic activity in sections 1.2.5 & 1.2.6.

Synaptic activity is known to increase the expression of certain genes. To highlight these genes within an appropriate biological context a selection of them will be discussed within each of the levels described above. These genes will also be summarised in section 1.4 and common features will be highlighted between them. The expression of many of these genes is increased within the hippocampus following neuronal excitation. This brain region, its structure and an overview of its function are discussed below.

1.1.2. The hippocampus and neural plasticity

As shown in Figure 1.2., the hippocampus is principally composed of 3 subfields: the dentate gyrus, CA1 and CA3.

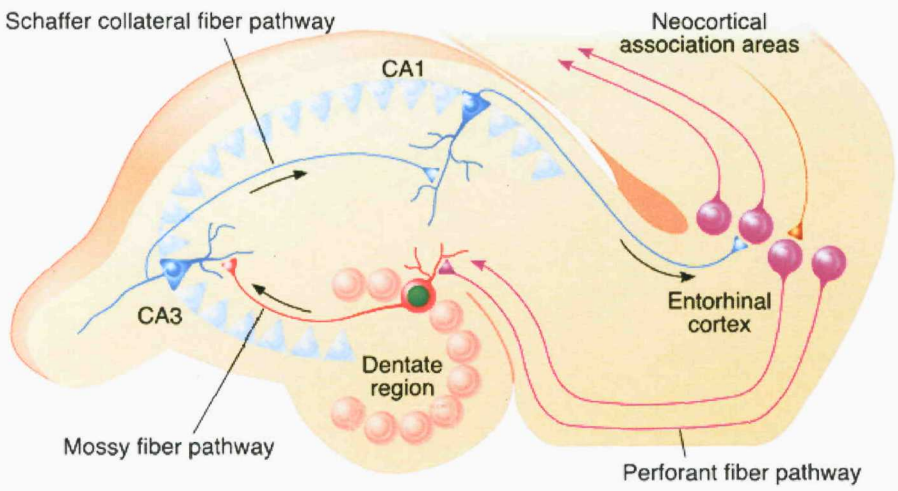

Figure 1.2. The rodent hippocampus. Input to the hippocampus originates primarily from the entorhinal cortex. These afferents form the perforant pathway, which synapse onto granule cells in the dentate gyrus. Axons from granule cells form the mossy fiber pathway that synapses onto CA3 pyramidal neurons. These neurons form the Schaffer collateral pathway which synapses onto neurons in the CA1 subfield. Finally, the hippocampal output returns back to the entorhinal cortex, which therefore forms a loop. Adapted from (Lie et al., 2004)

The hippocampus receives its input via the perforant path, which projects from the entorhinal cortex. The axons within this pathway synapse onto granule cell neurons within the dentate gyrus, as well as pyramidal neurons within the CA3 subfield. The CA3 pyramidal cells also receive an input via the mossy fibre axonal projection that

originates from the granule cells of the dentate. Axons from the CA3 pyramidal neurons project to CA1 neurons, which also receive input from the entorhinal cortex. Finally, CA1 neurons project to the subiculum, which sends its output back to the entorhinal cortex. The connections within the hippocampus therefore form a loop, which allows hippocampal input to be processed prior to its return to the entorhinal cortex (Martin and Clark, 2007).

In rodents, the hippocampus has been shown to be important for learning spatial information, such as identifying similarities and/or differences between particularly environments and remembering when this information was acquired (Martin and Clark, 2007). This therefore allows the time and place of specific events to be remembered. There are also other learning paradigms that can require the hippocampus such as contextual fear-conditioning, which involves the association of an aversive stimulus with a particular environment (Kim and Jung, 2006).

The likely cellular correlate of these complex behaviours involves activity-dependent changes in synaptic strength, such as long-term potentiation (LTP) and depression (LTD).

1.1.3. Long-term potentiation and depression as models of neuronal plasticity

As described above, a neuron will depolarise from an elevated resting membrane potential following synaptic activity. This change can be recorded either for a single cell or a population of cells. In 1973 Bliss and Lomo identified the long-lasting potentiation of the postsynaptic, granule cell, response in the dentate gyrus following high-frequency stimulation of the perforant path in anaesthetized rabbits (Bliss and Lomo, 1973). This potentiation was characterised by an increase in the amplitude of the response of the granule cell population to subsequent stimulation of the perforant path. This long-term potentiation (LTP) has been extensively studied in the subsequent 30 years and is assumed to contribute extensively to learning and memory (Bliss et al., 2003). As will be discussed in subsequent sections, the expression and maintenance of LTP is dependent on many of the levels described above. Some of these contribute to the 'early-phase' of LTP expression and others the protein synthesis dependent 'late-phase' of LTP maintenance (Malenka and Bear, 2004).

In contrast to LTP, long-term depression (LTD) involves a reduction in the postsynaptic response following low frequency stimulation, which has also been shown to be important for learning and memory (Malenka and Bear, 2004).

Both LTP and LTD exist in different forms depending on development age, cell type, synapse and stimulus protocol used (Malenka and Bear, 2004). Therefore, the expression and maintenance of these long-lasting changes in synaptic efficacy is dependent on the specific molecular and cellular events at particular synapses. This specificity is conferred by the complement of receptors, scaffolds and signalling molecules found at these synapses. Therefore in section 1.2.1. the glutamatergic synapse will be used illustrate the general organisation of synapses and how they can support activity-dependent changes in synaptic strength such as LTP.

1.2. Molecular events that support neural plasticity

Protein-protein interactions and posttranslational modifications are essential components used by neurons to organise the molecular events underlying plasticity. These mechanisms can allow the physical organisation of proteins within time and place, as well as the transfer of signals between regions of the cell. Following release of neurotransmitter, the first point of regulation for these molecular events is in the synapse.

1.2.1. The glutamatergic synapse and neural plasticity

Glutamate is a major excitatory neurotransmitter found within the central nervous system. It is a ligand for 3 classes of ionotropic receptors: AMPA (α-amino-3-hydroxy-5-methyl-4-isoazole), NMDA (N-methyl-d-aspartate), and kainate receptors. It is also a ligand for the metabotropic glutamate receptor (mGluR), which is composed of 3 groups. Many of these receptors are concentrated at the postsynaptic density (PSD), which is a protein rich thickening of the postsynaptic cell membrane. There are also many different types of cell adhesion molecules and ion channels in the postsynaptic membrane. Some of these proteins are illustrated in Figure 1.2. below.

As Figure 1.3. illustrates the proteins expressed with the postsynaptic membrane are bound to, and organised by, 'scaffolding proteins'. This class of proteins consists of modular protein-protein interaction domains, such as the PDZ (PSD-95, discs large,

zona occludens 1 domain; see Chapter 3), SH3 (Src homology 3) and guanylate kinase domains (GK).

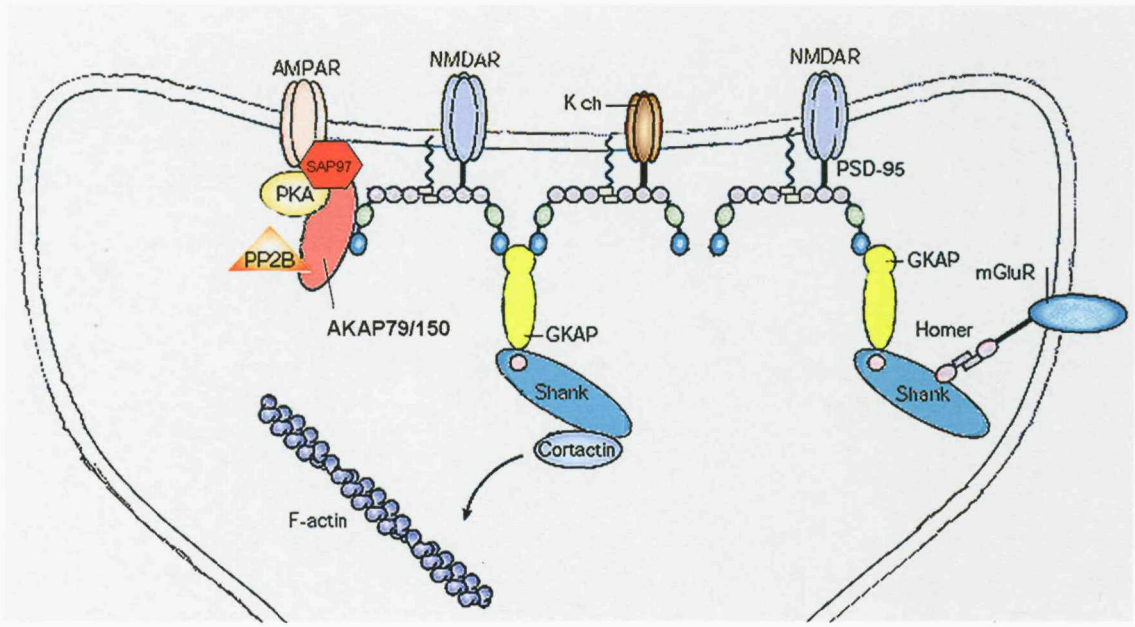

Figure 1.3. A selection of proteins expressed within glutamate receptor containing synapses. Receptors, scaffolds and signalling molecules described within the text are illustrated. Purple circles indicate PDZ domains within selected proteins and black lines indicate the C-terminal tails of proteins. Green and blue ellipses in PSD-95 indicate SH3 and GK domains, respectively. The grey arrow indicates binding of cortactin to the actin cytoskeleton. AKAP79/150, A-kinase anchor protein 79/150; AMPAR, AMPA (α-amino-3-hydroxy-5-methyl-4-isoxazole propionic acid) receptor; GK, guanylate kinase-like domain; GKAP, guanylate kinase-associated protein; K ch, potassium channel; mGluR, metabotropic glutamate receptor; NMDAR, NMDA (N-methyl-D-aspartate) receptor; PSD-95, postsynaptic density protein 95; Shank, SH3 and ankyrin repeat-containing protein. PP2B, protein phosphatases 2B (calcineurin). Adapted from (Kim and Sheng, 2004; Smith et al., 2006)

An example of a scaffolding protein that contains all 3 of these domains is postsynaptic-density protein 95 (PSD-95), which is illustrated in Figure 1.4. below.

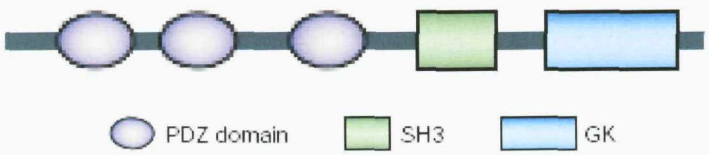

Figure 1.4. Domain structure of PSD-95.

Like many scaffolding proteins, PSD-95 can self-associate; PSD-95 achieves this by forming multimers, which appears to be mediated by head-to-head amino (N) terminal interactions (Hsueh and Sheng, 1999; Christopherson et al., 2003). Multimerization of scaffolding proteins may allow the clustering of functionally related proteins into

molecular networks at membrane specialisations such as the PSD. This function appears important for PSD-95 as it is localised to the postsynaptic membrane (Valtschanoff and Weinberg, 2001; Petersen et al., 2003), which therefore allows it to interact with receptors, ion channels and cell adhesion molecules. In fact, it is thought that PSD-95 can organise some of these proteins at the postsynapse; for example, PSD-95 can cluster the NMDA receptor and Shaker-type K+ channels when these proteins are heterologously expressed in cells (Kim et al., 1995; Kornau et al., 1995). However, PSD-95 may affect receptor internalisation and proper functional localisation of these proteins rather than clustering per se (Roche et al., 2001; Mori et al., 1998; Steigerwald et al., 2000). For example, heterologous cells and cultured neurons are able to internalise the NMDA receptor from their cell membranes; however, PSD-95 inhibits this process and deletion of the PDZ-binding motif in the NR2B subunit of the NMDA receptor increases internalisation within cultured neurons (Roche et al., 2001).

PSD-95 is therefore able to interact with receptors and affect their recruitment to the postsynapse. Receptors are also regulated by posttranslational modifications such as phosphorylation; therefore, are scaffolding proteins, such as PSD-95, also able to interact with signalling molecules, such as kinases?

The A-kinase anchoring proteins (AKAPs) represent an instructive example for how the synapse has chosen to organise functionally related signalling molecules. Both PSD-95 and a related member of the membrane-associated guanylate kinase family (MAGUK), SAP97, have both been shown to interact with AKAP79/150 (Colledge et al., 2000). This scaffolding protein can interact with PKA (Carr et al., 1992; Bregman et al., 1991), protein kinase C (Coghlan et al., 1995) and protein phosphatases 2B (calcineurin; Klauck et al., 1996). Therefore, these interactions allow for the formation of a signalling complex between the AMPA receptor, kinases and a phosphatase. The importance of this signalling complex is illustrated by the requirement for the SAP97-AKAP complex for phosphorylation the AMPA receptor GluR1 subunit (Colledge et al., 2000), which binds to SAP97. This subunit, and thus its interactions, is also required for down-regulation of AMPA receptor currents by calcineurin (Tavalin et al., 2002). Interestingly, AKAP150 (the murine homologue of human AKAP79) has been shown to be upregulated in the hippocampus during the maintenance phase of LTP (Genin et al., 2003), which suggests that the complex described above may be required during learning and memory.

The interaction between PSD-95/SAP97 and AKAP79/150 is mediated via the SH3 and GK domains of these MAGUKs (Colledge et al., 2000). However, these domains also mediate interactions individually. For example, the SH3 domain can interact with Pyk2 (Seabold et al., 2003), which is a kinase involved in the induction of LTP at CA1 hippocampal synapses (Huang et al., 2001). Also, as shown in Figure 1.3., the GK domain of PSD-95 can interact with guanylate kinase-associated protein (GKAP; Kim et al., 1997), which itself can interact with SH3 & ankyrin repeat-containing protein (Shank; Boeckers et al., 1999; Naisbitt et al., 1999; Tu et al., 1999). Shank can interact with the actin-binding protein cortactin via a proline-rich domain; this interaction therefore anchors the molecular complex mediated by PSD-95 with the actin cytoskeleton. Shank is also able to interact with the protein Homer (Tu et al., 1999).

The scaffolding protein Homer was initially identified as an immediate early gene product that was upregulated in the hippocampus following seizure activity (Brakeman et al., 1997; Kato et al., 1997). It was subsequently discovered there are different isoforms of Homer, which are illustrated by Figure 1.5. below. All Homer isoforms contain a EVH-like domain at their N-terminus that includes a GLFG motif (see Chapter 4), which mediates the interaction of Homer with type I mGluRs (Kato et al., 1998; Xiao et al., 1998; Brakeman et al., 1997). The short isoform of Homer, Homer1a only contains this domain and was the isoform identified by Brakeman et al & Kato et al.

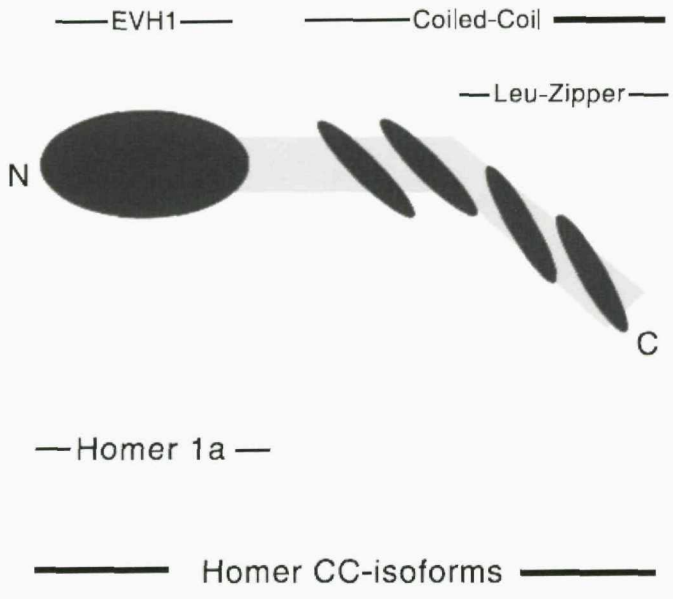

Figure 1.5. Different isoforms of Homer. All Homer isoforms contain a EVH-like domain at their N-terminus that includes a GLGF motif, which mediates binding to type I mGluRs. The 'CC' isoforms of Homer contain a coiled-coiled domain that also contains multiple leucine-zipper motifs, which allow self-association of the Homer proteins. Taken from (Thomas, 2002).

The long isoforms of Homer (e.g. Homer1b and 1c) also contain a coiled-coiled domain, which include multiple leucine-zipper motifs; these structural motifs allow self-association of Homer proteins. In contrast to Homer1a, Homer1b and 1c are constitutively expressed in non-neuronal as well as neuronal tissue (Kato et al., 1998; Xiao et al., 1998; Bottai et al., 2002; Sun et al., 1998). All of the Homer proteins are able to bind to group I mGluRs (e.g. mGluR1 and mGluR5) via there EVH1 domain (Kato et al., 1998; Xiao et al., 1998; Brakeman et al., 1997). Heterologous expression of type I mGluRs and Homer proteins appears to suggest that Homer proteins are involved in the trafficking of type I mGluRs into dendrites and/or axons by as yet unknown mechanisms (Reviewed in Ehrengruber et al., 2004).

The direct and indirect links between the receptors and their signalling molecules described above therefore illustrates the degree of molecular organisation within the synapse. How then does the synapse communicate with the nucleus to effect the transcription of plasticity related genes? Interestingly, other members of the MAGUK family, calcium/calmodulin-dependent serine protein kinase (CASK) and zona-occludens-1 (ZO-1), have been found to scaffold proteins at the cell membrane as well as proteins within the nucleus. These proteins illustrate one means of communication between the synapse and the nucleus which will be discussed in the next section.

1.2.3. Signalling from the synapse to the nucleus

One means by which the synapse can communicate with the nucleus is by direct translocation of a synaptic protein to the nucleus. The scaffolding protein ZO-1 is a tight junction (TJ) protein that interacts with TJ proteins, the cytoskeleton and signalling molecules (Gonzalez-Mariscal et al., 2000). In subconfluent MDCK cells ZO-1 is present in the nucleus; however ZO-1 is restricted to the cell junction in confluent cultures (Gottardi et al., 1996). In the nucleus ZO-1 interacts with ZONAB (ZO-1-associated nucleic acid binding protein) and regulates expression of the growth factor receptor ErbB2 (Balda and Matter, 2000). ZONAB is crucial for epithelial cell proliferation because knockdown of ZONAB levels in MDCK cells reduces proliferation (Balda et al., 2003). These studies illustrate the importance of the ZO-1-ZONAB complex for epithelial cell proliferation as well as illustrating the principle of

protein transfer between the cell membrane and the nucleus. Interestingly, another MAGUK, CASK, has also been shown to interact with a transcription factor and effect gene expression (Hsueh et al., 2000).

Immunogold electron microscopy has shown CASK expression in the pre and postsynapse and biochemical fractionation has also revealed CASK localisation in the PSD (Hsueh et al., 2000). Like other MAGUKs CASK contains a PDZ, SH3 and GK domain; however, it also contain a Ca^{2+}/Calmodulin-like kinase domain and 2 L27 domains (protein-protein interactions modules). Through these domains CASK has been found to interact with many neuronal and synaptic proteins, which has implicated it in neurotransmission, protein trafficking, dendritic spine morphology and synapse formation (Reviewed in Hsueh, 2006). However, like ZO-1 CASK can interact with a transcription factor, which has been identified as T-box element 1 (Tbr-1). The CASK-Tbr-1 complex can translocate to the nucleus and promote transcription of genes such as Reelin and the NR2B subunit of the NMDA receptor (Hsueh et al., 2000).

Although the two MAGUKs described above are suggestive of a direct translocation of a cell membrane/cytoplasmic protein to the nucleus a better characterised example can be found with the transcription factor NFATc4 (Graef et al., 1999). This transcription factor has been shown to translocate from the cytoplasm to the nucleus in hippocampal neurons following depolarizing of the cultured cells (Graef et al., 1999).

As Figure 1.6. shows, the translocation of NFATc4 is dependent on calcium entry through L-type voltage-gated calcium channels and calcineurin (Graef et al., 1999). Neuronal excitation can also lead to increases in nuclear calcium (Lipscombe et al., 1988), which can represent a signal for activity dependent transcription via the transcription factor downstream regulatory element antagonistic modulator (Carrion et al., 1999). DREAM is constitutively bound to downstream regulatory elements (DRE) which leads to repression of gene transcription. However, DREAM contains 3 E-F hand calcium binding motifs, which allows derepression of DREAM following an increase in nuclear calcium (Osawa et al., 2001; Carrion et al., 1999). This derepression leads to transcription of genes such as prodynorphin (Carrion et al., 1999).

Therefore, calcium entry through specific channels can lead to the translocation of a transcription factor to the nucleus. Calcium entry through these channels allows the preservation of signal specificity but little room for signal amplification. In contrast, a general increase in nuclear calcium allows for signal amplification but a loss of

specificity. In between these two extremes is another pathway that is illustrated by the transcription factor Ca^{2+}/cAMP responsive element binding protein (CREB).

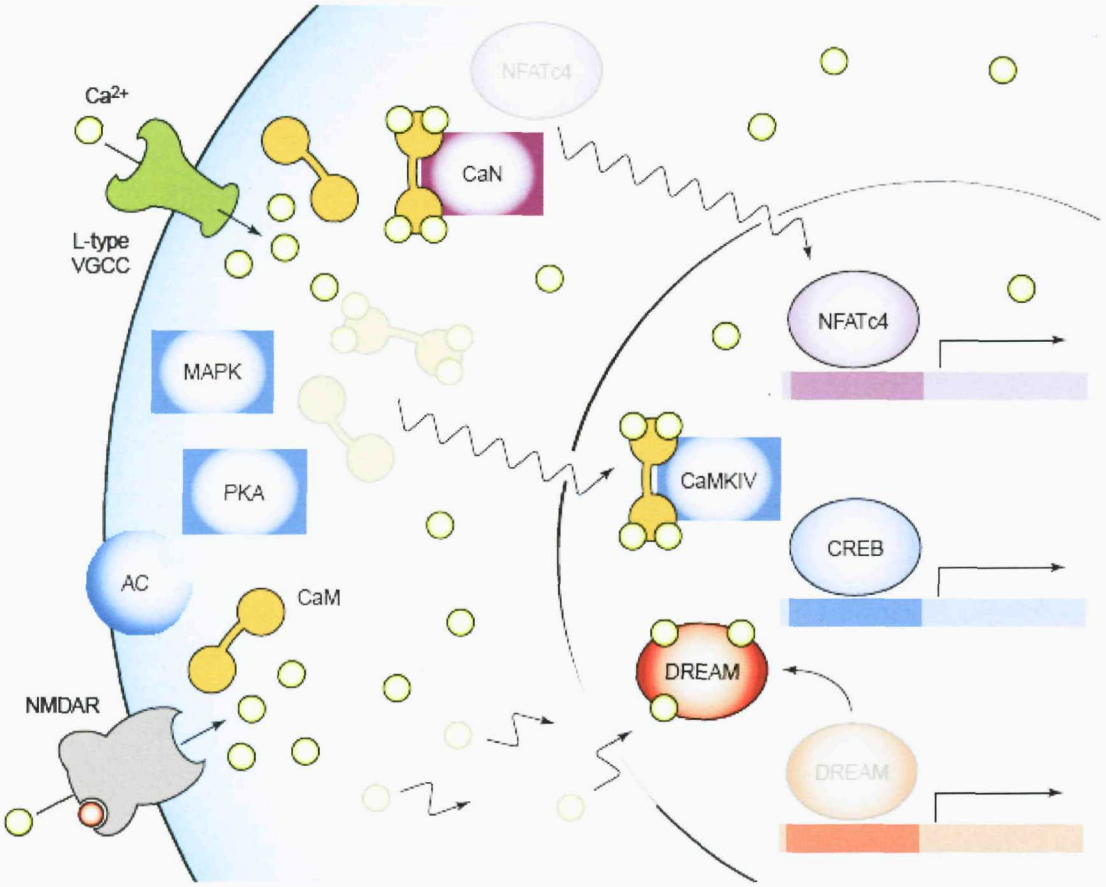

Figure 1.6. Signalling pathways between the cell membrane and the nucleus. Following a general rise in intracellular calcium DREAM dissociates from DNA leading to derepression of transcription. In contrast, specific entry of calcium through the NMDA receptor and L-type channels leads to translocation of calmodulin to the nucleus and activation of CaMKIV, which promotes phosphorylation of CREB. This route of calcium entry also leads to the dephosphorylation of NFATc4 by calcineurin, which causes it to translocate to the nucleus. VGCC, voltage-gated calcium channel. NMDA, N-methyl-d-aspartate; NFATc4, nuclear factor of activated T-cells; MAPK, mitogen-activated protein kinase; PKA, cAMP-dependent protein kinase; AC, adenylate cyclase; CaM, calmodulin; CaN, calcineurin; CaMKIV, CaM kinase IV; DREAM, downstream regulatory element antagonistic modulator; CREB, Ca^{2+}/cAMP responsive element binding protein. Taken from (Deisseroth et al., 2003).

CREB is constitutively bound to CRE (Ca2+/cAMP responsive element) regulatory sites and is primarily activated (i.e. released) by Ser-133 phosphorylation, which derives from a slow MAP kinase and fast CaM-dependent kinase signalling cascades (Wu et al., 2001), as illustrated in Figure 1.6. Interestingly, only calcium entry through two channels are able to activate CREB phosphorylation: the L-type calcium channels

and the NMDA glutamate receptor (Deisseroth et al., 1998; Ginty et al., 1993; Dolmetsch et al., 2001; Deisseroth et al., 1996). Elevation in calcium per se is not enough to promote activation of CREB; for example, nuclear calcium is not typically sufficient to activate CREB (Deisseroth et al., 1998; Dolmetsch et al., 2001) and even global (nuclear and cytoplasmic) chelation of calcium using EDTA cannot inhibit the activation of CREB (Deisseroth et al., 1996; Hardingham et al., 2001). It has also been shown that μM-scale localisation of L-type calcium channels in the plasma membrane and the presence of a calmodulin (CaM) bind motif are important for CREB phosphorylation (Weick et al., 2003; Dolmetsch et al., 2001). These studies therefore support the hypothesis that calcium exerts its effects on CREB phosphorylation by acting within a domain <1μM in radius from the source of entry (Deisseroth et al., 1996).

The importance of calmodulin for the effect of calcium on CREB phosphorylation has been illustrated by studies showing that following neuronal excitation Ca^{2+}-CaM can activate MAP kinase signalling (Wu et al., 2001; Hardingham et al., 2001; Dolmetsch et al., 2001) and/or translocate to the nucleus (Deisseroth et al., 1998; Mermelstein et al., 2001). In the nucleus, CaM activates nuclear CaM-dependent protein kinase kinase (CaMKK) and its target CaMKIV, which subsequently phosphorylates CREB on its Ser-133 residue (Wu et al., 2001; Kang et al., 2001). Following stronger stimulation the slower MAP kinase cascade also leads to Ser-133 phosphorylation of CREB (Wu et al., 2001).

In summary, calcium entry through the L-type calcium channel and the NMDA receptor lead to CaM kinase and MAP kinase activation, which leads to Ser-133 phosphorylation of CREB and derepression of transcription. The functional significance of CREB phosphorylation can be seen in learning and memory. For example, hippocampal-dependent forms of fear conditioning involve robust activation of CREB in the hippocampus (Wei et al., 2002) and targeted mutations in CREB lead to mice with deficiencies in long-term memory (Bourtchuladze et al., 1994).

The transfer of a signal to the nucleus can therefore proceed via a signalling cascade or directly through translocation of a membrane associated protein. How though are synapse associated proteins transferred to the nucleus? Nuclear import proceeds via the binding of nuclear localisation signals (NLS) on proteins to the α subunit of importin. Interestingly, both the α and β subunit of importin are found in the PSD and undergo NMDA receptor dependent trafficking to the nucleus (Thompson et al., 2004). The

importance of a NLS to the translocation of a synaptic protein to the nucleus has recently been illustrated for the PSD protein AIDA-1d (Jordan et al., 2007). These authors found that a mutation of the NLS within AIDA-1d leads to the inhibition of its translocation to the nucleus, which suggest that importins are involved in synapse to nuclear translocation.

AIDA-1d is able to affect nuclear structure and change protein synthesis; this property and other mechanisms that have been found to effect the nucleus following neuronal excitation will be discussed in the next section.

1.2.3. Neural Plasticity and the nucleus

Nuclear structure, chromatin, transcription and mRNA processing may all be effected by neuronal excitation. A recent example of synaptic activity affecting nuclear structure can be found with the protein AIDA-1d. AIDA-1d is a PSD protein that interacts with PSD-95 and translocates to the nucleus following stimulation of NMDA receptors; following translocation, AIDA-1d co-localises with Cajal bodies and promotes their association with nucleloar (Jordan et al., 2007). Prolonged stimulation results in an AIDA-1d-dependent increase in nucleolar number and protein synthesis (Jordan et al., 2007).

Although nuclear import of proteins has so far been discussed there is also evidence for neuronal activity leading to export of nuclear proteins; for example, the histone deacetylases (HDAC) HDAC-4 & -5 have been found to exit the nucleus following depolarisation of cultured hippocampal neurons (Chawla et al., 2003). This study and others that will be discussed illustrate the importance of chromatin modifications as a point of regulation following neuronal activity.

1.2.3.1. Chromatin modifications and plasticity

DNA is tightly packed into DNA-protein complexes called chromatin, which include histones as the major component (Figure 1.7).

Under basal conditions, transcription is repressed due to a strong interaction between DNA and the histones, which therefore occludes the required RNA polymerase II/DNA interaction (Reviewed inBerger, 2007). To initiate transcription, the structure of chromatin must therefore be disrupted. The acetylation of lysine residues by histone

acetyltransferases (HATs) is one means of achieving this conformational change (Berger, 2007; Lunyak et al., 2002).

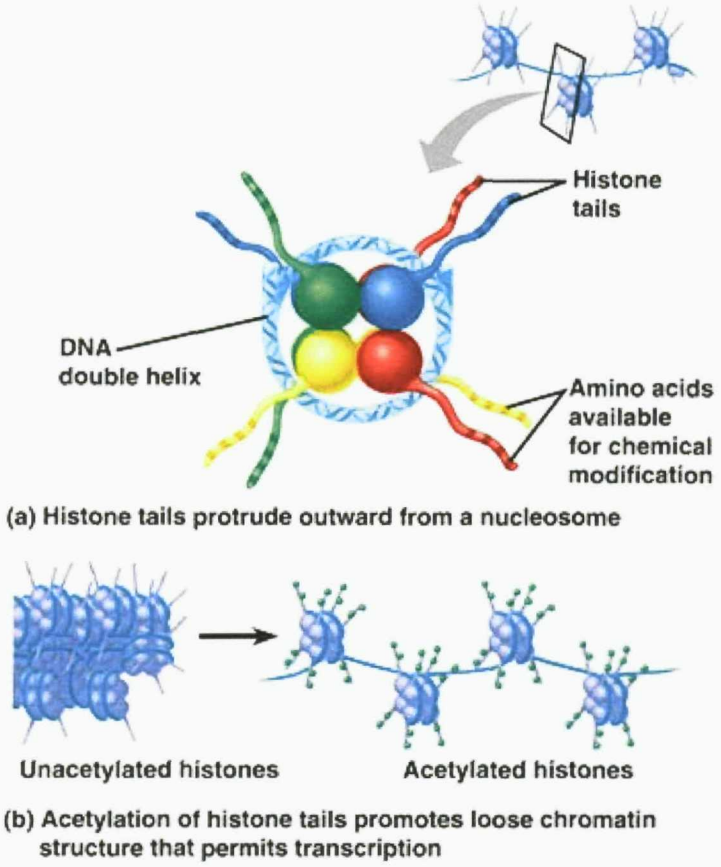

Figure 1.7. Structure and modification of chromatin. (A) chromatin consists of nucleosomes that contain an octamer of histones surrounded by the DNA duplex. The C-terminal tails of histones contain lysine residues that can be acetylated. (B) Following acetylation, chromatin becomes unwound, which allows transcription to occur. Chromatin can also be modified by phosphorylation, methylation, ubiquitination and sumolytation. (Modifed from Campbell and Reece, 2004).

Recent evidence suggests that regulation of chromatin modifications is an important process in learning and memory. For example, the HAT activity of CREB binding protein (CBP) has been implicated in the formation of long-term memories in rodents (Guan et al., 2002; Korzus et al., 2004; Alarcon et al., 2004). Also, it has been found that the acetylation and phosphorylation of histone H3 is increased by activation of extracellular signal regulated kinase (ERK) and the NMDA receptor in hippocampal slice preparations (Levenson et al., 2004). The study by Levenson et al further established that the acetylation and phosphorylation of histone H3 is also increase *in vivo* in the hippocampus following fear conditioning. Therefore, it appears that

activation of NMDA receptors can initiate a signalling cascade that affects gene transcription partly by altering chromatin structure.

Although acetylation of histones is the most studied form of chromatin modification there is also evidence for activity-dependent methylation of DNA (Miller and Sweatt, 2007). The study by Miller and Sweatt identify the upregulation of DNA methyltransferases (DNMTs) in the hippocampus following contextual fear-conditioning; the methylation of DNA is associated with repression of transcription.

The regulation of chromatin modifications may represent the mechanism that allows the rapid upregulation of immediate early genes (Sng et al., 2004). For example, the induction of status epilepticus in mice using kainate leads to hyperacetylation of the c-fos/c-jun promoter and an increase in their expression in the hippocampus (Sng et al., 2006).

1.2.3.2. Expression of immediate early genes following synaptic activity

The expression of IEGs is a common event following synaptic activity. Many of these genes code for transcription factors; for example, the expression of Zif268, c-fos and c-jun have all been found to increase following seizure activity (Saffen et al., 1988; Dragunow and Robertson, 1987; Morgan et al., 1987); and of these three IEGs, Zif268 is the most robustly activated following LTP inducing neuronal stimulation (Cole et al., 1989; Wisden et al., 1990; Richardson et al., 1992). The rapid expression of transcription factors following synaptic activity suggest that gene expression is an important component of the response of the neuron to strong or physiological important stimulation. For example, Zif268 has been found to increase the expression of synapsin I in PC12 cells (James et al., 2004). Synapsin I appears capable of affecting neurotransmitter release and the formation of synapses (Li et al., 1995; Ferreira et al., 1998).

Following transcription, the nascent transcript may undergo alternative splicing and/or degradation. These processes may be affected by synaptic activity and/or affect neuronal function themselves.

1.2.3.3. Activity-dependent alternative mRNA splicing

Most eukaryotic genes contain coding sequence (exons) separated by non-coding introns. Following transcription, the nascent transcript will contain both of these genomic elements and will require processing to remove the non-coding sequence. This

'splicing' of the pre-mRNA involves the inclusion of exons that are constitutively present and possibly some that are alternatively spliced into the mature mRNA. The alternative splicing of certain exons are regulated by cell type, stage of development and cellular activity (Lipscombe, 2005).

A basic outline of splicing is illustrated in Figure 1.7. below.

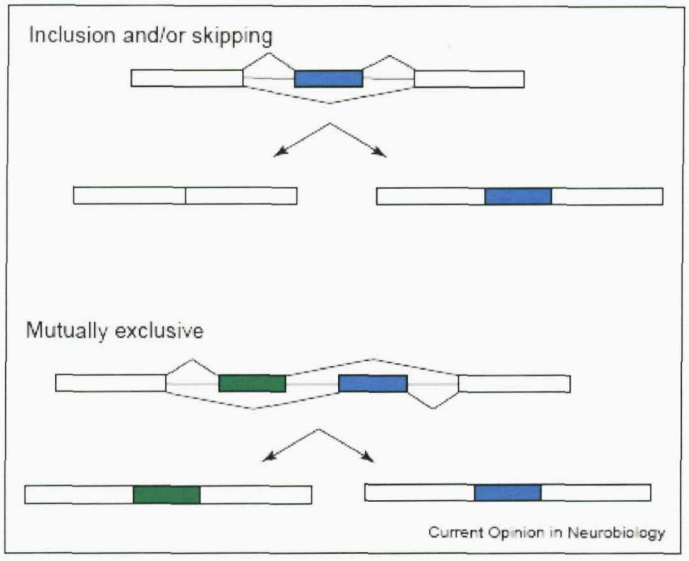

Figure 1.7. Different forms of alternative mRNA splicing. Eukaryotic genes consist of coding sequences called exons (boxes), which are separated by non-coding sequence (lines). Some exons are constitutively expressed within the final transcript (empty boxes) and some are alternatively spliced (green and blue boxes). The upper panel illustrate the inclusion or skipping of an alternatively spliced exon. The lower panel illustrates alternatively spliced exons that can only be included in the final transcript in a mutually exclusive fashion. (Modified from Lipscombe, 2005)

An example of splicing affecting scaffolding at the synapse can be found with SAP97. In the PSD, an alternative splice variant of SAP97 leads to recruitment of AMPA receptors specifically to cortical spines (Rumbaugh et al., 2003). This process depends on the presence of a cassette exon that defines a '13 domain', which is located between the SH3 and GK domains. The 13 domain binds to protein 4.1, which in turn can interact with the cytoskeleton and AMPA receptors. In cultures of cortical cells, the overexpression of this splice variant induces spine enlargement and facilitates synaptic transmission (Rumbaugh et al., 2003). The alternative splicing of SAP97 therefore represents a means for regulating the efficacy of glutamatergic synapses.

Synaptic activity can also regulate splicing. This can be illustrated by the alternative splicing of the NMDA receptor following changes in neuronal excitation (Mu et al.,

2003). Mu and co-workers initially established that accumulation of the NMDA receptor at the plasma membrane is regulated at the level of its export from the endoplasmic reticulum (ER), and that changes in the electrical activity of cortical cultures affected the surface expression of the NMDA receptor. These authors discovered that alternative splicing of the C2-C2' domain regulated export from the ER: C2 variants were retained in the ER during periods of increased neuronal activity, and C2' variants were released from the ER when activity is inhibited. They achieved this by increasing the electrical activity of cortical cultures using bicuculline or decreasing it using tetrodotoxin, with the inclusion of the C2 or C2' exon, respectively. The presence of the NMDA receptor at the plasma membrane is therefore inversely related to the level of activity at the synapse, which may allow this process to function in the homeostatic scaling of synaptic activity (Turrigiano and Nelson, 2004).

1.2.3.4. mRNA processing and plasticity

The 3'-untranslated (UTR) region of many transcripts contains AU-rich elements (ARE) that are implicated in RNA turnover (Reviewed in Malter, 2001). AU-rich elements are able to bind proteins that can regulate mRNA degradation and stability; for example, the RNA-binding protein HuD has been found to interact with and stabilise the transcript neuroserpin (Cuadrado et al., 2002). Neuroserpin is a serine protease inhibitor that is secreted from the growth cones of neurons and inhibits the enzyme tissue plasminogen activator. Neuroserpin appears to play a role in synaptogenesis in areas of the brain involved in learning and memory (Miranda and Lomas, 2006). The degradation of some transcripts have been found to be affected by synaptic activity; for example, the stability of PACAP (pituitary adenylate cyclase activating polypeptide) mRNA is increased by membrane depolarisation in cultured rat cortical neurons (Fukuchi et al., 2004).

As well as degradation, the 3'-UTR can also regulate targeting and translation of nascent transcripts. A number of mRNA's have been identified within the dendrites of hippocampal neurons; for example, the α-subunit of Ca^{2+}/calmodulin-dependent protein kinase II (CaMKII), activity-regulated cytoskeleton-associated protein (Arc) and the NR1 subunit of the NMDA receptor (Burgin et al., 1990; Lyford et al., 1995; Benson, 1997). The 3'-UTR of such transcripts contain Dendritic Targeting Elements (DTE's) that regulate the transport of these messages. For example, Miller et al (2002) have replaced the 3'-UTR of CaMKII with that for the bovine growth hormone to generate a

mutant mouse that exhibited reduced expression of CaMKII mRNA in the dendritic compartment of neurons. The targeting of these transcripts also appears to be regulated by synaptic activity. For example, the mRNA for both CaMKII and Arc is trafficked into dendrites following synaptic activity (Steward et al., 1998; Rook et al., 2000).

The 3'-UTR also contains cytoplasmic polyadenylation elements (CPE's) that are involved in the regulation of translation (Reviewed in Klann et al., 2004). The CPE's are bound by CPE-binding protein (CPEB) which initiates the recruitment of further proteins following its phosphorylation. This subsequently leads to the extension of the poly(A) tail of the mRNA, which promotes translation. The mRNA for the α-subunit of CaMKII has been found to contain 2 CPE's in its UTR (Wu et al., 1998). The CPE's are required for increased polyadenylation of α-CaMKII mRNA and the subsequent synthesis of α-CaMKII that is associated with NMDA receptor-dependent synaptic plasticity in the visual cortex (Wells et al., 2001).

The translation of mRNA can therefore be regulated by synaptic activity. This phenomena has been extensively studied in the context of local protein synthesis in dendrites.

1.2.4. Protein synthesis, metabolism and targeting

Using electron microscopy, polyribosomes have been observed in the dendrites of dentate granule cell neurons of the hippocampus (Steward and Levy, 1982). Also, synaptosomes purified using biochemical fractionation can incorporate radiolabelled amino acids into protein (Rao and Steward, 1991). Taken together these studies indicate that the machinery required for translation of proteins is present in dendrites; however, what it the function of dendritic translation in synaptic plasticity?

The first identified role for dendritic translation involved the rapid enhancement of synaptic transmission by the brain derived neurotrophic factor (Kang and Schuman, 1996). Kang and Schuman showed that BNDF-induced synaptic plasticity in hippocampal slice cultures was still viable when neurites had been isolated from their cell bodies. More recent studies have also implicated dendritic translation in plasticity. For example, isolated hippocampal dendritic fields can support protein synthesis-dependent forms of LTP (Cracco et al., 2005; Vickers et al., 2005); plus, localised application of protein synthesis inhibitors to dendrites in intact slices can inhibit late LTP (Bradshaw et al., 2003). Some transcripts, such as that for CaMKII are translated

in an activity-dependent manner (Ouyang et al., 1999). As described above, Miller and colleagues (2002) deleted the dendritic targeting element within the 3'-UTR of the CaMKII transcript; the transgenic mice showed significantly reduced expression of CaMKII in the PSD even though levels in the cell body were only modestly affected. This study therefore illustrates that local translation of proteins can supply the bulk of what is needed by the synapse and is not necessarily restricted to an ancillary role.

1.2.4.1. Activity-dependent proteolytic processing of proteins

The production and release of the protease tissue plasminogen activator (tPA) from neurons is known to increase across multiple brain regions following seizure and within the granule cells of the hippocampus following LTP-inducing stimuli (Qian et al., 1993). tPA has been shown to be required for the late (protein synthesis dependent) phase of hippocampal LTP using both tPA knockout mice and specific inhibitors of tPA (Huang et al., 1996; Baranes et al., 1998). The ability of tPA to affect L-LTP may be related to its proteolytic processing of the NMDA receptor (Nicole et al., 2001). Nicole and colleagues have shown that tPA can cleave the NR1 subunit of the NMDA receptor, which releases a 15-20kDa fragment from the N-terminus; this cleavage appears to increase Ca^{2+} influx through the NMDA receptor following pharmacological stimulation.

The expression levels, and therefore activity, of a protease can be regulated by neuronal excitation, which is illustrated by tPA above. However, a more direct method for affecting the activity of a protease can be found with the calpain family of calcium-sensitive cysteine proteases. Calpains exist as proenzymes that undergo autocatalytic processing into their active state via a Ca^{2+}-dependent mechanism. Therefore, calcium influx following neuronal stimulation may produce the calcium concentrations required to activate calpain (Lynch and Baudry, 1984). The μ isoform of calpain has been shown to cleave the glutamate receptor interacting protein (GRIP; Lu et al., 2001). This scaffolding protein interacts with the GluR2 subunit of AMPA receptors and is thought to affect its targeting and stabilisation within the postsynapse (Kim and Sheng, 2004). The degradation of GRIP by μ-calpain inhibits its interaction with GluR2 and therefore affects its ability to scaffold the AMPA receptor.

Cleavage of a protein such as GRIP can impair its function, but a more lasting means of removing the activity of a protein is to degrade it permanently. This can be achieved using the ubiquitin-proteasome system (UPS).

1.2.4.2. The UPS and synaptic plasticity

As illustrated in Figure 1.8. below, ubiquitin is a polypeptide that is covalently attached to lysine residues in target proteins. The generation of polymeric ubiquitin chains leads to recognition by the 26S proteasome, which results in proteolysis and recycling of the ubiquitin.

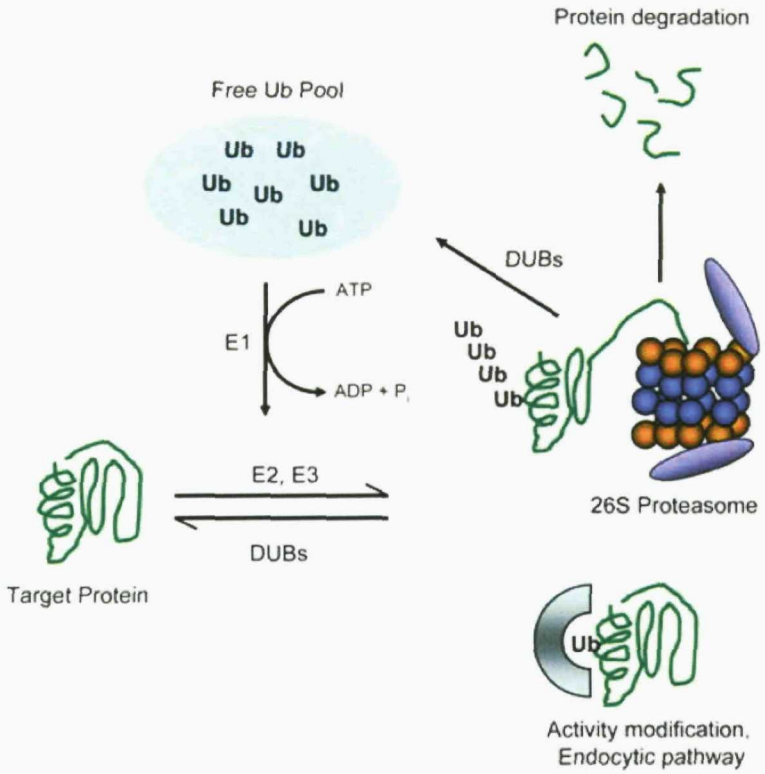

Figure 1.8. The ubiquitin proteasome system. Ubiquitin (Ub) is activated by an E1 activating enzyme in an ATP-dependent manner. This subsequently allows the conjugation of Ub to a target protein by sequential action of E2 conjugating enzymes and E3 ubiquitin ligases. The formation of polyubiquitin chains tags protein for degradation by the 26S proteasome. In contrast, monoubiquitination can modify the proteins activity. Ubiquitination is opposed by deubiquitination enzymes (DUBs).

Within the postsynapse the ubiquitination of proteins can be regulated by activity. For example, inhibiting activity within cultured hippocampal neurons leads to a 50% reduction in PSD associated proteins that are conjugated to ubiquitin; in contrast, increasing spontaneous activity facilitates the ubiquitination of proteins (Ehlers, 2003). Interestingly, many of the PSD proteins known to be ubiquitinated are scaffolding

protein such as Shank, GKAP, AKAP79/150 and PSD-95 (Colledge et al., 2003; Ehlers, 2003). As discussed earlier, these scaffolds contain multiple protein-protein interaction domains that allow them to organise numerous PSD proteins. This feature is particularly resonant considering that sets of proteins within the PSD accumulate and degrade with similar kinetics and magnitudes (Ehlers, 2003), which suggests that UPS-mediated turnover of a few 'master organising' proteins allows the regulation of large changes in the PSD.

Serum inducible kinase (SNK) is upregulated following synaptic activity (Kauselmann et al., 1999). This kinase phosphorylates Rap GTPase activating protein (SPAR) a PSD scaffolding molecule that binds both actin and PSD-95 (Pak and Sheng, 2003). Following phosphorylation, SPAR is targeted for degradation by the UPS, which also promotes the same fate for PSD-95. The loss of PSD-95 and SPAR from spines leads to the loss of actin stability and the breakdown of dendritic spines (Pak and Sheng, 2003) The induction of SNK by synaptic activity may therefore represent a negative feedback loop to reduce further activity by removing synapses/spines. The study by Pak & Sheng neatly illustrates the different levels over which plasticity can occur at the molecular level: firstly, a protein is induced by synaptic activity, this protein then promotes UPS-dependent degradation of a scaffolding protein, and finally the loss of an essential scaffold affects the integrity of the PSD and its supporting structure the spine. Therefore, this study illustrates how molecular plasticity can be converted into structural plasticity, which will be discussed shortly.

The affect of ubiquitin described above requires the generation of polyubiquitin chains. However, monoubiquitination has been implicated in various aspects of neuronal biology such as protein trafficking, protein activity, and protein-protein interactions (Reviewed in Yi and Ehlers, 2007). Also, ubiquitin-like polypeptides such as SUMO (small ubiquitin-like modifier protein) have been implicated in synaptic plasticity. For example, Martin et al (2007) have identified the SUMOlyation of the GluR6 subunit of kainate receptors as a regulator of activity-dependent (kainate application) endocytosis of these receptors in rat hippocampal neurons.

The insertion and removal of receptors into the plasma membrane represents a point of regulation following synaptic plasticity, which can be illustrated by the endocytosis of AMPA receptors.

1.2.4.3. Activity-dependent targeting of proteins

LTP inducing stimuli are known to induce rapid insertion of AMPA receptors into the postsynaptic membrane (Malenka and Nicoll, 1999). This process is dependent on posttranslational modifications such as PKA-dependent phosphorylation (Esteban et al., 2003). However, the long-term maintenance of LTP appears to require structural changes in synapse morphology, which is dependent on persistent changes in AMPA mediated currents (Reviewed in Matsuzaki, 2007). Therefore, how does the synapse achieve this persistent increase in AMPA-mediated currents?

Recently, the IEG Arc/Arg3.1 has been implicated in the activity-dependent endocytosis of AMPA receptors. Arc/Arg3.1 is an immediate-early gene whose expression is rapidly increased following NMDA receptor activation (Link et al., 1995; Steward and Worley, 2001). The mRNA for Arc/Arg3.1 has been shown to target to the dendrites of recently activated synapse (Steward and Worley, 2001).

Chowdhury et al (2006) have established that Arc/Arg3.1 interacts with endophilin 3 and dynamin 2, which are two protein involved in endocytosis of membrane proteins. These authors also show that the overexpression of Arc/Arg3.1 in dissociated hippocampal neurons downregulates the surface expression of AMPA receptors; this process is dependent on the endophilin/dynamin interaction as a mutant Arc/Arg3.1 does not affect AMPA receptor expression at the plasma membrane (Chowdhury et al., 2006). These results have been strengthened by the establishment of an Arc/Arg3.1 knockout mouse that shows a 2-fold increase in AMPA receptor surface expression with a concomitant decrease in endocytosis (Shepherd et al., 2006). The knockout mice appear to be impaired in long-term spatial, fear and taste memories (Plath et al., 2006), which reinforces the importance of AMPA-mediated currents for the consolidation of certain types of learning.

1.3. Activity-dependent changes in neuron morphology

As illustrated in Figure 1.1, neurons are composed of a cell body with neurites (dendrites and axons) that project from the soma. Dendrites contain thousands of spines which house synapses and a variable in terms of structure, plasticity, and function (Reviewed in Matsuzaki, 2007). The basic structure and an example of activity-dependent modification are illustrated in Figure 1.9.

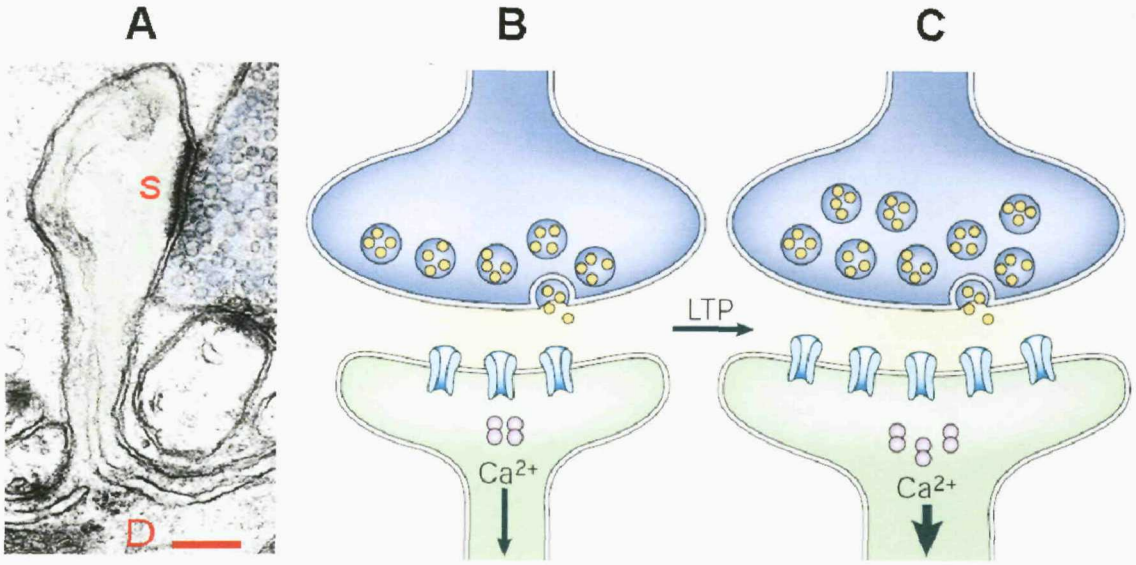

Figure 1.9. Activity-dependent modification of dendritic spines. (A) electron micrograph image of a dendritic spine. The spine (shaded green) projects from the dendrite (D) and forms a synapse (S) with a presynaptic bouton (shaded blue). The scale bar = 200nM. (B & C) Following LTP-inducing stimuli, the dendritic spine enlarges and the surface expression of AMPA receptors is increased. (Adapted from Lamprecht and LeDoux, 2004)

The variability of dendritic spines has been illustrated using live imaging of GFP-tagged actin in hippocampal neuronal cultures (Fischer et al., 1998). This structural variability appears closely correlated with activity at the synapse as shown by a number of studies. For example, Matsuzaki and colleagues have shown that the localised uncaging of glutamate (i.e. laser light mediated release of glutamate from a compound that renders glutamate inert) over individual spines leads to enlargement of spine heads which is dependent on Ca^{2+} influx through NMDA receptors and actin polymerisation (Matsuzaki et al., 2004). In fact, high-frequency stimulation is sufficient to enlarge some spines (Okamoto et al., 2004; Zhou et al., 2004). Both LTP and long-term depression (LTD) have been shown to affect the structure of spines. For example, LTP-inducing pharmacological stimulation of NMDA receptors leads to the enlargement of spines and LTD induced by low frequency stimulation causes some spines to shrink and even disappear (Otmakhov et al., 2004; Kopec et al., 2006). Therefore, LTP causes spine enlargement and LTD causes spine shrinkage, which suggests that spine structure may be closely related to those aspects of learning and memory that are correlated with these opposing aspects of neuronal physiology.

Dendritic spines are composed of two functional regions: a spine head and a spine neck. LTP is able to increase the width of spine necks as well as their head size (Noguchi et al., 2005). This increase in neck size may facilitate the entry of polyribosomes and mitochondria into spines (Ostroff et al., 2002; Li et al., 2004). As discussed in section 1.2.3., the local translation of proteins within dendrites is an important point of regulation for synaptic plasticity. Therefore, the enlargement of spine size following LTP may facilitate further plastic changes in the synapse. (Matsuzaki, 2007).

Spine structure is also closely linked with the actin cytoskeleton, which is present in the cytoplasm of the spine and interacts with the PSD (Reviewed in Tada and Sheng, 2006). Cytoskeletal dynamics have proven to be important for LTP; for example, the maintenance phase of LTP can be inhibited by bath application of actin polymerisation inhibitors (e.g. cytochalasin) to hippocampal slice preparations (Krucker et al., 2000). However, a specific involvement of the actin cytoskeleton within spines has been established for F-actin, which shows greater polymerisation following LTP induction in vivo (Fukazawa et al., 2003).

The actin cytoskeleton is closely associate with the PSD, which is a intimately involved in organising receptors as described in section 1.2.1. As discussed above, NMDA receptor transmission is important for regulating spine size or motility; however, it has been found that the AMPA type of glutamate receptor is involved in spine stabilisation. For example, application of AMPA to cultured hippocampal neurons reduces actin-dependent spine motility, which can be blocked using the specific AMPA receptor antagonist 6-cyano-7-nitroquinoxaline-2,3-dione (Fischer et al., 1998). The AMPA receptor therefore appears to stabilise spine structure, which has been confirmed by other studies. For example, removing synaptic input into the CA1 subfield of hippocampal slices leads to a reduction in spine density; however, bath application of AMPA can prevent this effect (McKinney et al., 1999). The study be McKinney and colleagues also established that blocking activity-dependent dependent glutamate release using tetrodotoxin had no effect on spine density whereas blocking both activity-dependent and independent glutamate release using botulinum toxin markedly reduced spine numbers. These two observations establish that basal spontaneous glutamate release is important for AMPA mediated stabilisation of spine density and suggest that AMPA receptor mediated transmission is important for maintaining plastic changes such as LTP. In fact, AMPA receptor numbers in spines have been shown to

increase following learning paradigms that induce LTP (Reviewed in Malinow and Malenka, 2002). As discussed earlier in section 1.2.1 neurotransmitter receptors such as AMPA are organised by scaffolding proteins into signalling complexes that include kinases and other signalling molecules. Therefore, is there evidence to show that scaffolding and signalling molecules are also required for activity-dependent changes in spine morphology?

As described earlier, the Shank family of proteins are part of the protein complexes that scaffold NMDA and mGluR glutamate receptors. Sala et al (2001) have shown that overexpression of Shank in cultured hippocampal neurons causes an enlargement of spine heads. This capacity of Shank appears dependent on its ability to recruit the constitutively expressed long isoforms of Homer (e.g. Homer1b). Interestingly, the short isoform of Homer, Homer1a, has a dominant-negative effect by reducing the density of spines and their head size (Sala et al., 2003). The report by Sala et al (2003) also established that expression of Homer1a in cultured hippocampal neurons decreased clusters of PSD-95 & the NMDA receptor as well as reducing the surface expression of AMPA receptors. These studies therefore suggest that Shank is critical for the maintenance of spine head size and synaptic function via an interaction with the constitutively expressed isoforms of Homer, but that synaptic activity can disrupt spine morphology and synaptic function via upregulation of Homer1a (Sala et al., 2003).

The morphology of spines is therefore affected by synaptic transmission with the possibility that the NMDA receptor and spine motility are important for 'learning' and AMPA receptors and spine stabilisation are important for 'memory' (Lamprecht and LeDoux, 2004). These structural changes therefore provide a relatively long-term mechanism for encoding physiological phenomena such as LTP. Long-term potentiation is dependent on certain patterns of activity such as high-frequency or coincidental stimulation (Bliss et al., 2003).

1.3.1. Activity-dependent changes in myelination

It has recently been suggested that the myelination of axons may be a point of regulation for activity-dependent plasticity due to its capacity to change conductance speed in axons (Fields, 2005). This form of structural plasticity would therefore contribute to synaptic efficacy by increasing the duration, strength, and possibly timing of synaptic inputs (Fields, 2005).

The activity-dependent myelination of axons appears to act through purinergic receptor signalling; for example, the cytokine leukaemia inhibitory factor (LIF) is secreted by astrocytes following the secretion of ATP by axons firing action potentials. LIF subsequently stimulates oligodendrocytes to form myelin within the CNS (Ishibashi et al., 2006).

Activity-dependent myelination is an example of structural plasticity in non-neuronal cells. This illustrates the extent that molecular events at the synapse can reach out beyond the synapse. However, activity-dependent myelination can also occur through generation of nascent oligodendrocytes from progenitor cells (Fields, 2005). This phenomenon is part of the wider topic of activity-dependent changes in cellular phenotype, which will be discussed in the next section.

1.4. Activity-dependent change in cellular phenotype

As mentioned above, ATP is known to be released by axons during the passage of an action potential (Stevens and Fields, 2000), which in the peripheral nervous system inhibits Schwann cell proliferation, differentiation and myelination. In contrast, release of adenosine following the passage of an action potential within the CNS leads to the proliferation and differentiation of oligodendrocyte precursor cells, which subsequently promotes myelination of dorsal root ganglion axons in culture (Stevens et al., 2002). The study by Stevens et al (2002) illustrates that neuronal excitation can affect the phenotype of cells which have a functional association with neurons. This type of neural plasticity has been illustrated for other types of neural precursors, for example, NG2+ cells.

NG2+ cells express the chondroitin sulphate proteoglycan NG2 and exhibit a multipotent phenotype which allows them to differentiate into neurons, astrocytes and oligodendrocytes (Goldman, 2003). Interestingly, these progenitor cells have been shown to synapse onto axons in the corpus callosum (Ziskin et al., 2007; Kukley et al., 2007). Both of these groups established that action potentials travelling along unmyelinated axons in the corpus callosum (i.e. the major white matter tract connecting the two hemispheres of the brain) caused the vesicular release of glutamate onto NG2+ cells that are known to express AMPA-type glutamate receptors. Using either reporter constructs or electrophysiology to identify NG2+ cell these authors showed: the release

of glutamate following action potentials, the presence of synaptic junctions using electron microscopy and synaptic components using immunohistochemistry, calcium-dependent vesicle release using latrotoxin, and a reduction in the postsynaptic (i.e. NG2+) response following inhibition of voltage-gated Ca^{2+} channels within the axon. Therefore, it is clear that activity-dependent release of vesicular glutamate onto NG2+ cells can lead to an AMPA-receptor mediated change in conductance.

Interestingly, NG2 has been shown to interact with the scaffolding protein GRIP (Stegmuller et al., 2003), which as described earlier interacts with the GluR1 subunit of AMPA receptors. This supports the hypothesis that the NG2+-axon connection is a genuine synapse and reinforces the concept that scaffolding is an essential component of synaptic function.

What is the function of this neuronal-glia signalling? Activation of AMPA receptors in cultured oligodendrocyte progenitor cells leads to an inhibition of both proliferation and differentiation (Gallo et al., 1996). The activation of AMPA receptors by these neuronal-glia synapses may therefore regulate the number and phenotype of the progenitor cells. Interestingly, NG2+ cells have also been found to form both AMPA and GABAergic (gamma-amino butyric acid) synapses with neurons and interneurons, respectively, in the hippocampus (Bergles et al., 2000; Lin and Bergles, 2004). As before, these neuronal-glia synapses may also regulate differentiation and proliferation of the progenitor cells in an activity-dependent manner (Gallo et al., 1996).

The reports described above concern plasticity of non-neuronal cells. However, a significant body of research also exists for neuronal plasticity, or neurogenesis.

1.4.1. Neurogenesis

Neurogenesis, or the birth of new neurons, has been most extensively characterised within two populations of the adult mammalian CNS: the subventricular zone (SVZ) and the subgranular zone (SGZ) within the dentate gyrus of the hippocampus (Ming and Song, 2005). However, there are also more recent neurogenic zones identified within the 3rd ventricle and white matter (Xu et al., 2005; Takemura, 2005). Stem cells in these 'germinal niches' are maintained in an astroglial phenotype, which can both proliferate and differentiate into neurons and glia (Alvarez-Buylla and Lim, 2004).

In the olfactory system, nascent neurons migrate along the wall of the lateral ventricle and into the olfactory bulb where they disperse into the outer cell layers of the bulb. In contrast, nascent neurons migrate only a short distance to the inner granule cell layer of

the dentate gyrus. The nascent neurons have been shown to extend neurites into appropriate target sites; for example, nascent granule cells in the dentate gyrus extend axons along the mossy fiber pathway to reach the CA3 pyramidal layer within 4-10 days following division, and these cell also extend dendrites into the molecular layer of the dentate gyrus within two weeks (Hastings and Gould, 1999; van Praag et al., 2002). How does activity-regulated the proliferation and differentiation of these progenitor cells?

Proliferating SVZ progenitor cells are able to detect neuronal activity via L-type Ca^{2+} channels and the NMDA receptor, which promotes their differentiation into neurons (Deisseroth et al., 2004). Also, neurotransmitters such as serotonin, noradrenaline and glutamate are able to regulate proliferation of progenitors (Kemperman, 02). Interestingly, the peptide PACAP has been shown to increase proliferation of progenitor cells in both the SGZ and SVZ (Mercer et al., 2004). As described earlier, the stability of PACAP mRNA has been found to increase following depolarisation of cultured cortical neurons (Fukuchi et al., 2004), which suggests a possible link between molecular and cellular plasticity. Neuronal activity, neurotransmitters and other molecules may underlie the well established ability of environmental stimuli to affect neurogenesis. For example, exposure of rodents to an enriched environment increases the survival of nascent neurons with the SGZ (Kempermann et al., 1997). Also, hippocampus-dependent learning tasks such as the Morris water maze also appear to increase survival of nascent granule cells in the hippocampus (Gould et al., 1999). Taken together these studies illustrate that synaptic activity can directly and indirectly affect the proliferation and differentiation of neuronal progenitors.

Throughout the sections described so far the expression of certain genes have been identified as regulated by synaptic activity. In the next section these genes will be summarised and common features between them identified.

1.4. Activity-dependent gene expression

As described above, the expression of some genes is increased following synaptic activity. A summary of these genes, including some not previously described, is given in Table 1.1 below.

Level	Gene	Method of Induction	Brain Region	Reference(s)
Scaffolding	AKAP150	LTP	Hippocampus	Genin, 03
	Homer	Seizure/LTP	Hippocampus	Brakeman, 97; Kato, 97
Signalling	SNK	LTP	Hippocampus	Kauselmann, 99
	Pim1	LTP	Hippocampus	Konietzko, 99
Transcription	Zif268	Sezuire/LTP	Hippocampus/cortex	Saffen, 88; Dragunow, 87; Morgan, 87; Cole, 89
	c-fos	Seizure		
	c-jun	Seizure		
Protein metabolism	tPA	Seizure/LTP	Hippocampus/cortex	Qian, 93
Protein targeting	Arc	Seizure/LTP	Hippocampus/cortex	Lyford, 95; Link, 95

Table 1.1. Gene expression affected by synaptic activity. Each activity-regulated gene functions within one of the levels described above and all the genes are upregulated in the hippocampus.

The genes listed above can all be described within the context of the various levels highlighted within this introduction. As discussed, AKAP150 and Homer are both involved in the scaffolding of glutamate receptors in the synapse (Smith et al., 2006; Ehrengruber et al., 2004). Serum inducible kinase (SNK) is upregulated in the hippocampus by LTP-inducing stimuli, and is involved in activity-dependent regulation of spine density/size (Kauselmann et al., 1999; Pak and Sheng, 2003). Another kinase whose expression is affected by activity is Pim1 (Konietzko et al., 1999). The expression of Pim1 is increased in the hippocampus following LTP-inducing stimuli and is required for the late-phase of long-term potentiation (Konietzko et al., 1999).

There are also well established examples of transcription factors that are upregulated following synaptic activity; for example, Zif268, c-fos and c-jun (Saffen et al., 1988; Dragunow and Robertson, 1987; Morgan et al., 1987). The increase in transcription factors supports that idea that de novo protein synthesis is required for the consolidation of long lasting forms of synaptic plasticity (Malenka and Bear, 2004). As well as the synthesis of new proteins, the metabolism and targeting of proteins is also a point of regulation following synaptic activity. For example, tissue plasminogen activator is increase in the hippocampus following LTP-inducing stimuli and may

affect synaptic function via proteolytic processing of the NMDA receptor (Qian et al., 1993; Nicole et al., 2001). Also, the targeting of AMPA receptors to the plasma membrane is affected activity-induced Arc/Arg3.1 (Link et al., 1995; Chowdhury et al., 2006).

The activity-dependent genes listed in Table 1.1 and described above are only a few amongst many hundreds that have been identified. The genes listed above have been chosen to illustrate the various levels discussed within this introduction; however, there are others that have a broad role in neural function. For example, brain-derived neurotrophic factor (BDNF) is an activity-regulated gene that has a broad role in neuronal growth and survival as well as synaptic physiology (Lessmann et al, 2003).

These genes also appear to have certain features in common: they are all expressed in the hippocampus following activity, and often in the dentate gyrus. Also, they are expressed as immediate early genes - that is, they are upregulated within the first hour following synaptic activity and do not require protein synthesis.

Another gene whose expression is affected by synaptic activity is microtubule-associated serine/threonine kinase 4, or MAST4 (French et al., 2001b). French et al identified a set of genes whose expression in the dentate gyrus was increased following electro-shock evoked maximal seizures (EMS). The MAST4 gene encodes a protein with a serine/threonine kinase domain and a PDZ domain, as shown in Figure 1.10.

Figure 1.10. Microtubule-associated serine/threonine kinase (MAST4). MAST4 contain a serine/threonine kinase (blue box), which includes a C-terminal extension (red box). MAST4 also contain PDZ protein-protein interaction domain (green box). Unlike the other members of the MAST family, MAST4 also contains an extension of its C-terminus, termed the C-domain.

The study by French et al (2001b) identified the upregulation of MAST4 as an immediate early gene, which has been confirmed during this study (see Chapter 3). Also, the presence of a kinase domain and PDZ domain suggests that MAST4 may be involved in signalling and scaffolding, which as discussed are points of regulation following synaptic activity. Also, as this study will describe, MAST4 may also contribute to nuclear function via its unique C-terminal extension ('C-domain').

MAST4 is part of a larger family that contain 5 members. These other members illustrate the capacity of the MAST family to contribute to signalling and scaffolding, both within the CNS and other tissues.

1.5. The MAST family of serine/threonine kinases.

The MAST family are characterised by the presence of a serine/threonine kinase domain and a PDZ domain, which is illustrated by Figure 1.11 below. The HUGO (Human Genome Organisation) Nomenclature Committee has reviewed the nomenclature for this family; the official names are listed below along with common aliases:

MAST1 = Syntrophin associated serine/threonine kinase

MAST2 = Microtubule associate serine/threonine kinase of 205kDa

MAST3 = FLJ14813

MAST4 = AK090136.1 (MAST4)

MAST-L = KIAA0561

This nomenclature has also been used for mouse/rat homologues and will be used throughout this report

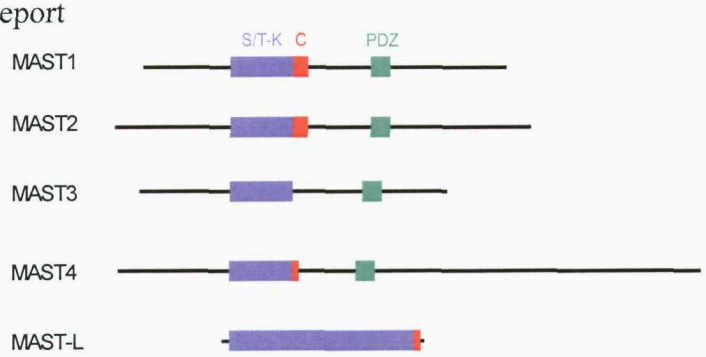

Figure 1.11. The MAST family of Proteins. All 5 members contain a kinase domain (S/T-K), which has a C-terminal extension in each case (C). Four members (MAST1-4) also contain a PDZ domain. MAST4 contains a noticeable extension at its C-terminal end, which contains no identifiable domains. Blue (S/T-K) = kinase domain; Red (C) = extension to kinase domain; Green = PDZ

All 5 members contain a kinase domain, although this domain is elongated in MAST-L; and 4 members - MAST1, MAST2, MAST3, and MAST4 - contain a PDZ domain. The kinase domains of the MAST family also contain a C-terminal extension which includes two phosporylation sites that regulate the kinase activity (Newton, 2003).

The first member of the MAST family to be identified, MAST2 (Microtubule-Associated Serine/Threonine Kinase of 205kDa), was originally identified during an attempt to characterise proteins that interact with and possibly modulate the function of microtubules during spermatogenesis (Walden and Cowan, 1993). MAST2 and the other members are described below.

1.5.1. MAST1 & MAST2 contribute to scaffolding in the dystrophin/utrophin associated protein complex.

In (1999), Lumeng et al identified an interaction between β2-syntrophin and MAST2, as well as a related protein they termed Syntrophin-Associated Serine/Threonine Kinase of 170kDa (MAST1). The syntrophin family of proteins are a component of the dystrophin- and utrophin-associated protein complex (DAPC and UAPC, respectively). The DAPC/UAPC are part of the cytoskeletal elements found at neuromuscular junctions (NMJs) and post-synaptic densities (PSDs), and link actin filaments to extracellular matrix components (ECM). Figure 1.12. below illustrates the UAPC.

The DAPC/UAPC are composed of dystroglycans, sarcoglycans, sarcospans, dystrobrevins, and syntrophins. The syntrophins (α1, β1, and β2) are 59kDa proteins found in the cytoplasm, which bind to the C-terminus of dystrophin, utrophin, and dystrobrevins (Ahn and Kunkel, 1995; Peters et al., 1997); they include a PDZ domain, two pleckstrin homology domains (PH), and a unique C-terminal domain. Lumeng et al (1999) hypothesised that the syntrophins link dystrophin and utrophin to other cellular structures and therefore screened for proteins that interact with the NMJ-specific β2-syntrophin.

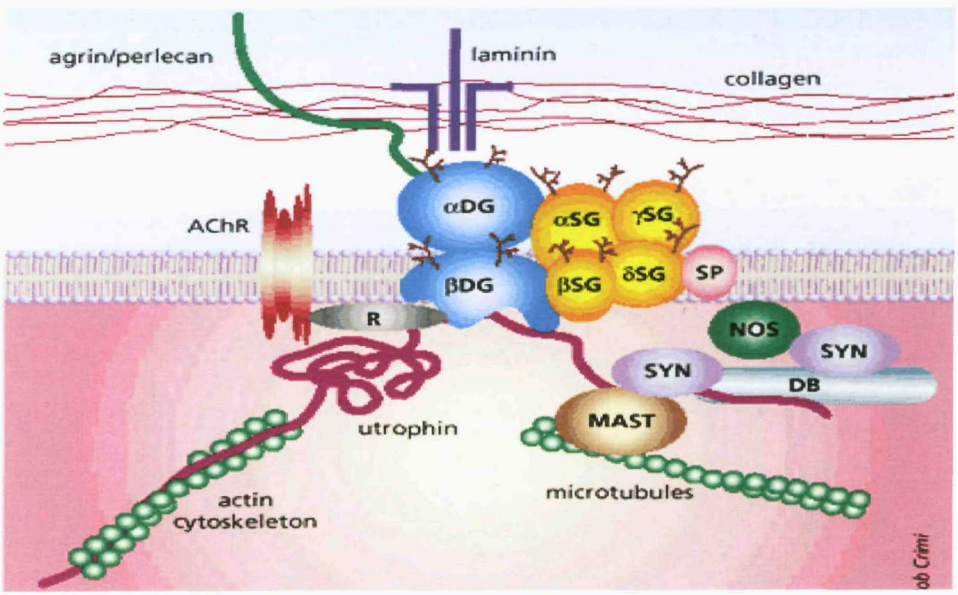

Figure 1.12. The Structure of the utrophin-associated protein complex. This complex acts as a receptor for laminin, agrin and perlecan, and functions to link the ECM to the actin cytoskeleton. It is also involved in clustering of acetylcholine receptors (AChRs). A central component, dystroglycan (DG), has a range of functions in different cell types. The dystrophin-associated protein complex is similarly organized accept that it does not interact with MAST2 Rapsyn, R; Syntrophin, SYN; dystrobrevin, DB; neuronal nitric oxide synthase, NOS; sarcospan, SP; sarcoglycan, SG. (Taken from Chamberlain, 1999)

The yeast-two hybrid system was used to search for proteins that interact with β2-syntrophin and both MAST1 and MAST2 were identified as potential candidates. Lumeng et al established that the PDZ domain of β2-syntrophin mediated the interaction with these MAST family members.

Using a northern blot, both MAST1 and 2 were shown to be expressed in mouse brain. Although antisera raised against both proteins only identified MAST1 expression within mouse brain homogenates. Microsome preparations showed that MAST2 and MAST1 are associated with muscle and brain membranes, respectively.

Further studies showed that MAST2 was localised to the NMJ, and in a pattern that overlaps with utrophin expression, which itself colocalizes with β2-syntrophin expression. Therefore, MAST2 may be linked to the utrophin-associated protein complex.

MAST1 expression was examined in relation to syntrophin, utrophin, and dystrophin. In the CNS, dystrophin and utrophin primarily localise to the vascular endothelium, postsynaptic regions, pia, and choroid plexus. In brain sections, anti-MAST1 antibodies detected a signal in vascular endothelium and in proximity to neuronal nuclei in both the cortex and cerebellum; MAST1 was also detected in the choroid plexus and ependymal cells. Taken together, it appears that the CNS vascular endothelium represents a major region for colocalisation of MAST1, β2-syntrophin, and utrophin.

The study described above demonstrated that two related kinases, MAST2 and MAST1, colocalize with either the DAPC or UAPC and may couple these complexes with signal transduction pathways.

1.5.2. Syntrophin-associated serine/threonine kinase of 124kDa (SAST124), a novel splice variant of MAST1.

Some years after the study by Lumeng et al, a splice-variant of MAST1 was identified and described by Yano et al (Yano et al., 2003). This study identified in rat a transcript homologous to mouse MAST1, and also another smaller transcript that was identical to this up to its Glu^{1089} residue. After this residue, MAST1 has another 481 amino acids; however, the variant MAST1 has only 28 residues, which are unique to this variant.

Using reverse-transcriptase PCR, mRNA for SAST124 was found to be exclusively expressed within the brain (Yano et al., 2003). The pattern of this expression was then further investigated using a monoclonal antibody.

Certain cell types and regions were labelled following immunostaining. These included cells in the subventricular zone and granule cells of the dentate gyrus. In neurons, immunoreactivity appeared to be confined to the nucleus. This observation was confirmed in cultured cerebellar granule cells, which displayed exclusive staining within the nucleus. This staining was punctate, which suggest that SAST124 is associated with particular structures inside the nucleus (Yano et al., 2003).

1.5.4. MAST2 is involved in the immune response

Phagocytes such as macrophages ingest invading pathogens as part of the immune response. Lipopolysaccharide (LPS) from bacteria can be used to stimulate the immune response in macrophages, which results in the coordinated activation of proinflammatory cytokines. One of these, IL-1 binds to IL-1 receptors on macrophages, which cause the activation of NF-kB and the synthesis/secretion of IL-12 (Figure 1.13).

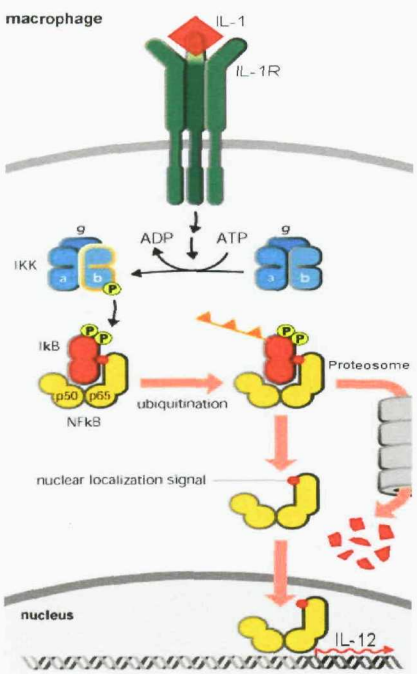

Figure 1.13. Synthesis and secretion of interleukin-12 following activation of the interleukin-1 receptor. Activation of the receptor leads to phosphorylation of IkB by activated IkB kinase (IKK). Phosphorylated IkB is ubiquitinated and subsequently degraded by the proteasome. An exposed nuclear localization signal on the p65 subunit of NF-kB causes its translocation to the nucleus where it activates transcription. Although poorly defined, the E3 ubiquitin ligase TRAF6 appears to play a role in activating IKK. (Adapted from http://www.stat.rice.edu/~siefert/Research/NfKB.html)

Interleukin-12 (IL-12) causes naïve T cells to differentiate into T helper 1 cells, and is therefore an essential component of the Th1 immune response. Following LPS stimulation of macrophages, MAST2 has been found to control the synthesis of the p40 subunit of IL-12 through activation of NF-κB (Zhou et al., 2004). This study found that inhibition of MAST2 synthesis using RNAi blocked LPS-induced IL-12 synthesis and

release. Therefore, MAST2 appears to be involved in the LPS signal transduction pathway that regulates the activity of NF-κB and subsequent expression of IL-12.

It has subsequently been found that the activation of NF-κB by MAST2 is mediated by an interaction with TRAF6 (Xiong et al., 2004). This protein is part of the TNF receptor associated family (TRAF), which mediate signal transduction from the TNF receptor superfamily. TRAF6 functions as a signal transducer in the NF-κB pathway that activates IκB kinase (IKK) in response to proinflammatory cytokines. However, this function is negatively regulated by its interaction with MAST2. Therefore, the increase in NF-κB activity shown by disrupting MAST2 function can be explained by the release of this negative regulation of TRAF6.

1.5.6. The MAST family and PTEN

As shown in Figure 1.14, stimulation of growth factor receptors, activates phosphatidyl inositol 3-kinase (PIK), which phosphorylates PIP_2 to PIP_3. PIP_3 then activates phosphoinositide dependent kinase (PDK) and integrin-linked kinase (ILK). These two enzymes phosphorylate PKB/Akt on Thr^{308} and Ser^{473}, respectively. Akt is a serine/threonine kinase that becomes activated following phosphorylation and functions to promote cell survival. PTEN is a phosphatase that can de-phosphorylate PIP_3 and therefore inhibit activation of Akt.

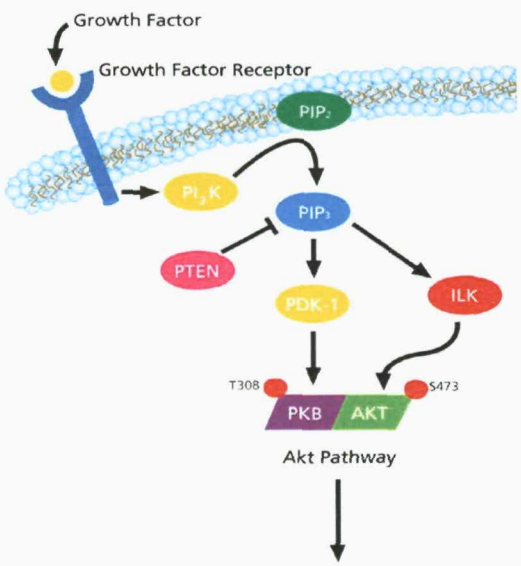

Figure 1.14. PTEN pathway. Growth factors can affect cell viability via the downstream activation of Akt. The phosphatase PTEN can inhibit this pathway. (Adapted from www.sigmaaldrich.com)

Some of the functions of PTEN are regulated by its phosphorylation status, which affects its stability, subcellular location and/or its association with regulatory molecules (Gericke et al., 2006). In relation, PTEN contains a C-terminus that consists of a functional PDZ-domain binding motif. PTEN has been found to bind to PDZ domain

containing proteins, for example MAST2 (Adey et al., 2000). Valiente et al (2005) have confirmed this interaction as well as describing further PDZ mediated interactions with MAST1 and MAST3, which appear to attenuate the degradation of PTEN. These authors also found that binding of PTEN to these 3 members of the MAST family facilitates phosphorylation of PTEN by their kinase domains. They suggest that phosphorylation of PTEN by these members of the MAST family may modulate its function by affecting which other proteins PTEN interacts with (Valiente et al., 2005). No interaction, or kinase activity, was identified between MAST4 and PTEN, and these authors chose not to investigate any possible interaction between PTEN and the PDZ deficient MAST-L.

1.5.7. MAST4, an inducible member of the MAST family

As previously described, another member of the MAST family, MAST4, has so far only been identified as an activity-regulated transcript in the dentate gyrus of the mouse hippocampus (French et al., 2001b). This study began as an attempt to identify seizure-induced gene expression in area CA1 of the mouse hippocampus. The differential expression of ≈ 9000 genes was examined using cDNA microarrays. *In situ* hybridisation was then used to confirm the differential expression of 14 transcripts that showed the highest modulation in the microarray screen. Only one gene, for the nuclear hormone receptor NGFI-B, showed significant up-regulation (≈ 2-fold) in area CA1; however, this transcript was more noticeably up-regulated (≈ 12-fold) in the dentate gyrus of the hippocampus. In addition, two other genes showed up-regulation in the dentate gyrus, Fos-like antigen 2, and an uncharacterised transcript deposited as an EST in GenBank (Acc. No AA145137).

The EST identified by this study was derived from the spleen of a 4 week old male mouse. The full length clone was isolated from the bone marrow stroma cells of a 5 month old female mouse (Acc. No AK090136) and was produced by the Riken Genome Exploration Research Group as part of an attempt to produce a full-length cDNA library of the mouse transcriptome. The Riken clone AK090136 (subsequently referred to as 'Riken clone') is 10621bp in length and contains an open reading frame between bases 273 to 8136, which produces a protein of ≈288kDa.

MAST4 is therefore induced during increased synaptic activity, contains domains capable of signalling and scaffolding, and has a unique C-terminus that may also

function. The available reports for other MAST family members also support the idea that these protein are involved in scaffolding and signalling. The protein-protein interactions a kinase is involved in can reveal potential substrates for its kinase activity. Therefore, what methods can be used to identify potential interacting proteins for MAST4?

1.6. Methods to identify and confirm potential interacting proteins for MAST4

A common method for characterising protein-protein interactions is the yeast-two hybrid system (YTH), which will be described shortly. However, to independently confirm the results of a YTH screen various other approaches can be taken. For example, cDNA isolated from a YTH screen can be used to heterologously express recombinant proteins within cells. This can allow cellular localisation to be investigated as well as revealing whether an interaction can be confirmed outside of the yeast-two hybrid system. The possibility that a potential interaction occurs *in vivo* can also be investigated by analysing the transcript and protein expression profiles for the interacting proteins.

1.6.1. The yeast-two hybrid system (YTH)

The YTH system is based on the reconstitution of a transcription factor by the interaction of two proteins. Transcription of reporter genes by this transcription factor therefore allows the interaction to be identified (Fields and Song, 1989)

Originally, the transcription factor was based on the yeast Gal4 DNA-binding domain (DBD) and activation domain (AD). However, in the LexA system the transcription factor is derived from the LexA DBD and the B42 acidic AD. Both of these proteins are derived from bacteria, which will reduce false positives as neither prokaryotic protein has any natural interacting partners within the eukaryotic yeast cell (Reviewed in Maple and Moller, 2007). As Figure 1.15. illustrates, the 'Bait' 'protein X' is expressed as a fusion with the LexA DBD, and the Prey 'protein Y' is expressed as a fusion with the B42 AD. If protein X and Y interact the transcription factor is reconstituted and the reporter gene is expressed. The Bait and Prey proteins can be

chosen based on a hypothesised interaction; alternatively, the Bait protein can be used to search for its 'Prey' within a library of potential interactors.

Expression of either the Prey or Bait proteins may be toxic to the yeast cells. Toxic proteins will arrest the growth of the yeast, and may even kill them (Reviewed in Maple and Moller, 2007). This will make Bait proteins unsuitable for screening, and may cause the loss of yeast containing Prey proteins that are involved in significant interactions. Therefore the LexA system has circumvented this problem by putting the expression of both proteins under the control of the inducible GAL1 promoter. This promoter will only allow transcription to be initiated if galactose is present in the growth media. Also, the plasmid copy number for the Bait and Prey proteins can be amplified *in vivo* by growth on non-inducing glucose containing media prior to screening, which will therefore increase the probably of detecting low abundance interactions.

This system also utilises two reporter genes: the LEU2 gene, which allows yeast to grow on leucine deficient media; and the LacZ gene, which encodes β-galactosidase. If X-gal is present in the growth media, β-galactosidase will hydrolyse it to produce a blue product, which thus allows the expression of the reporter gene to be visually assessed.

The major disadvantage of the YTH system is the potential for false positives (see Figure 1.16.). Both the Bait and Prey proteins may be able to activate transcription of the reporter genes independently of any interaction. This problem can be minimised by the use of appropriate controls. However, the major advantage of this system is that it allows easy access to the sequence information and cDNA clones of the interacting proteins.

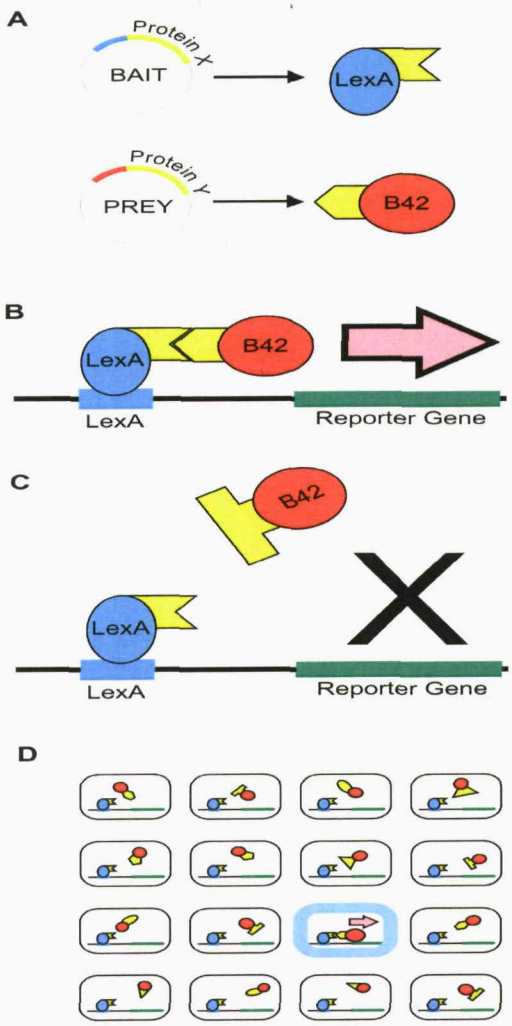

Figure 1.15. The LexZ Yeast-Two hybrid System.
A - Protein X is expressed fused to the LexA DNA binding domain. Protein Y is expressed fused to the B42 activation domain.
B - Protein X and Y interact, which allows transcription of the reporter gene.
C- Protein X and Y do not interact; therefore, the reporter gene is not expressed.
D - Screening of a library of proteins using the Bait construct results in an interaction. This is assayed by the expression of a reporter gene that turns the yeast blue.

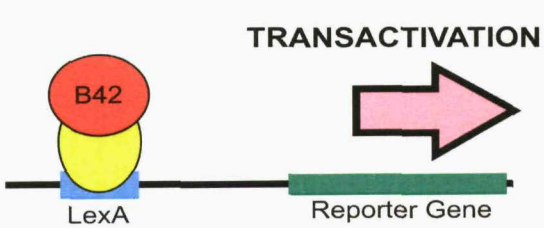

Figure 1.16. Transactivation of a reporter gene.
The fusion protein can bind to the LexA operator sequence and allow the B42 activation domain to initiate transcription.

To confirm the capacity of two proteins to interact independently of the YTH system are variety of different approaches can be used. The interaction can be investigated biochemically by using the glutathione-S-transferase 'pull-down' method. Alternatively, expression of the potential interacting proteins can be investigated within cells.

1.6.2. Heterologous expression of potential interacting proteins

The YTH system allows relatively easy access to the cDNA encoding the potential interacting proteins. These cDNA clones can be inserted in-frame into vectors which allow the interacting protein to be expressed as a fluorophore-tagged fusion protein. Following transfection of a standard cell line (e.g. HEK cell), the subcellular localisation of the fluorophore-tagged fusion protein can be identified using fluorescent microscopy. This can reveal valuable information about the potential localisation of the identified proteins and whether they are expressed in the same region of the cell as the bait protein. However, the bait protein and its potential interactor can also be co-transfected and possible co-localisation observed. Therefore, any change in expression observed following co-transfection can potentially confirm the presence of the interaction.

If the interaction(s) identified from the YTH system, and any confirmed in a separate study, occur *in vivo* the expression patterns of these genes should overlap.

1.6.3. Characterising the expression profile of genes across various tissues

The expression profile of a gene and its cognate protein can be investigated using a variety of techniques. For example, the expression of a genes transcript can be investigated using *in situ* hybridisation. A common variant of this technique involves the hybridisation of a radioactively labelled oligonucleotide to fixed sections of a particular tissue. This therefore allows the detection of the expressed transcripts and identification of the cells/regions within the tissue where they are expressed.

The protein product of the gene of interest can also be investigated using immunohistochemistry. This requires the generation of antisera (and/or a monoclonal antibody) against the target protein, which can be achieved using a peptide or purified protein derived from the gene of interest. Again, an expression profile of the target protein can be therefore be investigated and compared to the potential interacting proteins.

MAST4 is therefore an activity-inducible gene that contains domains know to be involved in signalling and scaffolding. These domains have been shown to perform these roles in other MAST family members. Therefore, the initial hypothesis was that MAST4 may contribute to signalling and scaffolding at the synapse following synaptic activity. To test this hypothesis the yeast-two hybrid system has been used to identify potential interacting proteins. Both a rationalised approach (based on known MAST family interacting proteins) and a screen for interacting proteins has been performed. The results from the YTH screen have been investigated further using heterologous expression within HEK cells. Also, to characterise the expression profile for MAST4, and other members of the MAST family, *in situ* hybridisation has been performed. This has allowed the expression profile for MAST4 to be compared to that for its potential interacting proteins. These results and others will be described within the following chapters.

Chapter 2 - Materials and Methods

2.1. Molecular Biology

Tables 2.1 and 2.2 below lists the oligonucleotides used for PCR amplification and the constructs and plasmids made using these amplicons.

Primer name	5'-3' sequence
inSAST PDZ EcoR1	GGA ATT CCA GCC CAT TGT CAT CCA CAG
INSAST PDZ Xho1	CCG CTC GAG TGG AGT AGT GGT GAT AGA CAC
SAST PDZ EcoR1	GGA ATT CAT CAC CAT CCA ACG CTC AG
SAST PDZ Xho1	CCG CTC GAG GGT CAC AGC TAC TTT GTT GC
MAST PDZ EcoR1	GGA ATT CAT CAT CAT CCA CCG AGC TGG
MAST PDZ Xho1	CCG CTC GAG AAT TGA TAC CTT GTT CCA CTC
xt inSAST fwd	CCG GAA TTC CAG GAG CTG ATT ACC TTG CT
xt inSAST rev	CCG CTC GAG CTC CTC TTG TGT CAC CTC TA
xt SAST fwd	CCG GAA TTC GCA CAG CTT CTA ATA TCT AGC
xt SAST rev	CCG CTC GAG CAG GCT GTG TTT GCG CAG T
C-Domain fwd	CCG GAA TTC ACA TCA ATC AAA ACG GGA CCA
C-Domain rev	CCG CTC GAG TTA GGA GGC CTT TTT GTG AG
Kinase fwd	CCG GAA TTC ATG GGG GAG AAA GTT TCC GA
Kinase rev	CGC GGA TCC GTC TCG GCT GGG AGA GGA AT
FP1 fwd	ACA TGC ATG CCA CAA AGA TAG CCA AGA TGA G
FP1 rev	ACG CGT CGA CTT AGG AGG CCT TTT TGT GAG
FP3 fwd	CGC GGA TCC GGT AAA GCC AGT GAC AGT TC
FP3 rev	ACG CGT CGA CCC CTC CAT TGG TGT TTT TCA G
FP4 fwd	TCC CCC CGG GAA GCA TCC ACC CAG ACA AG
MAST1-Y2 fwd	CCG GAA TTC GAA GTG GGT CAC CCT GAT T
MAST1-Y1 rev	CCG CTC GAG TCA TGG ACC TAA AGA TGC AG
C-Domain bglII	GGA AGA TCT TCA AGA AGC TGG CCA AGC AG
MAST3 Northern fwd	AAC CGT AAG AGC TTG GTC GTG
MAST3 Northern rev	GGT GGT GGA TAA AGC CCA AGA
MAST-L Northern fwd	TGA GGA GAA TGA AGG AGG TGC
MAST-L Northern rev	CGA AGG TAT GTG ACT GGC TAC

Table 2.1. List of oligonucleotides used for PCR amplification.

Name	Author	Method
pGilda	Origene	
PJG4-5	Origene	
pSH18-34	Origene	
pEG202MAX	Origene	
pJK101	Origene	
pQE-30	Qiagen	
pCR II	Invitrogen	
pGRFP	PG	mRFP & pEGFP cut BsrGI/AgeI
pFLCI-MAST4 (AK090136.1)	Riken	
pUC19-MAST	PW	
pJG4-5-SAST Full	KL	PCR amplification and RT-PCR
MAST1PDZ-pJG4-5	PG	PCR amplification insert into EcoR1/Xho1
MAST2PDZ-pJG4-5	PG	PCR amplification insert into EcoR1/Xho1
MAST4PDZ-PJG4-5	PG	PCR amplification insert into EcoR1/Xho1
xt MAST1PDZ-pJG4-5	PG	PCR amplification insert into EcoR1/Xho1
xt MAST4PDZ-pJG4-5	PG	PCR amplification insert into EcoR1/Xho1
MAST1-Y1 - pJG4-5	PG	PCR amplification insert into EcoR1/Xho2
MAST1-Y2 - pJG4-5	PG	PCR amplification insert into EcoR1/Xho3
CDomain-pGilda	PG	PCR amplification insert into EcoR1/Xho1
C-Domain - pEGFPC2	PG	C-Domain-pGilda cut EcoRI/XhoI and ligated into vector cut EcoRI/SalI
C-Domain - pCMV Tag2B	PG	
C-Domain - pGEX 5X	PG	
C-Domain - pGRFP	PG	
KinaseDomain-Pgilda	PG	PCR amplification insert into EcoR1/BamH1
xt MAST4PDZ-pGilda	PG	EcoR1/Xho1 lift from xt MAST4PDZ
FP1-pQE-30	PG	PCR amplification insert into Sph1/Sal1
FP2-pQE-30	PG	PCR amplification insert into Sph1/Sal2
FP3-pQE-30	PG	PCR amplification insert into BamH1/Sal1
FP4-pQE-30	PG	PCR amplification insert into Xma/Sal1
pEGFP - A6(SytXI)	PG	pJG4-5-candidate interactor cut EcoRI/XhoI and cloned into pEGFP cut EcoRI/SalI
pEGFP - B12(14-3-3 eta)	PG	
pEGFP - C5(ELL2)	PG	
pEGFP - G3(14-3-3 beta)	PG	
pEGFP - G6(NIPP1)	PG	
pEGFP - G10(ELL1)	PG	
pEGFP - I3(CK2 alpha chain)	PG	
pEGFP - K1(RTF1)	PG	
MAST3-pCR II	PG	TA cloning (Invitrogen)
MAST-L-pCR II	PG	TA cloning (Invitrogen)

Table 2.2. List of plasmids and constructs made. PG = Patrick Garland; KL = Kate Lidwell; PW = Paul Walden

2.1.1. Restriction Digests

Restriction digests were used to analyse plasmid DNA and generate complementary DNA ends for subcloning. Restriction endonucleases were supplied by New England Biolabs or Roche and used in accordance with their recommendations. A typical reaction would consist of:

5-10μg of DNA

1-5μl of restriction endonuclease* (10U/μl)

5μl 10X buffer

ddH_2O to a final volume of 50μl.

Restriction digests were analysed using agarose gel electrophoresis.

* one unit of restriction enzyme will digest 1μg of Lambda DNA within 1hr at 37^{O}C. Therefore, the number of units of restriction endonuclease used for each reaction was adjusted according to the size of the DNA used and number of restriction sites within it.

2.1.2. Agarose Gel Electrophoresis

DNA was separated according to size using electrophoresis through ethidium bromide containing agarose gels. To achieve optimal separation of the DNA, gels of various concentrations were prepared using the following components:

0.5-3g agarose (0.5-2% agarose)

1X Tris-acetate (TAE) to a final volume of 50ml (mini-gel), or 150ml(maxi-gel)

The TAE was prepared from a 50X stock (100ml/L 0.5M EDTA pH 8.0, 2M TrisBase, 57.1ml/L Glacial Acetic Acid, made up to 1L with ddH_20). The agarose was dissolved by heating the mixture in a microwave. The molten gel mix was then allowed to cool slightly before the addition of 1μl ethidium bromide (10mg/ml). The gel was then poured into a casting mould, allowed to set, and then placed into an electrophoresis chamber containing 1X TAE. Before loading samples were mixed with loading buffer (6X, Invitrogen; 30% (v/v) glycerol, 60 mM Tris-HCl (pH 7.5), 60 mM EDTA, 0.36% (w/v) XCFF, and 3.6% (w/v) Tartrazine) to achieve a 1X final concentration. A molecular weight marker (1Kb Plus DNA Ladder, Invitrogen) was included in an adjacent lane to asses the size of the separated DNA. Mini-gels were run at 75mV and large-gels 120mV. When necessary, DNA extraction was performed by cutting out the

appropriate band of DNA (under low-intensity UV light) and purifying it using the Qiagen Gel-Extraction Kit (Qiagen).

2.1.3. Polymerase Chain Reaction (PCR)

The polymerase chain reaction was routinely used to amplify DNA fragments for cloning or analytical purposes (e.g., Colony PCR).

In both cases, oligonucleotides were purchase from Invitrogen and their melting temperatures calculated using the Wallace rule (Wallace, 1979):

A/T = 2°C

G/C = 4°C

Cloning:

Platinum pfx (Invitrogen) was used to amplify inserts for use in subcloning. This is a proof reading enzyme with 3'-5' exonuclease activity.

On ice, the following components were added to a PCR reaction tube:

Template (10ng/µl)	5µl
Primers (20µM)	1µl

Buffer (10X)	5µl	Made as a 'master mix'
dNTP (10µM)	1.5µl	
Platinum pfx	0.5µl	
$MgSO_4$	1µl	
ddH_20	34.5µl	

The cycling parameters were as follows:

2min @ 94°C	25-35 cylces
15sec @ 94°C	
30sec @ oligo specific temperature	
1min/kb @ 68°C	
5min @ 68°C	

Following analysis using electrophoresis, PCR products were either column purified (Qiagen PCR Purification Kit) or gel extracted (Qiagen Gel Extraction Kit) according to the manufactures instructions.

Colony PCR:

On ice, a master mix was set-up and pipetted into an appropriate amount of sterile PCR reaction tubes:

Buffer (10X)	2.5µl
Primers (20µM)	0.35µl
dNTP (10µM)	0.31µl
Taq Polymerase (5U/µl)	0.125µl
ddH_20	21.36µl

Using an autoclaved pipette tip, a colony was picked, spotted onto a back-up plate and then left in the master mix for 3-5min. The reaction was then placed into a thermocycler, which was programmed with the following cycling parameters:

1min @ 94°C
40sec @ 94°C
40sec @ oligo specific temperature } 35 cycles
1min/kb @ 72°C
5min @ 72°C

The products of the PCR reaction were analysed using gel eletrophoresis.

2.1.4. Ligation reactions

Preparation of the vector:

1) The indicated vectors (Table 2.2) were digested with the appropriate restriction endonucleases.

2) The cut vector was purified using the Qiagen PCR purification Kit, or Qiagen Gel Extraction Kit depending on the size of DNA released from the digested vector.

3) If necessary, the vector was de-phosphorylated using the reaction conditions below:

Vector DNA	Xµl (2-4µg)
Buffer (10X)	5µl
Calf Intestine Alkaline Phosphatase (Roche)	1U/1pmol vector DNA
ddH_20	Up to 50µl

The reaction was allowed to proceed at 37°C for 60min.

4) The vector was purified using the Qiagen PCR Purification Kit.

Preparation of the insert:

1) The insert was digested with the appropriate restriction endonucleases directly from a plasmid or following amplification via PCR.

2) The insert was purified using the Qiagen PCR purification Kit, or Qiagen Gel Extraction Kit according to the manufactures instructions.

Both the insert and vector were run on an agarose gel to determine the quality and quantity of DNA prepared by each procedure. A ligation reaction was then set-up as follows:

Vector	50-100ng
Insert	3X the molar amount of vector
Ligase Reaction Buffer (Roche)	1-2µl
T4 DNA Ligase	1µl (i.e. 1U)
ddH_20	Up to 10-20µl

The reaction was allowed to proceed overnight at $12^{O}C$.

TA cloning was performed according to the manufactures instructions (Invitrogen).

2.1.5. Bacterial Strains

Strain	Supplier	Use
XL1-Blue	Stratagene	Routine use
M15(pREP)	Qiagen	Protein expression
BL21(DE3)	Stratagene	Protein expression

2.1.6. Bacterial Cultures

Luria Broth, LB (Tryptone 10g/L, Yeast Extract 5g/L, NaCl 10g/L, pH7.0), was used to grow bacterial cultures at $37^{O}C$ with shaking. LB agar plates were made by the addition of 15g/L of agar. Media intended for either cultures or plates was sterilized by autoclaving (LTE 300SH $121^{O}C$ for 15min at 1BAR). When required, antibiotics were included in the media, which was allowed to cool to $<50^{O}C$ when preparing plates (see Table 2.3, below).

Antibiotic	Stock Concentration	Final Concentration
Ampicillin	100mg/ml in water	50-100µg/ml
Tetracycline	5mg/ml in ethanol	50µg/ml
Kanamycin	50mg/ml in water	25-50µg/ml

Table 2.3. Antibiotics used for bacterial cultures.

2.1.7. Generation of Electrocompetent Cells

From a glycerol stock, single colonies of XL1-blue were made by streaking onto a tetracycline selective plate. One of these colonies was then picked and grown overnight at 37°C in 50ml of Yeast Extract Bacto Nutrient Broth, YENB (7.5g/L Yeast Extract, 8g/L Bacto Nutrient Broth, pH7.0). The overnight culture was diluted to an optical density (OD_{600}) of 0.1 by dilution in to 1L of YENB - this culture was then grown to an OD of 0.6. All subsequent steps were performed at 4°C, which included the use of apparatus that had been pre-chilled. The culture was dispensed into 2 centrifuge buckets and spun at 4000g (Sorvall Legend RT) for 10min. The supernatant was removed and the pellet resuspended in 20ml of sterile 10% (v/v) glycerol. This was again spun at 4000g for 10min, the supernatant removed, and the pellet resuspended in 3ml of 10% glycerol. Finally, 80µl of aliquots of the resuspended cells were then snap frozen into liquid nitrogen. The cells were stored at -80°C until used.

2.1.8. Electroporation

XL1-Blue strain of electrocompetent cells was used for standard transformations. A single aliquot of cells was thawed on ice and 1ng of dsDNA added. Following gentle mixing, the cells were transferred to a pre-chilled 2mm gap electroporation cuvette (Qbiogene). The cuvette was placed in the electroporation chamber in 2.5kV passed through the solution. The cells were then allowed to recover in LB for 1hr to allow the expression of the antibiotic resistance conferring gene. Selective LB agar plates were pre-warmed and allowed to dry under sterile conditions. The culture was then spread onto the antibiotic selective plates and incubated for 16hrs at 37°C.

2.1.9. Crude Extraction of Plasmid DNA from Bacteria

To screen bacterial colonies for target plasmid DNA a crude-miniprep protocol was used base on the alkaline lysis method (Bimboim, HC and Doly, J. 1979). The solutions for this procedure were supplied by Qiagen. A single, isolated colony was picked and grown overnight in 3ml of selective LB media. A 1.5ml eppendorf was then filled with the overnight culture and spun at 14,000rpm in a microcentrifuge for 1min. The pellet was resuspended in 100µl of Buffer P1 (50mM Tris-Cl, pH8.0, 10mM EDTA, 100µg/ml RNase A), and the cells lysed by adding 200µl of Buffer P2 (200mM NaOH, 1%SDS w/v) and gently inverting 5X. The lysate was neutralised by the addition of 150µl of Buffer P3 (3.0M potassium acetate, pH5.5) and again mixed by inversion 5X. The lysate was cleared by centrifugation at 14,000rpm for 5min (occasionally 10min if the lysate was not fully cleared). An eppendorf was filled with 900µl of 100% ethanol and 400µl of the cleared lysate was added. Following a brief vortex, the precipitated DNA was pelleted by centrifugation at 14,000rpm for 5min. The supernatant was removed and the pellet overlaid with 250µl of 70% ethanol, to remove residual salt, and spun at 14,000rpm again for 5min. The supernatant was removed and the pellet allowed to air dry for 1hr at room temperature before resuspension in 20µl of ddH_20.

2.1.10. High Quality Extraction of Plasmid DNA from Bacteria

To produce large amounts of high quality plasmid DNA, mini- and maxi-prep kits supplied by Qiagen were routinely used in accordance with the manufactures instructions.

2.1.11. Glycerol Storage of Bacterial Cultures

Bacteria were grown overnight in 3ml of selective media. Into an autoclaved cryogenic tube, 0.15ml of autoclaved 100% glycerol was added to 0.85ml of the overnight culture and vortexed to mix. This was snap frozen by immersion in liquid nitrogen. The tubes were then placed into a -80°C for long term storage. To recover the bacteria, a sterile loop was used to scrape the surface of the glycerol stock and then streaked onto a selective plate. The glycerol stock was then returned to the -80°C freezer and the plate incubated overnight at 37°C.

2.1.12. Sequencing

DNA sequencing was performed on each construct to ensure it was in-frame and correct. Plasmid DNA was sequenced using the ABI PRISM DNA sequencing kit. A typical reaction would consist of:

Template	250-300ng
Primer	1.6pmol
Terminator Ready Reaction Mix*	4µl
ddH_20	Up to a final volume of 10µl

* BigDye terminators (labelled with dRhodamine acceptor dyes), dNTPs, AmpliTaq DNA Polymerase, FS, rTth pyrophosphatase, magnesium chloride and buffer.

The cycling parameters for sequencing were:

10sec @ 96°C
5sec @ 50°C
4min @ 60°C
} 30 cycles

Following the sequencing reaction the DNA was precipitated. This was achieved by adding to each reaction:

10µl ddH_20
2µl 3M sodium acetate (pH4.6)
50µl 95% ethanol

The tubes were vortexed and then left at room temperature for 1hour to allow the dye-incorporated extension products to precipitate. The samples were then spun at 14,000rpm for 20min in a microcentrifuge. The supernatant was then removed and the pellet overlaid with 250µl of ice cold 70% ethanol. The sample was then briefly vortexed and spun again in a microcentrifuge for 10min at 14,000rpm. The supernatant was removed again and the pellet dried in a heat block for 1min at 90°C.

Automated sequencing was performed by the School of Biological Sciences, University of Southampton.

Commercial sequencing was performed by MWG Biotech. DNA (1-2µg) to be sequenced was lyophilised in an eppendorf using a SpeedVac (Savant). If necessary, a

sequencing oligonucleotide (10pmol/µl suspended in ddH_20). was also sent to MWG Biotech.

The quality of sequencing was visually checked by analysing chromatogram files with the software Chromas (Technelysium Pty Ltd). Sequences were then aligned (ClustalW) to the NCBI entry for each gene (Table 2.4).

Gene	Accession number
MAST1	BC054524.1
MAST2	U02313.1
MAST3	AK140821.1
MAST4	AK090136.1
MAST-L	AK030140

Table 2.4. MAST family sequences used to assess DNA sequencing.

2.1.13. Northern Blot

A mouse multiple tissue northern blot was purchase from Clontech. The cDNA probes used were made by digesting clones for MAST1, MAST2, and MAST4, and amplifying specific regions of MAST3 and MAST-L using PCR (see Table 2.5).

Gene	Position
MAST1	1-953
MAST2	4342-4845
MAST3	206-770
MAST4	1667-2470 & 8481-9132
MAST-L	79-980

Table 2.5. Position within each MAST family member (see Table 2.4) used to generate probes for northern blotting.

The sequence of each probe was checked for specificity using NCBI nucleotide-to-nucleotide BLAST searches. Each probe was labelled with [^{32}P] dCTP using the Rediprime random prime labelling kit (Amersham) according the manufactures instructions. The probes were then purified using ProbeQuant G-50 Micro Columns (Amersham). The quality of the labelling was assayed by measuring the cpm before and after the purification of the probe. The Total and Column count, respectively, was then used to calculate the percentage incorporation (typically 20-50%)

An incubator was pre-heated to 68°C, and set-up to rotate a hybridisation tube. The northern blot was placed RNA side face up into the hybridisation tube, and pre-hybridised with 10ml of hybridisation buffer for 1hr. The buffer consisted of:

5X SSC

5X Denhardt's Solution

0.1X Sodium dodecyl sulphate (SDS)

100μg/ml Salmon Sperm DNA

The radioactively labelled probe was denatured by heating for 5min at 95-100°C, and then chilled on ice for 2min. To 15ml of fresh hybridisation buffer, $2x10^6$ cpm/ml of the labelled probe was added. The pre-hybridisation solution was removed and the 15ml of fresh buffer added. The blot was incubated with the probe for 16hrs at 68^0C. The following day, the hybridisation buffer was removed and the blot rinsed 3X with Wash Solution 1:

2X SSC

0.05% SDS

The blot was washed for 15min with Wash Solution 1 three times at room temperature. The blot was then washed 2X for 20min at room temperature in the higher stringency Wash Solution 2:

0.1X SSC

0.1% SDS

The excess solution was shaken off and the blot carefully wrapped in Clingfilm.

The blot was then exposed to BioMax MS film for up to 7days at -80°C, and then developed using an X-ograph compact automatic developer.

2.1.14. Isolation of total RNA

To minimise contamination with RNases, a dedicated area, and appropriate equipment (e.g. pipettes, homogeniser,) were cleaned using solutions of 5% SDS, 1M NaOH and diethylpyrocarbonate (DEPC) treated ddH_20. Glassware was baked overnight at 150^0C, and plasticware/homogeniser autoclaved using an RNase removing cycle (121^0C for 30min).

Total RNA was isolated from mouse tissues using the Trizol method according to the manufactures instructions (Invitrogen). Briefly, tissue was homogenised

(PowerGen125, Fisher Scientific) in 1ml of Trizol reagent per 50-100mg of tissue. Homogenised sample was incubated for 5min at R/T and then 0.2ml of chloroform added per 1ml of Trizol reagent. Samples were shaken vigorously by hand for 15 seconds and then incubated at R/T for a further 3min. Samples were centrifuged at 12,000 x g for 15min at 4°C. The RNA containing upper aqueous phase was carefully removed. RNA was precipitated using isopropyl alcohol, washed with 70% ethanol, and stored under 70% ethanol at -80°C prior to use.

To assess RNA quality and quantity, RNA was separated using electrophoresis and visualised using ethidium bromide staining. The RNA pellet was spun at 7500g for 5min, the ethanol removed, and the pellet air dried for 10min. The pellet was then resuspended in an appropriate volume (based on expected yield) of DEPC-treated ddH_20 and incubated at 60°C for 10min. An electrophoresis tank was cleaned using 0.5% SDS, rinsed 3X with DEPC-treated ddH_2O, 1X 70% ethanol, and allowed to dry. 10µg of RNA was then denatured by heating to 70°C for 5min and then loaded onto an EtBr containing 1.5% agarose gel. The gel was run at 150V for 20-30 min.

2.1.15. Reverse-transcriptase PCR

First strand cDNA synthesis was performed using Superscript II Reverse Transcriptase (Invitrogen). The first-step of the reaction was set-up in a thin walled PCR tube:

OligodT primers (500µg/ml)	1µl
1µg of total RNA	xµl
dNTP (10mM each)	1µl
ddH_2O	up to 12µl

This mixture was incubated in a thermal cycler for 5min at 65°C, and then placed on ice for 2min. The following components were then added:

5X first-strand buffer	4µl
0.1M DTT	2µl
ddH_2O	1µl

The tubes were gently mixed by flicking, briefly centrifuged, and incubated for 2min at 42°C. 2µl of Superscript II was added to the tube, mixed by pipetting, and then incubated at 42°C for 50min. The mix was finally incubated at 70°C for 15min.

To amplify specific cDNA targets, a reaction was set-up as shown below:

cDNA	2µl
10X Buffer	5µl
dNTP (10mM)	1µl
Taq polymerase (Qiagen)	0.4µl
Gene specific primers (20µM)	1µl
ddH_2O	up to 50µl

The cycling parameters were: 1min @ 94°C, 35 cycles of (40sec @ 94°C, 40sec @ oligo specific temperature, 1min/kb @ 72°C), 5min @ 72°C. Products were visualised by electrophoresis on an EtBr containing agarose gel.

2.2. Yeast-two hybrid system

2.2.1. Media

Yeast Media Stock Solution:

100X Tryptophan (T)	4mg/ml	Filter sterilized
100X Uracil (U)	2mg/ml	
100X Leucine (L)	6mg/ml	
100X Histidine (H)	2mg/ml	

10X SD Dropout Mix (minus amino acids)		Autoclaved
20X Glucose (Glu)	40% w/v Glucose	
20X Galactose (Gal)	40% w/v Galactose	
20X Raffinose (Raf)	40% w/v Raffinose	
5X Yeast Nitrogen Base (YNB)	33.5g/L	
2X Yeast Nitrogen Base Agar	6.7g/L YNB	
	20g/L Agar	
	Up to 500ml ddH_20	

As with all the media above, YNB agar was brought to a 1X solution using SD Dropout Mix, an appropriate source of carbohydrate, and the relevant amino acids.

X-gal plates:

Plates were made as above accept for the addition of 1X BU Salts (1L 10X stock: 37g $Na_2 HPO_4$, 39g $NaH_2PO_4 \cdot H_20$, pH7.0, autoclaved) and X-gal to a concentration of 80mg/L. These plates were air dried under sterile conditions, foil wrapped, and stored at 4°C.

2.2.2. Glycerol Stock Storage of Yeast Strains

Yeast strains were grown overnight in 5ml of a selective media. Using a sterile cryogenic tube, 0.25ml of autoclaved 100% glycerol was added to 0.75ml of the overnight culture. The tube was then vortexed and placed at -80°C.

2.2.3. Small-Scale Yeast Transformation

A single colony was picked from a 2/3 day old plate and used to inoculate 5ml of appropriate media. This culture was grown overnight with shaking at 30°C. The overnight culture was used to inoculate 60ml of selective media to an OD_{600} of 0.1, which was then grown to an OD_{600} of 0.6-0.8. The cells were pelleted by centrifugation at 1500g for 5min, the supernatant removed, and pellet resuspended in 20ml of ddH_20. The cells were again spun at 1500g for 5min, the supernatant removed, and resuspended in 1ml of ddH_20. The cells were finally spun at 14,000rpm in a microcentrifuge and the supernatant completely removed. The cells were then resuspended in 300µl of TE/LiOAc (made immediately beforehand):

1 part 10X TE (100mM Tris pH7.5, 10mM EDTA, autoclaved)

1 part 10X LiOAc (1M Lithium Acetate, autoclaved)

8 parts ddH20 (autoclaved)

In a separate eppendorf tube, 100ng of the plasmid(s) to be transformed was added to 50µg of salmon carrier DNA. Then 100µl of the cell suspension was added to the tubes containing the DNA along with 300µl of TE/LiOAC/PEG (made immediately beforehand):

1 part 10X TE

1 part 10X LiOAc

8 parts PEG (50% w/v Polyethylene glycol-3350, autoclaved)

The DNA was mixed with the cells by gentle inversion, and then placed at 30°C for 30min. After this period, 70µl of dimethyl sulfoxide (DMSO) was added to the cells and they were heat-shocked in a water bath at 40-42°C for 15min. The cells were then put through 2 cycles of centrifugation and resuspension, 14,000rpm and 500µl of ddH_20, respectively. The cells were finally plated onto selective agar plates and incubated at 30°C for 3-4 days.

2.2.4. Library screening

A yeast-two hybrid screen of a rat brain cDNA library was conducted using the C-Domain of MAST4 as a bait (see Chapter 4). A 150ml culture (YNB(Glu)-HU) of EGY48 pre-transformed with pGilda-C-Domain and pSH18-34 was grown for 24hrs. This culture was diluted into 1L of YPD (20g Peptone, 10g Yeast Extract, 20g Glucose, up to 1L and autoclaved) to an OD_{600} of 0.3 (0.2-0.3) and grown to an OD_{600} of 1 in 5-6hrs. The culture was pelleted by centrifugation at 4550g for 20min. The supernatant was removed and the cells were resuspended in 500ml of TE and spun again at 4550g for 20min. The cells were washed by resuspension in TE/LiOAc, centrifugation at 4550g for 5min, and further resuspension in TE/LiOAc. The resuspended cells were then mix gently with 1mg of the library plasmid (pJG4-5 rat brain cDNA library) and 20mg of carrier DNA. Another 150ml of TE/LiOAc/PEG was added to the cell suspension and then the solution was left for 30min at 30°C (the tube was inverted every 5min). Following the addition of 17ml DMSO, the cells were heat-shocked for 15min at 40-42°C in a water bath (the tube was inverted every minute). The cells were then immediately placed on ice for 5min. In falcon tubes, the cells were washed twice by centrifugation and resuspension in 20ml of TE. Finally, 200µl of the resuspended cells was plated onto YNB(Glu)-HUT plates; a serial dilution was also made to assess the transformation efficiency.

The plates were incubated for 3 days at 30°C prior to harvesting; this was achieved by pre-chilling the plates in a cold room for 1hr (to harden the plates) and then scrapping the cells off the agar after pipetting 2X 2ml of ddH_20 onto the plates. The cells were collected in a 50ml tube and then centrifuged at 4550g for 5min. The supernatant was removed and the cells resuspended in sterile 50% glycerol equal to half the volume of the cell pellet. The resuspended cells were divided into 1ml aliquots and stored at -80°C.

2.2.5. Calculating the Number of Viable Cells

1ml aliquot of frozen transformants was thawed on ice and diluted into 10ml of YNB(Gal)-HUT, and grown for 4hrs to induce the Gal1 promoter and fusion-protein expression. Serial dilutions were made using 200µl of the cell culture (1-10,000 fold) and then 200µl of each dilution was plated out onto YNB(Gal)-HUT plates. The plates

were incubated for 3 days at 30°C. The number of viable transformants was calculated to be $2x10^8$ cfu/ml.

2.2.6. A yeast-two hybrid screen to identify interacting proteins for MAST4

The transformation efficiency was calculated as 2.51×10^4 cfu/ug, which therefore represented 25×10^6 clones amplified. It is recommended that 5X the number of clones amplified should be used to screen for interacting proteins. Therefore, 1.25×10^8 clones was required, which would require 625µl of the transformed cells. Due to an error in calculating the number of viable cells 251µl was used, which therefore represented 2.5X less cells screened than recommended.

1 aliquot of transformants was allowed to thaw and then 251µl of this was diluted into 10ml of YNB(Gal)-HUT and grown for 4hrs at 30°C. After incubation, 15.2ml of ddH_2O was added to the culture and 200µl was plated onto 125 YNB(Gal)-HUTL X-gal plates. Serial dilutions were also made and plated onto YNB(Gal)-HUT plates. Colonies were picked onto back-up YNB(Glu)-HUT plates at days 5, 8, and 14. These colonies were taken through 3 rounds of selection by streaking onto YNB(Gal)-HUTL X-gal plates. Colonies still exhibiting reporter gene expression were prioritized by simultaneously picking onto YNB(Gal)-HUTL X-gal plates and classifying them as 24, 48, 72, 96, and >96hr colonies. This classification was based on the strength of the growth under leucine selection and intensity of blue colouration.

2.2.7. Characterisation and Cataloguing of Clones

Crude plasmid DNA preparations were made from the yeast colonies produced by the screen. The cDNA inserts within the library plasmid pJG4-5 were amplified using primers positioned either side of the multiple cloning site (5'-TFP and 3'-TFP). 2µl of the crude yeast DNA extract was used in the PCR reaction, which used Taq polymerase (Qiagen) and the cycling parameters:

94°C 1min, (94°C 15s, 52°C 30s, 72°C 4min)×30, 72°C 10min

5µl of the PCR reaction was analysed using agarose gel electrophoresis, and another 5µl was used for restriction digest with the enzyme HaeIII (Roche). The restriction digest profile of the various PCR products allowed the identification of unique clones. These were subsequently cleaned using Microclean (Microzone ltd) and sequenced

commercially (MWG biotech). Sequencing was performed using the 5'-TFP and 3'-TFP oligonucleotides.

2.2.8. Plasmid rescue from yeast

The crude plasmid preparation contains the prey, bait, and reporter plasmids. Therefore, to obtain the cDNA encoding the candidate interactors, it is necessary to isolate the pJG4-5 prey plasmid. This was achieved by transforming XL1-Blue electrocompetent cells with 5µl of the crude yeast DNA preparation. The transformed bacteria were spread onto LB agar plates containing ampicillin, 40µl of IPTG (100mM), and 40µl X-Gal (100mg/ml). The XL1-Blue strain of bacteria are deficient for LacZ expression, therefore, bacteria containing the pSH18-34 reporter plasmid will express the LacZ gene and attain the ability to metabolise X-Gal. These colonies can therefore be excluded on the basis of their blue colour. The remaining white colonies were picked and use to inoculate 2ml of LB(amp), which was grown overnight and used to make crude minipreps. The plasmid DNA from these preps was digested EcoRI/XhoI, which releases the cDNA clone.

2.2.9. Post-screen controls

To confirm the expression of reporter genes by the candidate interactions, purified prey plasmids were re-introduced into EGY48 containing the C-Domain bait construct and reporter plasmid.

To determine whether the prey plasmids were capable of transactivation, the purified prey plasmids were re-introduced into EGY48 containing the reporter plasmid.

2.2.10. Interaction of the MAST family with the mGluRs

Yeast (EGY48) containing the reporter construct pSH18-34 were transformed with each PDZ-Prey reporter construct (see Chapter 4) and plated onto -UTL YNB, and -UT X-Gal, plates to assay transactivation of the reporter genes.

Following the control experiments, yeast were transformed (small-scale transformation, section 2.2.3) with the C-tails of the mGluRs (see Chapter 4) subcloned into the vector pGilda. To assay expression of the reporter genes, transformed yeast were plated onto -HUTL X-Gal plates.

2.3. Histology

2.3.1. Sectioning of Rat Brains

Adult male (200-250g) Wistar rats were sacrificed by cervical dislocation and their brains rapidly removed using an autoclaved (121°C for 30min - RNA removing cycle) dissection kit. Prior to the removal of the rat brains, a glass beaker was placed within a bucket containing dry ice. A small amount of 2-methylbutane was then dispensed into the beaker and an autoclaved holder for the brains was placed into the beaker. Following removal of the brain, a small amount of Tissue Tek (Bayer Diagnostics) was dispensed into the holder, the brain placed onto it, and then the brain completely covered with more Tissue Tek. The arrangement of the holder within the beaker allowed the brain and Tissue Tek to freeze gradually. The holder was also designed so that the shape of the frozen Tissue Tek, that contained the brain, would easily identify the brains orientation. The frozen brains were then stored at -80°C until required.

Brains from rats exposed to electroshock evoked maximal seizure (EMS) was derived from the study of (French et al., 2001a). EMS was induced in adult male Sprague-Dawley rats, which were supplied by Charles River, UK. Animals were subjected to a maximal fixed current (60 mA, 0.3s, 50Hz sine wave) applied via corneal electrodes. This procedure induced hind limb tonic extensor seizure in all animals. A control group of animals was exposed to the same procedure, but without stimulation. Brains were removed 1hr and 4hrs post-EMS, frozen on dry ice, and stored at -80^{0}C.

Two hours prior to sectioning, the brains were placed into a cryostat (Leica, CM3050S) set to a chamber temperature of -16°C to -18°C. The brains were then mounted onto the cryostat and 12μM sections were cut using a fresh paintbrush to manipulate the sections. The sections were thaw mounted onto slides (SuperFrost Plus, Fischer), allowed to dry on a heat block for 3-5min, and then another section placed onto the same slide. During sectioning, the sections were stored within the chamber of the cryostat; afterwards, the sections were stored at -80°C.

The rat brains were sectioned in 3 orientations: longitudinal, sagittal, and coronal. While cutting, the sections were checked under a microscope to ensure target areas were reached; however, every 10th section was subsequently Nissl stained to determine exactly where the sectioning had occurred.

2.3.2. *In situ* hybridisation - Criteria for Probe Choice

The probes were 45mer oligonucleotides supplied by Eurogentec. They were checked for self-annealing and hairpin formation (Oligonucleotide Properties Calculator), and the specificity of the sequence determined using NCBI nucleotide-to-nucleotide BLAST searches (no homology to other transcripts >60%).

2.3.3. *In situ* hybridisation - Radioactive Labelling of Probes

Oligonucleotides in both the antisense and sense orientation were labelled for in situ hybridisation.

A typical labelling reaction consisted of:

20ng oligonucleotide

3µl 5X TdT Reaction Buffer (Roche)

1.25µl [alpha-^{35}S] dATP (Amersham, 1000Ci/mmol, 10mCi/ml)

1.5µl $CoCl_2$

1µl Terminal Transferase, TdT (Roche)

Water to a final volume of 15µl

The reaction was placed in a 37°C water bath for 1hr.

Following the reaction, the labelled oligonucleotides were purified using ProbeQuant G-50 Micro Columns (Amersham) according to the manufactures instructions. To assess the quality of the labelling reaction the counts/min (cpm) were measure before and after the purification of the oligonucleotide, total count and column count respectively. These values were then used to calculate the specific activity of the probe. The calculation is as follows:

Terms used in the calculation:

Percentage incorporation = Column count/Total count X 100

Total cpm incorporated = Column count X reaction volume/volume counted

Average number of bases added to each oligo = % incorporation/100 X molar ratio of nucleotide to oligo in the reaction

Amount of DNA synthesized = Average bases added X 330(average mol. weight of base) X pmol of oligo present in the reaction

$$\text{Specific Activity} = \frac{\text{Total cpm incorporated}}{\mu g \text{ DNA template} + \mu g \text{ of DNA synthesized}}$$

For example, the Total count for the oligo 'MQ antisense' was 647,000cpm and its Column count 290,466cpm. A 12µl reaction was set up that contained 12.5pmol of ^{35}S dATP and 20ng (1.37pmol) of oligonucleotide:

Percentage incorporation	= 290466/647849 X 100	= 45%
Total cpm incorporate	= 290466 X 6	= $1.7x10^6$
Average number of bases added to each oligo	= 45/100 X 10/1.37	= 3.3/oligo
Amount of DNA synthesized	= 3.3 X 330 X 1.37	= 1.5ng
Specific activity	= $1.7x10^6$ / 0.025	= $6.8x10^7$ cpm/µg

Typically, the specific activity was in the range $1x10^7$-$1x10^8$ cpm/µg.

2.3.4. *In situ* hybridisation - Prehybridisation

To preserve the tissue, and prepare it for the hybridisation protocol, the section were fixed, delipidated, acetylated, and dehydrated. All solutions were made using diethylpyrocarbonate (DEPC) treated ddH_20 and all reagents used were 'molecular biology grade' (i.e. RNAase free)

The sections were removed from the -80°C freezer, placed into a slide-box, and allowed to thaw for 10min. The slides were then placed into coplin jars and fixed with 50ml of chilled 4% paraformaldehyde (made in phosphate buffered saline, PBS, pH7.0) for 5min. The slides were then rinsed twice with PBS. For each coplin jar, 50ml of TEA/AA solution was made immediately prior to use:

0.7ml Triethanolamine, TEA

0.125ml Acetic anhydride, AA

49.75ml DEPC-treated ddH_20

The slides were immersed in the TEA/AA solution for 10min to allow positively charged amine acid groups within the section to become acetylated, which will

subsequently reduce non-specific binding. The TEA/AA solution was removed and the sections dehydrated with graded ethanol solutions:

70% ethanol for 1min, pour off

80% ethanol for 1min, pour off

95% ethanol for 2min, pour off

100% ethanol for 1min, pour off

The sections were then delipidated with 50ml of chloroform for 5min. The sections were again dehydrated with 100% ethanol for 1min, followed by 95% ethanol for 1min. Finally, the sections were placed upright in a slide holder and left to air dry.

2.3.5. *In situ* hybridisation - Hybridisation

An incubator was pre-heated to 42°C and the hybridisation buffer placed within it to reach temperature. The hybridisation buffer contained:

50% Formamide

4X SSC (20X stock: 175.3g NaCl, 88.2g Sodium Citrate, up to 1L with DEPC-dd$H_2$0)

10% Dextran Sulphate

5X Denhardt's solution (100X Stock: 20g Ficoll, 20g Polyvinylpyrolidone, and 20ng Bovine Serum Albumin, up to 1L with DEPC-dd$H_2$0)

200micrograms/ml sheared salmon sperm DNA

100micrograms/ml long-chain polyadenylic acid

25mM Sodium phosphate (pH 7)

1mM Sodium pyrophosphate

* 20microL/ml of 1M DTT should be added to the hybridisation buffer prior to use.

A pencil was used to mark each slide with the probe, or control, used (see Chapter 3) Then 2-3µl of labelled probe (≈200,000cpm/100µl of buffer) was added to 100µl of hybridisation buffer and vortexed to mix. A 1000-fold excess of unlabelled probe was also included as a control where necessary. For each slide, 100µl of probe containing buffer was pipetted onto each slide (≈50µl per section) and gently covered with a parafilm coverslip using forceps - care was taken to ensure that the buffer was evenly spread over the section and that there were no air bubbles present in the buffer. Tissues saturated with 50% formamide and 4X SSC were placed into an appropriate box and the slides placed onto the tissue. The box was then sealed with parafilm and placed into the 42°C incubator overnight.

2.3.6. *In situ* hybridisation - Washing the sections after hybridisation

An incubator was set to 55°C and used to pre-heat 500ml of 1X SSC. The slides were transferred to a rack and then lowered into a bath of room temperature 1X SSC. After a few minutes, the parafilm coverslips were gently teased off the slides. The slides were then transferred to the 55°C bath of 1X SSC and left for 30min. Following this initial wash the sections were rinsed with room temperature 1X SSC for 1min, and then treated with a higher stringency 5min wash with 0.1X SSC. The sections were then dehydrated with 70% ethanol for 1min, followed by 95% ethanol for another 1min. Finally, the sections were left to dry for 30min before detecting the signal.

2.3.7. *In situ* hybridisation - Film autoradiography

The slides were first fixed to the bottom of a cassette using tape. The dull, emulsion covered side of the film was then placed face down onto the slides. The cassette was firmly closed, wrapped in a black plastic bag, and left at room temperature. The period of exposure depended on the strength of the signal, which itself depended on the abundance of the target mRNA and the specific activity of the probe used. The exposure time varied between 2-8 weeks (as indicated in the respective figure legends, Chapter 3).

2.3.8. *In situ* hybridisation - Emulsion autoradiography

Emulsion autoradiography involves covering labelled sections with a thin layer of autoradiographic emulsion. Post-staining of sections can therefore allow the identification of silver granules over specific cell types.

A light box fitted with a Kodak SafeLight No.1 filter was used throughout the procedure. This light source was kept away from the bench, and where practical, was either covered with Blue Roll or switched off to minimise the light intensity. 25ml of distilled water, plus one drop of glycerol, was warmed to 42°C in a 50ml falcon tube. Shreds of emulsion were added to the water to bring the solution up to 45ml and the solution warmed to 42°C to melt the emulsion. The solution was stirred manually a few times to mix while being careful not to produced any air bubbles. The solution was decanted into a pre-warmed coplin jar and each slide dipped into the solution. The back of the slides was wiped clean and the slide then placed onto a metal sheet, which had

been placed onto some ice. The slides were then left to dry for 10min. The slides were then taken off the metal sheet placed into slide holders and left to air dry in total darkness for >2hrs. Slides were then place in light proof slide boxes and kept at 4°C until ready for developing (3-5 fold the exposure time for film autoradiography).

In preparation, the slides were removed from the fridge and allowed to equilibrate to room temperature; Kodak D19 developer was diluted 1:1 with distilled water and Ilford Hypam fixer was diluted 1:4 with distilled water. Under the same safelight conditions as before, the slides were transferred to metal racks and placed into developer for 6min. The slides were then rinsed in distilled water and placed into fixer for 4min. The slides were then rinsed 2X in distilled water and left to air dry.

Sections were post-stained using cresyl violet (Section 2.3.9) for 1-2min.

2.3.9. *In situ* hybridisation - analysis and statistics

Autoradiographs were scanned using a Epson Perfection 4870. Analysis of the images was conducted using the programme ImageJ (NIH) and statistical analysis performed using SigmaStat. To analysis the activity-dependent expression of MAST4 (Chapter 3), the integrated density for the dentate gyrus was measured for each condition and normalised by reference to the cerebral cortex in each case. A Students t-Test was used to determine the statistical difference between each condition.

2.3.10. Cresyl violet staining of sections

Nissl staining of brain sections was routinely performed to visualise histological features. The protocol is as follows:

Fix in 10% formalin at 4°C	2min
Wash 2X in ddH^20	3min each
ddH_2O + acetic acid	3min.
0.25% cresyl violet (pH3.3)	10min
Wash in ddH_2O + acetic acid	5-10 seconds
70% ethanol	5-10 seconds
80% ethanol	5-10 seconds
95% ethanol	5-10 seconds
100% ethanol 1	30 seconds
100% ethanol 2	1min

Xylene I	3min (check under microscope)
Xylene 2	3min

Sections were then coverslipped using DPX mounting medium (RA Lamb).

2.4. Cell culture

2.4.1. Cell lines

HEK293 - Human embryonic kidney cells (ECACC No. 05030204). Epithelial cell line.

2.4.2. Culture conditions

Cells were routinely cultured in Dulbecco's Modified Eagles Medium (DMEM), which was supplemented with 10% (v/v) Fetal Bovine Serum (FBS) and Penicillin/Streptomycin (100U/ml). Cells were incubated at 37°C at 5% CO_2. Prior to, and during, transfections cells were culture in Opti-MEM reduced serum medium (Gibco). 25cm^2 flasks were used for routine culturing of cells.

2.4.3. Passaging cells

Cells were passaged when they reached 90% confluency. Media was removed and the cells washed with 2ml of PSA (150mM NaCl, 5mM KCl, 4mM $NaHCO_3$, 7mM Glucose, 100µM $CaCl_2$). 1ml of trypsin/versin solution was added and the cells left at R/T for 1min or until the cells had detached. 5ml of growth media was added to the cells and 50µl of this solution was added to a 25cm^2 flask containing pre-warmed media.

2.4.2. Storage of cells in liquid nitrogen

For a 25cm^2 flask, media was removed and cells were washed with 2ml of PSA. 1ml of versene/trypsin was added and the cells incubated at 370C for 1min or until cells had detached. Cells were then resuspended in 5ml of media and spun at 425g for 5min. Cells were resuspended in 5ml of DMEM supplemented with 10% serum and 10%

DMSO. 1ml of the resuspended cells was pipetted into a cryotube and placed into a polystyrene box; this was then placed in a -80^{0}C freezer for 3hrs before the cells were placed in liquid nitrogen.

To recover cells, an aliquot of cells was placed in a 37^{0}C water bath to rapidly thaw the cells. The cell solution was then pipetted into 5ml of media and the cells pelleted using a spin at 425g for 5min. Cells were then resuspended in 5ml of media and pipetted into a 25cm^2 flask.

2.4.4. Poly-L-lysine coated coverslips

When necessary, coverslips were coated in poly-l-lysine to improve attachment of cells. Poly-L-lysine (PLL) was dissolved in sterile ddH^2O to a concentration of 10µg/ml. Autoclaved coverslips were incubated in the PLL solution for 1hr at 37°C, washed 3X in sterile ddH_2O, and then dipped in 100% ethanol. The PLL coated coverslips were allowed to air dry prior to use.

2.4.5. Transfection

Lipofectamine 2000 (Invitrogen) was used to transfect cells with plasmid DNA constructs according to the manufactures instructions. Briefly, cells were passaged 24-36hrs prior to transfection. Prior to transfection, the media was changed to Opti-MEM reduced serum medium. DNA to be transfected was diluted in Opti-MEM and mixed gently by flicking the tube. Lipofectamine 2000 was gently mixed prior to use and an appropriate volume (2:1 DNA:Lipofectamine) diluted with Opti-MEM. The lipofectamine/Opt-MEM solution was incubated at R/T for 5min and then combined with the diluted DNA. This solution was incubated at R/T for 20min. The DNA-lipofectamine solution was then added to the cells, which were incubated at 37°C and 5% CO_2. After 5-6hrs the medium was changed to the standard culture medium (i.e. DMEM + FBS + antibiotics). Transgene expression was assessed after 18-48hrs.

2.4.6. Collection of cells

Cells were collected for western blotting. Media was removed from the cells, which were then washed X2 using cold 1X PBS. Then an appropriate volume (e.g. 500µl if using a 6well plate) of ice cold 1X PBS containing protease inhibitor (Complete, Roche) was added. A small volume of liquid nitrogen was dispensed onto the cells,

which were then allowed to thaw before being removed by a cell scraper. Collected cells were stored at -20°C prior to use.

2.5. Immunocytochemistry on cultured cells

Following transfection, cells were left for 24-48hrs before processing. The media was removed and the cells washed 3X with PBS. The cells were then fixed with 500µl of ice cold 4% (w/v) paraformaldehyde (PFA) for 10min. The PFA was removed and then quenched using 2X washes with ammonium chloride dissolved in PBS. Cells were washed a further 3X with PBS. The cells were permeabilised using 0.1% TX-100 in PBS for 10min.

Non-specific binding was blocked by incubation with 5% normal sera in PBS + 3% BSA. The primary antibody was diluted in PBS + 3% BSA and incubated with the cells for 90min at R/T. The cells were then washed 3X in PBS, and the secondary antibody applied for 60min. The cells were washed 3X before being mounted onto slides using Vectashield mounting medium (Vector labs), which also contained 4'-6-Diamidino-2-phenylindole (DAPI) for nuclei staining.

2.5.1. Antibodies used for immunocytochemistry

Antibody	Raised in	Dilution	Supplier
Anti-Flag	Rabbit	1:250	Sigma
Anti-GFP	Rabbit	1:500	BD Biosciences
Alex633 conjugate (anti-rabbit)	Goat	1:500	Molecular probes

Table 2.4. Antibodies used for immunocytochemistry.

2.6. Image capture and analysis

Heterologous expression of fluorophore tagged fusion proteins:

Images were obtained using a Nikon Eclipse E800 upright microscope using a 60X oil immersion objective. The parameters for the filter sets are described below (Table 2.5).

Flourophore	Excitation (nm)	LP (nm)
eGFP	460-500	510
mRFP	510-560	590
DAPI	330-380	420

Table 2.5. Fluorophores used and settings for detection.

Figure 2.1 below illustrates the degree of separation between the two fluorophores eGFP and mRFP. Due to the potential for bleed-through using the filter sets described in Table 2.1 and these two fluorophores the preparations were visually checked for the presence of combined (i.e. yellow) signals. Image analysis and scale bar addition was performed using the programme MetaMorph.

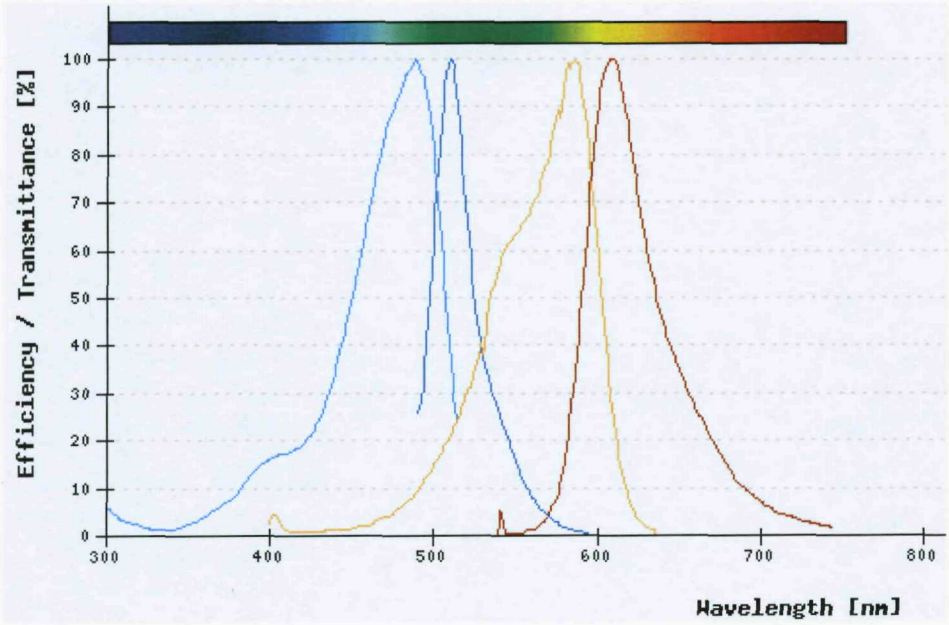

Figure 2.1. Degree of separation between the fluorophores eGFP and mRFP. Light-blue = eGFP excitation; dark-blue = eGFP = emission; light-brown = mRFP excitation; dark-brown = mRFP emission.

The transfection efficiency was typically >70%, which therefore allowed a large pool of transfected cells to be screened for the characteristic expression patterns for each

construct. The images illustrated in Chapter 6 are from a single transfection where at least 3 representative images were collected which reflected the patterns of expression observed for each individual transfection.

Emulsion autoradiography:

Images were obtained using a Zeiss Axioplan 2 using a 60X oil immersion objective. Images were also obtained with a Zeiss Axiovert using 5X and 40X objectives.

For each MAST family member tested, the antisense probe and two controls (see Chapter 3) was conducted using 1 slide (containing two sagittal sections) for each condition. Representative images were collected for the patterns of staining observed.

2.7. Biochemical Techniques

2.7.1. SDS-Polyacrylamide Gel Electrophoresis (SDS-PAGE)

The BioRad mini Protean II gel system was used for casting and running SDS-Page gels. The amounts of each reagent used to make the resolving and stacking gels is described in Table 2.5, below.

	Resolving Gel Strength (% Acrylamide)				Stacking
	15 12-43kDa	**10** 16-68kDa	**7.5** 36-94kDa	**5** 57-212kDa	
30% Acrylamide	5ml	3.3ml	2.5	1.7ml	5ml of stacker solution (0.01M Tris HCl (pH 6.8), 5% Acrylamide, 0.1% SDS)
Tris 3M (pH 8.8)	1.25ml	1.25ml	1.25ml	1.25ml	
SDS 10%	100µl	100µl	100µl	100µl	
APS 10%	50µl	50µl	50µl	50µl	50µl
ddH20	....top up to 10ml....				/
TEMED	10µl	10µl	10µl	10µl	10µl

Table 2.5 Amounts of reagents used to make SDS-PAGE gels. APS = ammonium persulphate, TEMED = N,N,N',N'-tetramethyl-ethylenediamine.

TEMED was added to the separating gel immediately prior to pouring, which was then overlaid with water and allowed to set. When the gel had set, the water was removed,

TEMED added to the stacking gel, and this was poured onto the separating gel. A comb was then placed into the stacking gel and it was left to set.

The gels were placed in the gel tank, which was filled with 1X Laemmli buffer (25mM Tris pH8.3, 192mM Glycine, 0.1% SDS). The samples were loaded into the well of the gel using a 50µl Hammilton syringe. A molecular weight marker (BioRad, Precision Plus Dual Color) was also included to determine the protein sizes. The gels were run at 30mA until the samples had run through the stacking gel, and then at 45mA per pair of gels.

2.7.2. Coomasie Staining

Gels were soaked overnight in Coomasie stain (Sigma). The gels were then soaked in destain (45% ddH_20, 45% Methanol, 10% Glacial acetic acid) until the protein bands became visible. Images of the gel were captured using an Alpha imager attached to a trans-illuminator.

2.7.3. Western blot

Western blotting was used to transfer proteins onto nitrocellulose membranes. Following electrophoresis, the gel was placed against a nitrocellulose membrane that had been pre-soaked in 1X Laemmli buffer containing 20% (v/v) methanol (transfer buffer). This was then sandwiched between 2 sheets of pre-soaked filter paper (Whatman 3mmm chromatography paper) and a sponge either side. The sandwich was then placed into the blotting tank the gel facing the negative side and the membrane the positive side. The tank was filled with transfer buffer and the proteins blotted overnight using 30V at 4°C. A magnetic stirrer was used to ensure circulation of the buffer.

Transfer of proteins was routinely confirmed using Ponceau S staining. The membranes were soaked in Ponceau S solution (2% Ponceau S, 3% tri-chloro acetic acid) for 15min and destained in dH_2O. The position of molecular weight markers was marked using a black biro.

The nitrocellulose membranes were incubated for 1hr in blocking buffer (Tris buffered saline (TBS, 25mM Tris, 0.15M NaCl, pH7.2) + 3% (w/v) BSA + 0.5% (v/v) Tween-20) to reduce non-specific binding. The membrane was then incubated with the primary antibody (diluted in blocking buffer) for 1-2hrs. Following this, the membrane was washed 3X for 5min in TBS Tween (TBS + 0.5% (v/v) Tween-20). The membrane was

then incubated for 1hr with the secondary antibody (horseradish peroxidase conjugated), which was diluted in blocking buffer. The membrane was again washed 3X for 5min in TBS Tween. The location of the secondary antibody was detected using an enhanced chemiluminescence kit (ECL, Amersham). Chemiluminescence was detected using BIOMAX light film (Kodak) and developed using an X-ograph automatic developer.

2.7.3.1 Antibodies used for western blotting

Antibody	Raised in	Dilution	Supplier
Anti-Flag	Rabbit	1:250	Sigma
Anti-GFP	Rabbit	1:500	BD Biosciences
Anti-rabbit horseradish peroxidase conjugate	Goat	1:10000	Jackson

Table 2.6. Antibodies used for western blotting.

2.7.4. Purification of his-tagged fusion proteins

2.7.4.1. Small-scale purification under denaturing conditions

Two protocols were used. The first involved using 8M urea as the denaturant:

An overnight culture was used to inoculate 50ml of LB to OD_{600} 0.1, which was then grown to an OD_{600} of 0.5-0.7. The culture was incubated with 1mM IPTG (Isopropyl-β-D-thiogalactopyranoside) for 3-4hrs, and then the cells pelleted with a 5min spin at 4550g. The cells were resuspended in 5ml of Buffer B (100mM NaH_2PO_4, 10mM Tris·Cl, 8 M urea, pH 8.0 prior to use) and put on a stirrer for 1hr. The solution was then spun at 14,000rpm in a microcentrifuge for 10min to pellet the cellular debris. The supernatant was removed and a 400µl aliquot incubated with 20µl of 50% resin for 30min at room temperature. The resin was then pelleted with a 10sec spin at 14,000rpm in a microcentrifuge. The supernatant was carefully removed and the resin washed X2 with 200µl of Buffer C (As Buffer B, but pH6.3 prior to use). The proteins were then eluted twice with 32µl of Buffer E (As Buffer B, but pH4.5 prior to use), and once with 32µl of 1X SDS sample buffer (62.5mM Tris pH6.8, 2%SDS w/v, 10% Glycerol w/v, 5% β-mercaptoethanol, 0.001% Bromophenol Blue w/v).

The 2nd protocol involved using guanidine hydrochloride as the denaturant:
An overnight culture was used to inoculate 5ml of fresh media to an OD of 0.1, which was then grown to mid-exponential phase. The culture was incubated with 1mM IPTG for 3-4hrs. The cells were first pelleted and then resuspended in lysis buffer (100mM NaH_2PO_4, 10mM Tris-Cl, 6M Guanidine hydrochloride, pH 8). The cells were gently vortexed until the solution became translucent. The solution was then spun for 10min in a microcentrifuge at 14,000rpm. The supernatant was then incubated with 50µl of 50% NiNTA resin for 30min at R/T. The resin was pelleted and resuspended 2X with 250µl of Wash buffer (as above, but pH 6.3). Finally, the resin was pelleted and resuspended 3X in Elution buffer (as above, but pH 4.5).

2.7.4.2. Large-scale purification under denaturing conditions

An overnight culture was used to inoculate 1L of fresh media to an OD_{600} of 0.1, which was grown to mid-exponential phase. The cells were then incubated with 1mM IPTG for 3-4hrs. Using the buffer system from the first protocol of section 2.4.7.1, the cells were pelleted and resuspended in 10ml Buffer B. The solution of cells was spun on a stirrer until the solution became translucent, and then centrifuged at 10,000g for 30min to remove the cellular debris. The supernatant was incubated with 1ml of 50% NiNTA resin for 1hr at R/T prior to centrifugation at 4335g for 5min. The supernatant was carefully removed and then resin was then washed 3X with 10ml of Buffer C . Protein was then eluted from the resin 2X using 500µl of Buffer E (as above), and a final elution was done using 1X SDS sample buffer.

2.7.4.3. Column purification under denaturing conditions:

An overnight culture was used to inoculate 1L of LB to an OD_{600} of 0.1, which was grown to an OD_{600} of 0.5-0.7. The culture was then incubated with 1mM IPTG for 4-5hrs. The cells were pelleted with a 15min spin at 4550g, and then resuspended in 40ml Buffer B. The cells were stirred for 60min at room temperature before centrifugation at 14,000rpm for 10min to remove the cellular debris.
The binding capacity of NiNTA resin is ≈5-10mg/ml; therefore, an appropriate volume of resin was pipetted into a capped column. Using the buffer system from the first protocol of section 2.4.7.1, the resin was firstly equilibrated with about 5 column volumes of Buffer B. The flow rate through the column was then set to 1ml/min and the cleared lysate applied to the column. After the lysate had passed through the column,

the resin was washed with Buffer B until the A_{280} reached ≈0.01 (≈5-10 column volumes). The resin was then more stringently washed with Buffer C until the A_{280} again reached ≈0.01 (≈10 column volumes). Protein was then eluted from the resin with Buffer E until the A_{280} reached 0.01.

For each step samples were taken for analysis and then equivalently loaded onto a SDS-PAGE gel for analysis.

2.7.5. Assessing the solubility of proteins

The solubility of proteins was assessed using high-speed centrifugation. Firstly, a 50ml overnight culture of XL1-blue transformed with a his-tagged fusion protein was used to inoculate 500ml of fresh selective LB media. This was grown to mid-exponential phase and then incubated with 2mM IPTG for 4hrs. The cells were pelleted and then resuspended in pre-breaking buffer (20mM HEPES, 0.5M KCl, pH7.4). The cells were pelleted again and resuspended in breaking buffer (As above, plus: 1 tablet/50ml of Complete Protease Inhibitor, 2mM $MgCl_2$, 0.5mM ATP). The resuspended cells were then passed 3X through a French Press to lyse the cells. The broken cells were spun at 20,000g for 30min. The pellet (P1) was resuspended in 25ml of breaking buffer, and the supernatant spun at 100,000g for 1hr. The pellet (P2) was resuspended in 25ml of breaking buffer, which required sonication. Loading was normalised by volume and the samples were run on an SDS-PAGE gel for analysis.

2.7.6. Equivalent loading of samples for SDS-PAGE gels

The OD_{600} was measured for bacterial cultures before and after induction of fusion proteins. This therefore allowed the density of bacteria between each culture to be assayed, which was subsequently used to calculate a volume of culture that contained an equivalent amount of bacteria. Therefore, by using the same quantity of bacteria the relative amount of protein expression between different conditions could be determined. Typically, 1ml of non-induced culture was centrifuged at 14,000rpm in a microcentrifuge and the pellet resuspended in a 100µl loading buffer; then a volume that was equivalently less than the increase in absorbance was used to resuspend the induced culture (e.g. for a 2-fold increase in absorbance 50µl would be used to resuspend the induced culture).

2.8. Generation of Antisera against MAST4

As described in Appendix A, the C-domain of MAST4 was expressed as a His-tagged fusion protein and column purified using the method described in section 2.7.4.3. The purified C-domain of MAST4 was used as an antigen to raise antisera against MAST4. The immunisation was conducted by Eurogentec using the protocol described in Table 2.7 below. Two rabbits were immunised according to this protocol.

Week	Immunisation	Bleed
1	1st	Pre-immunisation
2		
3	Boost 1	
4		
5	Boost 2	
6		Small Bleed
7		
8		
9	Boost 3	
10		Large bleed

Table 2.7. Immunisation protocol using the purified C-domain of MAST4.

The detection of the antisera and its characterisation was conducted using western blotting and immunocytochemistry as described in Appendix A.

2.9. Procedure for electroshock-evoked maximal seizure

As previously described (Upton et al., 1997), electroshock evoked maximal seizures (EMS) was induced in adult male Sprague-Dawley rats, which were supplied by Charles River, UK. The experimental work was conducted in compliance with Home Office Guidance on the operation of the Animals (Scientific Procedures) Act 1986, and was approved by the SmithKline Beecham Procedures Review Panel. In brief, animals were subjected to a maximal fixed current (60 mA, 0.3s, 50Hz sine wave) applied via corneal electrodes. This procedure induced hind limb tonic extensor seizure in all animals. A control group of animals was exposed to the same procedure, but without stimulation. Brains were removed 1hr and 4hrs post-EMS, frozen on dry ice, and stored at -80^0C.

Brains used to confirm the activity-dependent expression of MAST4 were derived from the study by French et al (2001a).

Chapter 3 - Expression of the MAST family of serine/threonine kinases

3.1. Introduction

As discussed in Chapter 1, the restriction of signalling events within a specific time and place is necessary to control the specificity of signalling networks (Wong and Scott, 2004; Kim and Sheng, 2004). These networks are organised by modular scaffolding domains, such as the PDZ domain. It is therefore interesting that the MAST family of kinases have evolved to include a PDZ domain, and can therefore potentially scaffolding its own signalling capacity. The MAST family of kinases below to the AGC branch of the kinome, which includes kinases such as PKA and PKC (Manning et al., 2002). The nearest phylogenetic neighbours of the MAST family include the nuclear Dbf2-related (NDR) family of kinase, which itself includes the large tumour suppressor (LATS) kinases (Reviewed in Tamaskovic et al., 2003). These kinases have been implicated in multiple aspects of cell division and morphogenesis, including regulation of the cytoskeletal network as well proliferation and survival of cells (Reviewed in Tamaskovic et al., 2003). Further along the same branch of the kinome that contains the NDR family, is the Rho-activated kinases, which include Rho-kinase (ROCK) (Manning et al., 2002). This kinase has also been implicated in the control of cell morphology; for example, by regulating inhibition of axonal growth following activation of Rho GTPases (Reviewed in Kubo et al., 2007).

Interestingly, the association with the cytoskeleton and a possible role in regulating cell morphology has been conserved for at least one member of the MAST family, namely MAST2 (Walden and Cowan, 1993; Walden and Millette, 1996). As described in Chapter 1, MAST2 has been shown to bind microtubules and appears to play a role in spermatid maturation (Walden and Millette, 1996). In the context of brain function, the association with the cytoskeleton appears to have been conserved for MAST1 & 2; however, these kinases have also been found to localise to protein complexes (UPAC/DAPC, Chapter 1) associated with membrane specialisations such as the synapse, as well as interact with metabotropic glutamate receptors {Lumeng, 1999 85 /id /pt "Pilkington BJ, PhD thesis; "}.

As described in Chapter 1, a functional role has been established for the kinase and PDZ domain of certain MAST family members in a variety of biological contexts. For example, MAST1-3 have been shown to interact with the tumour suppressor protein PTEN, which is also a substrate for their kinase domains (Valiente et al., 2005). MAST2 has been shown to play an important role in the production of IL-12 following

a LPS challenge, and both MAST1 & 2 have been found interact with syntrophins in the UAPC/DAPC (Xiong et al., 2004; Lumeng et al., 1999).

Taken together, the data described above suggest that the MAST kinase family have a broad role in a variety of biological contexts, which include multiple roles throughout the cell. In the context of brain function, MAST family members have been shown to localise to the nucleus as well as the plasma membrane (Yano et al., 2003; Lumeng et al., 1999). Interestingly, the expression of one member, MAST4, has been shown to be dynamically regulated by synaptic activity (French et al., 2001b), which suggests that this member may contribute the function of one or both of these subcompartments during plasticity.

The domain structure of the MAST family confers a utility that is evident by the conservation of these kinases from C.elegans to man. However, this branch of the kinome is relatively understudied. In particular, a full characterisation of the MAST family has not yet been conducted across multiple tissues and in brain.

Therefore, the expression patterns for the MAST family have been investigated across multiple tissues using reverse-transcriptase PCR and northern blotting. Four members, MAST1-4, were shown to be expressed in brain; therefore, *in situ* hybridisation has been used to clarify where these members are expressed in rat brain.

The expression patterns observed reflect the diverse roles attributed to this family and suggest that these MAST family have both distinct and overlapping functions within various tissues, and the CNS.

3.2. Results

3.2.1. Sequence Analysis

The percentage homology between the MAST family and their phylogenetic relationship can be investigated using sequence analysis (Table 3.1 and Fig 3.1). Table 3.1 illustrates the degree of homology between different regions of MAST1-4. MAST-like is distantly related to these members and does not contain a PDZ domain; therefore, its has not been included in this analysis. Interestingly, certain regions outside of the identifiable domains show a relatively high degree of homology; for example, the region N-terminal of the kinase domain shows a mean homology between MAST1-4 of >63%, which in some cases is as high as 70% (MAST1 vs MAST2); this region has been found to undergo polyubiquitination in MAST2 (Xiong et al., 2004). Similarly the region between the kinase and PDZ domains of MAST1-4 is noticeably well conserved between MAST1 and MAST2 compared to these members and the others; this region has been found to mediate microtubule-binding in MAST1 & 2 (Walden and Cowan, 1993; Lumeng et al., 1999). In contrast, sequence C-terminal to the PDZ domain for MAST1-4 is poorly conserved. A clear trend in Table 3.1 is that the regions/domains of MAST1-4 appear to have diverged independently of each other; this feature is illustrated in Figure 3.1, which shows the phylogenetic relationship between the MAST family and their identifiable domains.

Combo	N terminal	Kinase	Inter PDZ-Kinase	PDZ	C-terminal
M1 vs M2	70	90	50	81	35
M1 vs M3	62	88	32	77	42
M1 vs M4	66	89	35	75	43
M2 vs M3	59	87	32	77	53
M2 vs M4	69	90	37	76	36
M3 vs M4	57	88	31	78	44

Table 3.1. Percentage identity between domains/regions of MAST1-4. The kinase, PDZ and N-terminal region of MAST1-4 are relatively well conserved. The microtubule-binding region encompassed by the 'inter PDZ-kinase' region is noticeable well conserved between MAST1 & 2. The C-terminal region of the MAST family appears more variable between the members.

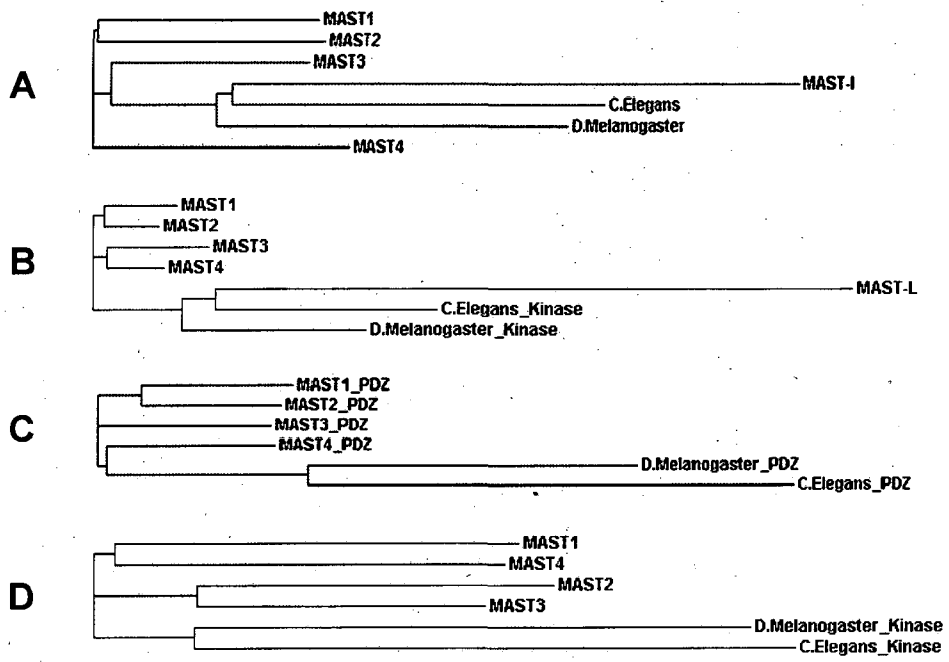

Figure 3.4 Phylograms for the MAST family of serine/threonine kinases. The phylogenetic relationship is indicated between the open reading frame (A), kinase (B), PDZ domains (C) and C-domain (D). The homology within the ORF and individual domains is not consistent across the family; for example, MAST1 & 2 show the highest degree of homology within their PDZ domain, but this is not the case for their kinase domains.

3.2.2. Multiple tissue analysis of MAST family expression.

The expression of the MAST family across multiple tissues has been examined using reverse-transcriptase polymerase chain reaction and northern blot analysis (Fig. 3.5). The amplicons generated for the RT-PCR analysis consisted of the PDZ domains of MAST1, 2 & 4, and regions of MAST3 and MAST-L as illustrated in Figure 3.5. For the northern blot analysis, the sequenced amplicons for MAST3 & MAST-L were used, plus digested fragments of MAST1, 2 and 4, as illustrated in Figure 3.5 and listed in Table 2.5 (Chapter 2).

RT-PCR analysis revealed both overlapping and distinct expression patterns (Fig 3.5A). For example, MAST1 and 2 are expressed in the same tissues, while MAST3 shows the strongest expression in brain and MAST-like is almost exclusively expressed in the testis.

The expression of the MAST family in multiple mouse tissues was confirmed using a poly(A) RNA northern blots purchased from Clonetech (Fig 3.5B). Using a rat poly(A) RNA northern blot, cDNA probes against MAST1 and MAST2 revealed bands at 5.2kb and 5.5kb, respectively. In contrast to the RT-PCR analysis, MAST1 appeared to be exclusively expressed in brain, although MAST2 was also detected in this tissue as well

as heart, kidney and testes. A specific band within the size range for full-length MAST4 was not detected using a single MAST4 cDNA probe.

Subsequently, a mouse poly(A) RNA northern blot (Clontech) was purchased and used to investigate expression of MAST3, 4 and MAST-like (Figure 3.6B) . A signal was not detected for MAST4 using two separate probes simultaneously, and a signal for MAST-L was also not detected. Using the MAST3 amplicon derived from the RT-PCR, an isolated signal was detected in the range of 6kb exclusively in brain. Following control experiments this blot was considered poor quality (i.e. poor signal for β-actin). Therefore, another mouse poly(A) RNA northern blot was obtained from Clontech, which yielded the same result as previously observed.

A signal for MAST4 and MAST-like was not detected using northern blots, which may reflect reduced sensitivity of northern blots compared to RT-PCR. Also, the production of standard northern blots can lead to poor recovery/transfer of large transcripts, which may have affected the detection of MAST4

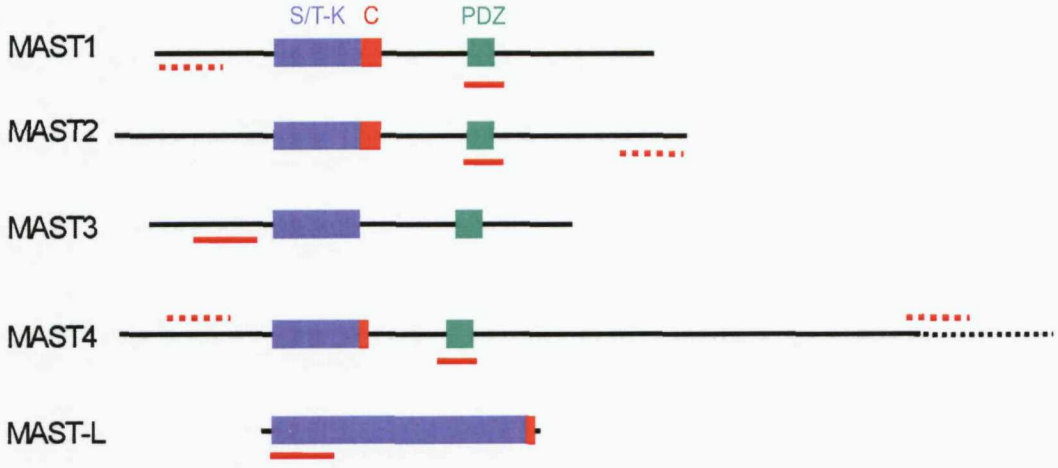

Figure 3.5. RT-PCR amplicons and northern probes used for MAST family multiple tissue expression analysis. Solid red bars indicate regions amplified by PCR for the RT-PCR. Dashed red bars indicate regions released from cDNA clones by restriction endonuclease. These regions, plus the amplicons for MAST3 & MAST-L, were used as probes for northern blot analysis. For MAST4 two northern probes were used, one of which partly covered the 3'-untranslated region (dashed black line). Blue (S/T-K) = kinase domain; Red (C) = extension to kinase domain; Green = PDZ domain.

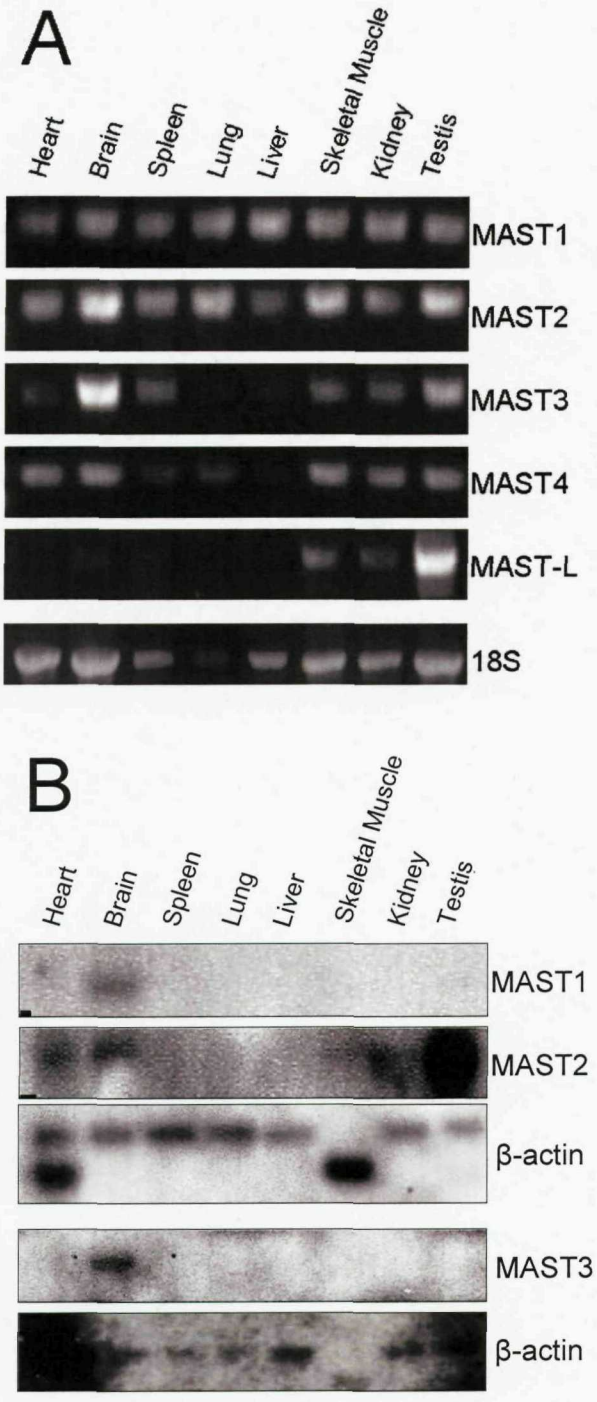

Figure 3.6. Multiple tissue analysis of MAST family expression.

(A) cDNA was generated from total RNA extracted from various mouse tissues. Non-homologous regions of each MAST family member where amplified using PCR. MAST1 and 2 are expressed in the same tissues, while MAST3 shows the strongest expression in brain and MAST-like is almost exclusively expressed in the testis. Loading and integrity of RNA was checked by amplification of 18S ribosomal RNA.

(B) ^{32}P labelled cDNA probes for MAST 1 & 2 were hybridised to a rat poly(A) northern blots, and a MAST3 probe to a mouse poly(A) northern blot. All three members show expression in brain: MAST1 (5.2kb), MAST2 (5.5kb), MAST3 (≈6kb)

3.2.3. In Situ Hybridisation

The positions of the probes for each MAST family member were (based on the cDNA clones listed in Table 2.4 of Chapter 2):

MAST1 = 63-107

MAST2 = 591-635

MAST3 = 3361-3405

MAST4 = 6372-6416

MAST-L = 2521-2565

These positions are illustrated by Figure 3.7., below

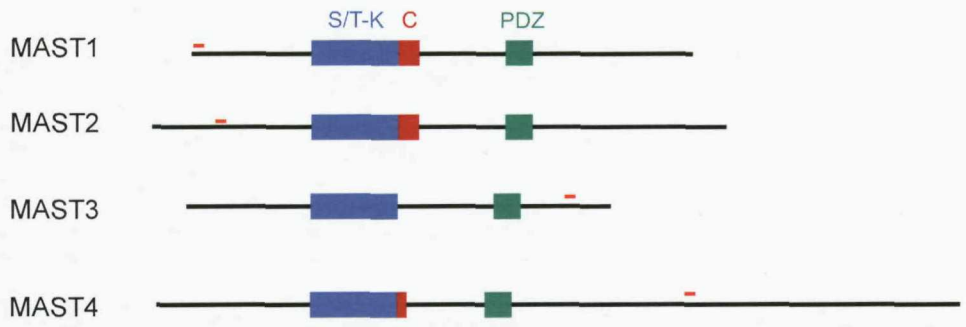

Figure 3.7. The position of *in situ* hybridisation probes within each member of the MAST family. The red bars indicate the position of each probe. MAST-L consists predominantly of a kinase domain, which has high homology to the kinase domain in the MAST family and other proteins. Therefore a probe for MAST-L was designed using the 3' untranslated region, which is indicated by the dashed line. Blue region (S/T-K) = kinase domain; Red region (C) = extension to kinase domain; Green region = PDZ domain.

To fully characterise the expression of each family member, rat brains were sectioned in three orientations: longitudinal, sagittal, and coronal (section 2.3.1). The probes described above were labelled, hybridised to the fixed rat brain sections, and detected using the method described in Chapter 2. The results for this set of experiments are described in the following section.

3.2.3.1. Film Autoradiography - anatomical expression

Figure 3.8 through to 3.16 show images taken of sections in three orientations and labelled with probes for MAST1, 2, 3, and 4. A signal for MAST-L was not detected using this technique. All images shown are derived from autoradiographic film that was

exposed to labelled sections for 7 weeks; also, sections were hybridised with equal amounts of equivalently labelled probes. Therefore, this allows for relative differences in expression levels to be assessed. Figures 3.8 to 3.16 show labelled images followed by the raw data. In situ experiments investigating the expression of MAST1, 2, and 4 were repeated 3X, and those investigating MAST3 and MAST-l expression 2X. Each run of experiments labelled two sections per condition.

The MAST family was found to be expressed in a variety of brain regions - this data is summarised in Table 3.2, below.

	MAST1		MAST2		MAST3		MAST4	
Structure	Rat	Mouse (Brain Atlas)	Rat	Mouse (Brain Atlas)	Rat	Mouse (Brain Atlas)	Rat	Mouse (Brain Atlas)
Hippocampus	++	++	++	++	+++	+++	+	-
Cortex	+	+	+	+	+++	+++	-	-
Cerebellum	++	++	++	++	-	-	++	-
3rd Ventricle	+	-	++	-	-	-	++	-
Striatum	-	-	-	-	+++	++	-	-
White Matter	-	-	-	-	-	-	++	-

Table 3.2. Brain structures showing expression of MAST family members. The members of the MAST family appear to show both distinct and overlapping expression in the brain. For comparison, the expression patterns documented by the Allen Brain Atlas are shown (see discussion). Relative expression levels have been indicated.

The hippocampus was labelled by probes for MAST1, 2, 3, and 4. These family members also labelled the cortex; however, the labelling for MAST3 was stronger in the upper layers of the cortex.

Probes for MAST1, 2, 4 produced a signal in the cerebellum. MAST1 and 2 appear to be expressed in the cellular layers of the cerebellum (Purkinje and/or granule cells). MAST4 may also be expressed in these layers, but this family member is more clearly expressed in the white matter of the cerebellum.

MAST1, 2, and 4 are expressed in the 3rd ventricle (see discussion) and MAST3 is expressed in the striatum.

A probe for MAST4 labelled multiple white matter containing structures, which are listed in Table 3.3, below.

Structure	Function
Corpus Callosum (cc)	Links hemispheres
Forceps minor of the corpus callosum (fmi)	Links hemispheres
Forceps major of the corpus callosum (fmj)	Links hemispheres
Internal capsule (ic)	Connects thalamus and cortex
External capsule (ec)	Connects putamen and claustrum
Dorsal hippocampal commissure (dhc)	Connects hippocampi
Ventral hippocampal commissure (vhc)	Connects hippocampi
Alveus of the hippocampus (alv)	Thin layer of fibres that coalesce to form fimbria
Fimbria (fi)	Major output pathwayof hippocampus
Cingulum (cg)	Connects cingulate gyrus to entorhinal cortex

Table 3.3. White matter containing brain structures labelled by a MAST4 specific probe. The regions listed above were identified using Paxinos (2007).

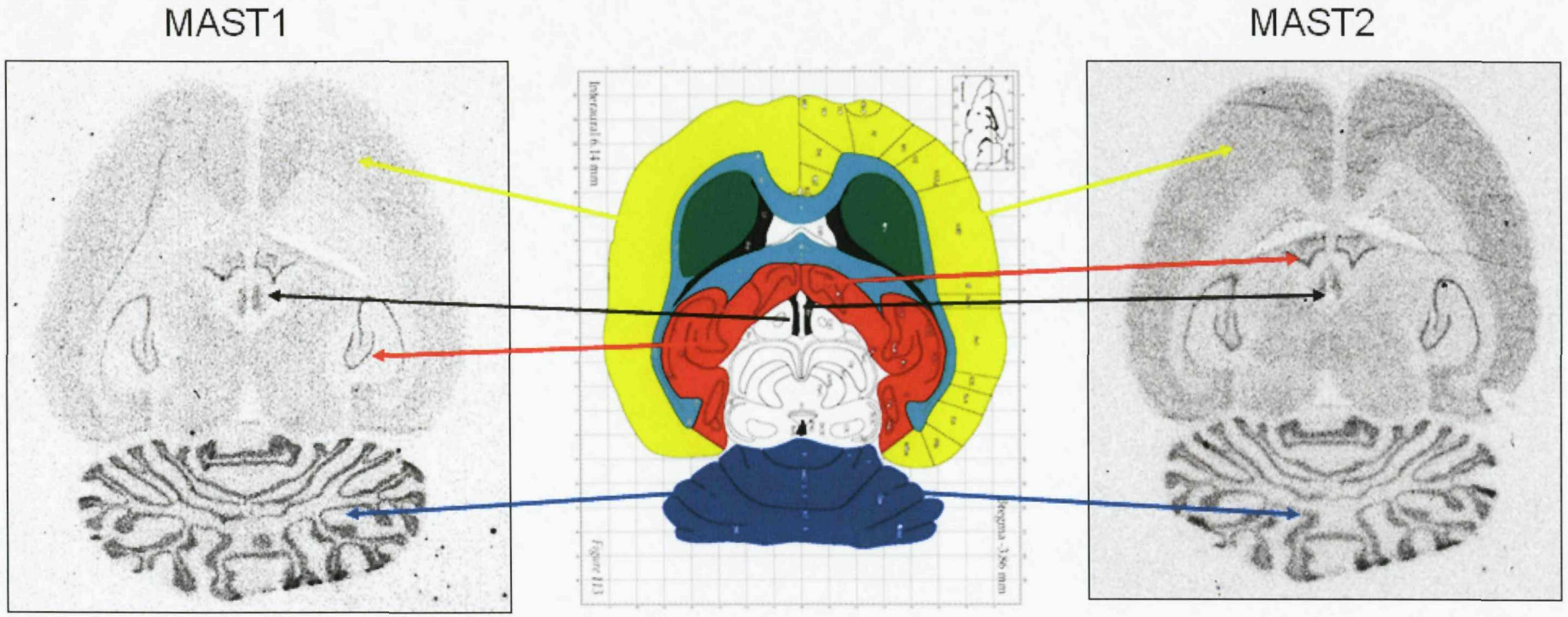

Figure 3.8. Expression of MAST1 & 2 in longitudinal sections. Both MAST1 & 2 are expression in the cortex, 3rd ventricle, hippocampus, and cerebellum. Image modified from Paxinos (2007). Sections were hybridised with equivalently labelled probes, and images shown are following 7 weeks exposure. The strength of expression of MAST1 and 2 appears similar within labelled brain regions. Cerebral cortex = yellow; white matter = light blue; striatum = green; hippocampus = red; cerebellum = dark blue; ventricle = black.

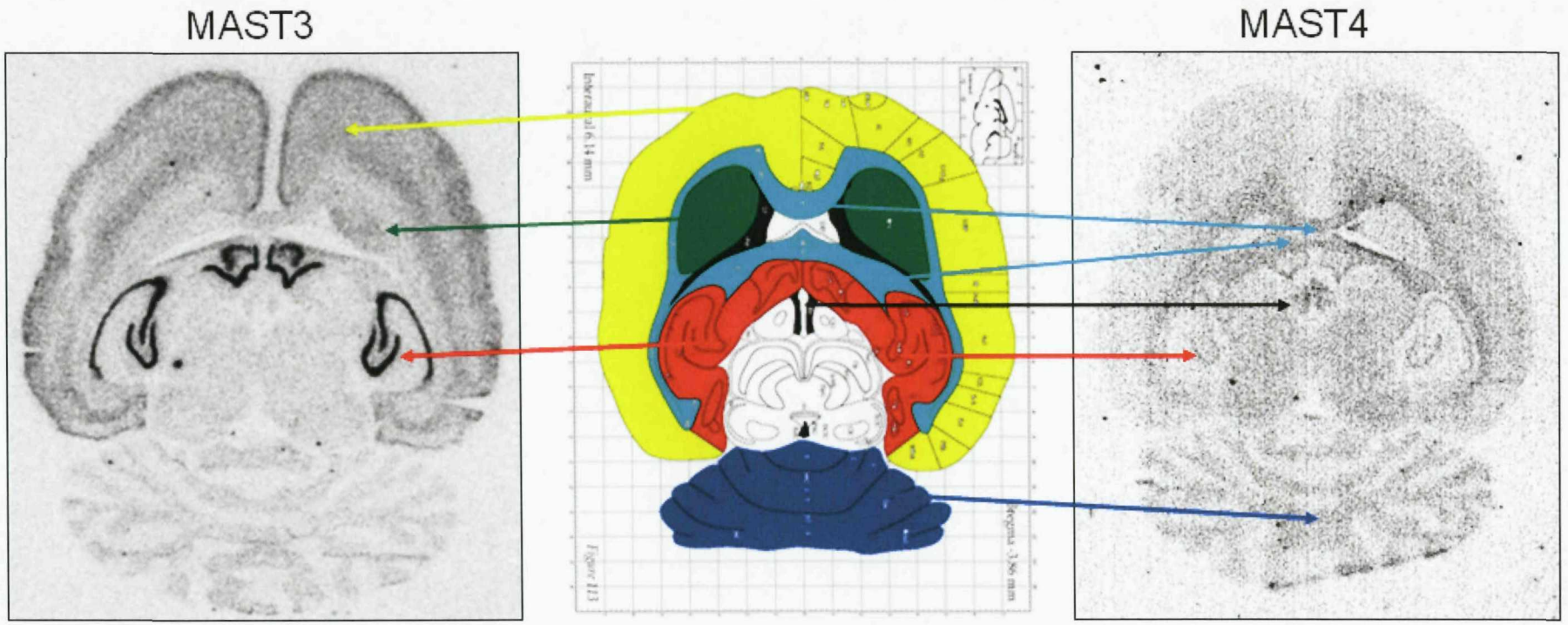

Figure 3.9. Expression of MAST3 & 4 in longitudinal sections. MAST3 is expressed in the cortex, striatum and hippocampus. MAST4 is expressed in the white matter, hippocampus and cerebellum. Image modified from Paxinos (2007). Sections were hybridised with equivalently labelled probes, and images shown are following 7 weeks exposure. MAST3 is more strongly expressed in the hippocampus than MAST4. Cerebral cortex = yellow; white matter = light blue; striatum = green; hippocampus = red; cerebellum = dark blue; ventricle = black.

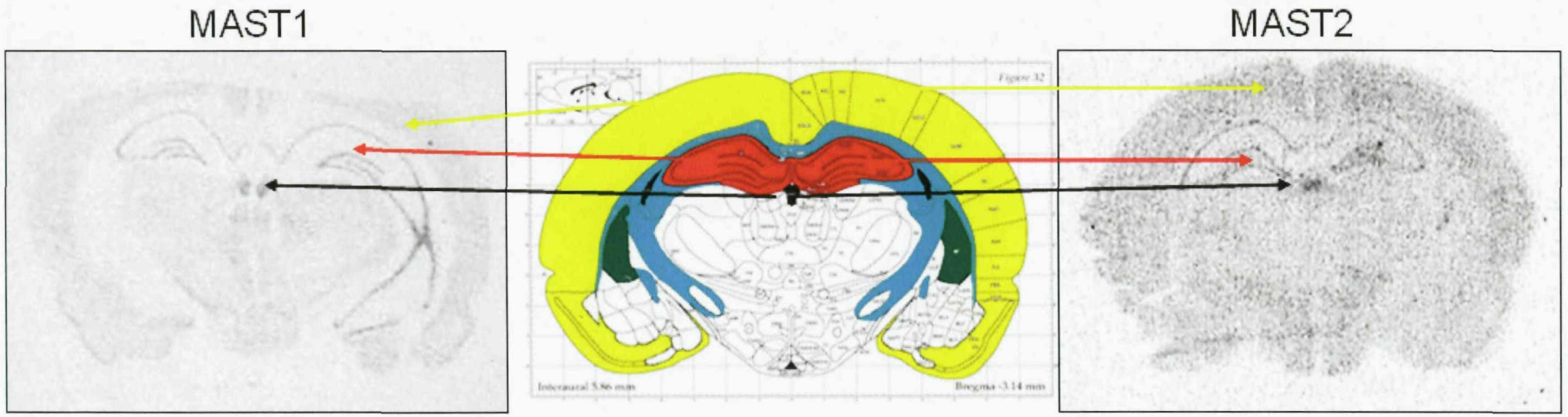

Figure 3.10. Expression of MAST1 & 2 in coronal sections. Both MAST1 and 2 are expressed in the cortex, hippocampus and 3rd ventricle. Image modified from Paxinos (2007). Sections were hybridised with equivalently labelled probes, and images shown are following 7 weeks exposure. The strength of expression of MAST1 and 2 appears similar within labelled brain regions. Cerebral cortex = yellow; white matter = light blue; striatum = green; hippocampus = red; ventricle = black.

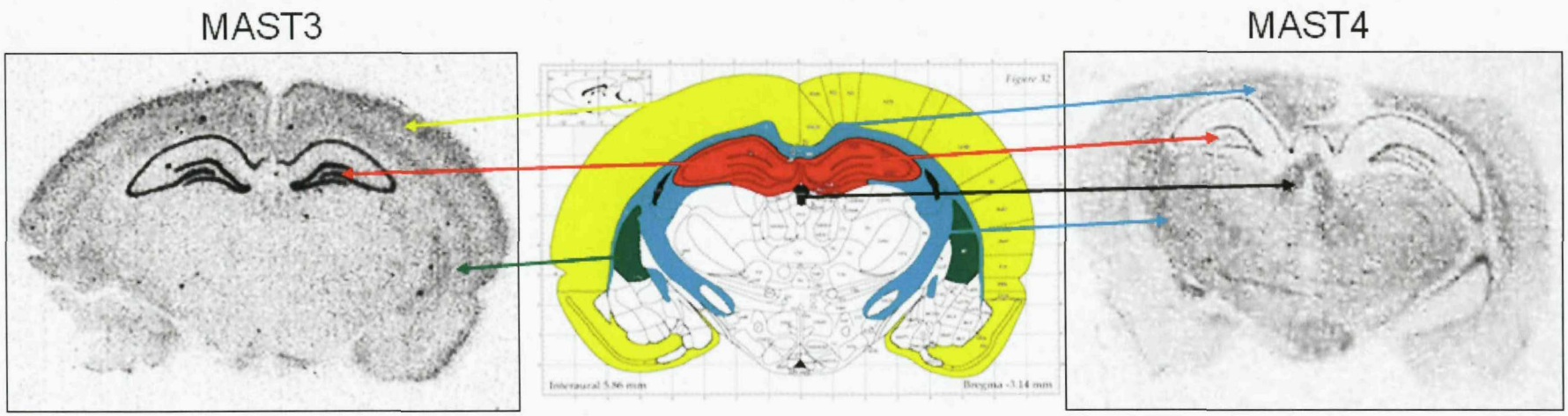

Figure 3.11. Expression of MAST3 & 4 in coronal sections. MAST3 is expressed in the cortex, striatum and hippocampus. MAST4 is expressed in the white matter, hippocampus and 3rd ventricle. Image modified from Paxinos (2007). Sections were hybridised with equivalently labelled probes, and images shown are following 7 weeks exposure. MAST3 is expressed more strongly in the hippocampus than MAST4. Cerebral cortex = yellow; white matter = light blue; striatum = green; hippocampus = red; ventricle = black.

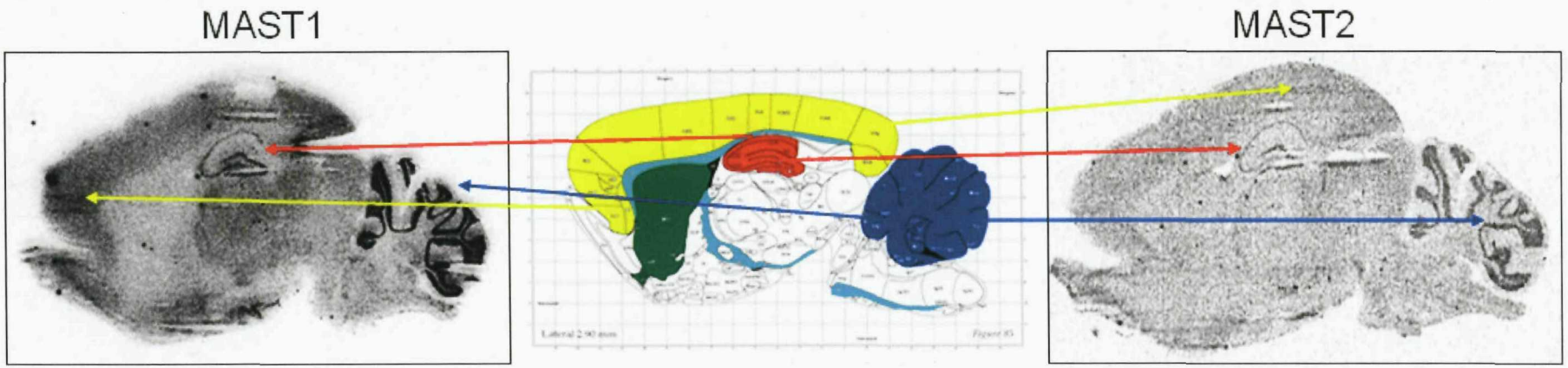

Figure 3.12. Expression of MAST1 & 2 in sagittal sections. Both MAST1 and 2 are expressed in the cortex, hippocampus and cerebellum. Image modified from Paxinos (2007). Sections were hybridised with equivalently labelled probes, and images shown are following 7 weeks exposure. Cerebral cortex = yellow; white matter = light blue; striatum = green; hippocampus = red; cerebellum = dark blue.

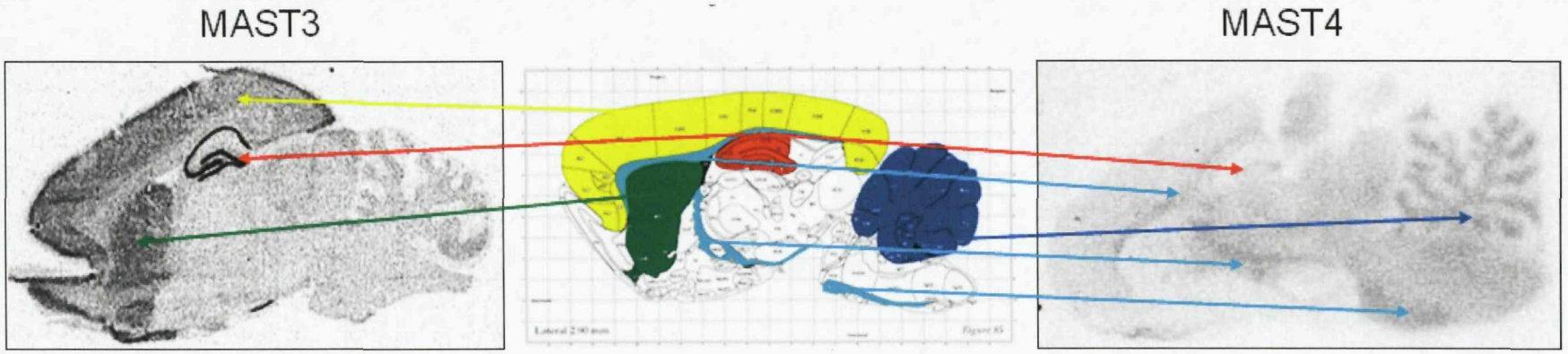

Figure 3.13. Expression of MAST3 & 4 in sagittal sections. MAST3 is expressed in the cortex, striatum and hippocampus. MAST4 is expressed in the white matter, hippocampus and cerebellum. Image modified from Paxinos (2007). Sections were hybridised with equivalently labelled probes, and images shown are following 7 weeks exposure. MAST3 is expressed in the hippocampus more strongly than MAST4. Cerebral cortex = yellow; white matter = light blue; striatum = green; hippocampus = red; cerebellum = dark blue.

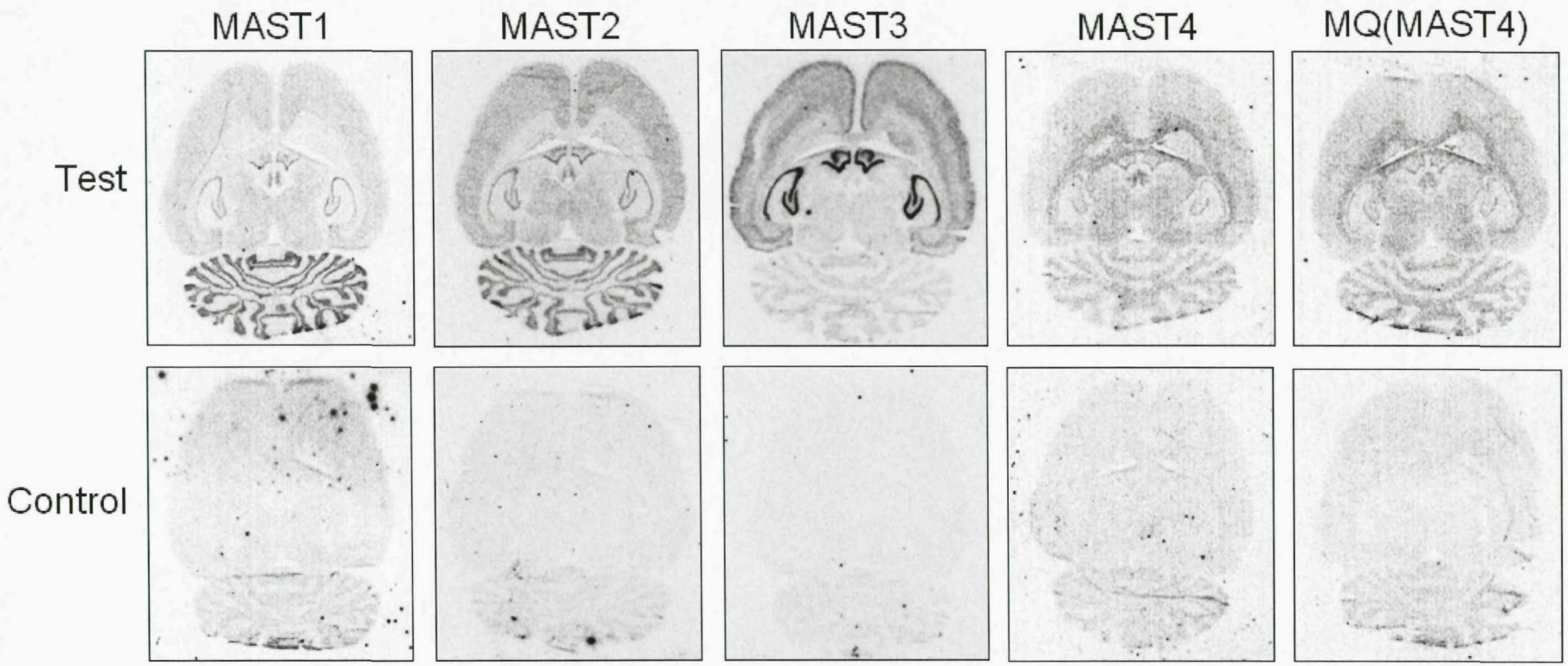

Figure 3.14. Raw data for MAST family expression in longitudinal sections. The control shown is the excess of unlabelled probe, which competes for the specific signals (see Chapter 2). The two probes used to separately assess MAST4 expression (MAST4 and MQ) produce equivalent results. Sections were hybridised with equivalently labelled probes, and images shown are following 7 weeks exposure.

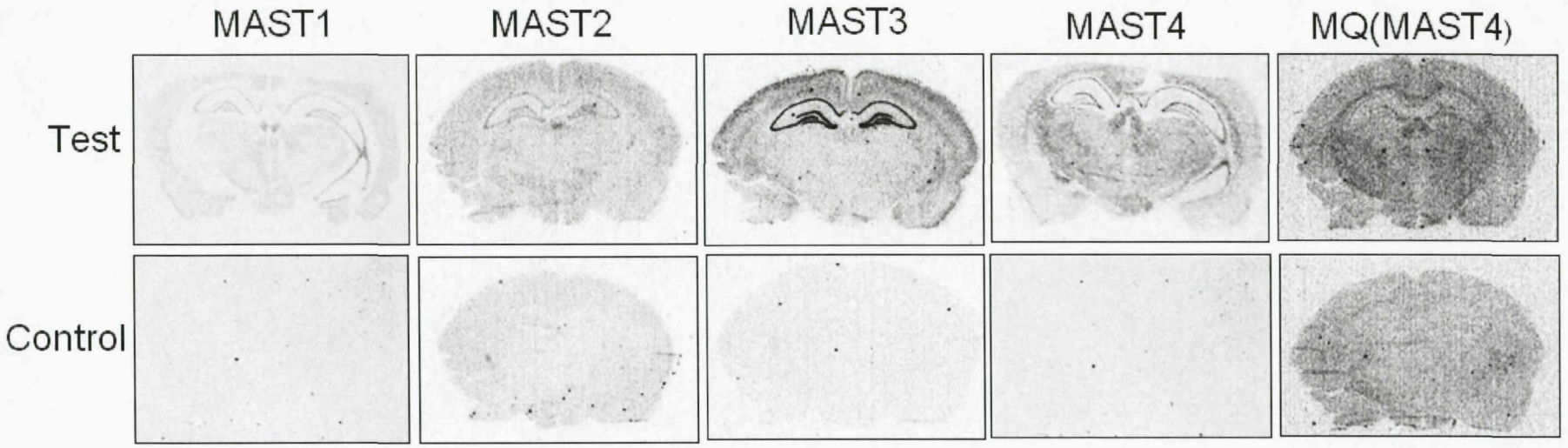

Figure 3.15. Raw data for MAST family expression in coronal sections. The control shown is the excess of unlabelled probe, which competes for the specific signal (see Chapter 2). The two probes used to separately assess MAST4 expression (MAST4 and MQ) produce equivalent results. Sections were hybridised with equivalently labelled probes, and images shown are following 7 weeks exposure.

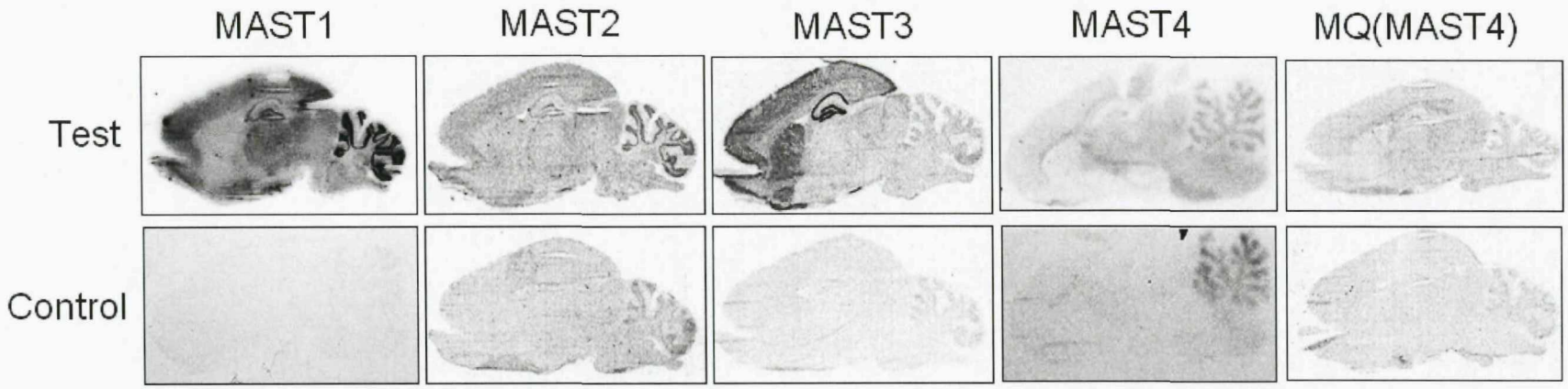

Figure 3.16. Raw data for MAST family expression in sagittal sections. The control shown is the excess of unlabelled probe, which competes for the specific signal (see Chapter 2). The two probes used to separately assess MAST4 expression (MAST4 and MQ) produce equivalent results. (2007). Sections were hybridised with equivalently labelled probes, and images shown are following 7 weeks exposure.

3.2.3.2. Emulsion Autoradiography - cellular expression

To delineate the expression patterns for the MAST family with cellular resolution emulsion autoradiography was performed for MAST1-4. This technique allows labelled sections to be covered with a thin layer of autoradiographic emulsion, which in combination with post-staining of the sections, allows identification of silver granules over specific cell types.

MAST1-4 are expressed in the neuronal cell types of the hippocampus. This is illustrated in Figure 3.17 with staining evident over the granule cell layer of the dentate gyrus (Figure 3.17 A-D). MAST1 & 2 also show expression in the granule cells of the cerebellum (Figure 3.17 E & F). The neuronal expression of MAST4 in the Purkinje cells of the cerebellum (Figure 3.17 H) is in contrast to its non-neuronal expression in oligodendrocytes of the cerebellar white matter (Figure 3.17 G). Figure 3.17 also illustrates the expression of MAST3 in the cerebral cortex and striatum. Although MAST3 appears to be expressed throughout the cerebral cortex, the strongest expression is in layer II (Figure 3.17 I). The expression of MAST3 in the striatum appears limited to medium sized neurons (Figure 3.17 J, black arrows) and not glia (white arrows).

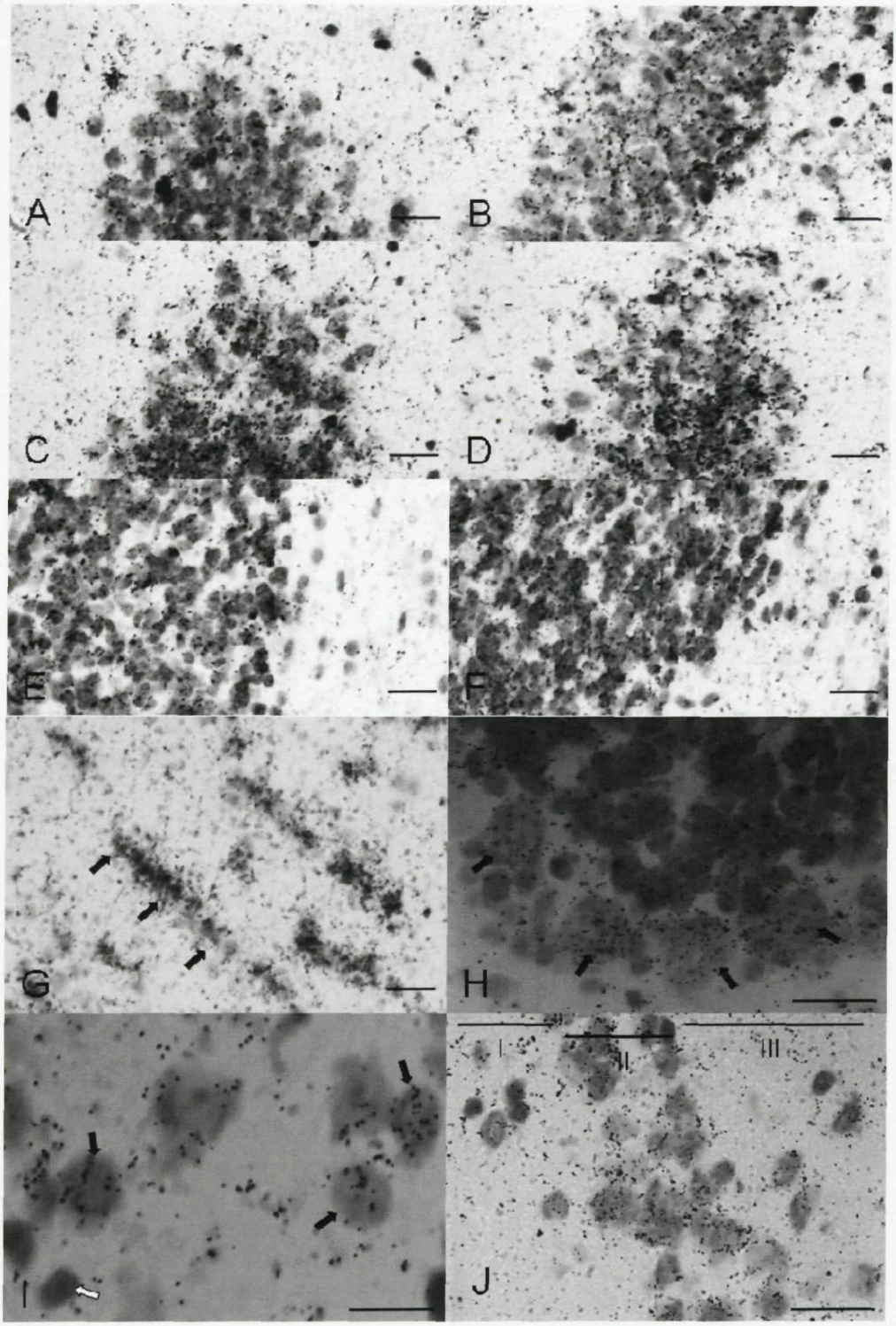

Figure 3.17. Cellular expression of the MAST family in rat brain. Figures A-J show emulsion autoradiographs performed using probes specific to MAST1-4 on rat brain sections. Figures A-D shows expression of MAST1 (A), MAST2 (B), MAST3 (C), and MAST4 (D) in the granule cells of the dentate gyrus. Figures E & F also show expression of MAST1 & 2 in the granule cells of the cerebellum. In contrast MAST4 shows expression in oligodendrocytes of the cerebellum (G), and purkinje cells (H). MAST3 shows expression in medium size neurons of the striatum (I, black arrows), but not non-neuronal cells (I, white arrow); Neurons in layer II of the cerebral cortex also show expression of MAST3 (J). Scale bars in A-F = 20μm, and H-J = 30μm.

3.2.4. The expression of MAST4 is increased following seizure-like activity

The activity-dependent expression of MAST4 has been reported previously in mouse brain (French et al., 2001b). To confirm this result and examine whether this increase also occurs in rat brain we have used in situ hybridisation on animals exposed to electroshock-evoked maximal seizure (Figure 3.18). Six sections from 3 separate rat brains were used for each condition (pre-seizure, 1hr post-seizure, 4hrs post-seizure). The expression of MAST4 in the dentate gyrus of the hippocampus can be seen to significantly ($p<0.02$, $n=3$) increase 1hr after seizure-like activity (Fig 3.19) The expression of MAST4 after 4hrs post-EMS returned to control levels.

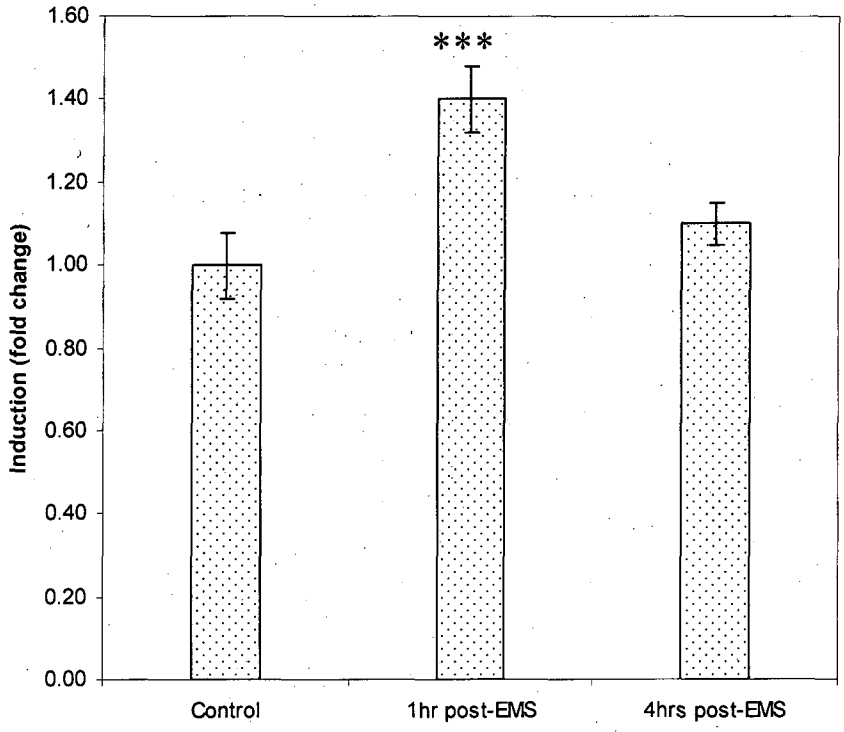

Fig. 3.19. Increase in MAST4 expression following EMS. The expression of MAST4 1hr post-EMS can be seen to significantly increase 1.4 fold from the control ($p<0.02$, $n=3$). However, after 4hrs post-EMS there is not a significant increase in MAST4 expression.

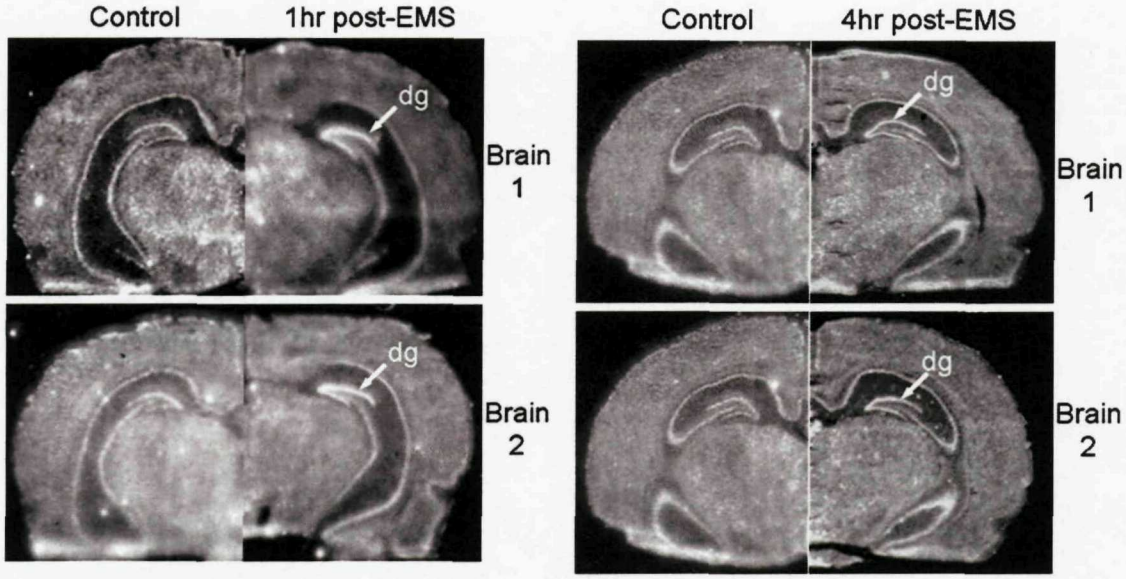

Figure 3.20. The expression of MAST4 is increased following seizure-like activity. The oligonucleotide used to assess expression of MAST4 in naïve tissue was used to probe rat brain coronal sections derived from animals subjected to EMS. The left hand panel shows an increase in MAST4 expression 1hr post-EMS within the dentate gyrus (dg), which returns to basal levels 4hrs post-EMS (right-hand panel).

Figure 3.21. The expression of MAST3 is not increased following seizure-like activity. To control for non-specfic upregulation of protein following EMS, the expression of MAST3 was investigated and found to remain at basal levels.

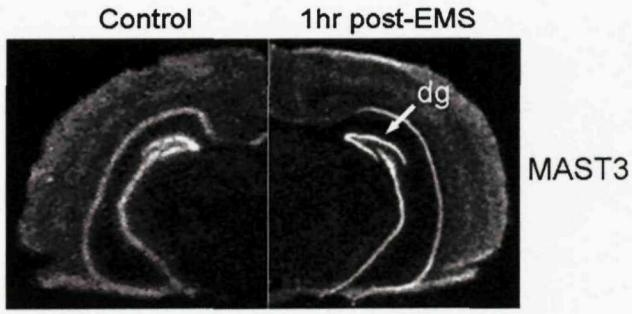

3.3. Discussion

This chapter describes the profiling of mRNA expression for the MAST family across multiple mouse tissues and rat brain. RT-PCR analysis has shown equivalent patterns of expression for MAST1 & 2 in multiple mouse tissues; MAST3, 4, and MAST-l exhibit stronger or more distinct expression in certain tissues. MAST1-4 all show expression in brain, which has been confirmed for MAST1-3 using northern blots.

The expression patterns in rat brain for MAST1-4 have been investigated using in situ hybridisation. The expression of MAST1 & 2 appears to overlap in the cortex, cerebellum, hippocampus, and 3rd ventricle. MAST3 is also expressed in the hippocampus; however, it is more strongly expressed in layer II of the cortex and is also expressed in the striatum. MAST4 is expressed in the hippocampus, 3rd ventricle, and white matter containing regions of the brain.

Both the RT-PCR (Figure 3.5) and in situ hybridisation (Figures 3.8, 3.10 & 3.12) analysis of MAST1 & 2 expression appears to show an overlap between these family members. MAST1 & 2 share a relatively high degree of homology in the microtubule-bind region (Table 3.1) between their kinase and PDZ domains. Also, these members have both been shown to bind microtubules (Lumeng et al., 1999). The study be Lumeng et al (1999) also established that these family members interact with the syntrophins (see Chapter 1, section 1.5.1). The syntrophins are components of the UAPC/DAPC. As described more fully in the Chapter 1, The UAPC/DAPC links the actin cytoskeleton to the extracellular matrix, particularly in postsynaptic cell membrane specialisations such as the neuromuscular junction and the postsynaptic density of central synapses. This structural role is augmented by interactions that support the clustering of receptors, signal transduction molecules, and associated proteins. These interactions are mediated by components of the complex such as the syntrophins. Lumeng et al (1999) hypothesis that MAST1 & 2 share the ability to link the UAPC/DAPC to cytoskeleton via an interaction with the syntrophins. Therefore, the overlap observed for MAST1 & 2 expression in this study may be rationalised by this shared capacity to organise scaffolding within the UAPC/DAPC.

The expression patterns reported for MAST1 protein by Lumeng et al (1999) also agree with the mRNA expression profile observed for this family member in rat brain (Figures 3.8, 3.10 & 3.12). For example, MAST1 protein colocalizes with DAPC/UAPC components in the vascular endothelium of the CNS, as well as neurons

in the cerebral cortex and cerebellum (Lumeng et al., 1999). And, as can be seen from Table 3.2, MAST1 is expressed in the cortex, cerebellum and 3rd ventricle, which contains many blood vessels.. Both this study and previous work report expression of MAST2 transcripts in mouse brain using northern blot analysis (Lumeng et al, 1999). However, the latter work was not able to characterise the expression pattern for MAST2 in brain (Lumeng et al., 1999). Therefore, the identification of overlapping expression patterns for MAST1 and 2 suggests that these family members share similar roles in the DAPC/UAPC.

As Table 1 shows, the regional expression of the MAST family in rat brain appears to generally overlap with those reported for mouse brain (Allen Brian Atlas). However, this study shows expression in the 3rd ventricle for MAST1, 2 & 4 and in the cerebellum for MAST2, which is not detected by the Allen Brain Atlas (Lein et al., 2007). This study used radioactively labelled probes and the Allen Brian Atlas uses a digoxigenin (DIG) labelling. Therefore, whereas this study can allow for prolonged exposure times to reveal low abundance transcripts, the Allen Brain Atlas can only take a 'snap-shot' of labelled transcripts within a tissue. This increase in sensitivity is most clearly illustrated by the characterisation of MAST4 expression, which is also not detected by the Allen Brain Atlas. As well as a more comprehensive characterisation of gross anatomical expression, this study also shows expression of MAST family members at the cellular level using emulsion autoradiography.

Using emulsion autoradiography, MAST1, 2, 3 and 4 show expression in the granule cells of the dentate gyrus (Figure 3.17 A-D). Figure 3.17 (E & F) also show expression of MAST1 & 2 in the granule cells of the cerebellum. In contrast MAST4 shows expression in oligodendrocytes of the cerebellum, and purkinje cells (Figure 3.17 G & H). MAST3 shows expression in medium size neurons of the striatum, but not non-neuronal cells (Figure 3.17 I); Neurons in layer II of the cerebral cortex also show expression of MAST3 (Figure 3.17 J).

Like MAST1 and 2, MAST3 is also expressed in brain (Figure 3.6). The database (NCBI) entry for murine MAST3 predicts an mRNA of between 3 to 4.4kb - this ambiguity is due to poor definition of the full-length transcript. However, the predicted size of full-length MAST3 for three other species is within the range detected: Macaca mulatta (6.3kb); Pan troglodytes (6.2kb); Homo sapiens (5.9kb). The predominant MAST3 transcript within mouse brain is therefore likely to be within the range of 6kb. Using autoradiographic film that had undergone equivalent times of exposure, the

expression of MAST3 in the hippocampus appears stronger than MAST1/2 (e.g., Figures 3.11 & 3.12). Unlike these family members, MAST3 also it has a more distinct pattern of expression in the cortex and striatum (e.g. Figure 3.13), which in the latter structure appears to be in the medium sized neurons (Figure 3.17 I).

The neurons showing expression of MAST3 in Figure 3.17 appear to constitute a large proportion of the cell types present; therefore, MAST3 appears to be expressed in the medium spiny projection neurons, which can constitute up to 95% of the neuronal population in the striatum (Kemp and Powell, 1971). This pattern of expression is particularly interesting in light of the interaction that has been identified between MAST1/2 and group I and II mGluRs (see Chapter 4). For example, Figure 3.21. below shows that mGluR5 is expressed in the cortex, hippocampus and the medium spiny neurons of the striatum (Testa et al., 1994; Testa et al., 1994). Further investigations are therefore needed to determine whether MAST3 can also interact with the mGluRs, especially as there is a precedent for functionally important serine phosphorylation of mGluR5 (Kim et al., 2005).

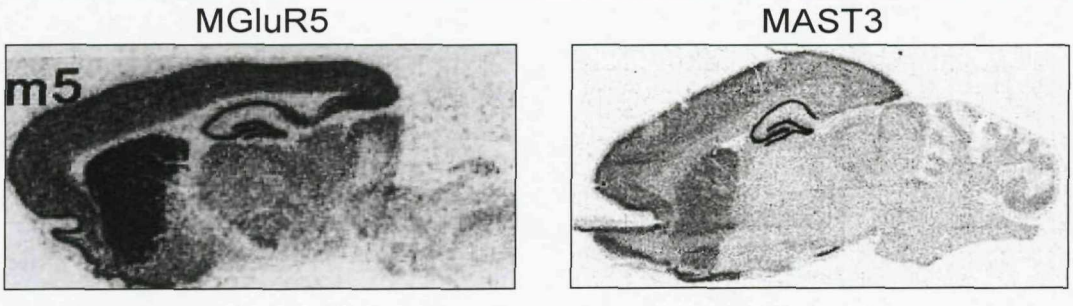

Figure 3.21. The pattern of expression for MGluR5 and MAST3 overlap. Expression of both transcripts can be seen in the striatum and hippocampus. A signal for MGluR5 can also be seen in the upper layer of the cortex.

Under basal conditions, MAST4 transcript is expressed in the 3rd ventricle, hippocampus and oligodendrocytes within white matter containing regions of the brain. However, following seizure-like activity there is a transient up-regulation of MAST4 mRNA within the dentate gyrus, which is consistent with an earlier study in mouse (French et al., 2001b). The temporary induction of MAST4 is reminiscent of immediate early genes (IEG) whose expression in the dentate gyrus has also been found to increase following seizure stimulus; for example, the transcription factors, zif268, c-fos, jun-B, and c-jun (Saffen et al., 1988) and the scaffolding protein Homer1a (Xiao et al., 1998). Immediate early genes are thought to support activity dependent changes in

synaptic function, and their expression following seizure may contribute to the aetiology of epilepsy (Hughes et al., 1999). The restricted up-regulation in the dentate gyrus over other sub-fields of the hippocampus may be related to the fact that this region of the brain contains glia-like stem cells that can differentiate into granule cells. This possibility may allow its expression in oligodendrocytes and the 3rd ventricle to be reconciled with its activity-dependent expression. It is known that the dentate gyrus and subventricular zone contain populations of stem cells (Ming and Song, 2005). Following seizure, these neural progenitor cells (NPC) are known to proliferate and differentiate into granule cells (Parent et al., 1997). These 'germinal niches', which have also been identified in the 3rd ventricle and white matter, maintain stem cells in an astroglial phenotype that can both proliferate and differentiate into neurons and glia (Alvarez-Buylla and Lim, 2004; Xu et al., 2005; Takemura, 2005). These studies therefore suggest that neurogenic cells within the dentate gyrus are more closely related to other glia cells than the neurons they can differentiate into. This proposition is supported by a recent report which shows that that transcriptome of hippocampal NPC show a stronger similarity to that of white matter containing brain regions than differentiated hippocampal tissue (Maisel et al., 2007). In the context described above, MAST4 may thus contribute to an aspect of glia phenotype which is required continuously in oligodendrocytes, but only transiently following seizure stimulus. This hypothesis is particularly interesting in light of the expression pattern of SAST124 (Chapter 1, section 1.5.2), which includes the dentate gyrus, subventricular zone and the pathway that nascent cells migrate along from this neurogenic region to the olfactory bulb (Yano et al., 2003). This pattern of expression has also lead Yano et al to propose a role for SAST124 in regulating/maintaining cellular phenotype in these regions. Interestingly, these authors also show expression of SAST124 in glia-like cells of the corpus callosum. The expression patterns of MAST4 and SAST124 therefore suggests that these family members may share similar functions.

In conclusion, this data reports the expression patterns of a poorly investigated branch of the mammalian kinome. Further studies are needed to confirm the expression of MAST family protein in the tissues and brain regions identified above. The characterisation of MAST family expression will support further investigation of their function; for example, by revealing co-localisation of potential interacting proteins (for example, see Figure 3.2.1). Also, an understanding of MAST family expression will

identify tissues/cell types that may utilise the functions reported for the MAST family and therefore focus further research into their function.

Chapter 4 - Interaction of the MAST family with the Metabotropic Glutamate Receptors

4. Introduction

MAST1 and 2 have been shown previously to interact with group I & II metabotropic glutamate receptors (mGluRs; Pilkington, BJ, PhD thesis). The metabotropic glutamate receptors (mGluRs) are seven transmembrane receptors that contain a large intracellular C-terminus which is coupled to a variety of signalling cascades; the mGluRs are involved in the generation of slow excitatory and inhibitory synaptic potentials, modulation of synaptic transmission and plasticity (Reviewed in Coutinho and Knopfel, 2002). As stated in Chapter 1, the working hypothesis was that MAST4 may contribute to scaffolding and signalling at the synapse following synaptic activity; and, as discussed in Chapter 1, there is precedent for an activity-regulated protein affecting mGluR scaffolding (e.g. Homer). Therefore, it was considered appropriate to investigate any possible interaction between MAST4 and the mGluRs.

As will be described below, the PDZ domain of MAST1 & 2 appears to mediate the interaction with group I & II mGluRs. As listed in Table 3.1 (Chapter 3), the PDZ domain of MAST4 has greater than 75% homology to the PDZ domains of MAST1 & 2. Therefore, the PDZ domain of MAST4 was used to investigate a potential interaction with the mGluRs. Also, to clarify and confirm the data reported by Pilkington et al, the minimal PDZ domain required to mediate the interaction between MAST1/2 & the mGluRs was investigated. It is unknown whether MAST4 can interact with the mGluRs and how much sequence from the MAST4 PDZ domain is required if its does. Therefore, investigating the minimal PDZ domain required to mediate the interaction between MAST1/2 and the mGluRs will provide a positive control that can be used as a model to rationalise what sequence to choose from MAST4 and how to interpret any interactions, if any, that are observed.

4.1.2. Structure of the PDZ domain and characteristics of its ligands

As described in Chapter 1, the PDZ domain facilitates scaffolding at the synaptic membrane by mediating protein-protein interactions. These interactions are often with the C-terminal tails of receptors and other membrane-bound proteins (Kim and Sheng, 2004). However, PDZ domains can also interact with each other via an internal peptide sequence that forms a β-hairpin conformation and mimics the usual C-terminal ligand (Hillier et al., 1999).

Figure 4.1 below illustrates the structure of a PDZ domain. A canonical PDZ domain consists of six β-strands (βA to βF) and two α-helices (αA to αB). The six β-strands form a partially opened barrel and the opening sides of the barrel are each capped with an α-helix. The βB strand and the αB helix form an extended groove, which has at one end a 'carboxylate binding loop', which the carboxylate of peptide ligands bind to (Doyle et al., 1996).

The amino acids at the 0 and -2 positions from the C-terminal end of a ligand are essential for binding PDZ domains – whereas the residues at the -1 and -3 positions, and possibly further N-terminal, are involved in fine-tuning the binding specificity (Reviewed in van Ham and Hendriks, 2003).

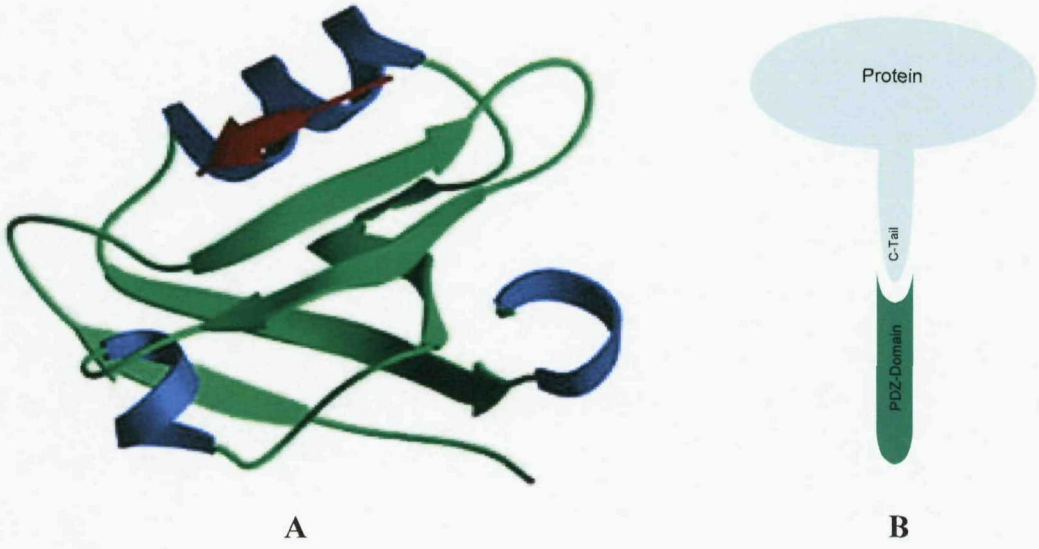

Figure 4.1. Structure of a PDZ domain. The diagram, **A**, shows the structure of a PDZ domain; the red arrow represents a ligand sitting within the groove formed by the βB strand (green) and αB helix (red). This interaction is shown schematically in **B**.

PDZ domains have been divided into three classes based upon the peptide motifs to which they bind. Class I bind the motif S/T-X-V, Class II bind F/L-X-V/L and Class III bind D/E-X-V (Reviewed in van Ham and Hendriks, 2003). By binding to group I & II mGluRs the PDZ domains of MAST1 & 2 can be classified as type I due to the high degree of homology between these mGluRs in their C-terminal tails.

4.1.2. Characteristics of the interaction between group I & II mGluRs and MAST1 & 2

A YTH screen using the C-terminal tails of mGluRs II and III has shown that these receptors interact with MAST1 and MAST2 (Pilkington, BJ, PhD thesis). The longest clones isolated from these screens encompassed the C-terminal half of each protein as illustrated in Figure 4.2.

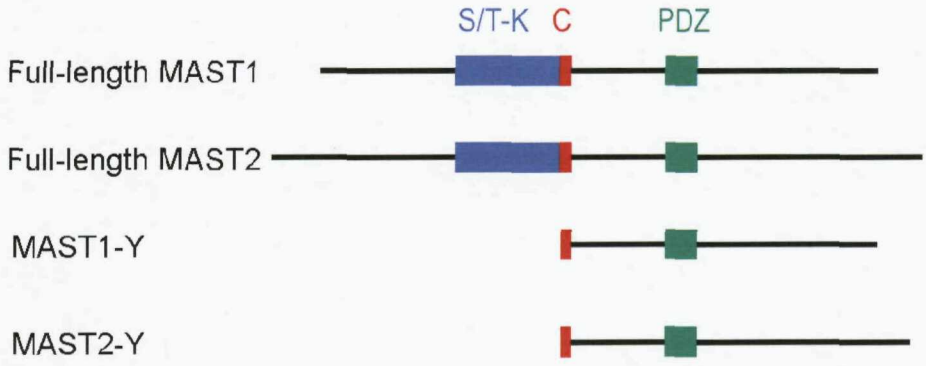

Figure 4.2. Regions of MAST1 & 2 shown to interact with group II mGluRs. Full-length MAST1 & 2 are shown in comparison to the longest clones shown to interact with group II mGluRs (MAST1-Y & MAST2-Y). Blue (S/T-K) = kinase domain; Red (C) = extension to kinase domain; Green = PDZ domain.

To investigate the characteristics of these interactions Ben Pilkington used the C-tails (the last 60 residues at the C-terminus), plus mutated forms of these C-tails in β-gal liquid assays. The clones isolated from YTH screen (as shown in Figure 4.2) interacted most strongly with group I mGluRs, less strongly with group II and not at all with group III. Truncation of the C-tails to remove the last 4 residues abolished the interaction with MAST1 and 2. Likewise, substitution of these residues with alanine reduced interaction. This data therefore reinforces the hypothesis that this interaction is PDZ mediated as the last 4 residues in PDZ ligands are essential for binding (Reviewed in van Ham and Hendriks, 2003). However, truncation of the C-tails to the last 18 amino acids also abolished the interaction with MAST1 & 2. This implies that sequence outside of the last 18 residues is important for mediating the binding with MAST1 & 2, which may explain why group I mGluRs interact more strongly with MAST1 & 2 than group II. Also, this suggests that the interaction between the mGluRs and MAST1 & 2 is more complex than a simple binding of the mGluR ligand to the PDZ domain.

4.2. Interaction of the isolated PDZ domains of MAST1, 2 & 4 with the mGluRs

To determine whether the isolated PDZ domain of MAST1, 2 & 4 is sufficient to mediate an interaction with the mGluRs, these domains were cloned in-frame with the B42 activation domain. The regions used to study the MAST family/mGluR interaction are listed below in Table 4.1 and shown schematically in Figure 4.3.below.

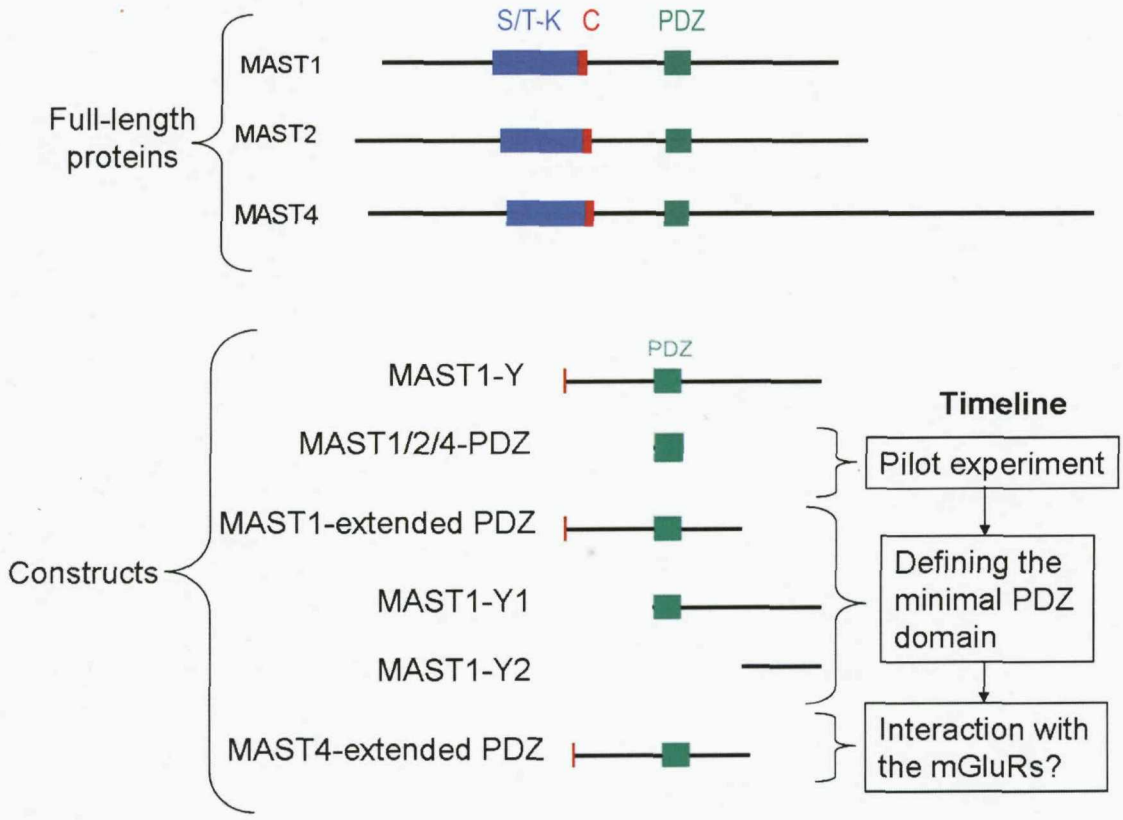

Figure 4.3. Constructs used to assess the interaction between the MAST family and the mGluRs. The upper panel illustrates the full-length proteins. The lower panel illustrates the constructs used to assess the mGluR interaction and the timeline over which these constructs were used. From top to bottom of the lower panel, the MAST1-Y clone was originally shown to interact with group I & II mGluRs. The isolated PDZ domains of MAST1, 2 & 4 were initially used to investigate any potential mGluR interaction. Subsequently, the minimal PDZ domain required to mediate this interaction was studied. Finally, an 'extended' PDZ domain of MAST4 was used to assess any interaction with the mGluRs. Blue (S/T-K) = kinase domain; Red (C) = extension to kinase domain; Green = PDZ domain.

Region	Position
MAST1 PDZ	2984-3232
MAST2 PDZ	3243-3489
MAST4 PDZ	3684-3947
xt MAST1 PDZ	1931-3943
xt MAST4 PDZ	2706-4688
MAST1-Y1	2984-4789
MAST1-Y2	3944-4789

Table 4.1. Transcript positions within the MAST family used to characterise their interactions with the mGluRs. Transcript positions for MAST1 (BC054524.1), MAST2 (UO2313) and MAST4 (AK090136.1) are listed for each construct.

Prior to assessing any potential interactions controls were performed to assess whether the isolated PDZ domain constructs were able to transactivate the reporter genes.

4.2.1. The isolated PDZ-prey constructs do not transactivate

Yeast (EGY48) containing the reporter construct pSH18-34 were transformed with the PDZ-Prey constructs and plated out onto two control plates: the first consisted of -UTL YNB agar plus galactose; and the second consisted of -UT plus X-gal. Therefore, if the PDZ-Prey construct is capable of transactivation, the yeast will grow on the first plate, and will turn blue on the second. The results for these two control experiments are shown in Figures 4.4. and 4.5. below.

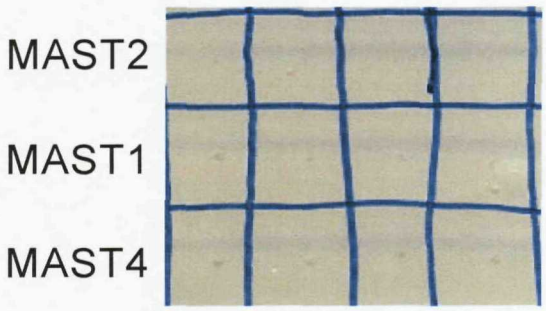

Figure 4.4. The MAST family PDZ-Prey constructs do not grow on -UTL Gal plates. Yeast (EGY48) containing pSH18-34 and PDZ-pJG4-5 were spotted four times onto -UTL gal plates.

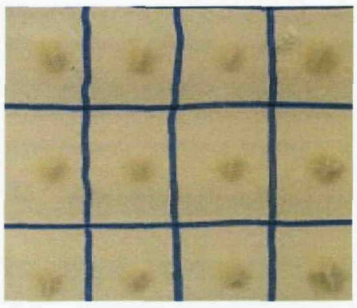

Figure 4.5. The MAST family PDZ-Prey constructs do not turn blue on -UT X-gal plates. Yeast (EGY48) containing pSH18-34 and MAST-PDZ-pJG4-5 were spotted four times onto -UT xGal plates.

Figure 4.4 above shows a -UTL Gal plate that has been spotted with yeast transformed with the PDZ-Prey constructs. If the PDZ-Prey constructs are capable of transactivation the yeast will produce leucine and be able to grow on these minus leucine plates; however, as Figure 4.4 shows no growth was seen for any of the family members. Figure 4.5 shows a -UT xGal plate that has been spotted with the same yeast as before. These plates contain leucine and so the yeast should grow on these plates, and as Figure 4.5 shows they have grown; however, these colonies will only turn blue if the PDZ-Prey construct is capable of activating the LacZ reporter gene, and as can be seen none of the colonies are blue. Therefore, these two control experiments confirm that the PDZ-Prey constructs are unable to cause transcription of the reporter genes.

4.2.2. The isolated PDZ domains of MAST1, 2 and 4 do not interact with the mGluRs.

Yeast containing the PDZ-Prey/reporter constructs were transformed with the C-tails of the mGluRs, which were subcloned into the 'Bait' vector pGilda. The sequence of the mGluR C-terminal tails is illustrated in Figure 4.6. below.

Figure 4.6. Sequence of mGluR C-tails used for interactions studies with the MAST family. (A) The sequence of the mGluR C-tails is illustrated for mGluR1 to 8, which have also been aligned to illustrate relative homology. (B) representation of a mGluR showing the C-terminal tail within the cytoplasm of the cell.

The pGilda plasmid allows the yeast to be grown on minus histidine plates. To assess the presence of any interactions the yeast were grown on -HUTL X-gal plates. These plates lack leucine and therefore only those colonies that contain interacting proteins

will activate the LEU2 reporter gene, and subsequently grow. These plates also contain X-gal and therefore only colonies with interacting proteins will activate the LacZ reporter gene and cause the colony to turn blue. Figure 4.7. below shows the results for this experiment.

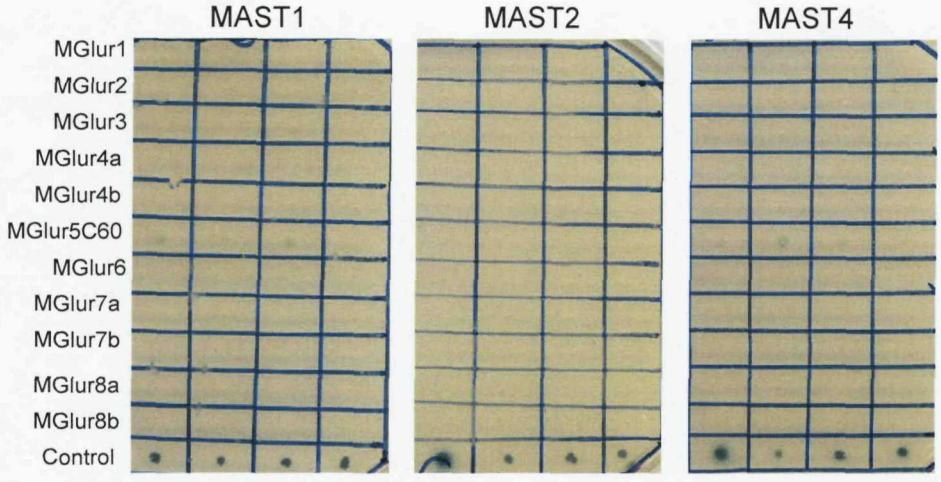

Figure 4.7. YTH experiment to determine the interaction of the mGluR C-tails with the isolated PDZ domains of MAST1, 2, and 4. Yeast (EGY48) containing pSH18-34, PDZ-pJG4-5, and mGluRx-pGilda (x = mGluRs1 to 8b) were spotted four times onto -HUTL xGal plates. The control (see text) can activate the LEU2 and LacZ genes and so grew, and turned blue, within two days. However, none of the test colonies grew, or turned blue over a two week period.

Figures 4.7. shows that yeast containing the PDZ-Prey/reporter constructs for each MAST family member did not grow/turn blue following transformation with any of the mGluR C-tails - this experiments was followed for 14days. This experiment therefore suggests that the PDZ domain of each family member that corresponds to the known consensus sequence is not capable of interacting with the C-tails of the mGluRs.

The control consisted of two proteins known to interact (from C.elegans, the last 70 aa of the C-tail of mgl-1, and the 3'-end of mpz-1 consisting of the last 4 PDZ domains), which was used to assess the viability of the plates to assay an interaction. In subsequent experiments, this control was replaced with yeast containing pGilda-mGluR2 + pJG4-5-MAST1-Y. This latter control can be used to assess the strength of the interaction for each construct relative to the original interaction, as well as providing information about the viability of the plates to measure an interaction.

4.3. Defining the minimal PDZ domain for the MAST1-mGluR interaction

The isolated PDZ domain for MAST1,2 and 4 did not appear to interact with any other the mGluR isoforms. Therefore, a set of experiments were conducted to determine the sequence within the MAST1-Y clone that is required to mediate the mGluR interaction. The failure to show expression of the reporter genes may be due to the absence of sequence flanking the PDZ domains that is required to mediate the interaction. Therefore, an 'extended PDZ' (xt-PDZ) domain was defined which included sequence either side of the isolated PDZ domain (Figure 4.3). As a potential interaction between the mGluRs and MAST4 was also considered, the extent of the xt-PDZ domain was defined by the degree of sequence identity between the MAST-Y clone and MAST4, as illustrated in Figure 4.3. & 4.8. Therefore, any subsequent interaction between these MAST family members and the mGluRs would potentially be due to homologous sequence. As shown in Figure 4.8. the xt-PDZ domain of MAST1 does not include all the C-terminal sequence found within the MAST-Y clone. Therefore, two extra regions of MAST-Y were also considered: MAST-Y1, which included the PDZ domain and all the C-terminal sequence of the MAST-Y clone (i.e. the 3'-end of MAST1); and, MAST-Y2, which consisted of the C-terminal sequence not included in the MAST1 xt-PDZ domain construct. These regions therefore encompasses all the sequence of the MASTY clone, from 5' to 3' end, in such a way that sequence necessary for the mGluR interaction can be identified.

The MASTY clone was originally found to interact with group I and II mGluRs. Therefore, mGluR 1, 2 and 3 were used for this set of experiments, but not mGluR 5 as it is known to transactivate the reporter genes (data not shown).

The appropriate regions (see Table 4.1 & Figure 4.3) were amplified by PCR and cloned in-frame into the pJG4-5 prey vector. Prior to conducting the test experiments controls were performed to assess whether these constructs were capable of transactivating the reporter genes.

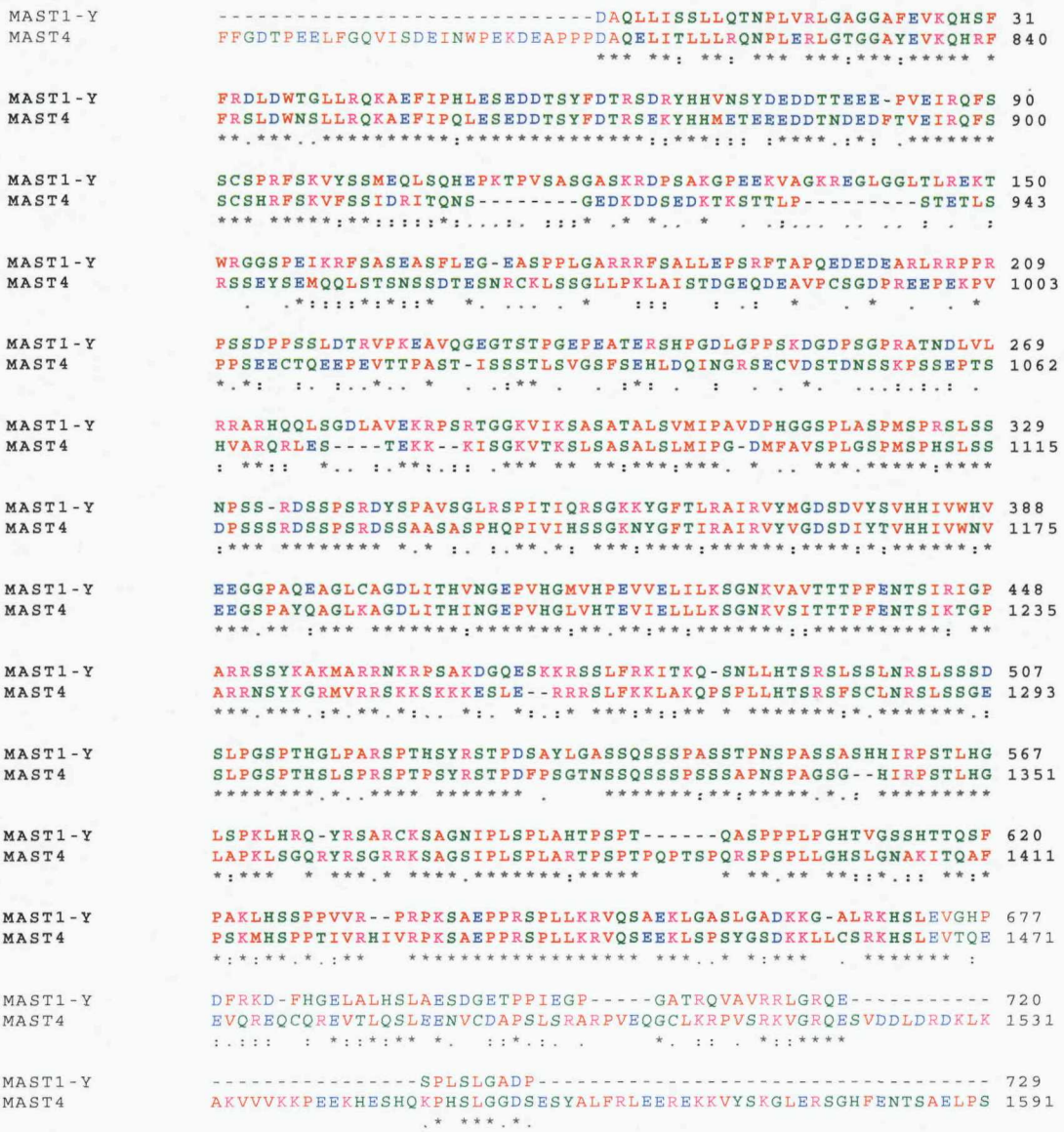

Figure 4.8. Alignment of MAST1-Y with MAST4. The highlighted residues represent the extended PDZ domain for MAST1, and 4. The positions within the full-length proteins are indicated by the numbers on the right.

4.3.1. The constructs MAST1-Y1, MAST1-Y2, and the extended PDZ domains of MAST1 and 4 do not transactivate

Yeast (EGY48) containing the reporter construct pSH18-34 were transformed with the appropriate Prey constructs and plated out onto two control plates: the first consisted of -UTL YNB agar plus galactose and the second consisted of -UT plus X-gal. Therefore, if the extended PDZ-Prey construct is capable of transactivation, the yeast will grow on the first plate, and will turn blue on the second. The results for these two control experiments are shown in Figure 4.9.

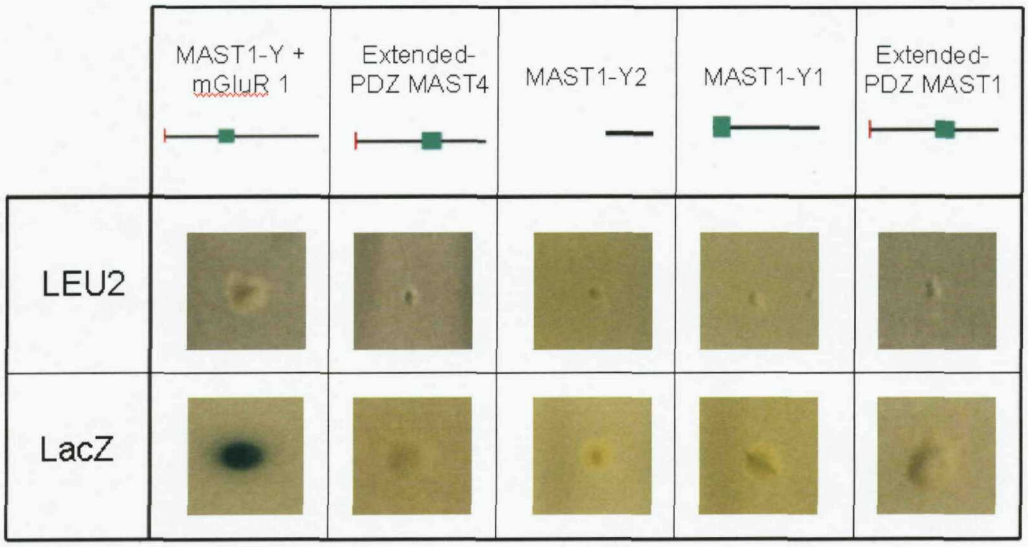

Figure 4.9. Controls for prey constructs used to characterise the minimal PDZ domain. Yeast (EGY48) containing pSH18-34 and each prey construct were spotted four times onto -UTL gal & -HUTL x-Gal plates. The control is able to activate the LEU2 & LacZ reporter genes and therefore grow on the minus leucine plates and turn blue on the x-Gal containing plates. None of the prey constructs grew on minus leucine plates or turned blue on x-Gal containing plates

Figure 4.9 above shows expression of the LEU2 by the control and therefore growth on minus leucine plates. If the Prey constructs are capable of transactivation the yeast will also be able to grow on these minus leucine plates; however, as Figure 4.9 shows no growth was seen for any of the Prey constructs. Figure 4.9 also shows the control can activate the LacZ gene and cause transformed yeast to turn blue. Again, yeast containing the Prey constructs do not express this reporter gene and grow without any blue colouration.

Therefore, these two control experiments confirm that the Prey constructs of MAST1 and 4 are unable to cause transcription of the reporter genes.

The control for these experiments was MAST1-Y co-transformed with mGluR1; therefore, this control allows a direct comparison between the original interaction observed for MAST1 and that observed for the extended PDZ domain construct.

4.3.1. Characterising the MAST1 sequence required to mediate an interaction with group I & II mGluRs

Following the control experiments, yeast containing the Prey and reporter constructs were transformed with the C-tails of mGluRs 1, 2 and 3. Transformed yeast were grown on -HUT plates and then spotted 4X onto -HUTL x-Gal plates for assaying of

reporter gene expression. The results for this set of experiments are shown in Figures 4.10 to 4.12.

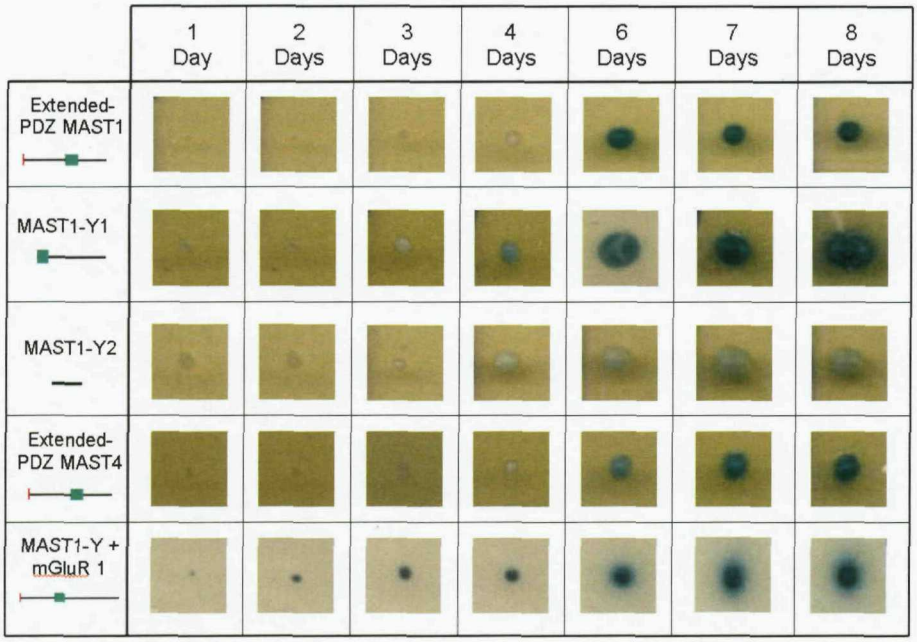

Figure 4.10. Interaction of the Prey constructs with mGluR 1. Yeast (EGY48) transformed with pSH18-34, pJG4-5-Prey construct and the pGilda-mGluR 1 C-tail were spotted 4X onto -HUTL x-Gal plates - a representative colony is shown. The control (MAST1-Y + mGluR 1) can strongly activate both the LEU2 and LacZ reporter genes and so grew and turned blue within one day.

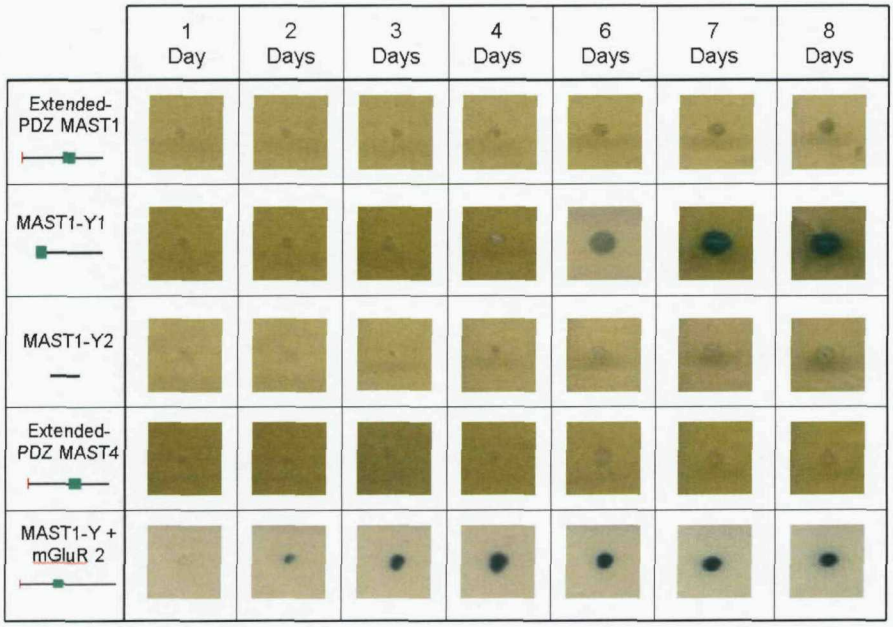

Figure 4.11. Interaction of the Prey constructs with mGluR 2. Yeast (EGY48) transformed with pSH18-34, pJG4-5-Prey construct and the pGilda-mGluR 2 C-tail were spotted 4X onto -HUTL x-Gal plates - a representative colony is shown. The control (MAST1-Y + mGluR 1) can strongly activate both the LEU2 and LacZ reporter genes and so grew and turned blue within one day.

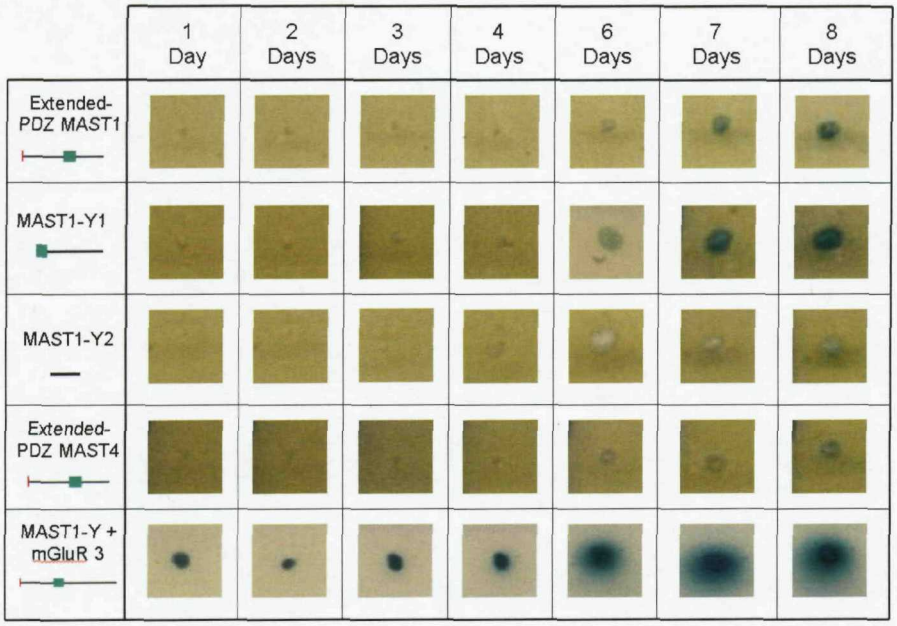

Figure 4.12. Interaction of the Prey constructs with mGluR 3. Yeast (EGY48) transformed with pSH18-34, pJG4-5-Prey construct and the pGilda-mGluR 3 C-tail were spotted 4X onto -HUTL x-Gal plates - a representative colony is shown. The control (MAST1-Y + mGluR 1) can strongly activate both the LEU2 and LacZ reporter genes and so grew and turned blue within one day.

The reporter gene expression illustrated in Figures 4.10 to 4.12 has been scored and tabulated as shown in Table 4.2 below.

	Prey Construct	Score
mGluR 1	Control	+++++
	MAST-Y1	+++
	MAST-Y2	+
	xt PDZ MAST1	++
	xt PDZ MAST4	++
mGluR 2	Control	+++++
	MAST-Y1	++
	MAST-Y2	-
	xt PDZ MAST1	-
	xt PDZ MAST4	-
mGlurR 3	Control	+++++
	MAST-Y1	++
	MAST-Y2	+
	xt PDZ MAST1	++
	xt PDZ MAST4	-

Table 4.2. Scoring of reporter gene expression for mGluR-MAST1 & 4 interaction. The maximum score is 5, which has been assigned to the control.

The reporter gene expression for MAST-Y1 is relatively weak compared to the control but is slightly stronger than for the xt-PDZ domain of MAST1. This construct also shows the strongest reporter gene expression when co-transformed with mGluR 2. However, the expression of reporter genes for MAST-Y1 is still significantly below the MASTY control in all cases.

The xt-PDZ domain of MAST4 appeared to cause a relatively weak expression of the reporter genes when co-transformed with mGluR1. Therefore, to determine if this region of MAST4 may interact more strongly with other isoforms of the mGluRs it was co-transformed with the full complement of mGluR C-tails.

4.4. Interaction of the xt-PDZ domains of MAST4 with the mGluRs.

The xt-PDZ domain of MAST4 was co-transformed into yeast with the pSH18-34 reporter construct and the mGluR C-tails cloned into the pGilda Bait vector. Following growth on -HUT plates, four colonies were spotted onto -HUTL x-Gal plates to assaying reporter gene expression. Figure 4.13. below shows the results for this set of experiments.

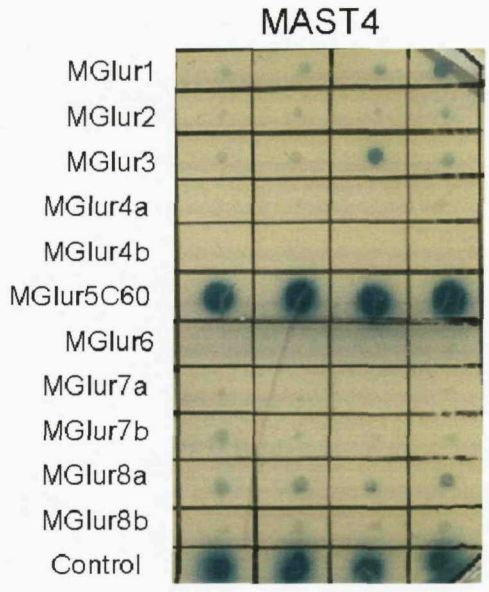

Figure 4.13. YTH experiment to determine the interaction of the mGluR C-tails with the extended PDZ domains of MAST4. Yeast (EGY48) containing pSH18-34, xt-PDZ MAST4-pJG4-5, and mGluRx-pGilda (x = mGluRs1 to 8b) were spotted four times onto -HUTL xGal plates. The control (MASTY + mGluR 1) can activate the LEU2 and LacZ genes and so grew, and turned blue, within two days.

The C-tail for mGluR V (M5C60) is known to show transactivation after 3-4 days, which was not any quicker after co-transformation with the xt-PDZ domain of MAST4. The image shown in Figure 4.13 is after 14 days incubation; therefore, there is no clear expression of the reporter genes for any combination of mGluR isoform and the xt-PDZ domain construct.

4.5. Discussion

Previous work has shown an interaction between MAST1 and 2 and group I & II mGluRs (B.J. Pilkington, PhD thesis). Using C-terminal tail mutants of group II mGluRs, this interaction appeared to be mediated via the PDZ of MAST1 & 2. This chapter has described the attempt to define the sequence within MAST1 that is required to mediate its interaction with the mGluRs. Also, the degree of sequence identity between the PDZ domains of MAST1/2 and MAST4 suggests that MAST4 may also interact with the mGluRs.

Initially, the PDZ in isolation was used to assess whether this domain is necessary and sufficient to mediate the interaction with the mGluRs. The isolated PDZ domains of MAST1, 2 & 4 did not show expression of reporter genes when co-transformed with an of the mGluR isoforms. This implies that there is sequence outside of the PDZ domain that is required to support the mGluR interaction; this may be through direct binding of residues outside of the PDZ domain to the mGluR C-tail, or indirectly through supporting the conformation of the PDZ domain.

To determine what sequence is required for the interaction between MAST1 and group I & II mGluRs, 3 regions of MAST1 were considered (Figure 4.3). An extended PDZ domain was defined according to the relative homology between the sequence flanking the PDZ domains of MAST1 & 4. This xt-PDZ domain for MAST1 included all the DNA sequence 5' of the PDZ and part of the DNA sequence 3' to the PDZ domain. As this construct did not include all the 3' sequence another was defined (MAST-Y1) that included the PDZ domain and all of the sequence 3' of this that is found in the MASTY clone (i.e. the 3' end of MAST1). Finally, to differentiate between MAST-Y1 and the xt-PDZ domain of MAST1 another region was chosen (MAST-Y2) that only included the 3' sequence not found in the xt-PDZ domain of MAST1.

None of the constructs tested were able to activate the reported genes as strongly as the MASTY clone. The strongest activation of the reporter genes appeared to be with the MAST-Y1 construct. This construct included the PDZ domain and all of the C-terminal sequence of MAST1. This implies that residues C-terminal to the PDZ domain are important either for the integrity of the PDZ domain structure or are directly involved in binding to the C-tails.

Although the xt-PDZ domain of MAST4 appear to show a relatively weak interaction with mGluR1, this region of MAST4 was not able to cause a stronger activation of the reporter genes when co-transformed with any of the other mGluR isoforms.

The set of experiments described in this chapter clearly show that sequence outside of the isolated PDZ domain is required to mediate the interaction with the mGluRs. However, to more clearly determine the role played by the PDZ domain in these interactions, this domain would need to be mutated at specific residues that are known to be required for such interactions. For example, the carboxylate binding loop contains the highly conserved signature Gly-Leu-Gly-Phe (GLGF) motif, as well as an arginine (sometimes a lysine) residue three amino acids upstream, that are critically involved in the hydrogen bond formation between the carboxylate of a ligand and the PDZ domain (Doyle et al., 1996). Mutation within this loop can affect binding of a PDZ domain to its ligand; for example, substitution of a lysine and an aspartic acid in the carboxylate binding of the PDZ domain of PICK1 (protein interacting with C kinase 1) abolishes its interaction with protein kinase C (Staudinger et al., 1997).

As described earlier, the residues within a PDZ ligand at positions 0 & -2 from the C-terminus are essential for binding, while those at -1, -3 and further N-terminal are involved in determining specificity (Songyang et al., 1997; van Ham and Hendriks, 2003). For example, deletion of 11 amino acids preceding the C-tail of the Kir2.1 channel abolishes binding to the 1st and 2nd PDZ domain of PSD-95 (Pegan et al., 2007).

In the context of the MAST family, the specificity of PDZ domains is neatly illustrated by the study of Valiente (2005). These authors report that MAST1-3 bind to PTEN. However, they also report that MAST4 does not interact with PTEN. Considering that MAST4 shows on average >75% homology between its PDZ domain and that of MAST1-3 (78% between these family members), it is revealing that its PDZ domain can discriminate between other MAST family ligands.

Most studies of PDZ structure have used the 80-90 residues that normally occur in the canonical PDZ domain (van Ham and Hendriks, 2003). However, sequence outside of this canonical motif is known to be important for regulating the binding properties of the PDZ domain; for example, binding of the Rho GTPase, Cdc42, to the CRIB domain of the cell polarity protein Par6 causes a conformation change that increase 13-fold the binding of the Par6 PDZ domain to its ligand (Peterson et al., 2004). Structural studies by Peterson et al (2004) suggest that the free PDZ domain of Par6 does not conform to

the standard PDZ conformation, with a low affinity for its ligand; however, following binding of Cdc42 to the CRIB domain in the native protein, the PDZ domain forms a standard PDZ conformation with a high affinity for its ligand.

Taken together, the studies described above illustrate that PDZ-ligand interactions are more complex than simple binding of the C-tail; and, that sequence outside of the canonical PDZ domain can affect its binding properties.

Chapter 5 - A YTH screen to identify interacting partners for MAST4

5. Introduction

As described in Chapter 1, the yeast-two system can be used to identify interactions between proteins. It is known that different members of the MAST family interact with other proteins and can affect their function through phosphorylation (see Chapter 1). These interaction have been found to occur through the PDZ domain of the MAST family as well as sequence outside of this domain. Like MAST1-3, MAST4 contains a PDZ domain, as well as a noticeable extension of its C-terminus. These regions of MAST4 may support protein-protein interactions, which the yeast-two hybrid system can be used to identify. The open reading frame for MAST4 is 8kb. The 290kDa protein produced from this ORF would be too large to use in a yeast-two hybrid screen (Maple and Moller, 2007). Therefore, MAST4 was separated into 3 subdomains (see Figure 5.1).

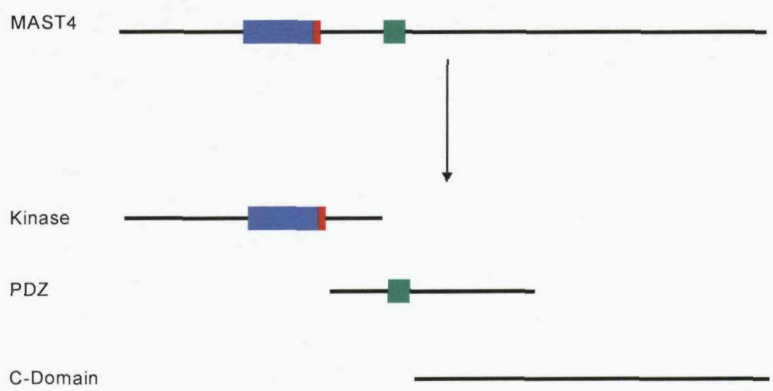

Figure 5.1. Subdomains of MAST4. Blue = kinase domain; Red = extension to kinase domain; Green = PDZ domain.

As stated in Chapter 1, analysis of the sequence for MAST4 has shown it to contain putative kinase and PDZ domains. Because the function of the kinase domain is likely to be limited to signal transduction, the PDZ and C-Domain were chosen as potential Baits to search for interacting proteins.

As described in Chapter 4, the interaction between the PDZ domain of MAST1 and the mGluRs appears to require flanking sequence outside of the canonical PDZ domain. Therefore, the extended PDZ domain used in Chapter 4 (Table 4.1) was also used as a potential bait. As discussed in Chapter 1 & 3, the C-terminus of the MAST family is variable, with the large C-terminal region of MAST4 being unique to this family member. Interestingly, this region of MAST4 predominantly sits within a single large

(3.9kb) exon. This suggests this region may have been introduced as part of a gene translocation, which may subsequently have allowed MAST4 to assume a novel function. The 'C-domain' of MAST4 does not appear to contain any known domains, which again suggests this region of MAST4 may constitute a novel domain(s).

The organisation of the YTH screen is illustrated below in Figure 5.2.

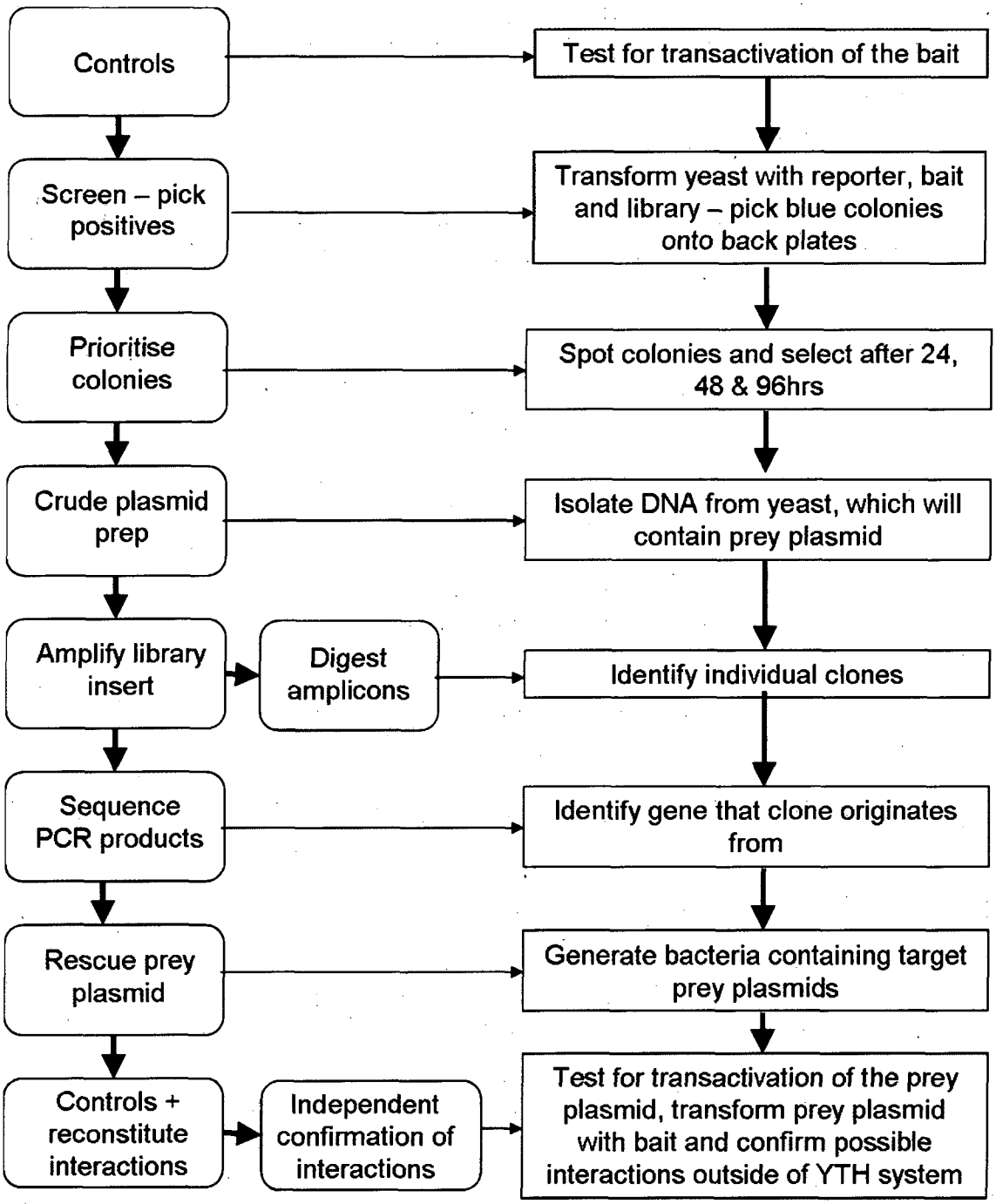

Figure 5.2. Organisation of the YTH screen.

5.1. Controls

The PDZ and C-Domains of MAST4 were fused in-frame to the LexA DNA binding domain. These potential Baits were then subjected to two sets of controls:

Repression assay - a Bait construct must be able to enter the nucleus of the yeast cell and express the Bait fusion protein. This can be assessed by cotransforming the Bait construct with the plasmid pJK101. pJK101 contains two LexA operators between the LacZ gene and the Gal1 promoter. Therefore, if the Bait protein is expressed in the nucleus its LexA DNA binding domain will interact with the LexA operators and repress transcription of the LacZ gene. The plasmid pEG202-Max constitutively expresses a LexA DBD containing protein, which is used as a 'high repression, negative control. The plasmid pJK101 allows yeast to grow on minus uracil plates; therefore, this assay was conducted on YNB(Gal)-HU X-gal plates to selective for the plasmids used and assay the expression of the reporter gene. A positive control was also included by plating yeast transformed with pJK101 onto YNB (Gal)-U X-gal plates; under these conditions the reporter gene is constitutively expressed, which represents 'no repression'.

The results for this experiment are shown in Figure 5.3. below.

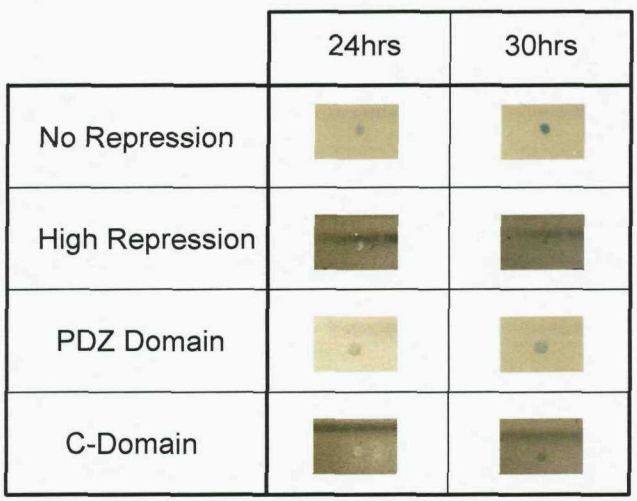

Figure 5.3. Repression assay to determine the nuclear targeting of the C-Domain and PDZ domain Baits. The C-domain bait is able to repress transcription of the reporter gene (LacZ = blue product) more effectively than PDZ domain bait.

Figure 5.3. shows that with no repression the yeast turn blue after 24hrs; however, with high repression the yeast are white after 24hrs, but eventually turn blue after 30hrs. Yeast transformed with the PDZ domain Bait are slightly blue after 24hrs, and clearly blue after 30hrs. In contrast, yeast transformed with the C-Domain Bait construct are

white after 24hrs and only slightly blue after 30hrs. Therefore, compared to the controls, the C-Domain exhibits high repression of the LacZ reporter gene and the PDZ domain exhibits low repression. This indicates the C-Domain enters the nucleus more effectively than the PDZ domain (assuming the two prospective baits express equally).

Transactivation assay - the Bait proteins may be capable of activating the reporter genes independently of any interaction.

To test for transactivation of the LacZ gene, the Bait constructs were cotransformed into EGY48 with the reporter construct pSH18-34. This plasmid contains the LacZ gene, which will cause the yeast to turn blue if it is activated by the Bait proteins. The reporter construct was also cotransformed with the plasmid pSH17-4, which strongly activates LacZ and therefore acts as a positive control. A negative control was included by cotransforming pSH18-34 with the plasmid pRFHM1, which does not activate the LacZ gene. This assay was conduced on YNB(Gal)-HU X-gal plates.

The results for this control assay are shown below in Figures 5.4 & 5.5.

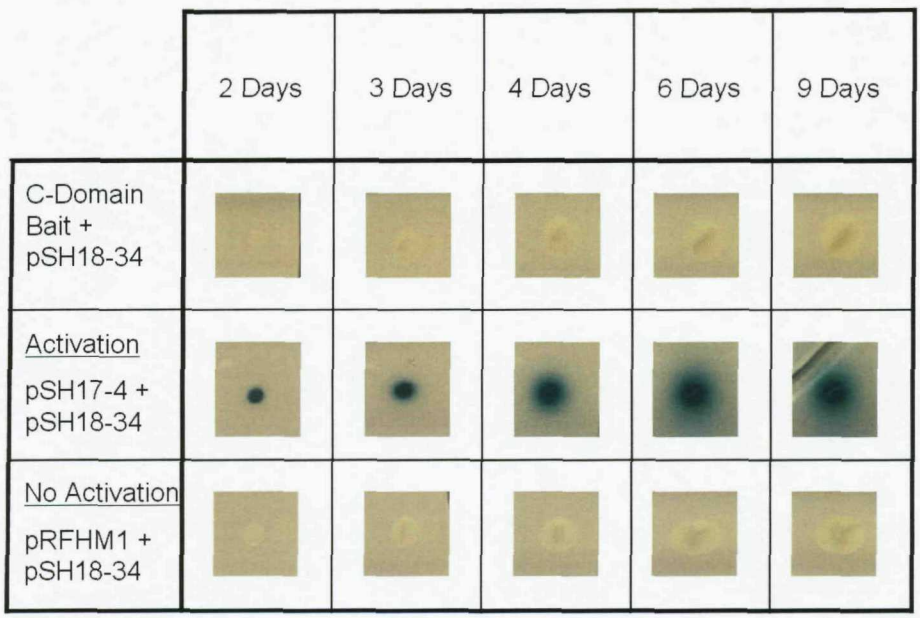

Figure 5.4. The C-Domain does not transactivate the LacZ gene. EGY48 transformed with the C-Domain Bait construct and pSH18-34 do not turn blue after 9 days.

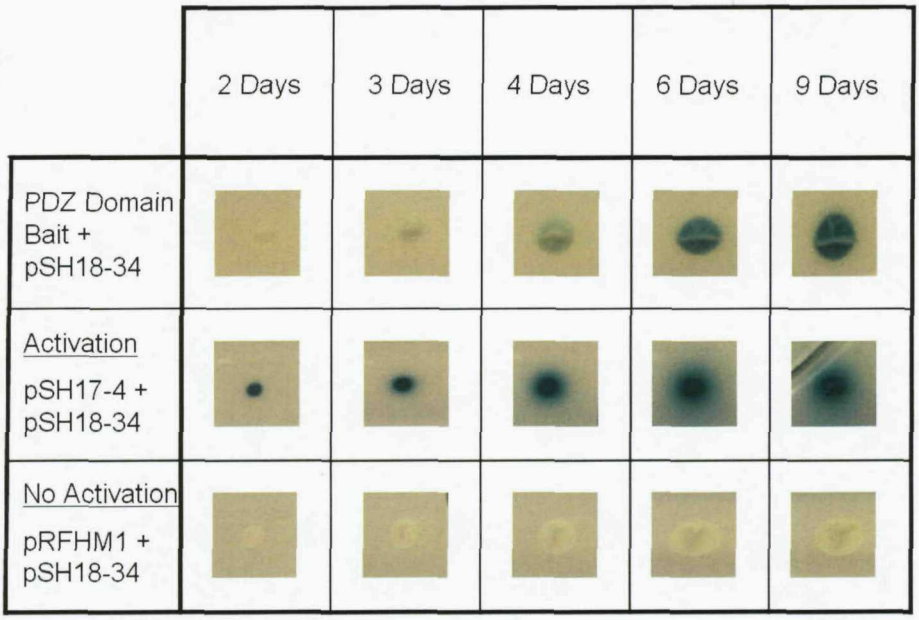

Figure 5.5. The PDZ domain can transactivate the LacZ gene. EGY48 transformed with the PDZ domain Bait construct and pSH18-34 turn blue after 3 days.

Figures 5.4 above show that after 9days yeast transformed with the C-Domain Bait and pSH18-34 shows no activation of the LacZ gene. The growth and colour are comparable to the No Activation control, and therefore indicate that the C-domain does not transactivate the LacZ gene.

In contrast, Figure 4.18 shows that yeast transformed with the PDZ domain Bait and pSH18-34 gradually turn blue during the 9day period, which indicates that this Bait is able to transactivate the LacZ gene.

Transactivation of the LEU2 reporter gene can also be assessed by transforming yeast with the pSH18-34 reporter, the Bait construct, and then growing them on minus leucine plates. If the bait is able to activate the LEU2 gene the yeast will grow on these plates, which can be compared to the same yeast grown on leucine containing plates. Consequently, this assay was conducted on YNB(Gal)-HUL plates, and YNB(Gal)-HU plates, respectively.

The results for this control assay are shown in Figures 5.7 and 5.7 below.

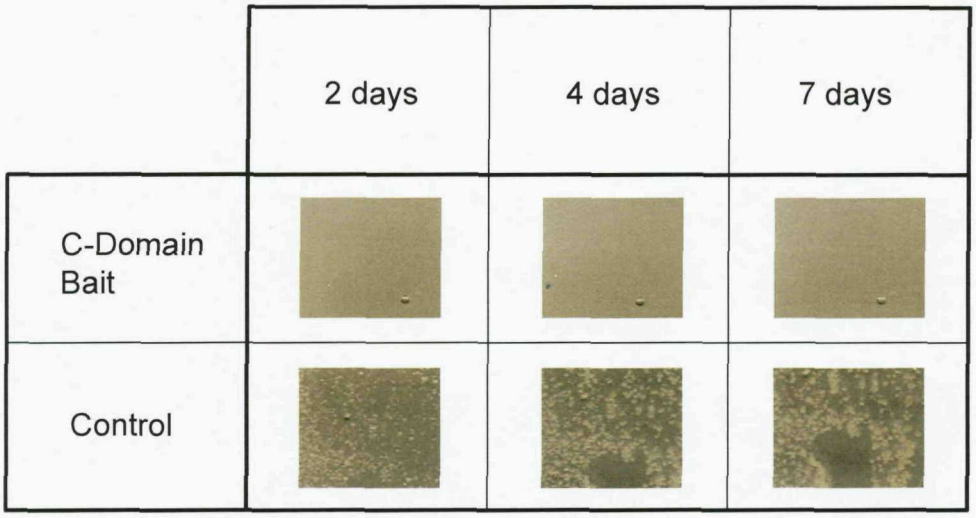

Figure 5.6. The C-Domain does not transactivate the LEU2 reporter gene. EGY48 transformed with the C-Domain Bait construct and pSH18-34 do not grow on minus leucine plates after 7 days.

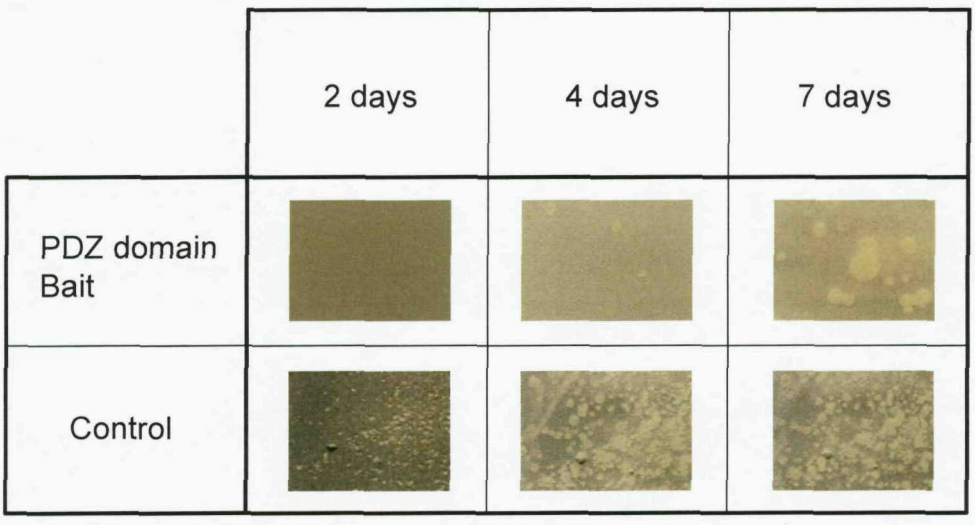

Figure 5.7 The PDZ domain can transactivate the LEU2 reporter gene. EGY48 transformed with the PDZ domain Bait construct and pSH18-34 grow on minus leucine plates after 4 days.

Figure 5.6 above shows that over the course of 7 days none of the yeast transformed with the C-Domain Bait/pSH18-34 grew, although they did grow on leucine containing plates. In contrast, EGY48 transformed with the PDZ domain/pSH18-43 did begin to grow after 4 days, which indicates that this Bait can transactivate the LEU2 gene.

	Transactivation		Repression
Bait	LacZ	LEU2	
C-Domain	No	No	Yes
PDZ	Yes	Yes	Partial

Table 5.1. Summary of the data for the potential C-Domain and PDZ Domain baits. The C-domain bait does not transactivate and can enter the nucleus more effectively than the PDZ domain bait. The C-domain bait is therefore more suitable to screen for MAST4 interacting proteins.

The results for this set of control experiments (see Table 5.1) show that the C-Domain Bait is able to enter the nucleus without exhibiting any transactivation. In contrast, the PDZ domain Bait appears to enter the nucleus less effectively than the C-Domain Bait, and shows clear transactivation of both reporter genes. Therefore, the C-Domain Bait was used within a YTH screen to look for interacting protein for MAST4.

5.2. The screen

The full details of the YTH screen performed using the C-domain of MAST4 are described in Chapter 2 (section 2.2). Briefly, yeast (EGY48) containing the pSH18-34 and the C-domain-pGilda bait were transformed with a rat brain cDNA library and plated onto YNB(Glu)-HUT plates. Transformed cells were collected, the viable count was calculated, and an appropriate density of cells were plated onto YNB(Gal)-HUTL x-Gal plates to assay reporter gene expression. Positive colonies were picked on day 5, 8, and 14 onto back-up YNB(Glu)-HUT plates. These colonies were re-streaked onto YNB(Gal)-HUTL x-Gal plates 3X to ensure maintenance of reporter gene expression. After the three rounds of selection there were 850 colonies consistently showing reporter gene expression.

5.3. Prioritisation of selected colonies

Due to the large number of positive colonies, the colonies were prioritised according to the strength of reporter gene expression. This was taken to be an indication of the strength of the protein-protein interaction occurring in the yeast and therefore allows the discrimination between low-to-high affinity interactions (Maple and Moller, 2007).

Colonies derived from the three rounds of selection were spotted onto YNB(Gal)-HUTL x-Gal plates to assay reporter gene expression. The amount of each colony spotted was crudely standardised ('equal' amounts picked onto a sterile tip) so that any subsequent difference in growth and colouration would represent an actual difference in reporter gene expression. At each time point the largest and bluest colonies were selected. Colonies were selected at time points 24, 48, 72, 96, and >96hrs. Colonies from time points up to 72hrs (157) were selected for further characterisation.

5.4. Cataloguing of prioritised library clones

Cataloguing of the prioritised colonies allows selected clones to be sequenced. PCR was performed on crude yeast extracts using pJG4-5 specific primers that flank the cDNA clone. The PCR product was then digested using the restriction endonuclease, *HaeIII*. Therefore, both the size and restriction digest profile was used to determine which clones were unique. The PCR product for unique clones was sequenced using the pJG4-5 specific primer, 5'-TFP. This primer allows sequencing over the fusion site between the cDNA clone and the acidic blob activation domain. Therefore, it is possible to determine if the clone is able to translate a protein that is in frame with the activation domain. The identity of sequenced clones was established using nucleotide-to-nucleotide BLAST searches (NCBI).

5.5. Profile of screen

The process of cataloguing prioritised clones led to the identification of a set of potential MAST4 interacting proteins, which are summarised in Table 5.2. The clones listed in Table 5.2 represent only those that were shown to be in-frame with the activation domain. Also, Table 5.2 shows how many times each in-frame clone was identified amongst the first '72hr' colonies (i.e. 157) and how many of these represented independent regions of the identified gene.

Clone identified	Number of times identified	Number of independent clones
Suppressor of K+ transport defect 3 (SKD3)	4	1
Synaptotagmin XI	7	2
14-3-3 beta	1	1
14-3-3 eta	8	1
14-3-3 theta	4	1
Nuclear inhibitor of PP1 (NIPP1)	32	1
Casein kinase II, alpha 1 polypeptide	1	1
WD repeat domain 5	1	1
Rtf1	8	1
Elongation factor RNA polymerase II	9	2
Elongation factor RNA polymerase II 2	30	1

Table 5.2. Summary of clones identified as potential interacting partners for the C-domain of MAST4. Only clones that were in-frame with the B42 activation domain are listed.

The primary sequence for these potential MAST4 interactors was analysed for the presence of identifiable domains. This process allows the identification of common features which may rationalise the interaction identified between these proteins and the C-domain of MAST4. The results of this analysis are illustrated below.

5.5.1. Suppressor of K+ transport defect 3 (SKD3)

The gene encoding SKD3 produces a protein with 677 residues that contains an ankyrin repeat domain and a AAA ATPase. This protein and the region encompassed by the identified clone are illustrated in Figure 5.8. This clone contains both the identifiable domains.

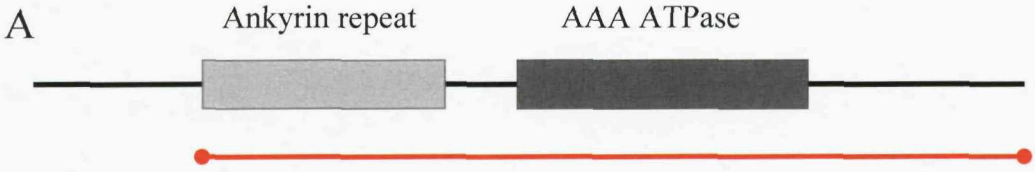

B

mmlsavlrrtapaprlflglikspslqsrggaynrsvitgdrgepqrlrtaawvrpga
ssvlfpgrgaatggrrgerteipyltaassgrgpspeetlpgqdswngvpnkaglgmw
alamalvvqcynknpsnkdaalmeaarannvqevrrllsegadvnarhklgwtalmva
aishnesvvqvllaagadpnlgddfssvyktaneqgvhslevlvtreddfnnrlnhra
sfkgctalhyavladdysivkellggganplqrnemghtpldyaregevmkllktset
kymekqrkreaeerrrfpleqrlkehiigqesaiatvgaairrkengwydeehplvfl
flgssgigktelakqtakymhkdakkgfirldmsefqerhevakfigsppgyigheeg
gqltkklkqcpnavvlfdevdkahpdvltimlqlfdegrltdgkgktidckdaifimt
snvasdeiaqhalqlrqealemsrnriaenlgdvqisdkitisknfkenvirpilkah
frrdeflgrineivyflpfchseliqlvnkelnfwakrakqrhnitllwdrevadvlv
dgynvhygarsikheverrvvnqlaaayeqdllpggctlritvedsdkqllkspelps
pqaekrpptlrleiidkdskthkldiqaplhpekvcyti

Figure 5.8. Domain structure of SKD3 and its primary sequence. A. The domain structure of SKD3. SKD3 contain an ankyrin repeat domain (light grey) and a AAA ATPase (dark grey). The region encompassed by the identified clone is illustrated in red. **B** - The primary sequence of rat norvegicus SKD3. The ankyrin repeat domain and AAA ATPase are illustrated in light grey and dark grey shaded areas, respectively. The region encompassed by the identified clone is illustrated by the red underline.

5.5.2. Synaptotagmin XI (SytXI)

The gene encoding SytXI produces a protein with 429 residues that contains two C2-1 domains and a transmembrane domain ™. This protein and the region encompassed by the identified clones are illustrated in Figure 5.9. Both clones contain the 2 C2-1 domains.

The synaptotagmin family of proteins are known to functional as calcium sensors in vesicle release at the plasma membrane (Reviewed in Sudhof, 2004). However, the C2 domain of synaptotagmin IV & XI do not bind calcium, which suggests that have a novel function (von Poser et al., 1997).

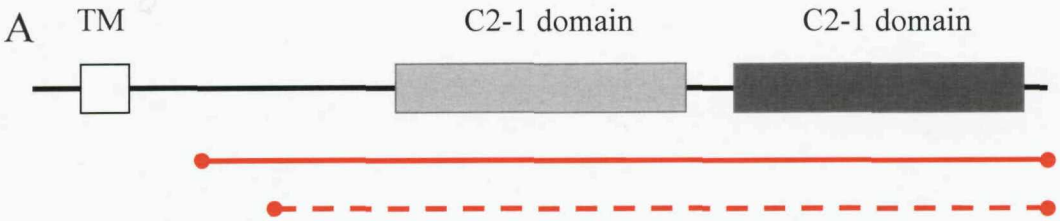

B

maeitnirpsfdvspvaagligasvlvvcvsvtvfvwtcchqqaekkhktppykfihm
lkgisiypetlsnkkkiikvrrdkdgshresgrgnllvnaesgllshdrdprgpspas
cidqlpikrdygeelrspmtsltpgeskptspsspeedvmlgsltfsvdynfpkkalv
vtiqeahglpvmdgqtqgsdpyikmtilpdkrhrvktrvlrktldpvfdetftfygip
ysqlqdlvlhflvlsfdrfsrddvigevmvplagvdpstgkvqltrdiikrniqkcis
rgelqvslsyqpvaqrmtvvvlkarhlpkmditglsdpyvkvnvyygrkriakkkthv
kkctlnpifnesfiydiptdllpdisieflvidfdrttknevvgrlilgahsvttsga
ehwrevcesprkpvakwhslsey

Figure 5.9. Domain structure of SytXI and its primary sequence. **A**. The domain structure of SytXI. SytXI contain two C2-1 domains (light grey) and a transmembrane domain (TM). The regions encompassed by the two identified clone are illustrated in red. **B** - The primary sequence of rat norvegicus SytXI. The two C2-1 domains are illustrated by the grey shaded areas. The regions encompassed by the 2 identified clones are illustrated by the red underline.

5.5.3. 14-3-3 beta

The gene encoding 14-3-3 beta produces a protein with 246 residues that contains a region homologous between the different 14-3-3 isoforms. This protein and the region encompassed by the identified clone is illustrated in Figure 5.10. This clone covers the full length of the 14-3-3 beta protein.

14-3-3 proteins exist as homo- and hetero-dimers that bind to phosphoserine containing motifs in various proteins (Reviewed in Darling et al., 2005). The 14-3-3 protein regulate various pathways including, signal transduction, apoptosis and the cell-cycle (Reviewed in Darling et al., 2005)

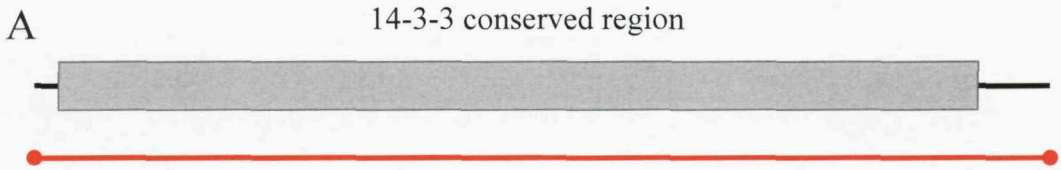

B

mtmdkselvqkaklaeqaeryddmaaamkavteqghelsneernllsvayknvvgarr
sswrvissieqkternekkqqmgkeyrekieaelqdicsdvlelldkylilnathaes
kvfylkmkgdyfrylsevasgdnkqttvsnsqqayqeafeiskkemqpthpirlglal
nfsvfyyeilnspekacslaktafdeaiaeldtlneesykdstlimqllrdnltlwts
enqgdegdagegen

Figure 5.10. Domain structure of 14-3-3 beta and its primary sequence. A. The domain structure of 14-3-3 beta. 14-3-3 beta contains a region that is homologous between each 14-3-3 isoform (light grey). The region encompassed by the identified clone is illustrated in red. **B** - The primary sequence of rat norvegicus 14-3-3 beta. The 14-3-3 homologous region is illustrated by the light grey shaded areas. The region encompassed by the identified clone is illustrated by the red underline.

5.5.4. 14-3-3 eta

The gene encoding 14-3-3 eta produces a protein with 246 residues that contains a region homologous between the different 14-3-3 isoforms. This protein and the region encompassed by the identified clone is illustrated in Figure 5.11. Apart from one residue at the N-terminus, this clone covers the full length of the 14-3-3 eta protein.

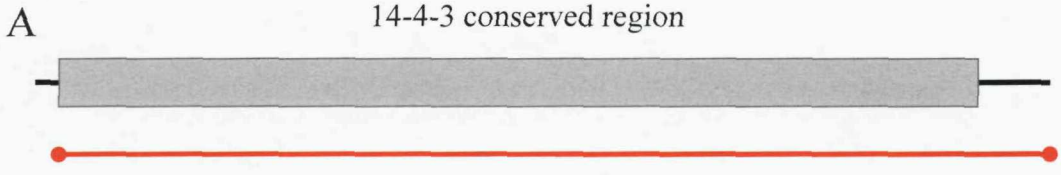

mgdreqllqrarlaeqaeryddmasamkavtelneplsnedrnllsvayknvvgarrs
swrvissieqktmadgnekklekvkayrekiekeletvcndvlalldkflikncndfq
yeskvfylkmkgdyyrylaevasgekknsvveaseaaykeafeiskehmqpthpirlg
lalnfsvfyyeiqnapeqacllakqafddaiaeldtlnedsykdstlimqllrdnltl
wtsdqqdeeagegn

Figure 5.11. Domain structure of 14-3-3 eta and its primary sequence. A. The domain structure of 14-3-3 eta. 14-3-3 eta contains a region that is homologous between each 14-3-3 isoform (light grey). The region encompassed by the identified clone is illustrated in red. **B** - The primary sequence of rat norvegicus 14-3-3 eta. The 14-3-3 homologous region is illustrated by the light grey shaded areas. The region encompassed by the identified clone is illustrated by the red underline.

5.5.5. 14-3-3 theta

The gene encoding 14-3-3 theta produces a protein with 245 residues that contains a region homologous between the different 14-3-3 isoforms. This protein and the region encompassed by the identified clone is illustrated in Figure 5.12. This clone covers the full length of the 14-3-3 theta protein.

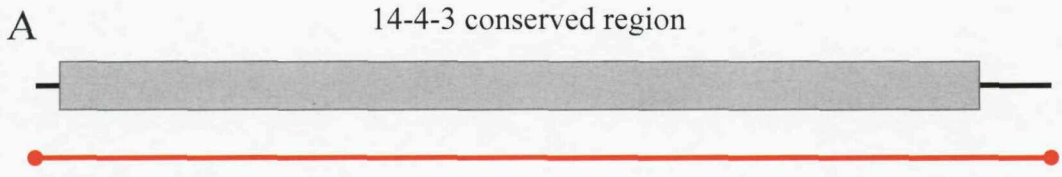

B

mekteliqkaklaeqaeryddmatcmkavteqgaelsneernllsvayknvvggrrsa
wrvissieqktdtsdkklqlikdyrekveselrsicttvlelldkylianatnpeskv
fylkmkgdyfrylaevacgddrkqtiensqgayqeafdiskkemqpthpirlglalnf
svfyyeilnnpelactlaktafdeaiaeldtlnedsykdstlimqllrdnltlwtsds
ageecdaaegaen

Figure 5.12. Domain structure of 14-3-3 theta and its primary sequence. A. The domain structure of 14-3-3 theta. 14-3-3 theta contains a region that is homologous between each 14-3-3 isoform (light grey). The region encompassed by the identified clone is illustrated in red. **B** - The primary sequence of rat norvegicus 14-3-3 theta. The 14-3-3 homologous region is illustrated by the light grey shaded areas. The region encompassed by the identified clone is illustrated by the red underline.

5.5.6. Nuclear inhibitor of PP1 (NIPP1)

The gene encoding NIPP1 produces a protein with 351 residues that contains forkhead-associated (FHA) domain. This protein and the region encompassed by the identified clone is illustrated in Figure 5.13. This clone covers the N-terminal half of NIPP1, which includes the FHA domain.

NIPP1 has been implicated in transcriptional repression via the inhibition of protein phosphatase 1 (PP1) as well a PP1-independent affect on spliceosome assembly (Reviewed in Ceulemans and Bollen, 2004).

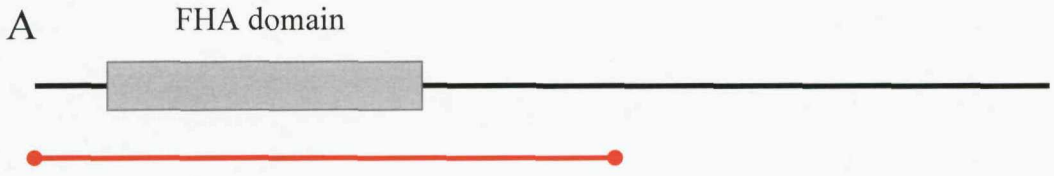

B

maaavnsgsslplfdcptwagkpppglhldvvkgdkliekliidekkyylfgrnpdlc
dftidhqscsrvhaalvyhkhlkrvflidlnsthgtflghirlephkpqqipidstvs
fgastraytlrekpqtlpsavkgdekmggeddelkgllglpeeeteldnltefntahn
kristltieegnldiqrpkrkrknsrvtfsdddeiinpedvdpsvgrfrnmvqtavvp
vkkkrmegsgslgleesgsrrmqnfafsgglygglppthsepgsqphgihgtaliggl
pmpypnlapdvdltpvvpsavtinptpnpavynpeavnepkkkkyakeawpgkkptps
lli

Figure 5.13. Domain structure of NIPP1 and its primary sequence. **A**. The domain structure of NIPP1. NIPP1 contains a forkhead-associated domain (light grey). The region encompassed by the identified clone is illustrated in red. **B** - The primary sequence of rat norvegicus NIPP1. The FHA domain is illustrated by the light grey shaded areas. The region encompassed by the identified clone is illustrated by the red underline.

5.5.7. Casein kinase 2 (CK2), alpha 1 polypeptide

The gene encoding CK2 alpha 1 polypeptide produces a protein with 391 residues that contains a serine/threonine kinase domain. This protein and the region encompassed by the identified clone is illustrated in Figure 5.14. This clone covers almost the full-length of the alpha 1 polypeptide, which includes the kinase domain.

Within the brain, CK2 has been associated with regulating synaptic transmission and plasticity (e.g. LTP), development and neuritogenesis (Reviewed in Blanquet, 2000).

A

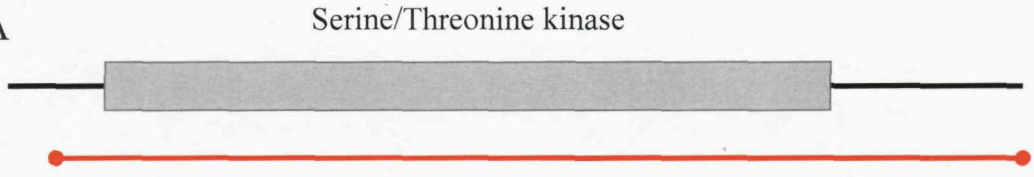

B

msgpvpsrarvytdvnthrpreywdyeshvvewgnqddyqlvrklgrgkysevfeain
itnnekvvvkilkpvkkkkikreikilenlrggpniitladivkdpvsrtpalvfehv
nntdfkqlyqtltdydirfymyeilkaldychsmgimhrdvkphnvmidhehrklrli
dwglaefyhpgqeynvrvasryfkgpellvdyqmydysldmwslgcmlasmifrkepf
fhghdnydqlvriakvlgtedlydyidkynieldprfndilgrhsrkrwerfvhsenq
hlvspealdfldkllrydhqsrltareamehpyfytvvkdqarmssagmaggstpvss
anmmsgissvptpsplgplagspviaaanslgipvpaaagaqq

Figure 5.14. Domain structure of CK2 and its primary sequence. **A**. The domain structure of CK2. CK2 contains a serine/threonine kinase domain (light grey). The region encompassed by the identified clone is illustrated in red. **B** - The primary sequence of rat norvegicus CK2 alpha 1 polypeptide. The kinase domain is illustrated by the light grey shaded areas. The region encompassed by the identified clone is illustrated by the red underline.

5.4.8. WD40 repeat domain 5 (Wdr5)

The gene encoding Wdr5 produces a protein with 334 residues that contains 7 WD40 repeats. This protein and the region encompassed by the identified clone is illustrated in Figure 5.15. This clone covers almost the full-length of Wdr5 protein, which includes the 7 WD40 repeats.

Wdr5 regulates the association between histone H3 and the MLL (mixed-lineage leukaemia 1) methyltransferase complex (MT), which promotes activation of gene transcription (Reviewed in Crawford and Hess, 2006).

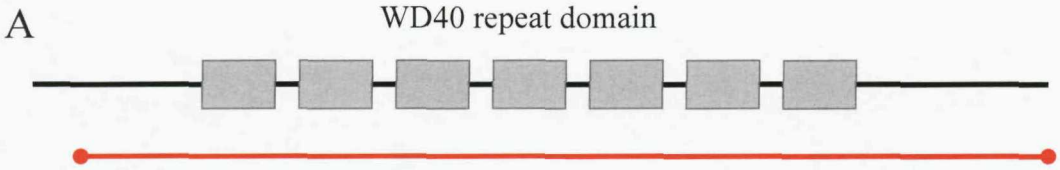

B

mateekkpeteaaraqptpsssatqskptpvkpnyalkftlaghtkavssvkfspnge
wlasssadklikiwgaydgkfektisghklgisdvawssdsnllvsasddktlkiwdv
ssgkclktlkghsnyvfccnfnpqsnlivsgsfdesvriwdvktgkclktlpahsdpv
savhfnrdgslivsssydglcriwdtasgqclktlidddnppvsfvkfspngkyilaa
tldntlklwdyskgkclktytghknekycifanfsvtggkwivsgsednlvyiwnlqt
keivqklqghtdvvistachpteniiasaalendktiklwksdc

Figure 5.15. Domain structure of Wdr5 and its primary sequence. **A**. The domain structure of Wdr5. Wdr5 contains 7 WD40 repeats (light grey). The region encompassed by the identified clone is illustrated in red. **B** - The primary sequence of rat norvegicus Wdr5. The WD40 repeats are illustrated by the light grey shaded areas. The region encompassed by the identified clone is illustrated by the red underline.

5.4.9. Rtf1

The clone identified aligns to the predicted rat homologue of the Paf1 complex component, Rtf1. The gene produces a protein with 715 residues that contains a Plus3 domain. This protein and the region encompassed by the identified clone is illustrated in Figure 5.16. This only encompasses the region containing the Plus3 domain.

Rtf1 is a component of the Paf1 complex, which is involved in regulating the elongation stage of transcription (Reviewed in Sims, III et al., 2004).

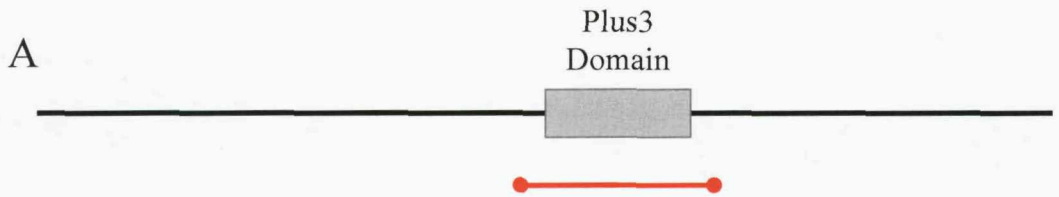

B

mrgrlcvgraaavaaavvaavavplaggqegspdgvrrgsrgttmvkkrkgrvvidsd
tedsgsdenldqellslakrkrsdseekeppvsqpaassdsetsdsddewtfgsnknk
kkgkarkvekkgamkkqankaassgssdrdssaessapeegevsdsdsnsssssdsd
ssssedeefhdgygedlmgdeedrarleqmtekereqelfnriekrevlkrrfeikkk
lktakkkekkekkkkqeeeqekkkltqiqesqvtshnkerrskrdekldkksqameel
kaerekrknrtaellakkqplktsevysddeeeedddksseksdrssrtsssdeeeek
eeippksqpvslpeelnrvrlsrhklerwchmpffaktvtgcfvrigignhnskpvyr
vaeitgvvetakvyqlggtrtnkglqlrhgndqrvfrlefvsnqeftesefmkwkeam
fsagmqlptldeinkkefsikealnykfndqdieeivkekerfrkappnyamkktqll
kekamaedlgdqdkakqiqdqlneleeraealdrqrtknisaisyinqrnrewnives
ekalvaeshnmrnqqmdpftrrqckptivsnsrdpavqaailaqlnakygsgalpdap
kevskgqgkdkdlnsksasdlsedlfkvhdfdvkidlqvpsseskalaitskappakd
gaprrslnledykkrrgli

Figure 5.16. Domain structure of Rtf1 and its primary sequence. **A**. The domain structure of Rtf1. Rtf1 contains a Plus3 domain (light grey). The region encompassed by the identified clone is illustrated in red. **B** - The primary sequence of rat norvegicus Rtf1. The Plus3 domain is illustrated by the light grey shaded area. The region encompassed by the identified is illustrated by the red underline.

5.4.10. ELL1, RNA polymerase II elongation factor

The clones identified align to the predicted rat homologue of the gene encoding ELL1 (eleven-nineteen lysine-rich leukaemia protein 1). This gene produces a protein with 634 residues that contains a region homologous between the ELL family and Occludin. This protein and the regions encompassed by the identified clones are illustrated in Figure 5.17. The longest clone covers the C-terminal half of ELL1, and both clones include the occludin homology region.

The ELL family of proteins are known to promote the elongation rate of transcription by inhibiting transient pausing through chromatin (Reviewed in Sims, III et al., 2004).

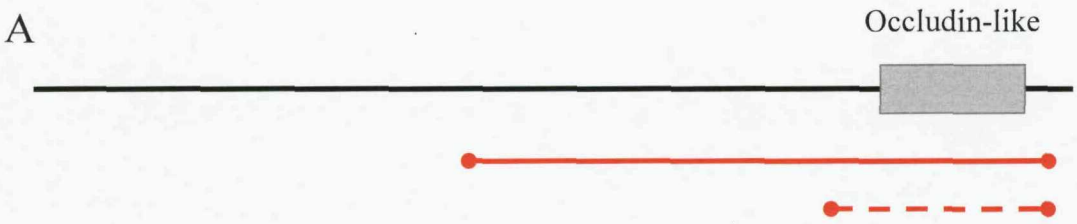

B

mqhvgwrrggagrregavaeeggggvmvakmaalkearsyglscgrvsdgsrvsvfhv
kltdsalkafesyrahqdsvslrpsirfegsqghisipqpdcpeevrafsfylsnigr
dspqgsfdciqqyvsshgdvhldclgsiqdkvtvcatddsyqkarqsmaqaeeetrsr
saivikaggrymgkkvqfrkpapgaadavpsrkratpinlasairkssggggassvvqr
pfrdrvlhllalrpyrkaelllrlqkdgltqadkdtldsllqqvasvnpkdgtctlqd
cmyknvqkdwpgysegdqqllkrvlmrklcqpqsattdssppprehrgsaspsqkrsqq
tdfidplaskkprishftqraqpilngrlgapnghetllpapvptpsdtlssshlppr
lepprthdpladvsndlghstqdykhqeatpapasrlglplltdfpqaeqpassshvh
srpkkkskkhkdkerppeerppapqpdsstapalptdapglngdcasvptstsetpdy
llkypaissseqrqsykndfnaeyseyrslharieqitrrftqldaqlrqlsqgseey
ettrgqilqeyrkikktntnysrekrrceylhrklahikrliaeydqrqlqawp

Figure 5.17. Domain structure of ELL1 and its primary sequence. **A**. The domain structure of ELL1. ELL1 contains a region homologous to that found in occludin (light grey). The regions encompassed by the identified clones are illustrated in red. **B** - The primary sequence of rat norvegicus ELL1. The occludin region is illustrated by the light grey shaded areas. The regions encompassed by the identified clones are illustrated by the red underline.

5.4.11. ELL2, RNA polymerase II elongation factor 2

The clone identified aligns to the predicted rat homologue of the gene encoding ELL2 (eleven-nineteen lysine-rich leukaemia protein 2). This gene produces a protein with 624 residues that contains a region homologous between the ELL family and Occludin. This protein and the region encompassed by the identified clone is illustrated in Figure 5.18. This clone encompasses the Occludin homology region.

B

maaggaaglreeqryglacgrlgqdnitvlhvkltetairaletyqsqklmkipkndp
fnevhnfnfylsnvgkdnpqgsfdciqqtlsssgasqlnclgfiqdkitvcatndsyq
mtrermtqaeeesrnrstkvikpggpyvgkrvqirkapqaisdavperkrstpmnpan
tirkmhggssvsqrpyrdrvihllalkaykkpellarlqkdgvnqkdknslgailqqv
anlnpkdlsytlkdyvfkelqrdwpgysetdkqtldlvlsrklnpsqnagtsrpespm
csskdaasspqkrpldsdfidpltnkkarishltnrvpptlnghlnptnekscasllp
ppaaaaiptpsplpsthlpvsnptqtvnsnsnspstpegrgtqdlpvdsfsqnssife
dqqdkytsrtcleetlpsssallkcpkpmeeehpvshkkskkkskkhkekdqikkhdi
esreekekdlqreetaklsndspnpnegvkeectasmepsstielpdylikyiaivsy
eqrqnykddfnaeydeyralharmetvarrfikldaqrkrlspgskeyqnvheevlqe
yqkikqsspnyheekyrceylhnklahikrligefdqqqaeswh

Figure 5.18. Domain structure of ELL2 and its primary sequence. **A**. The domain structure of ELL2. ELL2 contains a region homologous to that found in occludin (light grey). The region encompassed by the identified clone is illustrated in red. **B** - The primary sequence of rat norvegicus ELL2. The occludin region is illustrated by the light grey shaded areas. The region encompassed by the identified clone is illustrated by the red underline.

5.5. Post-screen controls

To confirm that each clone is only capable of activating the reporter genes in the presence of the C-domain bait, the purified prey plasmids were tested for transactivation and the original interaction re-constituted.

Each identified clone was rescued into the electrocompetent bacterial strain XL1-blue and crude DNA preparations were made. Restriction digests of the DNA using EcoRI/XhoI allowed selection of bacterial colonies containing the pJG4-5 vector, which contains the library clone. High quality DNA preparations were then made and the construct sequenced to confirm its identity.

The purified prey plasmids were transformed back into yeast containing the pSH18-34 reporter construct. Transformed yeast were then spotted 4X onto YNB(Gal) -HUTL x-Gal plates to assay reporter gene expression. None of the purified prey plasmids were able to grow or turn blue on the test plates and therefore did not exhibit transactivation of the reporter genes.

To re-constitute the original interaction, yeast containing the prey plasmid and pSH18-34 were transformed with the C-domain bait. Transformed yeast were spotted 4X onto -YNB(Gal) HUTL x-Gal plates to assay reporter gene expression. The results for this experiment are illustrated in Figure 5.19.

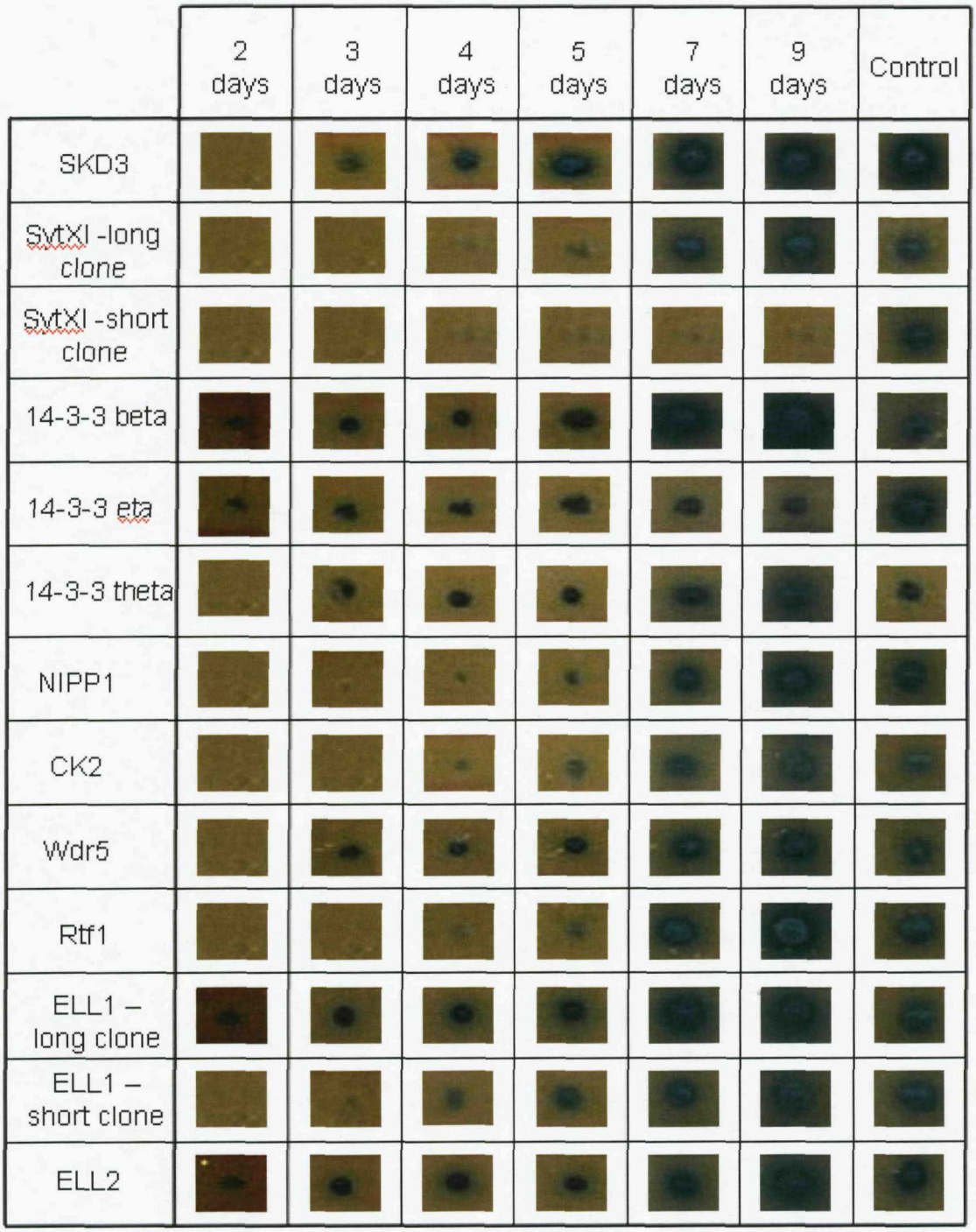

Figure 5.19. Reconstituted interactions from the YTH screen with the C-domain of MAST4. Yeast (EGY48) containing pSH18-34 were sequentially transformed with the purified prey plasmid (pJG4-5+library clone) and the C-domain bait (pGilda). Transformed yeast were spotted 4X onto YNB(Gal) -HUTL x-Gal plates and reporter gene expression followed over 9 days. A representative colony is illustrated for each interaction. In each case, the control is the colony originally showing reporter gene expression for this clone (from 7day time point). See text for abbreviations.

The reporter gene expression illustrated in Figure 5.19 has been scored and tabulated as shown in Table 5.3 below.

Clone	Score
Suppressor of K+ transport defect 3 (SKD3)	+++
Synaptotagmin XI - long clone	+
Synaptotagmin XI - short clone	-
14-3-3 beta	++++
14-3-3 eta	++++
14-3-3 theta	+++
Nuclear inhibitor of PP1 (NIPP1)	++
Casein kinase II, alpha 1 polypeptide	+
WD repeat domain 5	+++
Rtf1	+
Elongation factor RNA polymerase II - long clone	++++
Elongation factor RNA polymerase II - short clone	+++
Elongation factor RNA polymerase II 2	++++

Table 5.3. Scoring of reporter gene expression for potential MAST4 interacting partners. Reporter gene expression was scored according to the emergence, number (of colonies) and intensity of reporter gene expression for each clone.

5.6. Discussion

The LexA yeast-two hybrid system has been used to identify potential interacting proteins for MAST4. Following the appropriate controls, the C-terminal half of MAST4 (called the 'C-domain') was used as the bait to screen a rat brain cDNA library for potential interacting proteins.

The YTH screen identified 11 separate proteins that may potentially interact with the C-domain of MAST4. Some of these proteins were identified multiple times and/or independently. The 11 proteins described above were only those that were in-frame with the B42 activation domain and did not transactivate the reporter genes.

The original interactions were reconstituted using the purified library clones. This experiment confirmed the original interactions as well as allowing the relative strength

of the interaction to be assessed; the relative strength of interactions in the YTH system generally correlates with in vitro biochemical studies (Estojak et al., 1995). The results for this control experiment clearly showed that the RNA polymerase II elongation factors and the 14-3-3 proteins lead to the strongest interactions as assayed by reporter gene expression. However, these two sets of proteins, like the potential interactors in general, do not appear to share any common features which may rationalise the interaction with MAST4. This observation is illustrated by the sequence analysis described in section 5.4, which shows there are no common domains between the various proteins.

Due to the lack of any obvious candidates to prioritise for further analysis, it was decided to perform a secondary screen. This screen involved expressing the C-domain of MAST4 fused to monomeric red fluorescent protein (mRFP) with each candidate fused to green fluorescent protein (GFP). This would therefore allow co-localisation of the interacting proteins to be observed, which would confirm the interaction identified from the YTH screen as well as revealing information about the expression of these proteins.

The results of this set of experiments, and a fuller description of the candidate interactors, are described in Chapter 6.

Chapter 6 - Expression analysis of MAST4 candidate interactors

6. Introduction

The expression analysis described in chapter 3 suggests that MAST4 may play a role in specific tissues and brain regions. In particularly, the expression of MAST4 in the dentate gyrus is dynamically regulated by synaptic activity. The domain structure of MAST4, like the MAST family in general, suggests that this role may involve protein interactions via its PDZ domain and signalling via its kinase domain. However, unlike these family members MAST4 contains a noticeable extension of its C-terminus (labelled as its 'C-domain'), which may allow the PDZ & kinase domains to function within a context specific to MAST4.

To investigate the function conferred by the C-domain of MAST4 the yeast-two hybrid system was chosen to identify potential interacting partners. This screen identified multiple candidates with a variety of functions. Although some of the candidates appeared to interact more strongly than others (e.g. the isoforms of 14-3-3 and ELL proteins, Table 5.3), there was not a common structural element between the candidates that could rationalise the observed interactions. Therefore, it was decided to perform a secondary screen using co-expression in HEK293 cells. This involves the generation of fluorophore-tagged fusion protein for each of the candidate interacting partners & the C-domain of MAST4. These are then used in single or double transfections (i.e. with or without the C-domain of MAST4). The single transfections can potential reveal important information about the subcellular localisation of fluorophore-tagged protein, which can be compared to known expression patterns in vivo. Following, co-transfection with the C-domain of MAST4, the candidate interacting proteins may change subcellular localisation and/or exhibit co-localisation. A change in the expression pattern of a candidate interactor will strongly suggest binding to the C-domain of MAST4, which will confirm the interaction outside of the YTH system; and, co-localisation will suggest targeting of the two potential interacting proteins to the same region of the cell. Therefore, the expression analysis can confirm an interaction observed in the YTH system and provide initial data on whether it occurs in vivo.

To allow observation of co-localisation, the C-domain of MAST4 was cloned in-frame into the mRFP expressing vector pGRFP, and cDNA for each candidate interacting protein (from the YTH screen) was cloned in-frame into the vector pEGFP. Due to problems with subcloning (e.g. a point mutation in the cloning site, internal restriction

sites) the cDNA for some of the candidate interactors only 8 clones from the YTH screen were characterised further (Table 6.1). Prior to assessing any potential co-localisation, the molecular weight of the fluorophore tagged proteins was assayed using western blot analysis.

6.1. Biochemical characterisation of expression constructs

Western blotting was used to confirm the expression constructs used within this study were off the correct size. Each construct was transiently transfected into HEK293 cells using the lipofectamine method (Invitrogen). Cells were collected, resuspended in 1X SDS sample buffer and electrophoresed through a 10% SDS-Polyacrylamide gel. Following transfer to nitrocellulose, the immobilised proteins were probed using a GFP specific primary antibody and visualised using enhanced chemiluminescence.
The predicted size of the expression constructs are listed in Table 6.1 below.

Name	Size of clone (kDa)	Predicted size of GFP fusion protein (kDa)	Predicted size equals size on a western blot
SytXI	≈41.6	≈68.6	Yes
14-3-3 beta	≈28.1	≈55.1	Yes
14-3-3 eta	≈28.1	≈55.1	Yes
NIPP1	≈22.5	≈49.5	Yes
CK2	≈44.2	≈71.2	Yes
Rtf1	≈18.2	≈45.2	Yes
ELL1	≈18.7	≈45.7	Yes
ELL2	≈24.5	≈51.5	Yes

Table 6.1. Size of GFP-tagged fusion proteins use for expression analysis.

As well as the candidate interacting proteins, the expression of the C-domain tagged to GFP was also investigated using western blotting.
The results for this western blot are illustrated in Figure 6.1 below. As can be seen, all of the candidate interactors resolve to molecular weights that generally match those predicted. The GFP-tagged C-domain construct should produce a protein of ≈180kDa. However, the protein actually detected is ≈80kDa. This may due to the protein being

tagged C-domain was fully sequenced, and due to overlap in the sequencing the region covering the truncated protein was sequenced 2-3 times. Therefore, this protein may being cleaved before/during the extraction process even though a protease inhibitor was included in the extraction buffer. Alternatively, there may be secondary structure within this region which blocks translation of the DNA sequence.

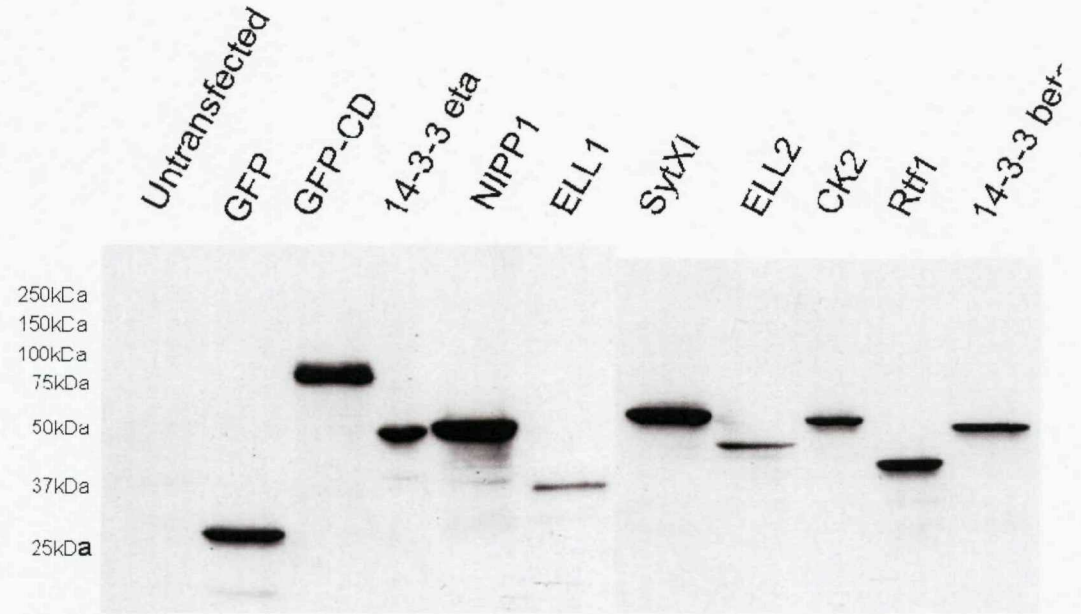

Figure 6.1. Western blot of C-domain and candidate interactors fused to EGFP. HEK293 cells were transiently transfected with each expression construct. Cell extracts were electrophoresed through a 10% gel, transferred and probed with a EGFP specific primary antibody. Bound primary was visualised using a horseradish peroxidase conjugated secondary antibody and enhanced chemiluminescence.

The following sections describe the expression patterns observed for the fluorophores used, the C-domain of MAST4 and its candidate interactors. The transfection efficiency was typically >70%, which therefore allowed a large pool of transfected cells to be screened for the characteristic expression patterns for each construct. The images illustrated are from a single transfection where at least 3 representative images were collected which reflected the patterns of expression observed for each individual transfection.

6.2. Expression of EGFP and mRFP in HEK293 cells

The C-domain of MAST4 and each of the interactors were tagged to fluorophores that may effect the targeting of these proteins within the cell. Therefore, to clarify if the fluorophores are targeted to any particular region of HEK293 cells their expression was investigated. As can be seen from Figures 6.2 & 6.3, the expression of both fluorophores is generally diffuse. There is some fluorescence within the nucleus, but this may be due to both fluorophores being smaller than the exclusion limit for passive diffusion into this subcellular compartment (i.e. everything >40kDa is excluded). However, there is also some atypical aggregation of these expression constructs within the transfected cells. This may be due to excessively high levels of the expression constructs being present following transfection.

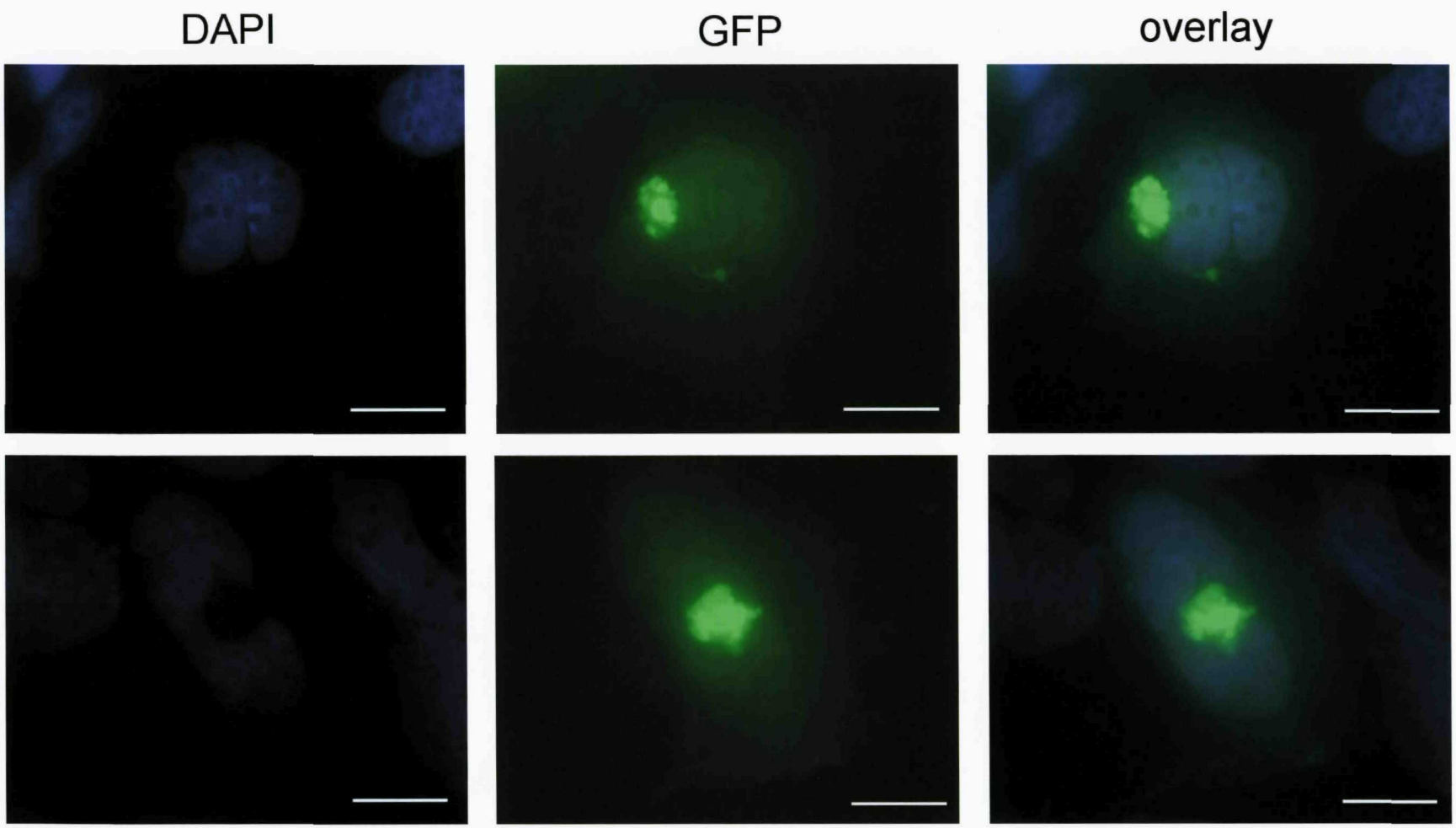

Figure 6.2. Expression of enhanced green fluorescent protein (EGFP) in HEK293 cells. HEK293 cells were transiently transfected with pEGFP. Following fixation with 4% PFA, cells were stained with DAPI and mounted. Both the upper and lower panel illustrate representative cells expressing eGFP. Scale bar = 35µm.

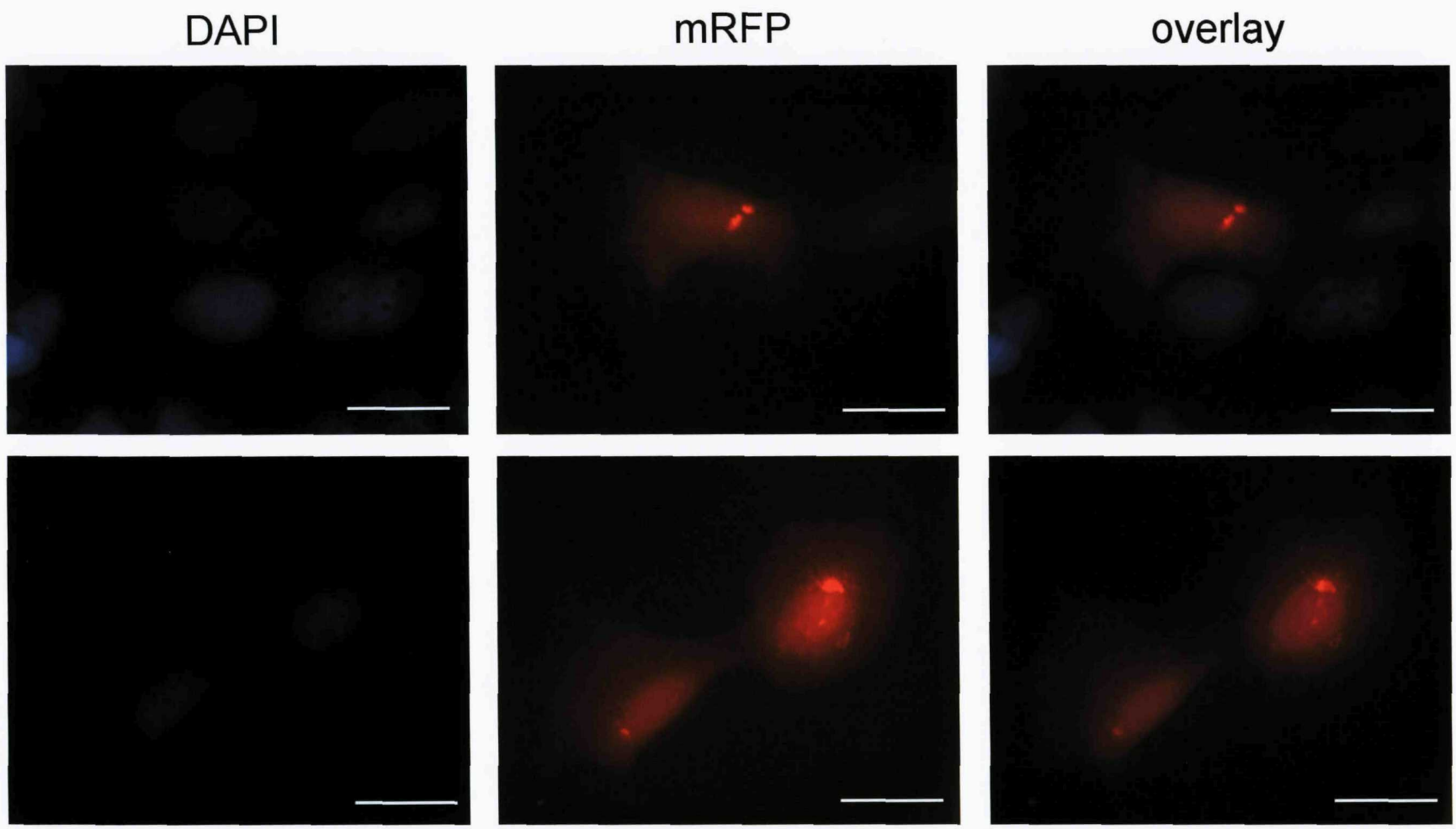

Figure 6.3. Expression of monomeric red fluorescent protein (mRFP) in HEK293 cells. HEK293 cells were transiently transfected with pGRFP. Following fixation with 4% PFA, cells were stained with DAPI and mounted. Both the upper and lower panel illustrate representative cells expressing mRFP. Scale bar = 35µm.

6.3. Expression of EGFP-CD and mRFP-CD in HEK293 cells

The expression of the C-domain of MAST4 was investigated by cloning the cDNA used for the YTH screen into the vectors pGRFP and EGFP. This therefore allowed the C-Domain to be expressed as a mRFP and GFP-tagged fusion proteins, respectively. The expression of these constructs is illustrated in Figures 6.4 to 6.6.

As can be seen from Figures 6.4 & 6.5 the C-domain of MAST4 is exclusively expressed within the nucleus of HEK293 cells. This expression appears localised to regions of the nucleus that are not stained by DAPI and therefore deficient in chromatin (Kapuscinski, 1995). This is most clearly illustrated by Figure 6.6, which also reveals a more distinct pattern of expression within substructures of these chromatin deficient regions.

Throughout this expression study there was a persistent problem with generating sufficient contrast within bright field images. Therefore, nuclei were stained with DAPI to reveal the morphology of the nucleus and thus the viability of the cell. This problem is best illustrated by Figure 6.4, which shows the result of an extensive effort to generate a bright field image using phase contrast. Therefore, where necessary nuclei have been stained with DAPI to verify the viability of imaged cells.

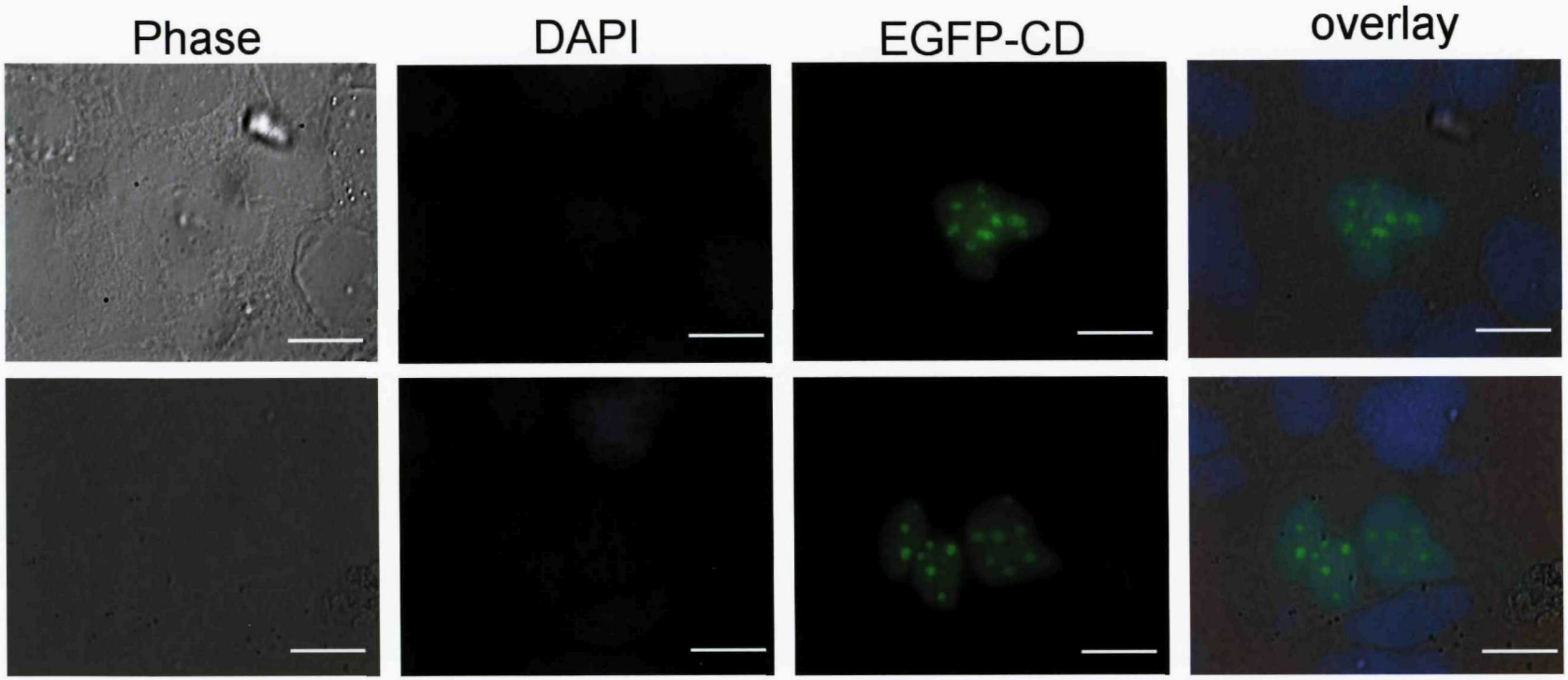

Figure 6.4. Expression of MAST4 C-domain fused to EGFP (EGFP-CD) in HEK293 cells. HEK293 cells were transiently transfected with pGRFP-CD. Following fixation with 4% PFA, cells were stained with DAPI and mounted. Both the upper and lower panel illustrate representative cells expressing pEGFP-CD. The expression of EGFP-CD appears confined to particular structures within the nucleus. Scale bar = 35µm.

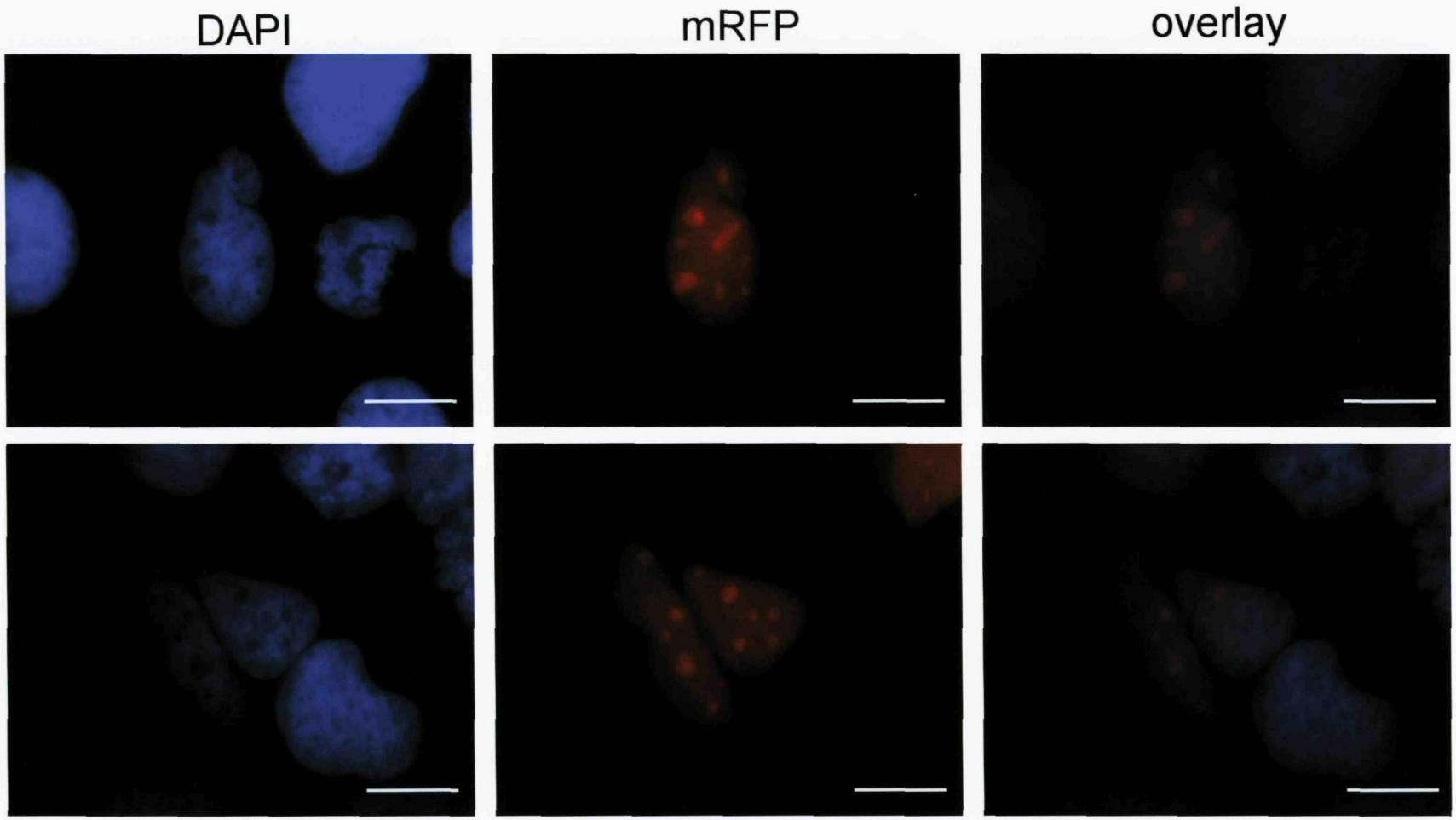

Figure 6.5. Expression of MAST4 C-domain fused to mRFP (mRFP-CD) in HEK293 cells. HEK293 cells were transiently transfected with mRFP-CD. Following fixation with 4% PFA, cells were stained with DAPI and mounted. Both the upper and lower panel illustrate representative cells expressing mRFP-CD. The expression of mRFP-CD appears confined to structures within the nucleus. Scale bar = 35µm.

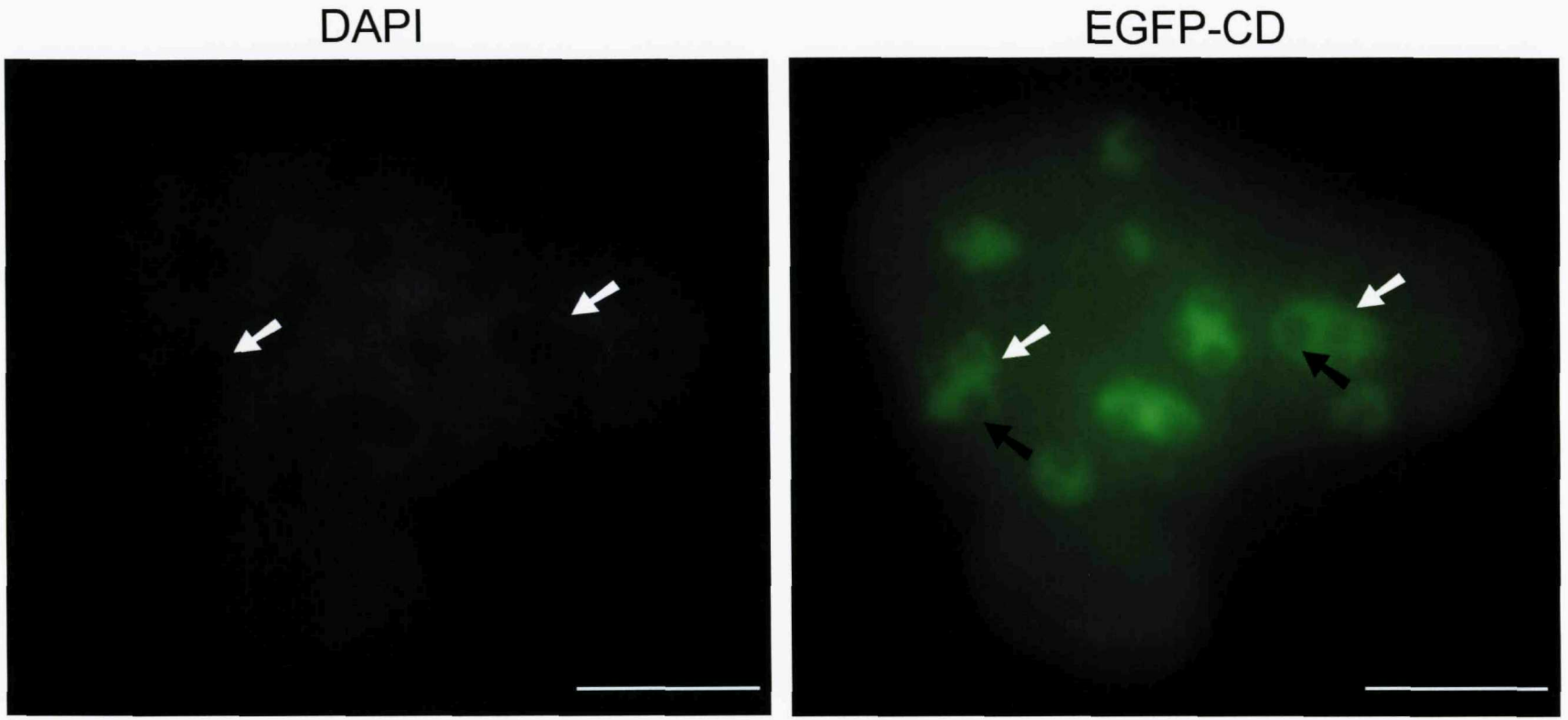

Figure 6.6. The C-domain of MAST4 is expressed in chromatin deficient regions of HEK293 cell nuclei. HEK293 cells were transiently transfected with pEGFP-CD. Following fixation with 4% PFA, cells were stained with DAPI and mounted. EGFP-CD appears localised in chromatin deficient regions (white arrows). However, these regions also contain structures that do not express EGFP-CD (black arrows). Scale bar = 35µm.

6.4. Expression of Synaptotagmin XI and co-expression with the C-domain of MAST4

Figure 6.7 illustrates the expression pattern for the Synaptotagmin XI clone isolated from the YTH screen when fused to EGFP. This patterns exhibits as small puncta within the nuclei of transfected HEK293 cells. Figures 6.8. and 6.9. illustrate the pattern of expression found by co-transfecting mRFP-CD and EGFP-SytXI. The fluorescence observed with a EGFP specific filter exhibits the same pattern of expression as that observed with the single transfection of EGFP-SytXI, as shown in Figure 6.7. The pattern of expression observed with an mRFP specific filter is similar to the single transfection of mRFP-CD illustrated in Figure 6.5. However, there are also potential points of specific co-localisation other than the general expression of both constructs within the nucleus.

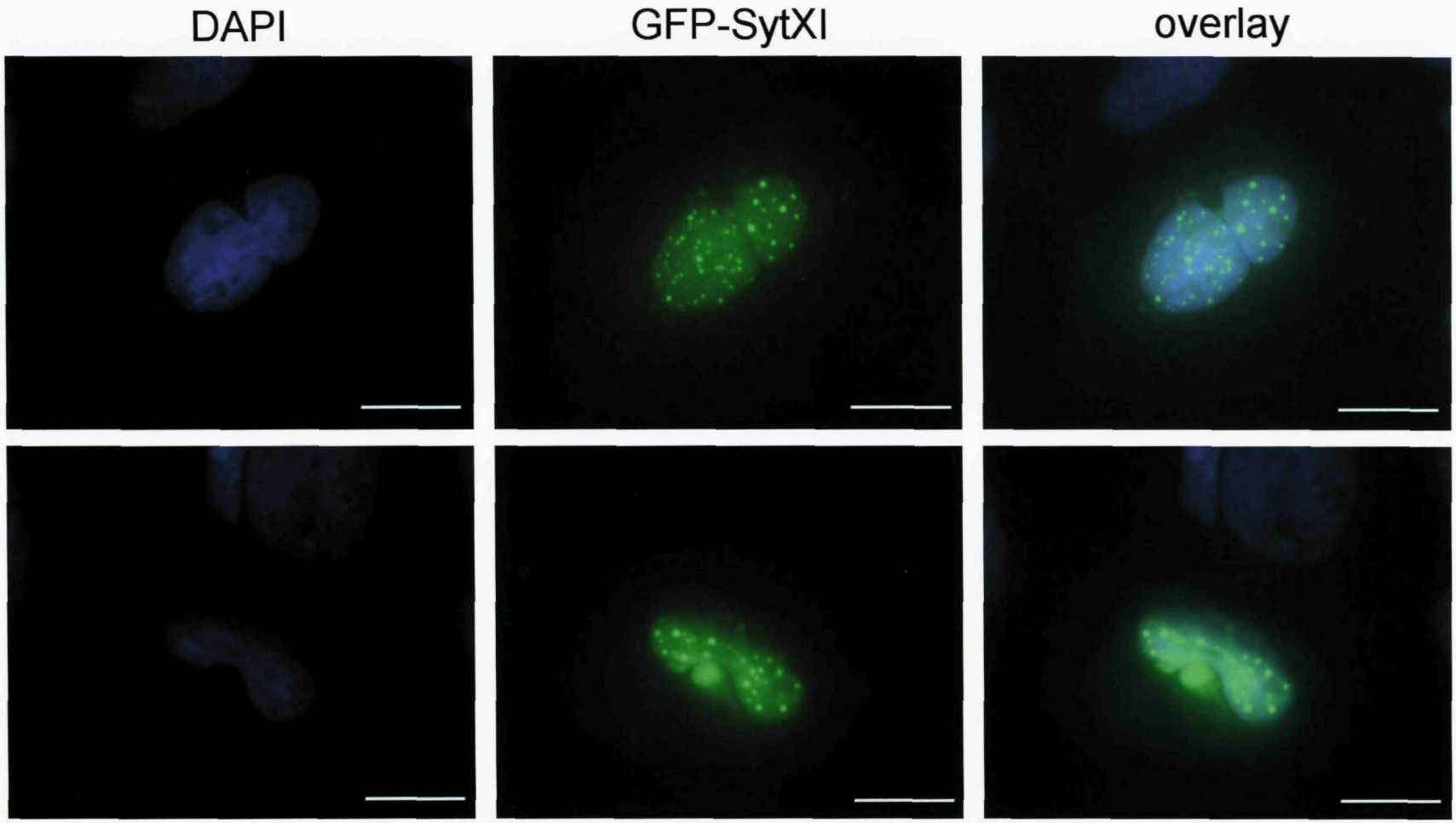

Figure 6.7. Expression of Synaptotagmin XI fused to EGFP (EGFP-SytXI) in HEK293 cells. HEK293 cells were transiently transfected with EGFP-SytXI. Following fixation with 4% PFA, cells were stained with DAPI and mounted. Both the upper and lower panel illustrate representative cells expressing EGFP-SytXI. The expression pattern for EGFP-SyXI appears punctuate in the nucleus of transfected cells.
Scale bar = 35µm.

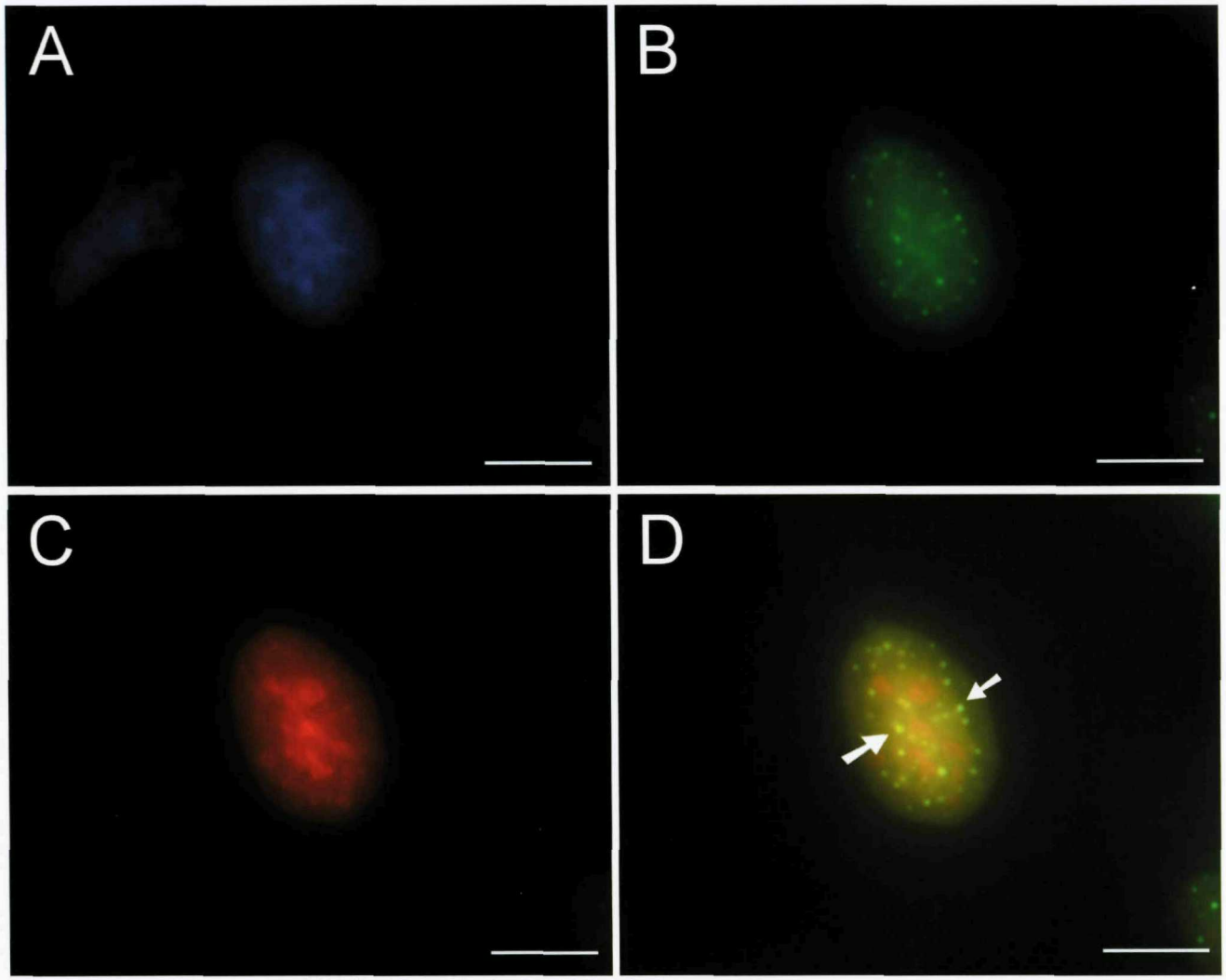

Figure 6.8. Co-expression of EGFP-SytXI & EGFP-CD in HEK293 cells. HEK293 cells were transiently transfected with EGFP-SytXI & EGFP-CD. Following fixation with 4% PFA, cells were stained with DAPI and mounted. (A) HEK293 cell stained with DAPI. (B) Fluorescence derived from a EGFP selective filter. (C) Fluorescence derived from a mRFP selective filter. (D) Overlay of EGFP and mRFP fluorescence. Representative regions of co-localisation are indicated with white arrows Scale bar = 35µm.

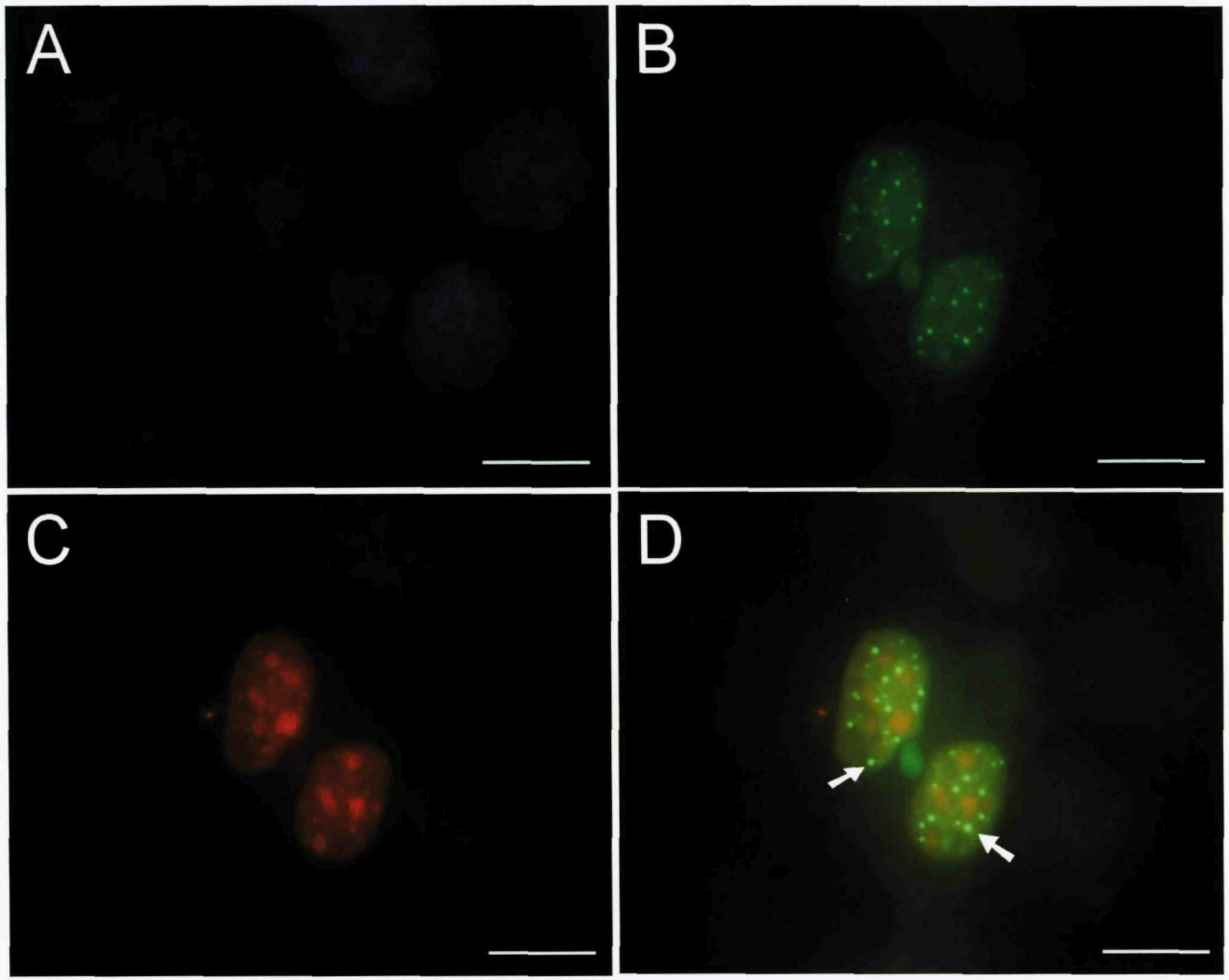

Figure 6.9. Co-expression of EGFP-SytXI & mRFP-CD in HEK293 cells. HEK293 cells were transiently transfected with EGFP-SytXI & EGFP-CD. Following fixation with 4% PFA, cells were stained with DAPI and mounted. (A) HEK293 cell stained with DAPI. (B) Fluorescence derived from a EGFP selective filter. (C) Fluorescence derived from a mRFP selective filter. (D) Overlay of EGFP and mRFP fluorescence. Representative regions of co-localisation are indicated with white arrows Scale bar = 35µm.

6.5. Expression of 14-3-3 beta and co-expression with the C-domain of MAST4

Figure 6.10 illustrates the expression pattern for the 14-3-3 clone isolated from the YTH screen when fused to EGFP. This patterns exhibits as puncta within the nuclei of transfected HEK293 cells. Figures 6.11. and 6.12. illustrate the pattern of expression found by co-transfecting mRFP-CD and EGFP-14-3-3 beta. The fluorescence observed with a EGFP specific filter exhibits the same pattern of expression as that observed with the single transfection of EGFP-14-3-3, as shown in Figure 6.10. The pattern of expression observed with an mRFP specific filter is similar to the single transfection of mRFP-CD illustrated in Figure 6.5. Other than the general expression of both constructs within the nucleus, there does not appear to be any evidence of a specific colocalisation of the expressed proteins.

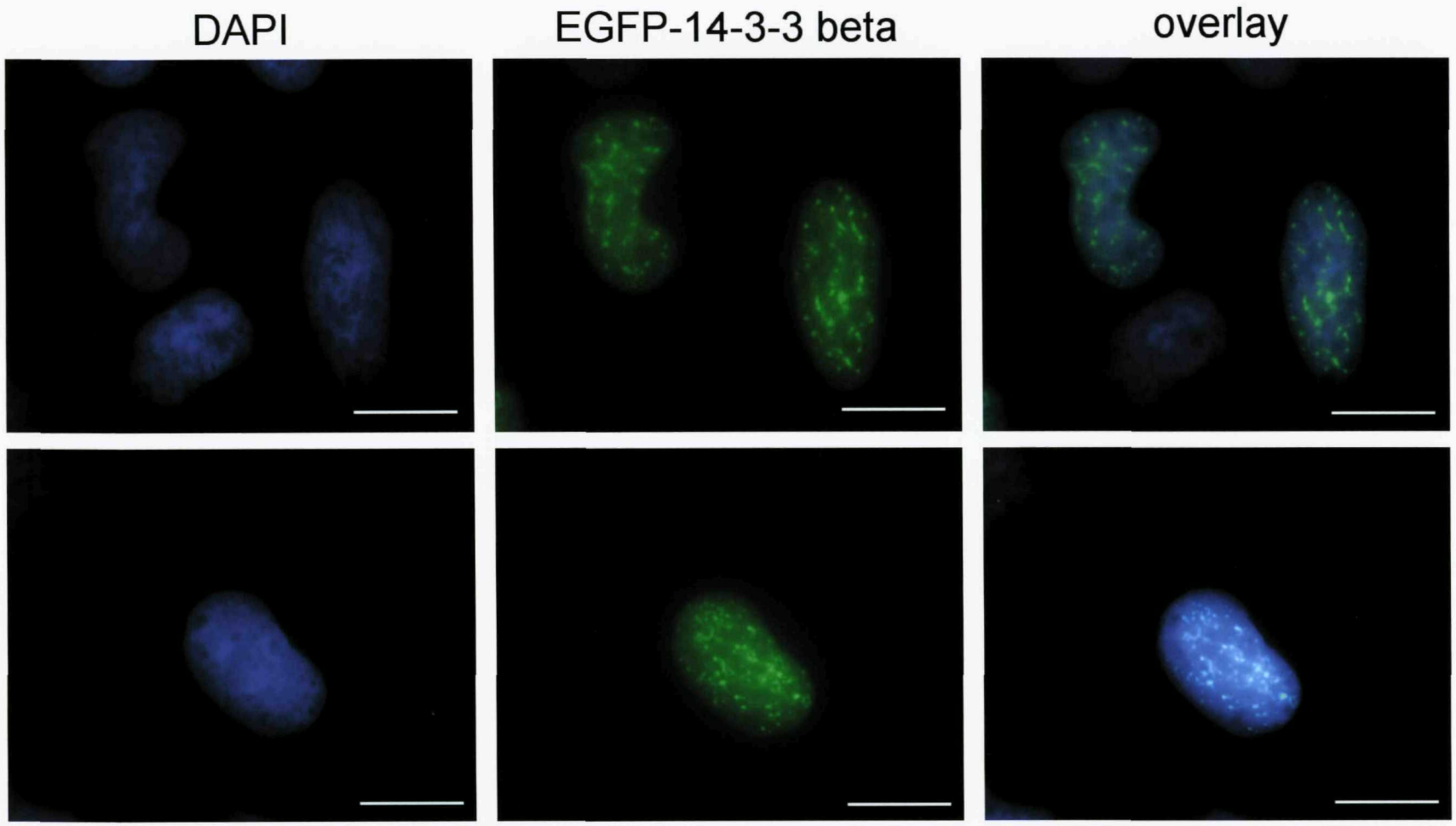

Figure 6.10. Expression of 14-3-3 beta fused to EGFP (EGFP-14-3-3 beta) in HEK293 cells. HEK293 cells were transiently transfected with EGFP-14-3-3 beta. Following fixation with 4% PFA, cells were stained with DAPI and mounted. Both the upper and lower panel illustrate representative cells expressing EGFP-14-3-3 beta. The expression of EGFP-14-3-3 beta appears punctuate within the nuclei of transfected cells. Scale bar = 35µm.

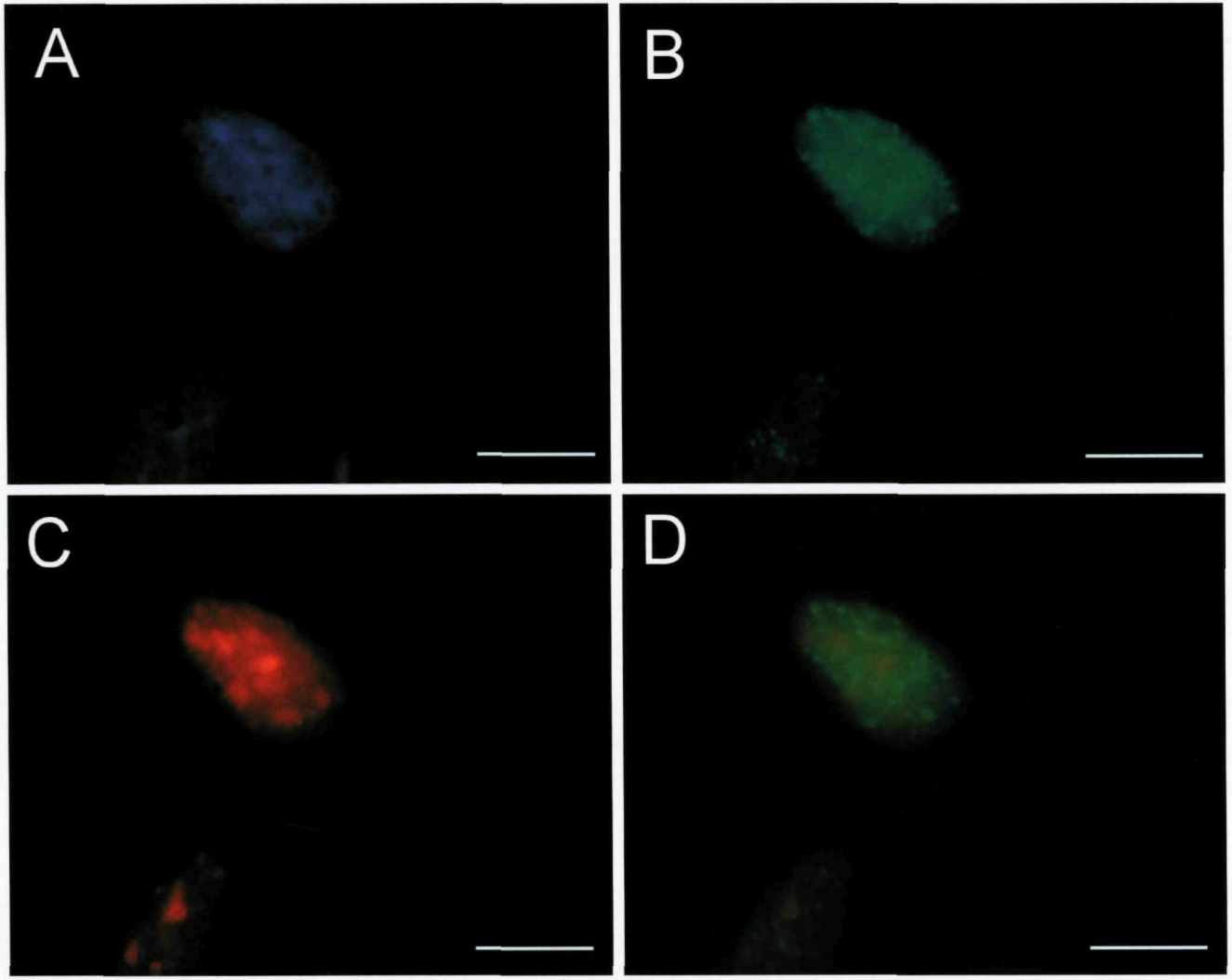

Figure 6.11. Co-expression of EGFP-14-3-3 beta & mRFP-CD in HEK293 cells. HEK293 cells were transiently transfected with EGFP-14-3-3 beta & EGFP-CD. Following fixation with 4% PFA, cells were stained with DAPI and mounted. (A) HEK293 cell stained with DAPI. (B) Fluorescence derived from a EGFP selective filter. (C) Fluorescence derived from a mRFP selective filter. (D) Overlay of EGFP and mRFP-CD fluorescence. Scale bar = 35μm.

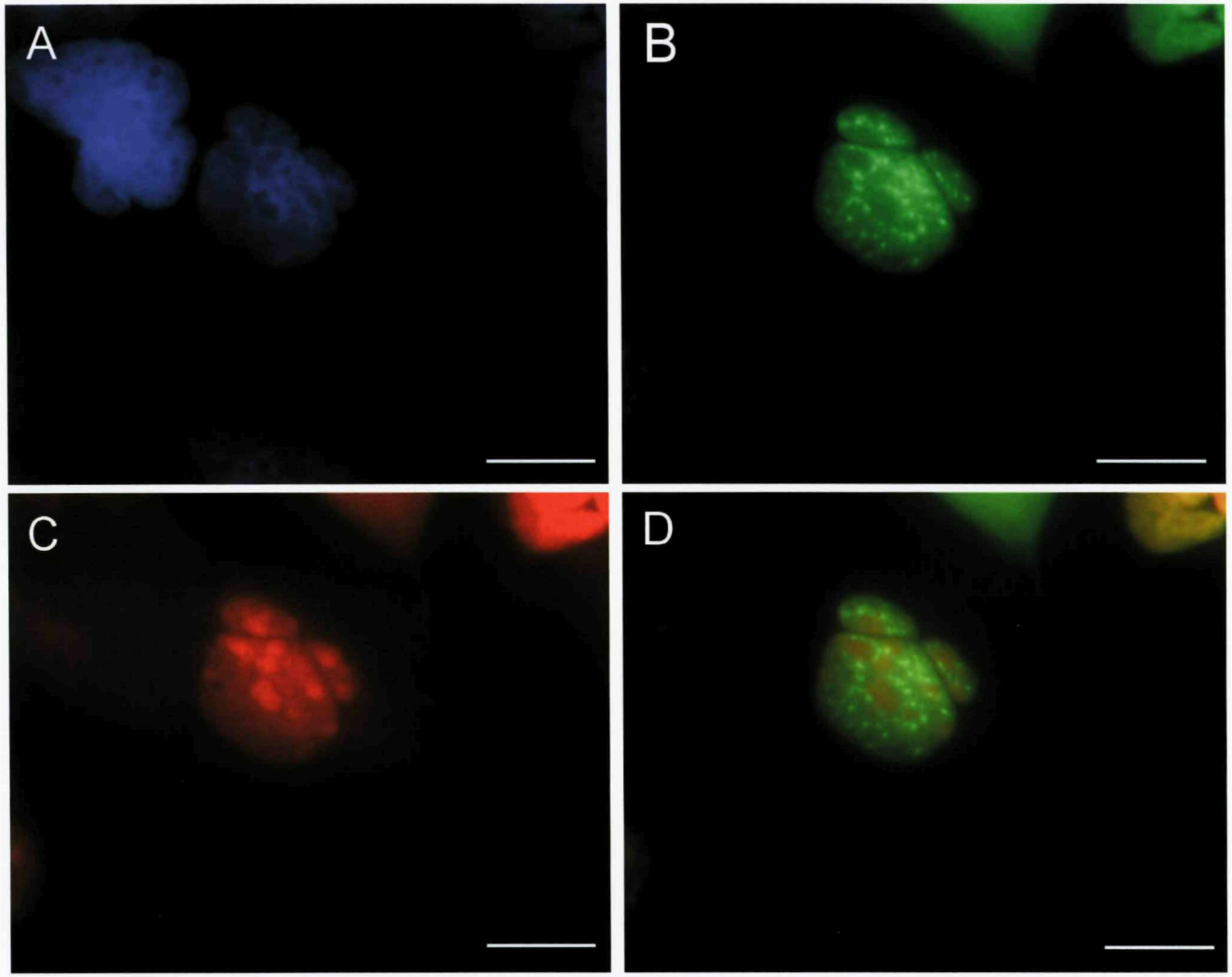

Figure 6.12. Co-expression of EGFP-14-3-3 beta & mRFP-CD in HEK293 cells. HEK293 cells were transiently transfected with EGFP-14-3-3 beta & EGFP-CD. Following fixation with 4% PFA, cells were stained with DAPI and mounted. (A) HEK293 cell stained with DAPI. (B) Fluorescence derived from a EGFP selective filter. (C) Fluorescence derived from a mRFP selective filter. (D) Overlay of EGFP and mRFP-CD fluorescence. Scale bar = 35µm.

6.6. Expression of 14-3-3 eta and co-expression with the C-domain of MAST4

Figure 6.13. illustrates the expression pattern observed following transfection of EGFP-14-3-3- eta into HEK293 cells. Two patterns of expression were observed: in the majority of cases, EGFP-14-3-3 eta was diffusely expressed throughout the HEK cells, however, in some cases it was excluded from the nucleus. Examples for both of these patterns of expression have been given in Figure 6.13.

The diffuse pattern of expression could also be observed when a GFP specific filter was used to visualise EGFP-14-3-3 eta following co-transfection with mRFP-CD (Figure 6.14). A filter specific for mRFP revealed a pattern of expression similar to that seen for the single transfection of mRFP-CD as seen in Figure 6.5. No evidence of co-localisation was observed following the co-transfection of mRFP-CD and EGFP-14-3-3 eta, as shown in Figure 6.14.

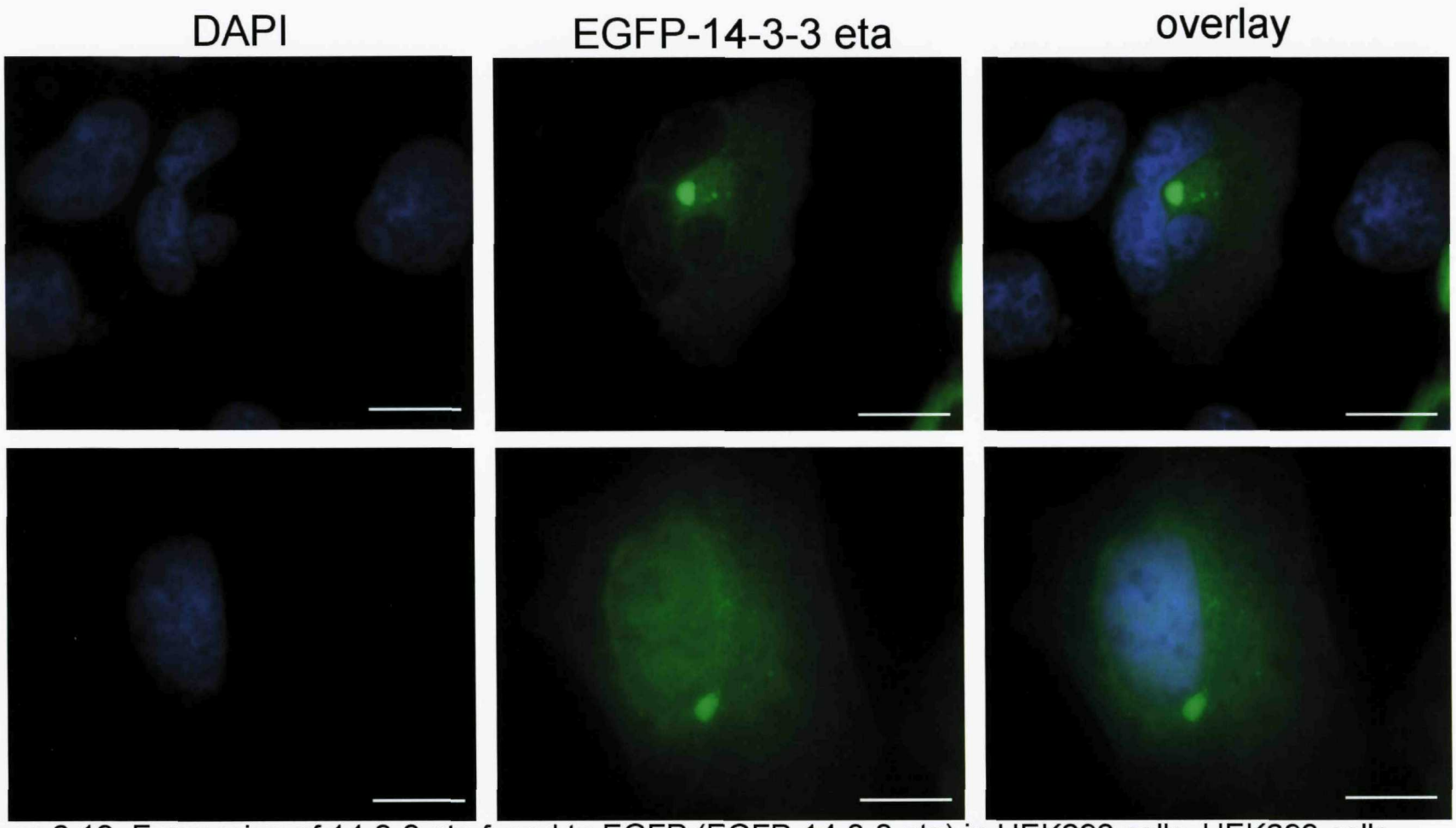

Figure 6.13. Expression of 14-3-3 eta fused to EGFP (EGFP-14-3-3 eta) in HEK293 cells. HEK293 cells were transiently transfected with EGFP-14-3-3 eta. Following fixation with 4% PFA, cells were stained with DAPI and mounted. Both the upper and lower panel illustrate representative cells expressing EGFP-14-3-3 eta The expression pattern for EGFP-14-3-3 eta appears diffuse throughout the cell. Scale bar = 35µm.

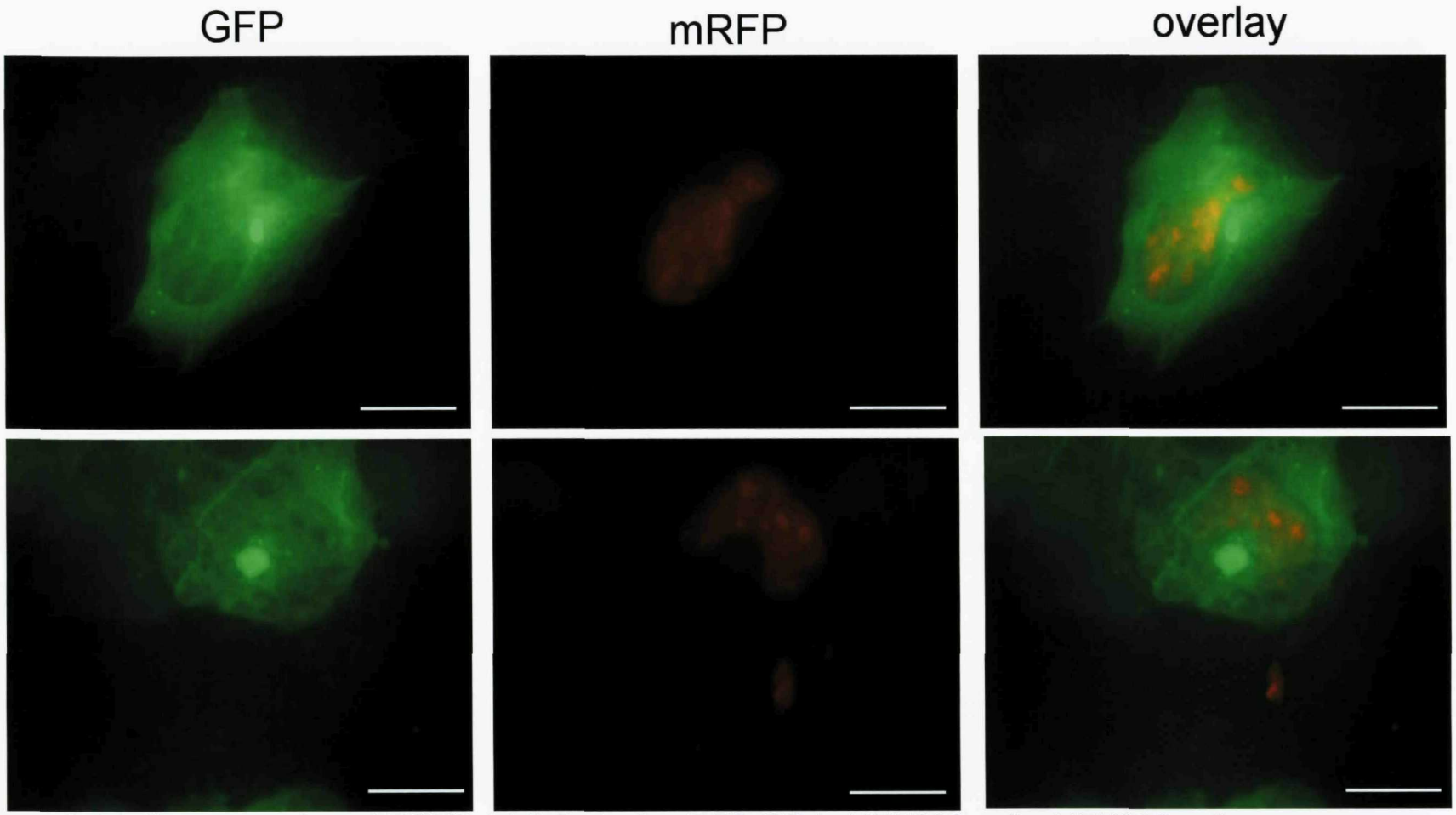

Figure 6.14. Co-expression of EGFP-14-3-3 eta & mRFP-CD in HEK293 cells. HEK293 cells were transiently transfected with EGFP-14-3-3 eta & EGFP-CD. Following fixation with 4% PFA, cells were stained with DAPI and mounted. Both the upper and lower panels illustrate, from left to right, fluorescence derived from a GFP specific filter, a mRFP specific filter, and an overlay of the two fluorescent signals. Scale bar = 35µm.

6.7. Expression of NIPP1 and co-expression with the C-domain of MAST4

Figure 6.15. illustrates the pattern of expression observed following the transfection of EGFP-NIPP1. EGFP-NIPP1 appears to express diffusely within the nucleus of the transfected HEK293 cells; however, there is also evidence of small puncta within the nucleus. Some of these puncta localise to chromatin deficient regions of the nucleus, as indicated in Figure 6.15.

The pattern of expression for EGFP-NIPP1 appears unchanged following co-transfection with mRFP-CD, as shown in Figure 6.16. & 6.17. The pattern of expression for mRFP-CD within this co-transfection also appears similar to that observed following single transfection, as shown in Figure 6.5. Other than the general expression of both proteins within the nucleus, there is no clear evidence of a specific co-localisation of the expressed proteins illustrated in Figures 6.16. & 6.17.

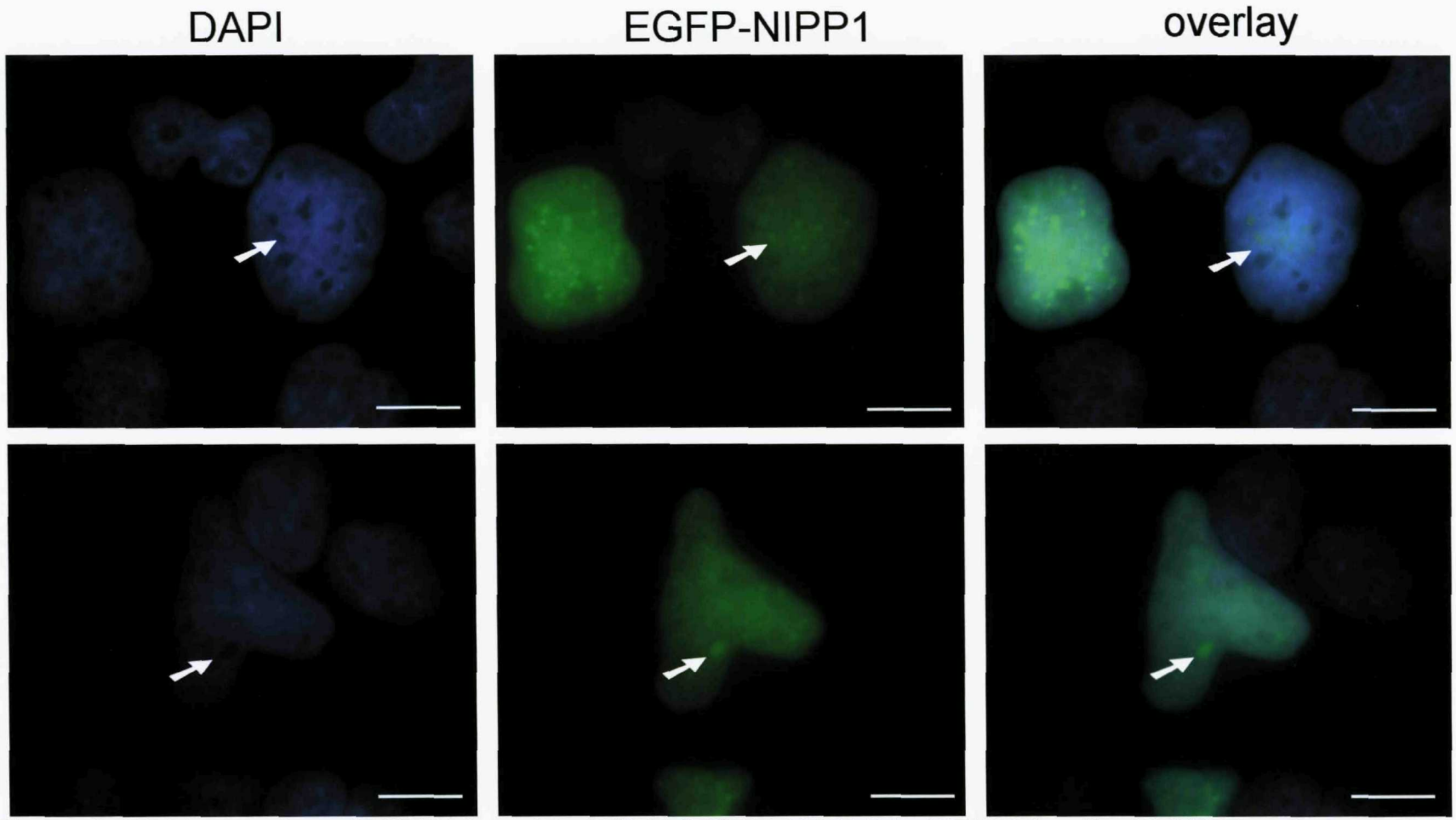

Figure 6.15. Expression of NIPP1 fused to EGFP (EGFP-NIPP1) in HEK293 cells. HEK293 cells were transiently transfected with EGFP-NIPP1. Following fixation with 4% PFA, cells were stained with DAPI and mounted. Both the upper and lower panel illustrate representative cells expressing EGFP-NIPP1. The expression pattern of NIPP1 appears diffuse within the nucleus, with possibly small puncta. However, there is evidence of localisation to chromatin deficient regions (white arrows) Scale bar = 35μm.

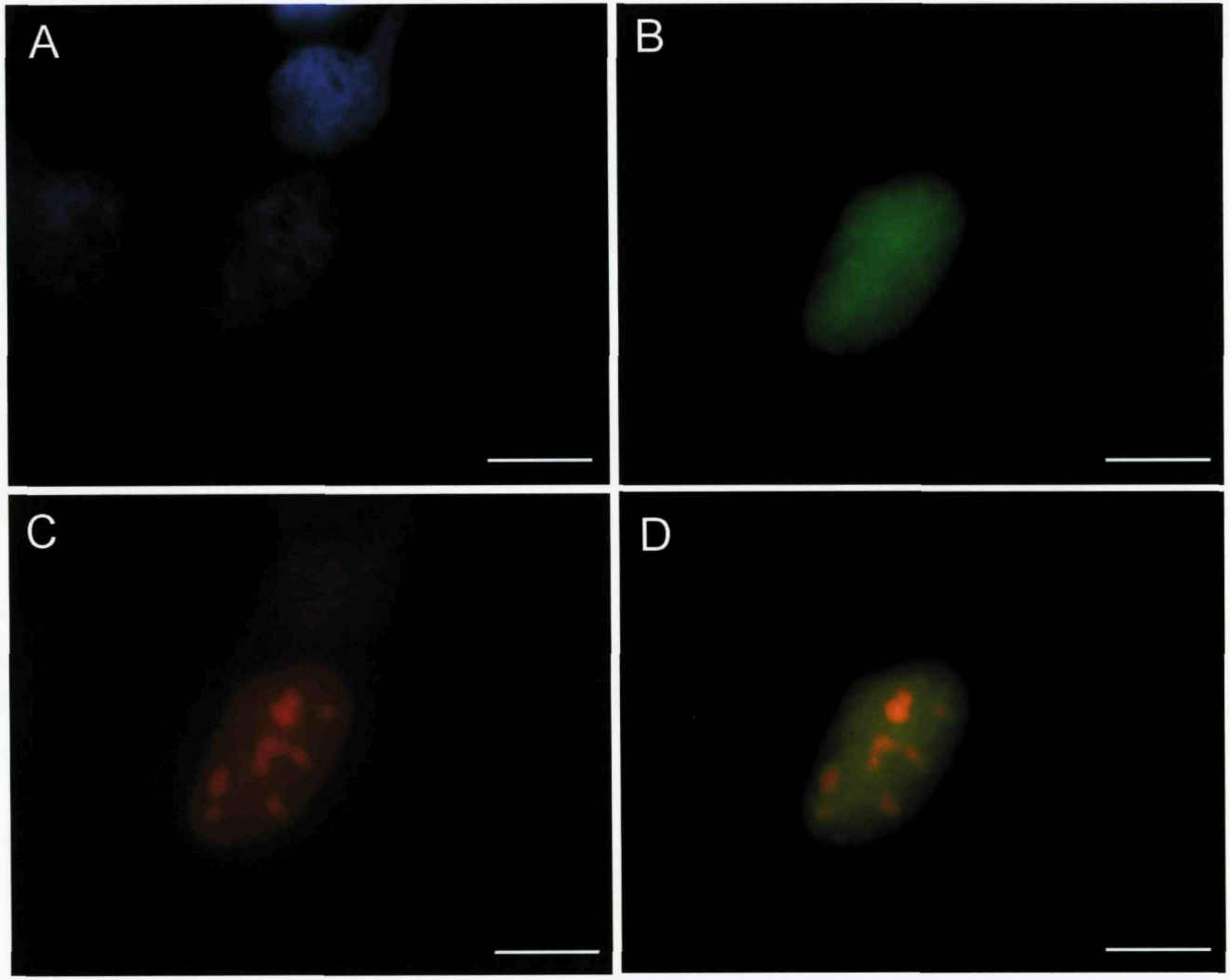

Figure 6.16. Co-expression of EGFP-NIPP1 & mRFP-CD in HEK293 cells. HEK293 cells were transiently transfected with EGFP-NIPP1 & EGFP-CD. Following fixation with 4% PFA, cells were stained with DAPI and mounted. (A) HEK293 cell stained with DAPI. (B) Fluorescence derived from a EGFP selective filter. (C) Fluorescence derived from a mRFP selective filter. (D) Overlay of EGFP and mRFP-CD fluorescence. Scale bar = 35µm.

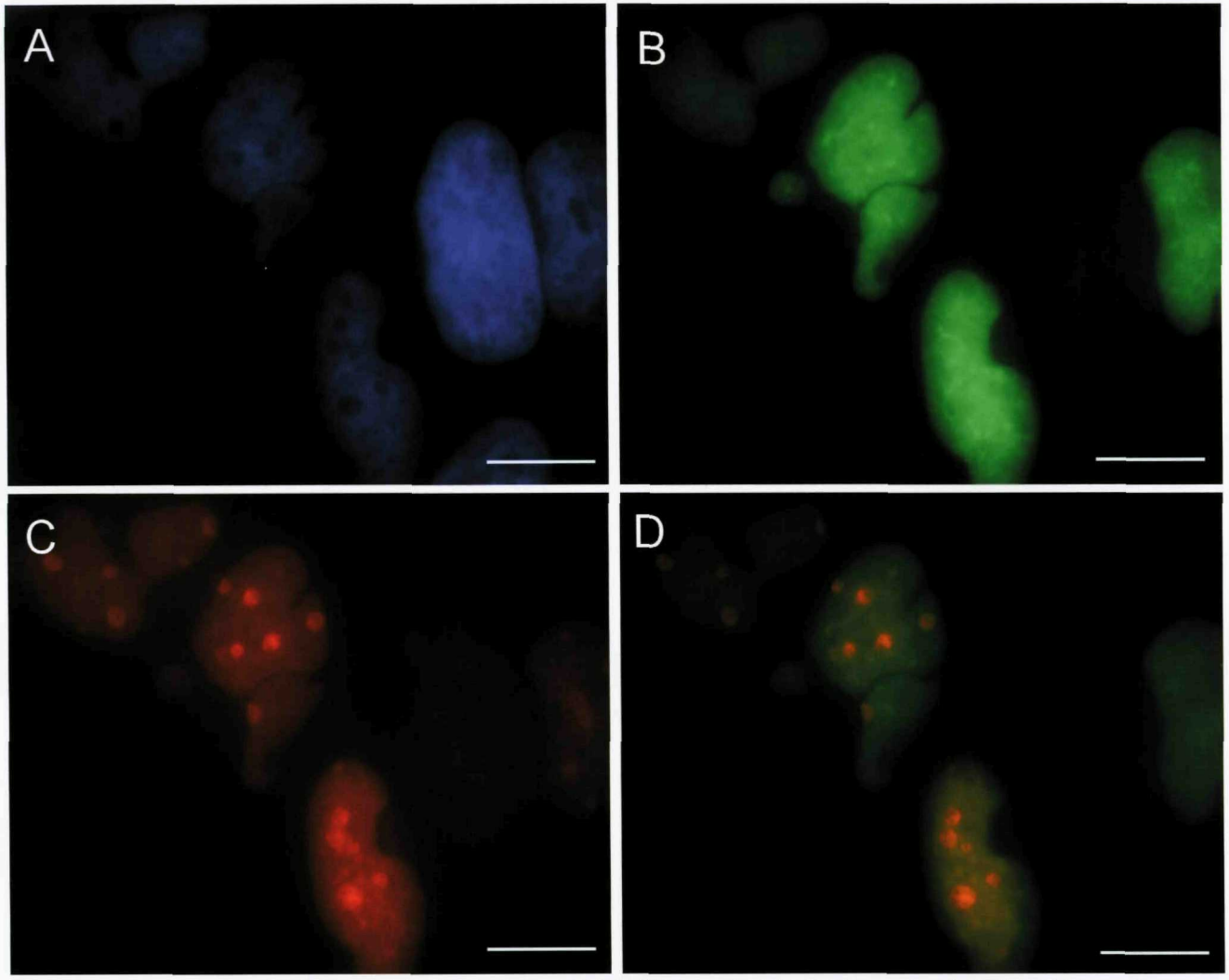

Figure 6.17. Co-expression of EGFP-NIPP1 & mRFP-CD in HEK293 cells. HEK293 cells were transiently transfected with EGFP-NIPP1 & EGFP-CD. Following fixation with 4% PFA, cells were stained with DAPI and mounted. (A) HEK293 cell stained with DAPI. (B) Fluorescence derived from a EGFP selective filter. (C) Fluorescence derived from a mRFP selective filter. (D) Overlay of EGFP and mRFP-CD fluorescence. Scale bar = 35μm.

6.8. Expression of Casein kinase 2 α1 polypeptide and co-expression with the C-domain of MAST4

Figure 6.18. illustrates the pattern of expression observed following the transfection of EGFP-CK2. EGFP-CK2 appears to express diffusely throughout the HEK293 cells, but is particularly strong within the nucleus. There is also some evidence of punctate expression within the nucleus.

The expression pattern of EGFP-CK2 is possibly more confined to the nucleus following co-transfection with mRFP-CD, as shown in Figures 6.19 & 6.20. The expression observed for mRFP-CD appears similar to that observed following a single transfection, as shown in Figure 6.5. Other than the general expression of both constructs with the nucleus, there is no specific evidence of co-localisation for the expressed proteins.

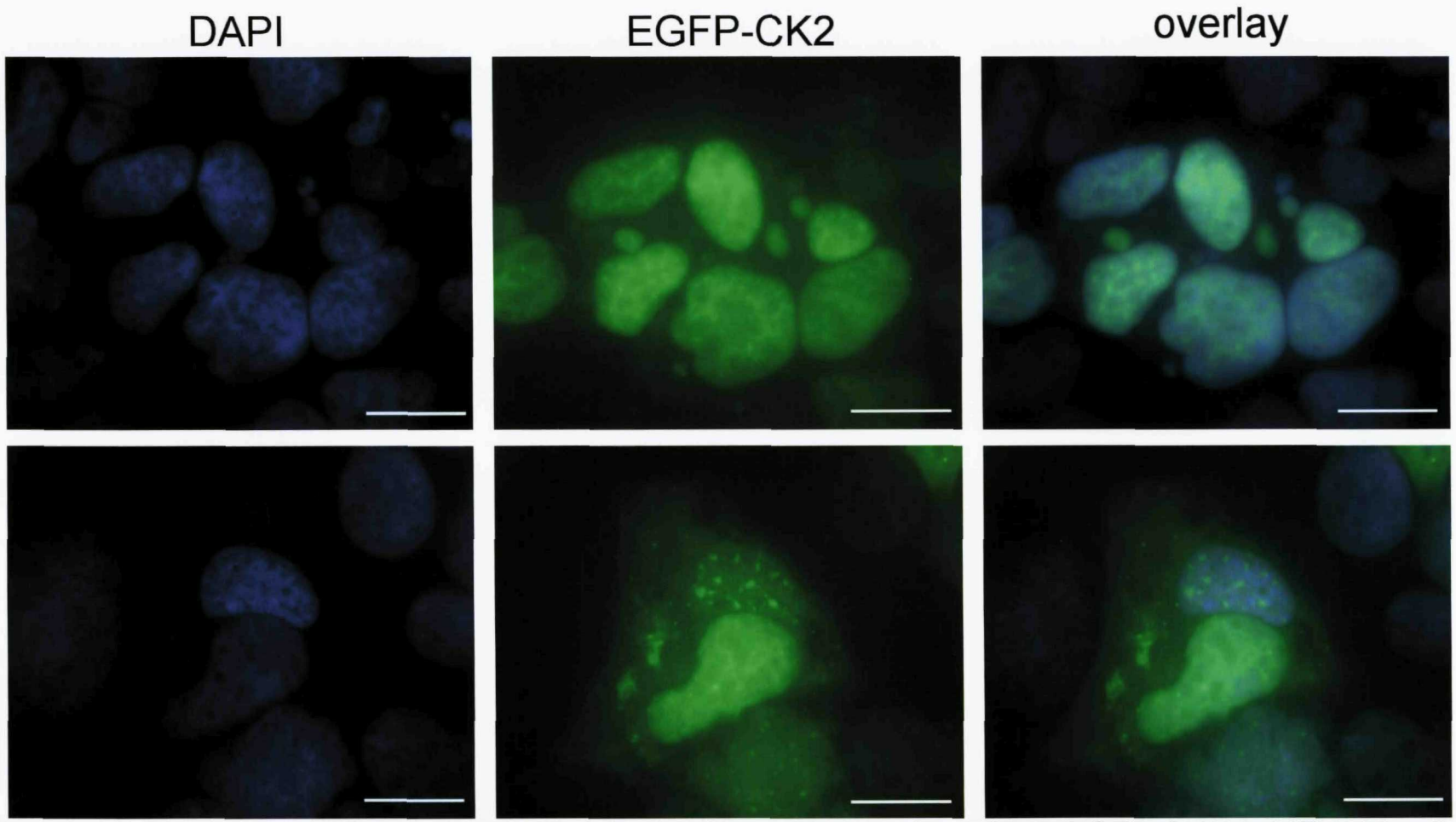

Figure 6.18. Expression of Casein kinase II alpha I polypeptide fused to EGFP (EGFP-CK2) in HEK293 cells. HEK293 cells were transiently transfected with EGFP-CK2. Following fixation with 4% PFA, cells were stained with DAPI and mounted. Both the upper and lower panel illustrate representative cells expressing EGFP-CK2. The expression pattern for EGFP-CK2 appears diffuse throughout the cell, but particular strong within the nucleus. There is also some evidence of punctuate expression within the nucleus. Scale bar = 35μm.

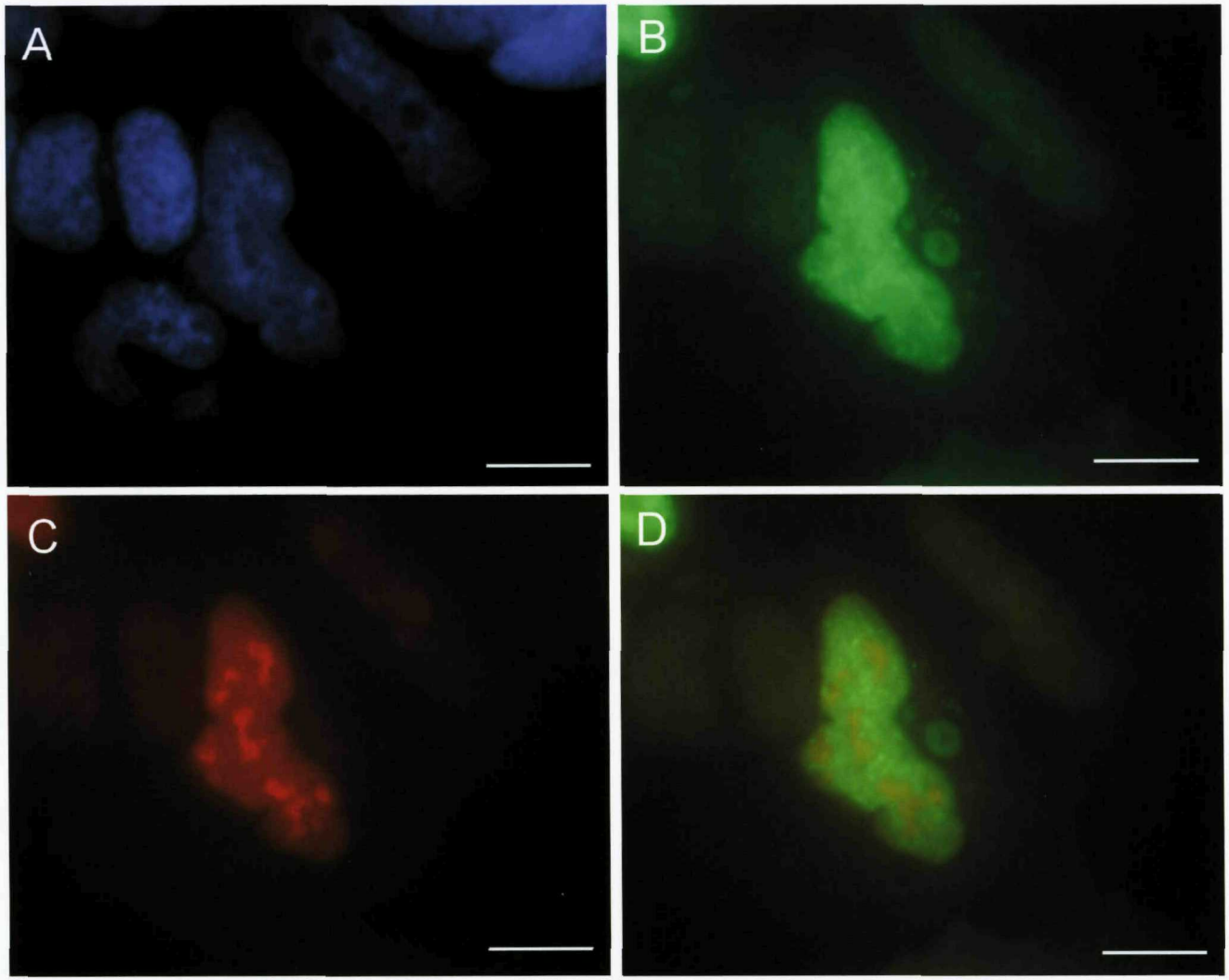

Figure 6.19. Co-expression of EGFP-CK2 & mRFP-CD in HEK293 cells. HEK293 cells were transiently transfected with EGFP-CK2 & EGFP-CD. Following fixation with 4% PFA, cells were stained with DAPI and mounted. (A) HEK293 cell stained with DAPI. (B) Fluorescence derived from a EGFP selective filter. (C) Fluorescence derived from a mRFP selective filter. (D) Overlay of EGFP and mRFP-CD fluorescence. Scale bar = 35μm.

6.9. Expression of Rtf1 and co-expression with the C-domain of MAST4

Figure 6.21. illustrates the pattern of expression observed following the transfection of EGFP-Rtf1. EGFP-Rtf1 appears to express diffusely throughout the HEK293 cells, but is particularly strong within the nucleus.

Following co-transfection with mRFP-CD, the expression pattern for EGFP-Rtf1 remains unchanged, as shown in Figure 6.22. Similarly, the expression pattern for mRFP-CD is also unchanged to that observed in Figure 6.5. Therefore, there does not appear to be any specific co-localisation of these protein when expressed in HEK293 cells. However, these two constructs do express in the same subcellular compartment.

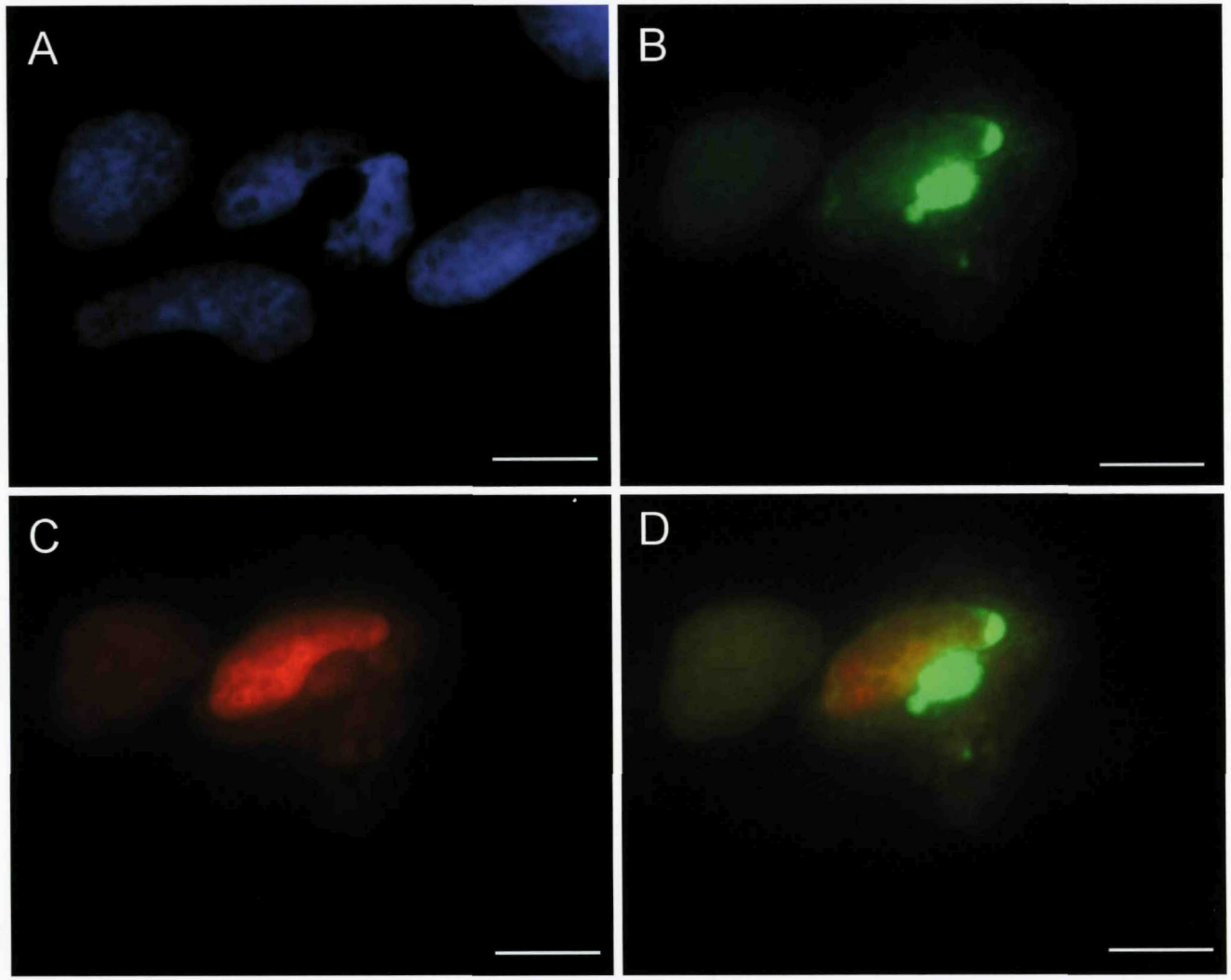

Figure 6.20. Co-expression of EGFP-CK2 & mRFP-CD in HEK293 cells. HEK293 cells were transiently transfected with EGFP-CK2 & EGFP-CD. Following fixation with 4% PFA, cells were stained with DAPI and mounted. (A) HEK293 cell stained with DAPI. (B) Fluorescence derived from a EGFP selective filter. (C) Fluorescence derived from a mRFP selective filter. (D) Overlay of EGFP and mRFP-CD fluorescence. Scale bar = 35um.

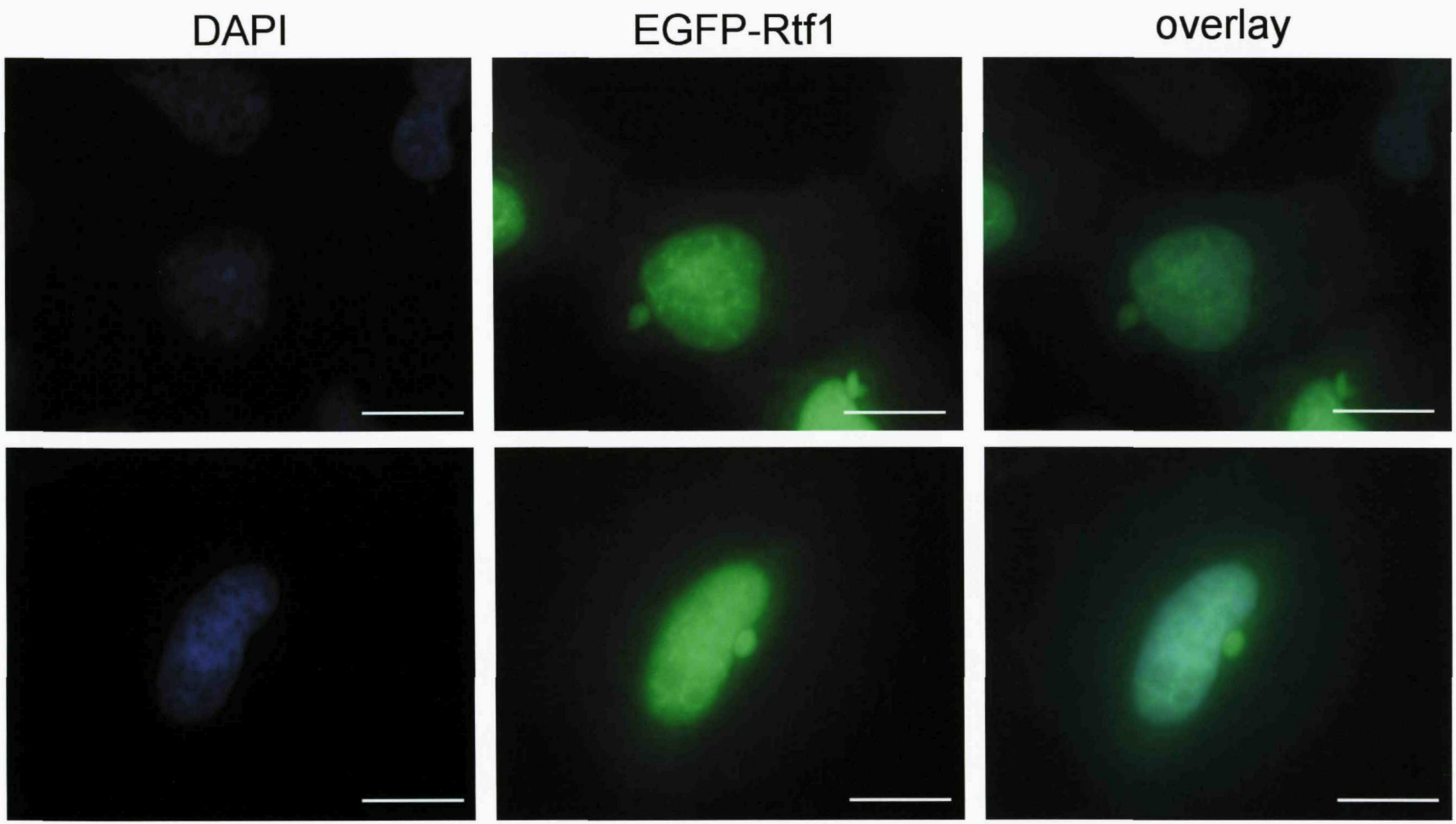

Figure 6.21. Expression of Rtf1 fused to EGFP (EGFP-Rtf1) in HEK293 cells. HEK293 cells were transiently transfected with EGFP-Rtf1. Following fixation with 4% PFA, cells were stained with DAPI and mounted. Both the upper and lower panel illustrate representative cells expressing EGFP-Rtf1. The expression pattern for EGFP-Rtf1 appears diffuse throughout the cell and is particular strong in the nucleus. Scale bar = 35µm.

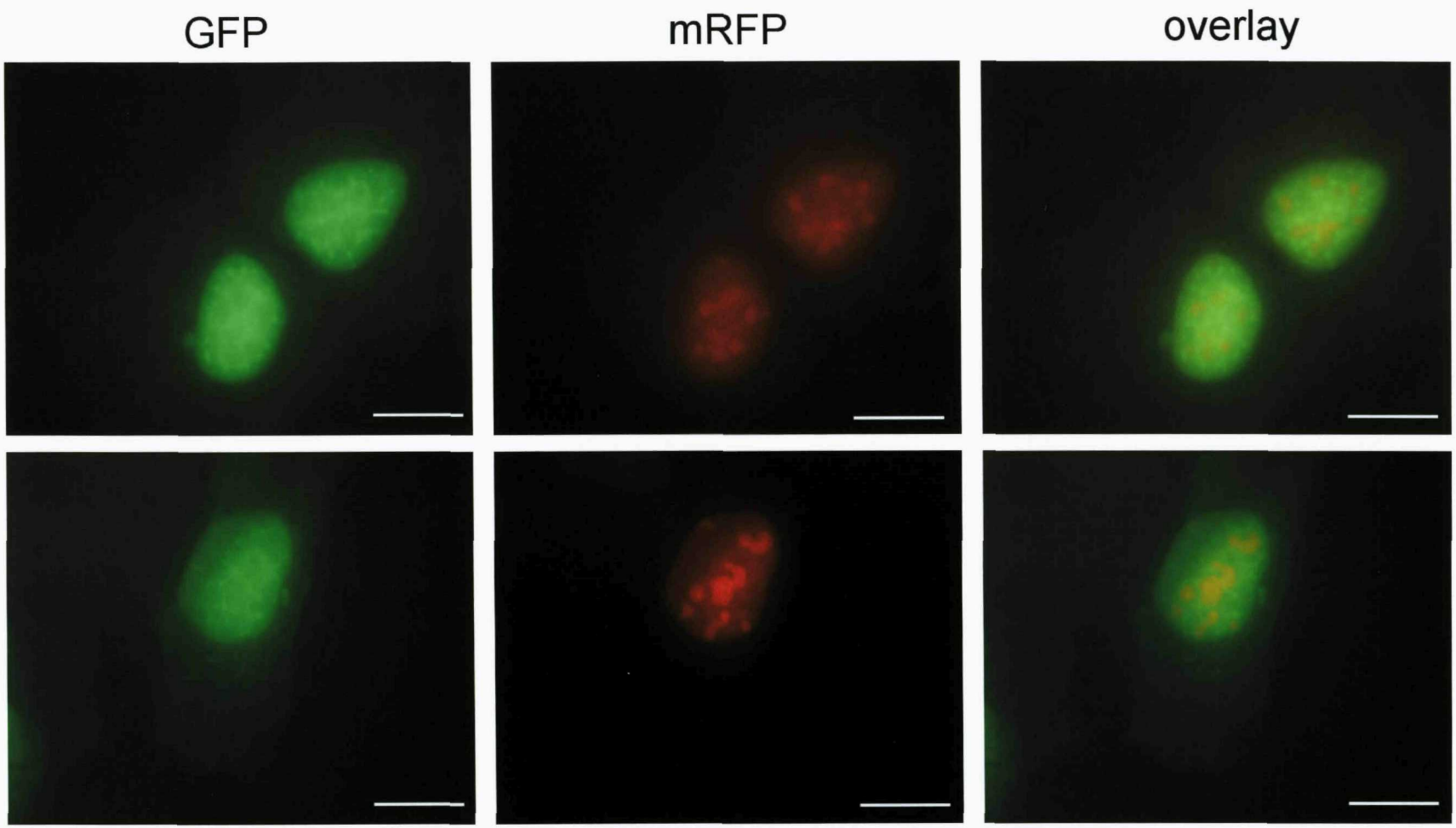

Figure 6.22. Co-expression of EGFP-Rtf1 & mRFP-CD in HEK293 cells. HEK293 cells were transiently transfected with EGFP-Rtf1 & EGFP-CD. Following fixation with 4% PFA, cells were stained with DAPI and mounted. Both the upper and lower panels illustrate, from left to right, fluorescence derived from a GFP specific filter, a mRFP specific filter, and an overlay of the two fluorescent signals. Scale bar = 35μm.

6.10. Expression of ELL1 and co-expression with the C-domain of MAST4

Figure 6.23 illustrates the pattern of expression observed following the transfection of EGFP-ELL1. EGFP-ELL1 appears to be expressed throughout the HEK293 cells, with slightly stronger localisation within the nucleus.

Following co-transfection with mRFP-CD the expression pattern for EGFP-ELL1 noticeably changes. Figures 6.23 & 6.24 show the expression of EGFP-ELL1 becomes significantly more nuclear, and more importantly, the expression co-localises with that for mRFP-CD.

As before, the expression of mRFP-CD is similar to that observed in Figure 6.5. That is, the expression appears localised to chromatin deficient regions of the nucleus. In contrast to the expression of EGFP-ELL1 when singly transfected, the expression of EGFP-ELL1 also localises to these chromatin deficient regions of the nucleus. When the two fluorescent signals for each fluorophore are overlaid, as shown in Figures 6.23. & 6.24, the two fusion proteins can be seen to clearly co-localise.

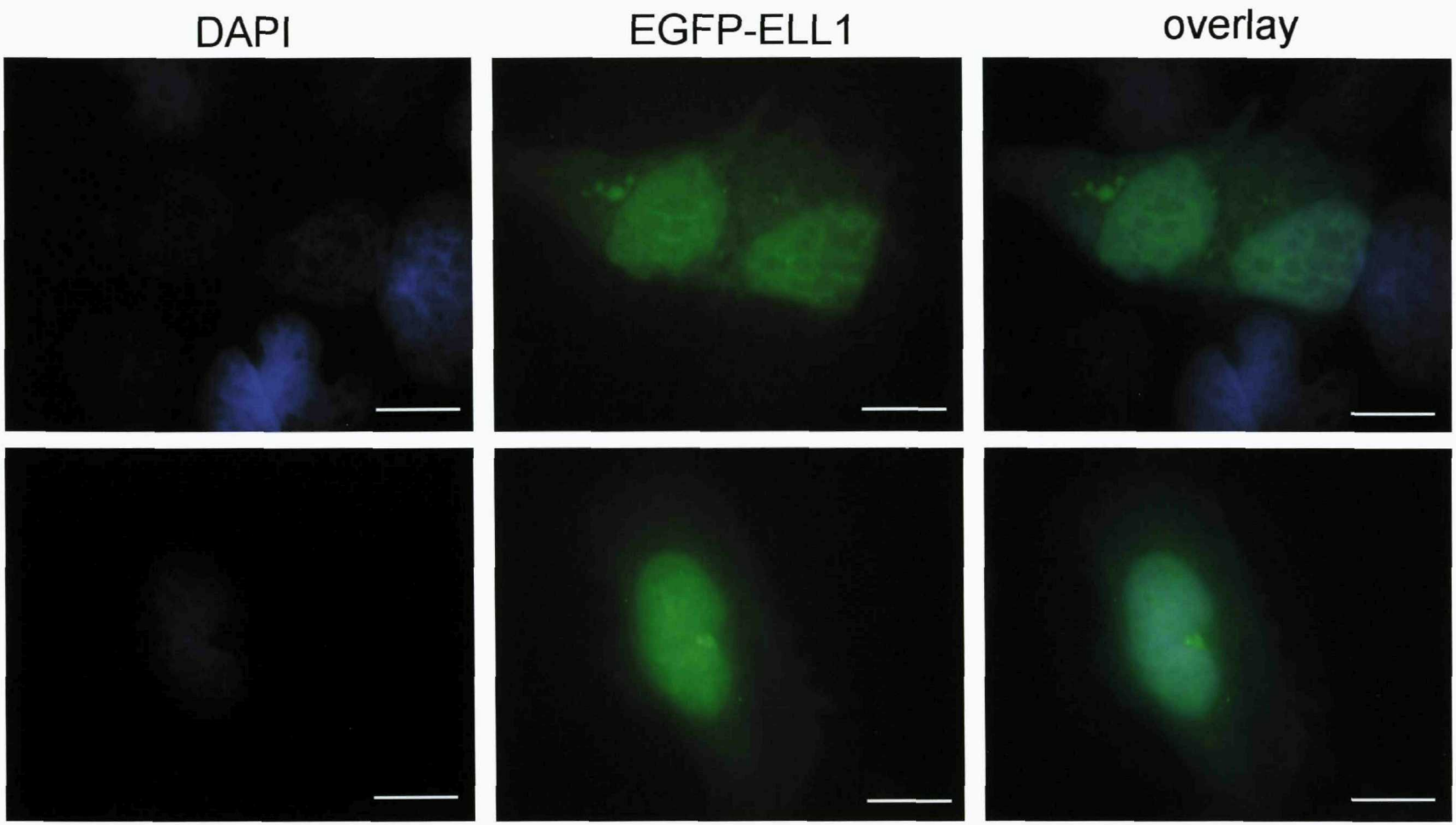

Figure 6.23. Expression of Eleven-nineteen lysine rich leukaemia isoform 1 (ELL1) fused to EGFP (EGFP-ELL1) in HEK293 cells. HEK293 cells were transiently transfected with EGFP-ELL1. Following fixation with 4% PFA, cells were stained with DAPI and mounted. Both the upper and lower panel illustrate representative cells expressing EGFP-ELL1. The expression pattern for EGFP-ELL1 appears diffuse within the cell, but is particular strong in the nucleus. Scale bar = 35µm.

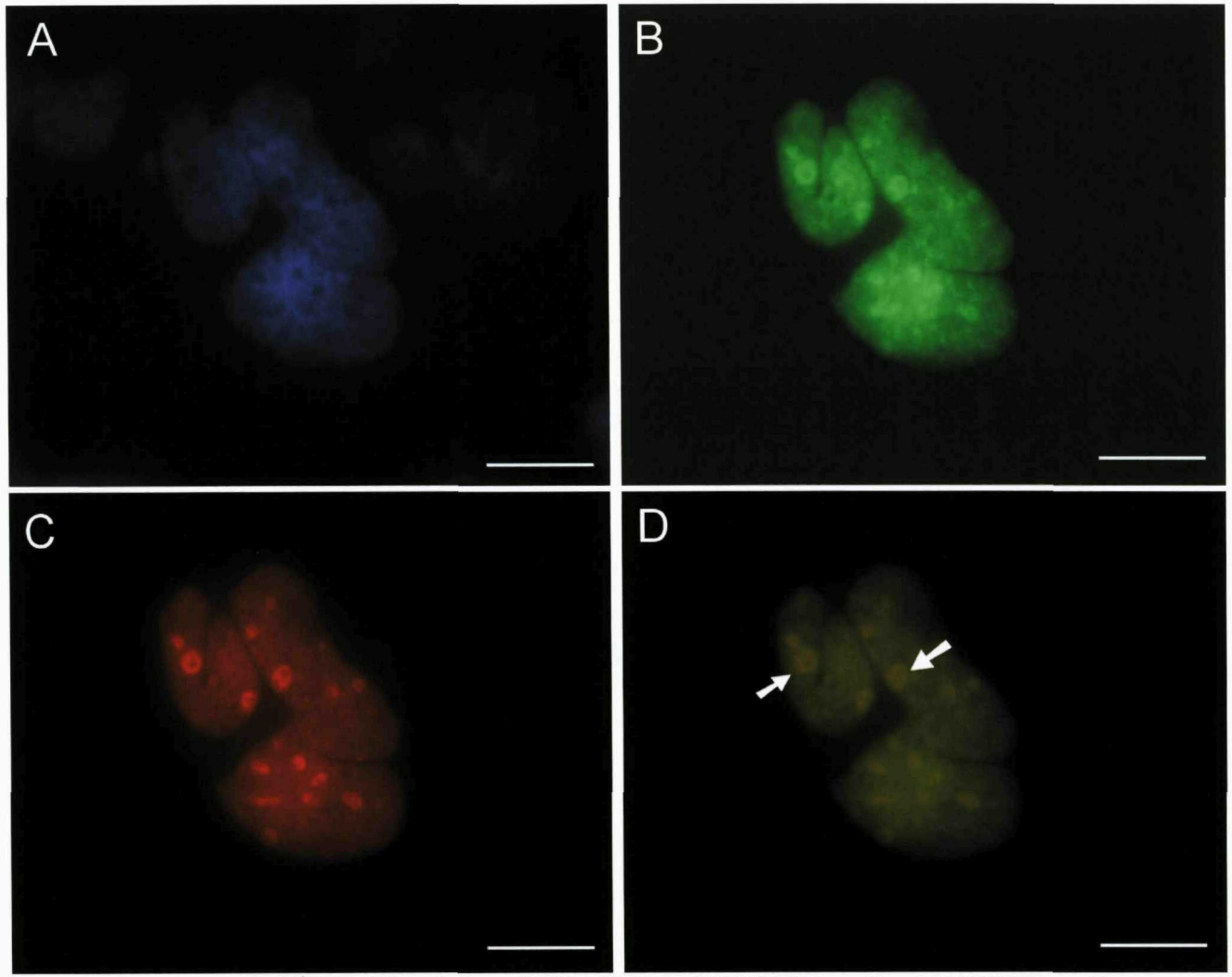

Figure 6.24. Co-expression of EGFP-ELL1 & mRFP-CD in HEK293 cells. HEK293 cells were transiently transfected with EGFP-ELL1 & EGFP-CD. Following fixation with 4% PFA, cells were stained with DAPI and mounted. (A) HEK293 cell stained with DAPI. (B) Fluorescence derived from a EGFP selective filter. (C) Fluorescence derived from a mRFP selective filter. (D) Overlay of EGFP and mRFP-CD fluorescence. Representative regions of co-localisation are indicated with white arrows. Scale bar = 35µm.

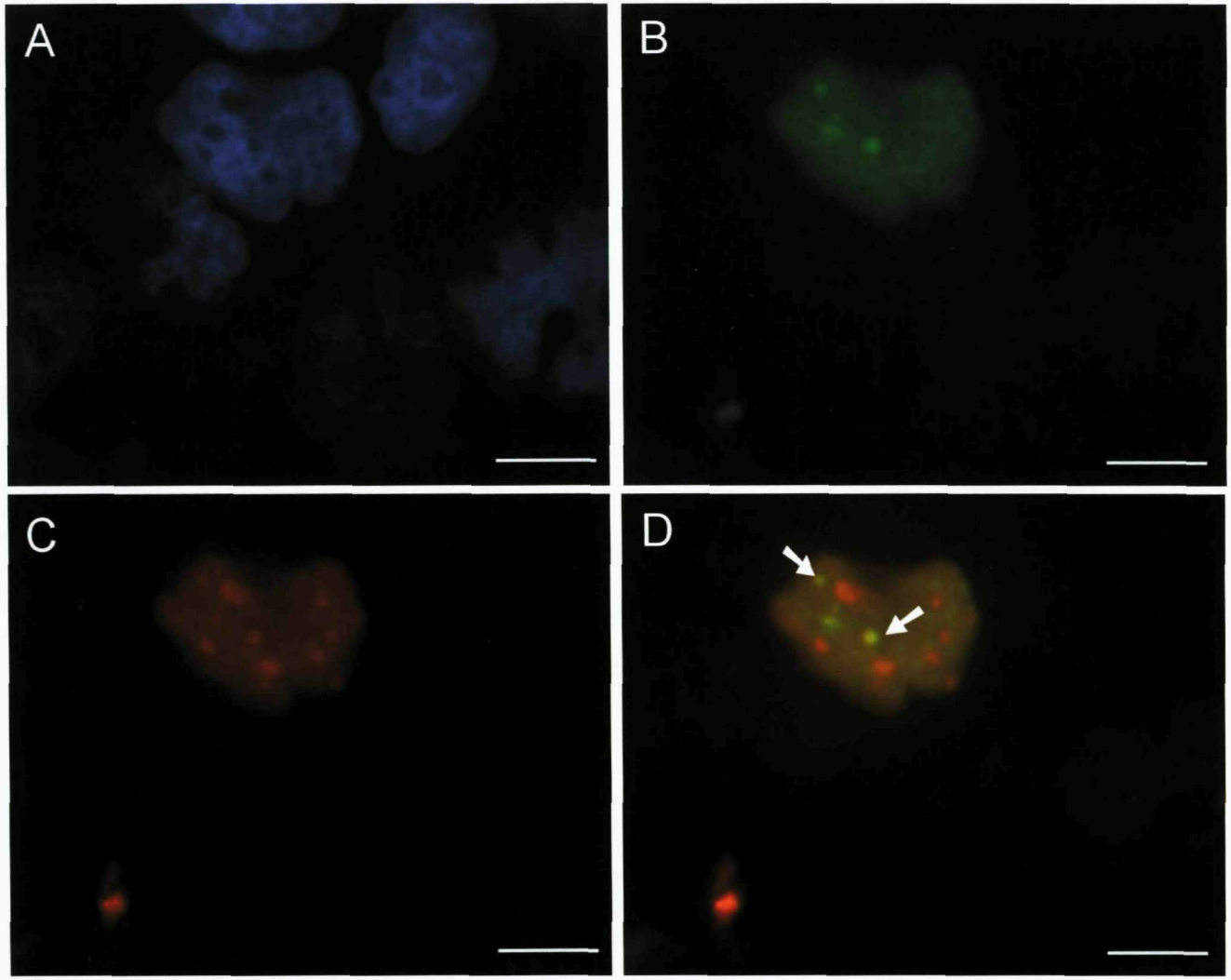

Figure 6.25. Co-expression of EGFP-ELL1 & mRFP-CD in HEK293 cells. HEK293 cells were transiently transfected with EGFP-ELL1 & EGFP-CD. Following fixation with 4% PFA, cells were stained with DAPI and mounted. (A) HEK293 cell stained with DAPI. (B) Fluorescence derived from a EGFP selective filter. (C) Fluorescence derived from a mRFP selective filter. (D) Overlay of EGFP and mRFP-CD fluorescence. Regions of co-localisation are indicated with white arrows. Scale bar = 35μm.

6.10. Expression of ELL2 and co-expression with the C-domain of MAST4

Figure 6.26 illustrates the pattern of expression observed following the transfection of EGFP-ELL2. EGFP-ELL2 is diffusely expressed throughout the HEK293 cells.

Following co-transfection with mRFP-CD the expression pattern for EGFP-ELL1 noticeably changes. Figure 6.27 shows the expression of EGFP-ELL becomes clearly nuclear, and more importantly, the expression co-localises with that for mRFP-CD.

As before, the expression of mRFP-CD is similar to that observed in Figure 6.5. That is, the expression appears localised to chromatin deficient regions of the nucleus. In contrast to the expression of EGFP-ELL2 when singly transfected, the expression of EGFP-ELL2 also localises to these chromatin deficient regions of the nucleus. When the two fluorescent signals for each fluorophore are overlaid, as shown in Figure 6.27, the two fusion proteins can be seen to clearly co-localise.

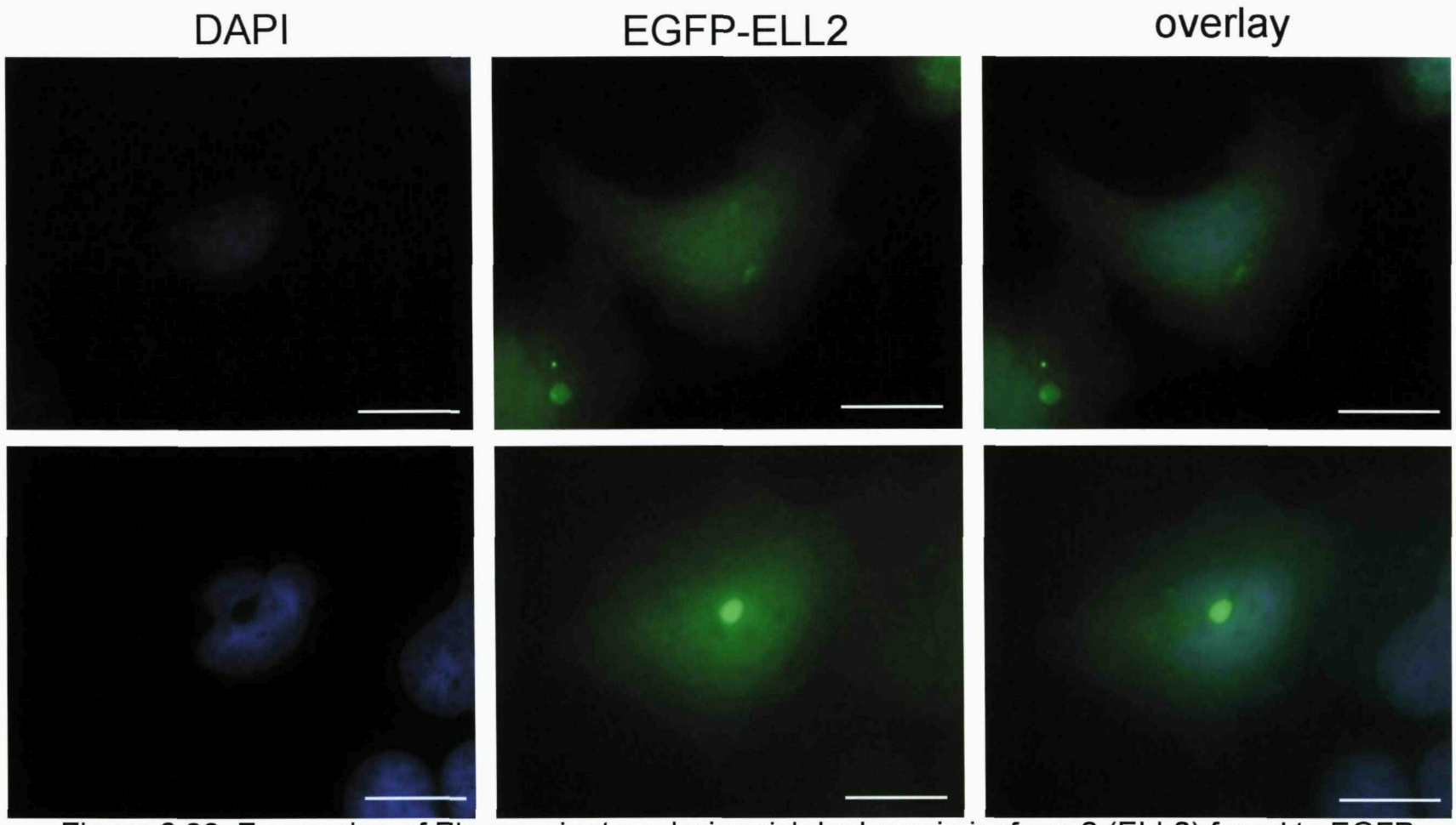

Figure 6.26. Expression of Eleven-nineteen lysine rich leukaemia isoform 2 (ELL2) fused to EGFP (EGFP-ELL2) in HEK293 cells. HEK293 cells were transiently transfected with EGFP-ELL2. Following fixation with 4% PFA, cells were stained with DAPI and mounted. Both the upper and lower panel illustrate representative cells expressing EGFP-ELL2. The expression of EGFP-ELL2 appears diffuse throughout the HEK293 cell. Scale bar = 35µm.

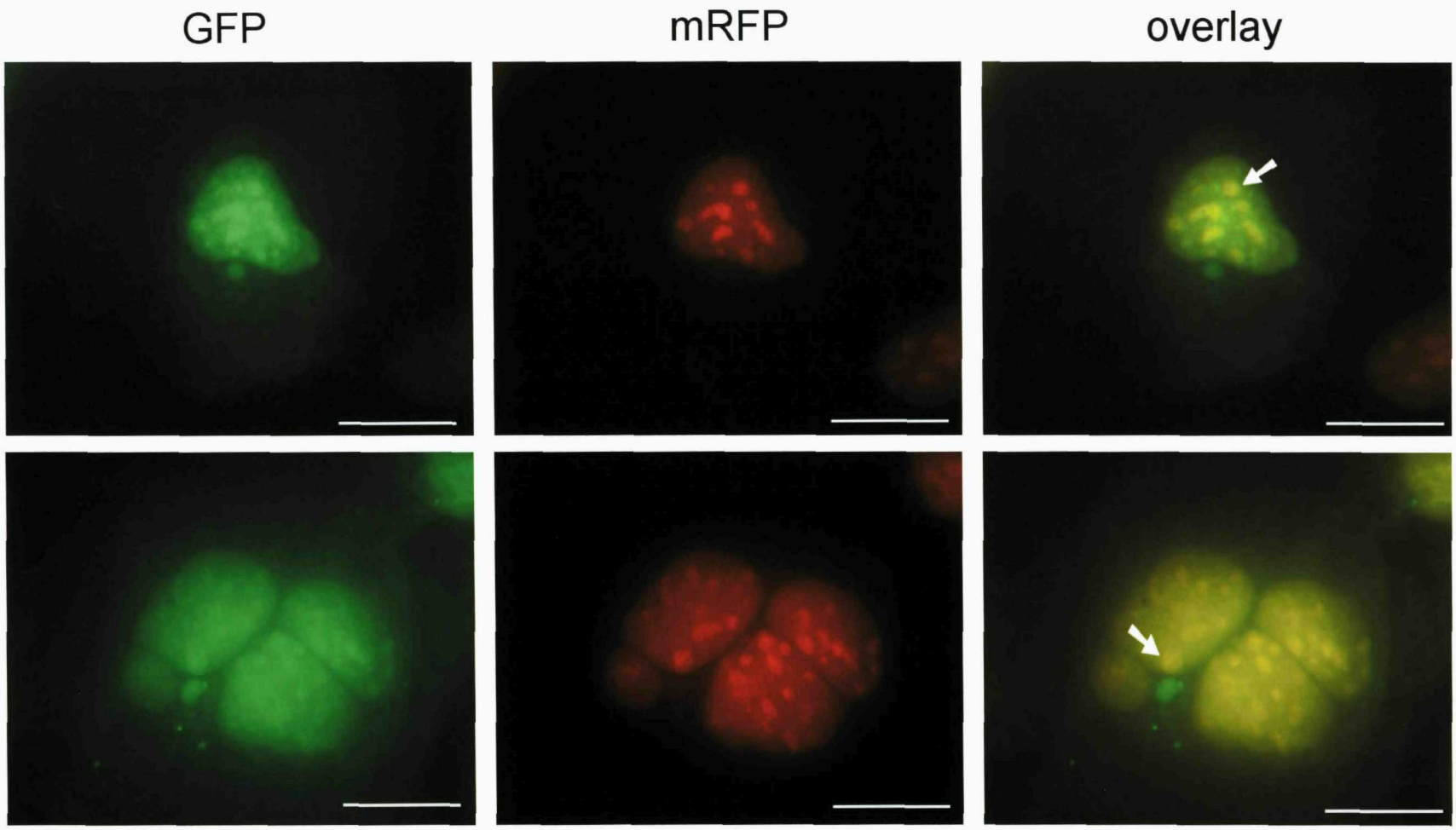

Figure 6.27. Co-expression of EGFP-ELL2 & mRFP-CD in HEK293 cells. HEK293 cells were transiently transfected with EGFP-ELL2 & EGFP-CD. Following fixation with 4% PFA, cells were stained with DAPI and mounted. Both the upper and lower panels illustrate, from left to right, fluorescence derived from a GFP specific filter, a mRFP specific filter, and an overlay of the two fluorescent signals. Representative regions of co-localisation are indicated with white arrows. Scale bar = 35µm.

6.2. Discussion

Chapter 5 described the use of the C-domain of MAST4 as a bait to screen for potential MAST4 interacting proteins. There was not any common structural element within any of the MAST4 interactors that could rationalise their interaction with MAST4. Therefore to confirm these interactions outside of the yeast two hybrid system, and gather information about the subcellular localisation of these protein, a secondary screen was performed. This expression analysis involved the use of fluorophore tagged constructs: the C-domain was fused in-frame to mRFP, and each potential interactor was fused in-frame to EGFP. These constructs were then transfected and co-transfected into HEK293 cells to investigate their expression.

The C-domain of MAST4 fused to mRFP & GFP (mRFP-CD & GFP-CD), as illustrated in Figures 6.4 to 6.6 clearly localises to the nucleus of transfected cells. As Figure 6.6. illustrates, the C-domain of MAST4 appears to localise to regions of the nucleus that do not stain with DAPI and are therefore deficient in chromatin. These regions of the nucleus are known to contain the nuclear substructure called nuclear speckles (Reviewed in Lamond and Spector, 2003). Nuclear speckles contain pre-mRNA splicing factors, which are recruited to actively transcribing genes (Lamond and Spector, 2003; Misteli et al., 1997). This recruitment requires kinase activity to phosphorylate serine residues in the splicing factors (Misteli et al., 1997; Misteli et al., 1998). For example, expression of cdc2-like kinase in A431 (Human epithelial carcinoma) cells leads to hyperphosphorylation of splicing factors and disruption of nuclear speckles (Sacco-Bubulya and Spector, 2002). The possibility that MAST4 may be involved in alternative mRNA splicing will be discussed in the General Discussion.

The expression data presented above for the GFP-tagged fusion proteins with and without co-transfection of mRFP-CD has been summarised in Table 6.2. below. It is clear that most of the GFP-tagged proteins are localised to the nucleus and/or diffusely expressed within the HEK293 cells. Following co-transfection, the expression patterns for most of the interactors remains unchanged. However, the expression patterns for both ELL1 & ELL2 markedly changes to a strong nuclear expression with clear localisation with mRFP-CD. Although the two isoforms of ELL show clear localisation there is also a general co-localisation of mRFP-CD with a selection of the potential interactors, as described in Table 6.2.

Protein	Single	Double	Change in expression pattern	General co-localisation	Specific colocalisation
SytXI	nuclear/punctate	Nuclear/punctate	No	Yes	Yes
14-3-3 beta	nuclear/punctate	Nuclear/punctate	No	Yes	No
14-3-3 eta	diffuse	Diffuse	No	No	No
NIPP1	nuclear	Nuclear	No	Yes	No
CK2	diffuse/nuclear	diffuse/nuclear	No	Yes	No
Rtf1	diffuse/nuclear	diffuse/nuclear	No	Yes	No
ELL1	diffuse/nuclear	nuclear	Yes	Yes	Yes
ELL2	diffuse	nuclear	Yes	Yes	Yes

Table 6.2. Summary of data for expression analysis of potential MAST4 interacting partners. Many of the potential interactors show general co-localisation in the nucleus. However, SytXI and ELL1/ELL2 show specific co-localisation.

To interpret the expression patterns summarised in Table 6.2. they need to be compared to the known subcellular localisation of the proteins. This can therefore provide support for the expression patterns observed as well as rationalising any differences. Also, where any of the potential interactors are expressed within brain this can be compared to the expression of MAST4 described in Chapter 3.

Table 6.3. below lists reports showing which of the interactors are expressed within brain, where these genes are expressed in the brain (using the Allen Brain Atlas), and what subcellular structure they are localised in. The expression patterns for brain reported by the Allen Brain Atlas (Lein et al., 2007) are illustrated in Figure 6.25. This database has utilised high-throughput in situ hybridisation to characterise the expression of mouse brain transcripts (Lein et al., 2007).

Synaptotagmin XI is expressed in brain, particularly the hippocampus and is localised to the cytoplasm and perinucleus (von Poser et al., 1997; Huynh et al., 2003; Lein et al., 2007). The expression of EGFP-SytXI in HEK293 cells, as illustrate in Figure 6.7, is clearly punctate within the nucleus. However, in vivo synaptotagmin XI localises to perinuclear regions, and exhibits punctate staining within axons that suggest localisation to synapses (Huynh et al., 2003). The discrepancy between the expression pattern observed for EGFP-SytXI and synaptotagmin XI in vivo may be accounted for by the size of the clone identified from the YTH screen. This clone does not contain the transmembrane domain that allows the synaptotagmin isoforms to associate with the

plasma membrane. Therefore, although synaptotagmin XI is expressed in the hippocampus, the co-localisation observed with mRFP-CD is probably non-specific.

Gene	Expression in brain	Brain region (Allen Atlas)	Subcellular structure	Reference
SytXI	Yes	Gen, Hp	Perinuclear, membrane bound	von Poser, 97; Huynh, 03
14-3-3 beta	Yes	Gen, Hp (Baxter, 02)	Cytoplasm/nucleus	Takashi, 03; Baxter, 02; Brunet, 02
14-3-3 eta	Yes	Hp, Cb	Cytoplasm/nucleus	Takashi, 03; Baxter, 02; Brunet, 02
NIPP1	Yes	Gen, Hp, Cb	Nucleus (speckles)	Trinkle-Mulcahy, 99
CK2	Yes	Gen, Hp	Nucleus, cytoplasm	Blanquet, 00
Rtf1	Yes	Gen, Hp	Nucleus	Stolinski, 97
ELL1	Yes	Gen, Hp	Nucleus	Shilatifard, 96
ELL2	Yes	Gen (low level)	Nucleus	Shilatifard, 97

Table 6.3. In vivo expression patterns for potential MAST4 interactors. All genes are expressed in brain, and the hippocampus. Most of the potential interactors are expressed in the nucleus. Gen = General expression; Hp = hippocampus; Cb = cerebellum.

14-3-3 proteins are predominantly cytoplasmic (Reviewed in Takahashi, 2003). However, there is evidence they can localise to the nucleus when they are not bound to their interacting proteins (Brunet et al., 2002). Therefore, the expression of EGFP-14-3-3 beta/eta, as illustrated in Figures 6.10 & 6.13, can both be rationalise based on the available data. Both of these isoforms of 14-3-3 are also expressed in the hippocampus (Lein et al., 2007; Baxter et al., 2002). Therefore, the general co-localisation of at least 14-3-3 beta with mRFP-CD in the nucleus may be specific, although there is no evidence of an actual specific co-localisation of the two proteins.

NIPP1 is expressed in the hippocampus of the brain and localises to nuclear speckles (Lein et al., 2007; Trinkle-Mulcahy et al., 1999). The expression of EGFP-NIPP1 is also clearly nuclear with some evidence for localisation to the chromatin deficient regions that harbour nuclear speckles. This might be expected as the clone identified by the YTH screen contains the forkhead-associated domain that mediates localisation to nuclear speckles for this protein (Jagiello et al., 2000). As well as a general role as a inhibitor of protein phosphatase 1 (PP1), NIPP1 has also been implicated in alternative

mRNA splicing (Beullens and Bollen, 2002). Beullens et al (2002) established that NIPP1 is involved in the later stages of spliceosome assembly, which is a role not dependent on its inhibition of PP1.

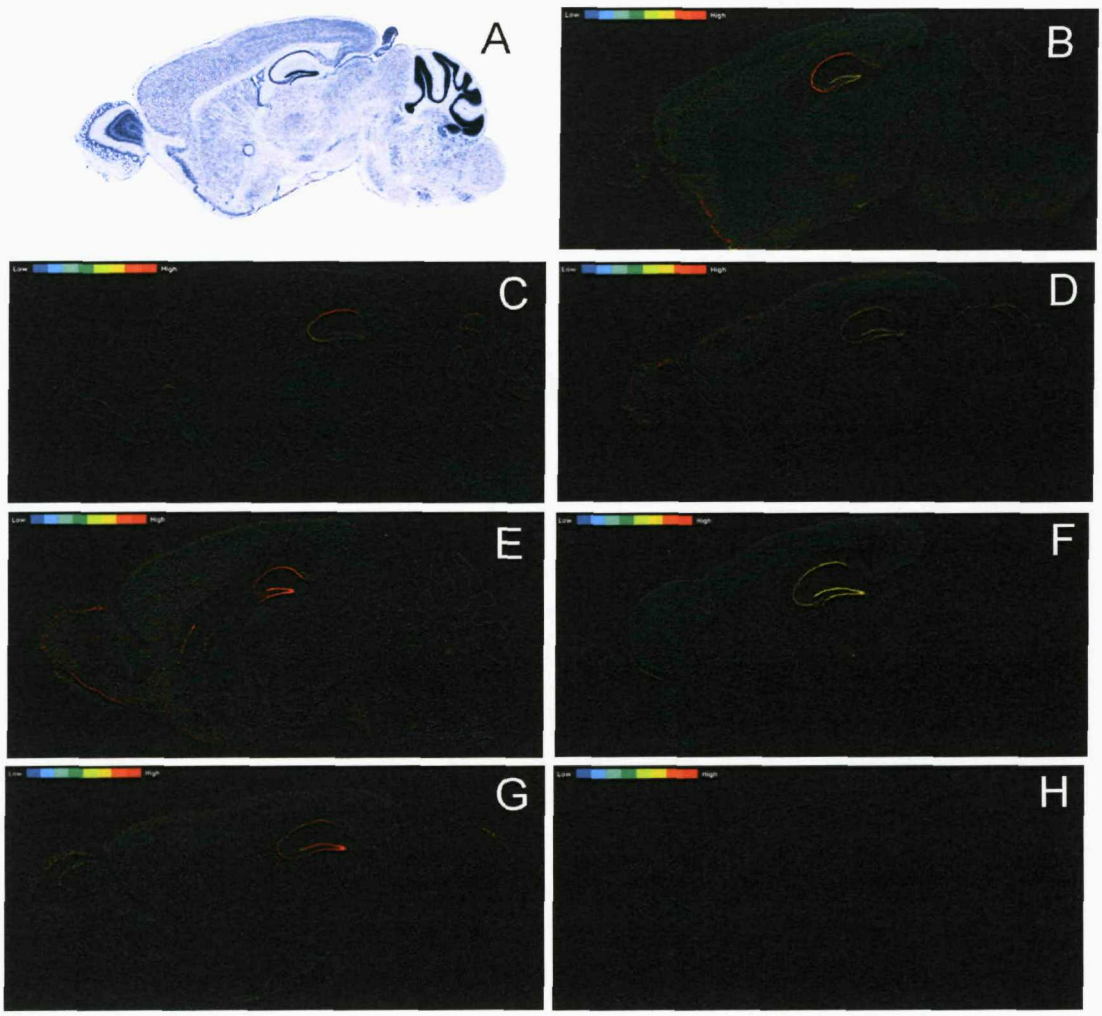

Figure 6.25. Expression of the MAST4 interactors as reported by the Allen Brain Atlas. (A) A Nissl stained section taken from the same region as figures B to H. (B) SytXI. (C) 14-3-3 eta. (D) NIPP1. (E) CK2. (F) Rtf1.(G) ELL1. (H) ELL2. The expression patterns of figure B to H are summarised in Table 6.2. However, most transcripts are expressed in the hippocampus. The coloured box (top left) indicates intensity of staining: blue = low; red = high.

The expression of EGFP-NIPP1 therefore generally agrees with available *in vivo* data for NIPP1. When EGFP-NIPP1 was co-transfected with mRFP-CD there was only evidence of a general co-localisation, rather than a specific co-localisation in the chromatin deficient regions. However, the expression of mRFP-CD within these regions is stronger than that for EGFP-NIPP1, which may obscure the co-localisation

that exists. The co-expression of MAST4 and NIPP1 in the hippocampus and their localisation within the nucleus suggests therefore that these two protein may genuinely interact.

The α1 polypeptide of casein kinase 2 is expressed in the hippocampus, and is localised in the nucleus and cytoplasm (Lein et al., 2007; Blanquet, 2000). The expression of EGFP-CK2 is also cytoplasmic and nuclear, as shown in Figure 6.18. Therefore, the expression of EGFP-CK2 agrees with the known expression pattern for CK2. When co-transfected with mRFP-CD there is no obvious specific co-localisation, only the general co-localisation due to their nuclear expression. CK2 is abundantly expressed in the brain and has been associated with a variety of functions, including: synaptic transmission and plasticity (e.g. LTP), development and neuritogenesis (Reviewed in Blanquet, 2000).

The protein Rtf1 is a component of the yeast Paf1 complex that is conserved from yeast to humans (Sims, III et al., 2004; Tate et al., 1998). This complex is important for the elongation stage of transcription due to an effect on chromatin modifications (Sims, III et al., 2004). The Rtf1 subunit is itself required for histone monoubiquitination and DNA methylation (Wood et al., 2003; Krogan et al., 2003; Ng et al., 2003).

Due to its role in transcription this protein would be expected to localise to the nucleus, although this has not been directly shown in mammalian cells. However, EGFP-Rtf1 does localise to the nucleus, as shown in Figure 6.21. Although, there is no evidence of specific co-localisation, as shown in Figure 6.22, this may be accounted for by the strength of the interaction, which in the YTH system was relatively weak (see Table 5.3). The two fusion proteins localise to the nucleus and the expression of Rtf1 in brain appears strongest in the hippocampus (Lein et al., 2007). Therefore, the expression of mRFP-CD and EGFP-Rtf1 in the nucleus may indicate a possible interaction between MAST4 and Rtf1.

The ELL isoforms show the clearest evidence of specific co-localisation, as illustrated by Figures 6.23, 6.24 and 6.27. There are 3 isoforms of ELL (ELL1, ELL2, and ELL3) within the human genome (Shilatifard et al., 2003).

All 3 isoforms are known to suppress the pausing of transcription and therefore stimulate the transcriptional rate (Shilatifard et al., 1996; Shilatifard et al., 1997; Miller et al., 2000). The transcript for ELL1 is expressed in brain, and ELL1 protein localises to the nucleus (Thirman et al., 1994; Shilatifard et al., 1997). Interestingly, although ELL2 is expressed in the brain at low levels, its is markedly upregulated in the dentate

gyrus following electroconvulsive seizure (Ploski et al., 2006); ELL2 is also localised to the nucleus (Shilatifard et al., 1997).

The expression of EGFP-ELL1 was diffuse within transfected HEK293 cells, with slightly more expression in the nucleus, as shown in Figure 6.23. The expression of ELL2 is diffuse throughout transfected cells, as shown in Figure 6.26. The discrepancy between the expression of the GFP-tagged proteins and their in vivo expression may be due to the size of the clones identified from the YTH screen, which only contain the occludin-like domain. Following co-transfection with mRFP-CD there is a significant redistribution of the ELL isoforms to the nucleus with clear colocalisation, as shown in Figures 6.24, 6.25 & 6.27.

A possible role for elongation rate in alternative mRNA splicing has been suggested, which will be considered within the General Discussion. This is particularly interestingly in light of the subcellular localisation of mRFP-CD and its interaction with NIPP1 & Rtf1. The activity-dependent expression of ELL2 may allow the formation of a complex that can affect gene transcription and/or mRNA processing, which will be discussed shortly.

In summary, a selection of the potential MAST4 interactors are expressed in the nucleus. However, the ELL isoforms show a marked change in expression, and clear co-localisation, following co-transfection with mRFP-CD. This change in expression patterns strongly suggests that the interaction has been confirmed outside of the YTH system. The interaction of the C-domain of MAST4 with the ELL isoforms was the strongest shown in the YTH system, as described in Table 5.3 (Chapter 5). This may help to rationalise the change in expression patterns observed following co-transfection of the GFP-tagged ELL isoforms with mRFP-CD. Some of the potential interactors that were expressed in the nucleus, but did not show clear specific co-localisation, interacted less strongly with the C-domain in the YTH system than the ELL isoforms (i.e. NIPP1, CK2 & Rtf1). The 14-3-3 isoforms also show a relatively strong interaction with the C-domain of MAST4, although there was not any evidence of a specific co-localisation in co-transfected cells.

The possibility that some of these interactions may allow MAST4 to contribute to transcription and/or mRNA processing will be considered in the General Discussion.

Chapter 7 - General Discussion

The domain structure of the MAST family suggests that they can interact with other proteins via their PDZ domain and/or contribute to signalling events via their kinase domain. The capacity of these domains to perform these functions has been confirmed for some MAST family members. For example, the PDZ domains of MAST1, 2 & 3 have been found to interact with the phosphatase PTEN, which is also a substrate for their kinase domains (Valiente et al., 2005). The interactions identified for the MAST family are required within many tissues as reported by this study and others (Valiente et al., 2005). This suggests that the MAST family functions within a wide variety of biological contexts. The expression of MAST1 & 2 transcripts across multiple tissues has been reported, as well as MAST1 protein in brain (Lumeng et al., 1999). However, a full characterisation of MAST family expression across multiple tissues and within brain has not yet been conducted. Therefore, as part of this study, the expression of MAST family transcripts was investigated using northern blot analysis, reverse-transcriptase PCR and *in situ* hybridisation on rat brain. As described in Chapter 3, the expression of MAST1 & 2 transcripts appears similar across a variety of mouse tissues using RT-PCR. In contrast, transcripts for MAST3, 4 and MAST-like show a more selective expression. Similarly, the expression of MAST1 & 2 in rat brain is similar, and MAST3 and 4 is selective. This data would suggest that MAST1 and 2 share similar functions, while MAST3 and 4 have unique functions. This study has focused on characterising the function of MAST4.

Like other members of the MAST family, MAST4 contains a PDZ domain and kinase domain. The expression of this family member has also been shown, by this study and others, to increase in the hippocampus following seizure-like activity (French et al., 2001b). PDZ domain containing proteins are often involved in scaffolding at the plasma membrane (Kim and Sheng, 2004). For example, as described in Chapters 3 & 4, MAST1 & 2 have been shown to interact with scaffolding proteins at the plasma membrane, as well as metabotropic glutamate receptors {Lumeng, 1999 85 /id /ft "; Pilkington, BJ, PhD thesis"}. Therefore, the initial hypothesis was that MAST4 may contribute to scaffolding and signalling at the synapse following changes in synaptic activity. To test this hypothesis, the yeast-two hybrid system was used to identify potential interacting partners for MAST4, which would also suggest possible substrates for its kinase domain.

As described in Chapter 4, both MAST1 & 2 have been shown to interact with group I mGluRs (Pilkington, BJ. PhD thesis). Therefore, it was considered appropriate to test

whether MAST4 may also interact with these receptors. However, no evidence of any interaction was observed between the C-tails of the mGluRs and the PDZ domain of MAST4.

As no interaction was observed between the mGluRs and MAST4, it was decided to screen for interacting proteins using the YTH system. Full-length MAST4 is too large to use in a YTH screen, therefore, MAST4 was separated into a kinase, PDZ, and C-domain. The PDZ and C-domain were chosen as possible baits for a YTH screen. However, the PDZ domain construct proved unsuitable as it was able to activate the reporter genes autonomously. Therefore, the C-domain of MAST4 was used to screen for interacting proteins.

The YTH screen for MAST4 interacting proteins produced a variety of potential candidates; however, their was not a common structural element amongst these potential interactor that could rationalise their interaction with MAST4. Therefore, a secondary screen was performed to confirm the potential interactions identified by the screen and gather information about the subcellular localisation of the interactors.

The expression patterns observed for MAST4 and its possible interactions suggest possible roles in both neuronal and glia biology. These possibilities are discussed below.

Under basal conditions MAST4 is expressed in neurons of the hippocampus and oligodendroglial cells in white matter containing regions of the brain, as described in Chapter 3. However, following synaptic activity there is a significant upregulation of MAST4 transcript in the dentate gyrus, as shown by this study and French et al (2001). Therefore, is this upregulation in glia or neurons? Due to time constraints, it was not possible to directly answer this question using emulsion autoradiography and/or immunohistochemistry (see Appendix A) on brains from animals subjected to EMS. However, as will be argued below, neurons and glia share various aspects of their biology that may allow these expression patterns to be resolved.

The upregulation of MAST4 following EMS suggests that MAST4 is regulated by activity at the synapse. This hypothesis is supported by a recent report showing upregulation of MAST4 following stimulation of synaptic NMDA receptors (Zhang et al., 2007). These authors used dissociated hippocampal neuronal cultures to investigate the effects of synaptic and extrasynaptic NMDA receptor stimulation on gene expression. The transcriptome of cultured cells was investigated following treatment with the $GABA_A$ antagonist bicuculline or bath glutamate application of glutamate. The

former treatment caused burst firing and therefore vesicular release of glutamate onto postsynaptic NMDA receptors, whereas the latter treatment caused activation of both synaptic and extrasynaptic receptors. MAST4 was one of 108 genes found to be upregulated by bicuculline treatment, but not bath glutamate application; this suggests that MAST4 is upregulated by synaptic NMDA receptors. The identity of genes upregulated by synaptic NMDA receptors suggested a transcriptional profile that promotes neuroprotection (Zhang et al., 2007).

The report by Zhang et al suggests that MAST4 is upregulated in neurons following an increase in synaptic activity. However, both NMDA receptors and functional synapses have been identified within glia. For example, treatment of adult rats with NMDA decreases both the proliferation of neural progenitors and survival of nascent granule cells in the dentate gyrus (Cameron et al., 1995); this effect may be mediated by NMDA receptors whose expression in neural progenitors and differentiating granule cells has recently been characterised (Nacher et al., 2007). Although, the report by Nacher et al (2007) does not provide direct evidence for expression of NMDA receptor in neuron-glia synapses, this does not exclude the possibility that these NMDA receptors may preserve some of the signalling pathways and effects associated with synaptic NMDA receptors. Therefore, as noted in Chapter 3, MAST4 may be expressed in this population of radial-glia cell progenitors and its upregulation following activity may occur through glutamatergic transmission. Interestingly, the glutamate-aspartate transporter has recently been shown to be selectively expressed in both radial-glia cells of the dentate gyrus as well as oligodendrocytes in white matter containing regions (Regan et al., 2007). This suggests that these distinct populations of glia share aspects of glutamatergic signalling. In fact, as described in Chapter 1, the presence of axosomatic synapses between unmyelinated callosal axons and NG2+ cells suggest that glutamatergic signalling may play an important role in the proliferation and survival of oligodendrocyte precursors (Ziskin et al., 2007). Although, these axosomatic synapses predominantly expressed AMPA receptors, Ziskin et al also report the presence of low levels of NMDA receptors, which again may rationalise the expression of MAST4 within white matter regions.

In summary, whether the expression of MAST4 is affected by NMDA receptor signalling or not, the population of cells that express MAST4 share aspects of glutamatergic signalling which may rationalise the expression of MAST4 within neurons and/or glia.

Does the YTH analysis of MAST4 interacting partners suggest what function this kinase has in neurons and/or glia?

In the both the YTH system and expression analysis, the strongest and clearest interaction was observed with the isoforms of the elongation factor, ELL. Interestingly, ELL2 was also found by to be upregulated by bicuculline treatment in cultured hippocampal neurons (Zhang et al., 2007); and, as stated before, the expression of this isoform of ELL is upregulated in the dentate gyrus by electroconvulsive seizure (Ploski et al., 2006). ELL2, and possibly the other isoforms of ELL, therefore represent possible *in vivo* interacting partners for MAST4. What might be the function of this interaction?

The ELL isoforms are known to promote the rate of transcription, but why would they interact with a kinase? The progress of RNA polymerase II (PolII) through chromatin is separated into initiation (i.e. recruitment to a promoter), elongation, and termination. The C-terminal domain (CTD) of PolII is not phosphorylated during transcription initiation, but is hyperphosphorylated on serine residues during transcription elongation (Phatnani and Greenleaf, 2006). The CTD of PolII has been found to be phosphorylated by many kinases; therefore, MAST4 could potentially contribute to phosphorylation of this regulatory domain. What genes might be regulated by this complex?

The drosophila homolog of ELL (dELL) has a non-redundant and essential role in fly development (Eissenberg et al., 2002). Interestingly, this appears to involve a preferential effect on relatively large genes, such as Notch (Eissenberg et al., 2002). The Notch signalling pathway has been suggested to play a role in plasticity and the regulation of cellular phenotype (Costa et al., 2005; Alvarez-Buylla and Lim, 2004). For example, mice heterozygous for a null mutation in the gene encoding Notch1 show impairment in the formation of long-term memories in the Morris water maze (Costa et al., 2003). Also, activation of Notch in postnatal subventricular zone cells suppresses neuronal differentiation and promotes a quiescent multipotent phenotype (Chambers et al., 2001). There are therefore two scenarios suggested by the reports above that may rationalise the upregulation of ELL2 in the dentate gyrus and possibly its interaction with MAST4. Firstly, upregulation of Notch in neurons may support plastic changes in synaptic strength that are required following synaptic activity, or secondly, increased expression of Notch may regulate differentiation of glial progenitors. Interestingly, Notch signalling plays an essential role in promoting differentiation of precursor cells into oligodendrocyte (Nicolay et al., 2007). Therefore, Notch signalling may represent

a shared feature amongst the cell types that express MAST4, which can rationalise its interaction with the ELL isoforms.

As described above, the drosophila homolog of ELL preferentially affects the transcription of large genes (Eissenberg et al., 2002). ELL isoforms are only present in metazoan eukaryotes and not bacteria and yeast, which Eissenberg et al (2003) interpret as resulting from the increased size of transcriptional units in metazoans. This difference is largely to the increased size and number of introns, which they suggest may require the regulation of elongation rate. An adjunct to this hypothesis can be found with the observation that introns size and number are functionally linked to the emergence of alternative splicing in eukaryotes (Kim et al., 2007). In particular, Kim et al (2007) report that cassette exons that can undergo skipping (i.e. are not included in the mature mRNA) are flanked by relatively long introns. In principle, it would take longer to transcribe short introns than long ones; therefore, this may represent a coupling between the kinetics of transcription and alternative mRNA splicing. This 'kinetic coupling model' has been described more comprehensively in the context of transcription factor and chromatin modification effects on elongation rate (Kornblihtt, 2006). The kinetic coupling model suggests that an increase in elongation rate promotes the skipping of cassette exons as a result of differential strength in 3' splice sites (Kornblihtt, 2006). If synaptic activity upregulates ELL2 in neurons and therefore increases elongation rate then it would be expected that certain transcripts will not contain alternatively spliced cassette exons. McKee et al (2007) have in fact shown that elevation of calcium in neuroblastoma cells leads to an increase of transcripts with skipped exons. These authors also established that alternative spliced exons were enriched at the 3' end of transcripts, which again suggests a coupling between transcriptional rate and splicing.

So, if elongation rate and alternative mRNA splicing are coupled how might an interaction between MAST4 and the ELL isoforms affect this? A useful model to answer this question involves the p110 (110kDa) isoform of Cdk11. Cdk11(p110) is localised to both nuclear speckles and the nucleoplasm (Loyer et al., 1998). Using the yeast-two hybrid system, Cdk11(110) has been found to interact with the general splicing factor RNPS1 and ELL2 (Loyer et al., 1998; Trembley et al., 2002). Interestingly, Cdk11(110) also interacts with CK2, which was shown to phosphorylate the CTD of PolII (Trembley et al., 2003). It has subsequently been established that immunodepletion of Cdk11(110) from cellular extracts reduces splicing of β-globulin

mRNA in an *in vitro* splicing assay (Hu et al., 2003). Taken together, these studies clearly illustrate that a kinase, in this case Cdk11(110), can scaffold multiple proteins that are functionally related to mRNA splicing. It is compelling that MAST4 has also been shown to interact with both ELL2 and CK2 in the YTH system, and confirmed for ELL2 using expression analysis of fluorophore tagged fusion proteins. Equally, it is unusual that MAST4, at least within the YTH system, has also been shown to interact with Rtf1 and NIPP1. As stated in Chapter 6, Rtf1 has been implicated in transcription elongation via an effect on chromatin modifications and NIPP1 has been implicated in mRNA splicing. Some or all of the interactions may combine to allow MAST4 to contribute to transcription and/or mRNA processing following synaptic activity.

The kinase activity of MAST4 may contribute to an effect on transcription by phosphorylating the CTD of PolII as suggested above; however, there is also evidence for phosphorylation directly effecting mRNA splicing. The MAST family are phylogenetically related to the cAMP-dependent class of serine/threonine kinases (PKA; Manning et al., 2002). In the context of transcription, the catalytic C subunit of PKA is known to passively diffuse into the nucleus and phosphorylate CREB (Reviewed in Karin and Hunter, 1995). However, Kvissel et al (2007) have also reported that the C subunit of PKA localises to nuclear speckles, regulates splicing and can phosphorylate splicing factors. Therefore, MAST4 exists within a branch of the kinome known to regulate both transcription and mRNA splicing.

The discussion above has assumed that full-length MAST4 is expressed in the nucleus. However, MAST4 may be expressed in multiple regions of the cell and/or functionally cleaved. As described in Appendix A there is some evidence using antisera raised against the C-domain of MAST4 that it undergoes a specific cleavage. Also, the function of the PDZ domain of MAST4 has not been resolved; and, as stated before, PDZ domain containing protein in neurons are often localised to the synaptic membrane. Therefore, it may be the case that MAST4 is localised to both the synapse and nucleus and the full protein or a cleavage product can translocate to the nucleus. Is there any precedent in the literature that may support this hypothesis?

The crystal structure for the C-terminus of occludin has been resolved and a large positively charged region within it shown to mediate binding to the MAGUK, ZO-1 (Li et al., 2005). Due to the high degree of homology between the C-terminus of occludin and the occludin-like domain in the ELL isoforms, Li et al hypothesis that the ELL isoforms may also bind to ZO family members. As described in Chapter 1,

MAGUK family members, ZO-1 and CASK, are known to translocate to the nucleus and bind transcription factors. Therefore, it is interesting that the ELL proteins may be subject to similar regulation by these proteins. If the ELL proteins are subject to this type of regulation then they may also be regulated by other MAGUK like proteins - that is, proteins that contain multiple scaffolding domains and function at the plasma membrane and the nucleus. MAST4 may be able to perform this role through its PDZ and C-domain. The potential proteolytic cleavage of MAST4 may also expose nuclear localisation signals which allow the C-domain to translocate to the nucleus and localise to chromatin deficient regions as illustrated for the fluorophore-tagged C-domain. This domain may then scaffold multiple proteins into a complex that can mediate transcription and/or splicing. These possibilities are illustrated in Figure 7.1 below.

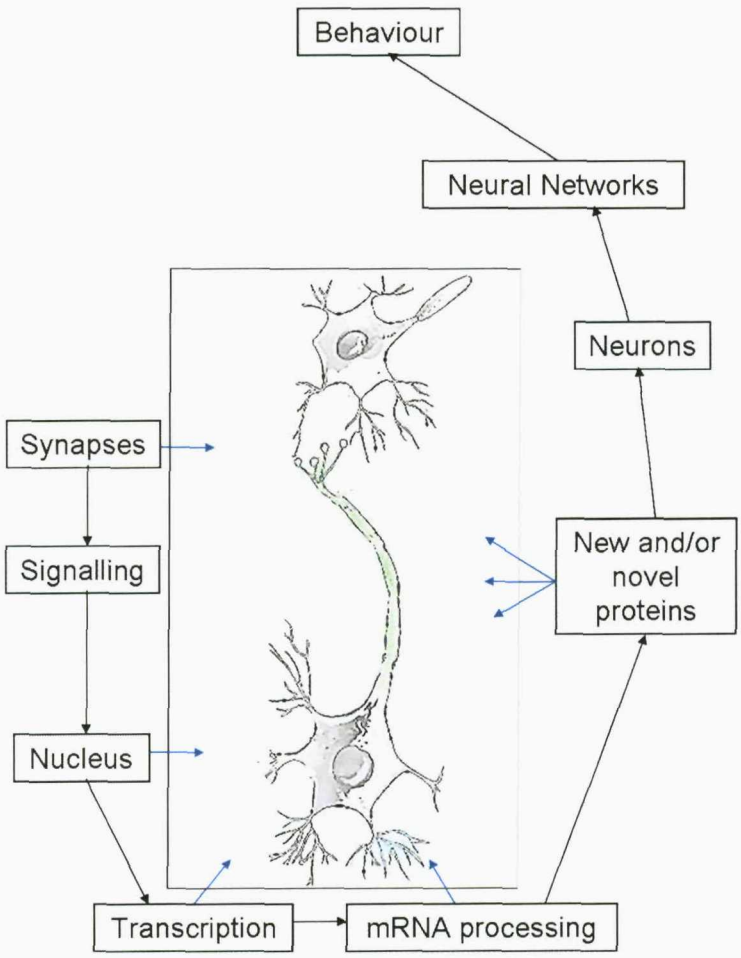

Figure 7.1. Possible effects of MAST4 on neuronal cell biology. MAST4 may be expressed at the synapse and scaffold proteins via its PDZ domain. The full-length protein or the cleaved C-domain may signal to the nucleus via translocation. Within the nucleus MAST4 may affect transcription and/or mRNA splicing. This will lead to production of new and/or novel proteins which ultimately affect neuronal, network and animal behaviour

The possible roles of MAST4 in neuronal biology described above could be investigate with a variety of experiments, which are outlined below.

If MAST4 forms a complex with nuclear related proteins then it may be possible to immunoprecipitate this complex. The limiting factor may be the avidity of antibodies raised against MAST4. As described in Appendix A, antisera has been raised against the C-domain of MAST; however, this antisera needs to be purified and tested for its suitability for this type of application. Alternatively, there are various companies that supply antisera raised against MAST4. If a suitable antibody can be raised against MAST4 then immunohistochemistry can be used to characterise the protein expression of MAST4 in brain, and were possible its co-localisation with candidate interactors.

Immunohistochemistry would potentially resolve the issue of whether MAST4 is expressed at the synapse and/or the nucleus. Also, this technique would clarify whether MAST4 is expressed in neuroprogenitors or neurons in the dentate gyrus, and confirm its expression in oligodendrocytes.

If MAST4 was found to be expressed at the synapse in neurons then it would be reasonable to assume it undergoes a PDZ mediate interaction. The PDZ domain bait construct transactivated in the YTH system; therefore, an alternative approach would be to express the PDZ domain as a GST-fusion protein and perform GST-pulldown assays using naïve or seized brain tissue.

If the experiments described above provided support for the interactions identified during this study then it would suggest that MAST4 is involved in transcription and/or mRNA splicing. To investigate this a set of experiments would need to be designed that look at the transcriptional profile of cells/tissues with and without the complex formed by MAST4.

As stated above Zhang et al (2007) identified the upregulation of MAST4 following bicuculline induced burst firing in cultured hippocampal cells. In itself this culture system could be used to investigate the cell biology of MAST4; however, it might also be possible (as Zhang et al did with some of the upregulated genes) to knockdown MAST4 expression using RNA interference. It would then be possible to analyse the transcriptome of cultured cells using standard or 'exon-centric' microarrays. The latter type of microarray allows the identification of spliced variants of particular genes. Alternatively, there are transgenic MAST4 mice that are commercially available which could be similarly used to investigate the transcriptome of hippocampal cells following seizure.

Both of the approaches described above would require independent confirmation of possible targets. This could be achieved using reverse-transcriptase PCR and/or immunohistochemistry.

If a role for MAST4 in transcription and/or splicing was established then it would be useful to develop *in vitro* assays to determine the key interactions and conditions required for the effect observed *in vivo*.

Finally, if MAST4 was found to be involved in neural plasticity it would be possible to investigate any behavioural phenotypes present in the transgenic mice; for example, by using learning paradigms such as the Morris water maze, or contextual fear conditioning.

The interactions identified for MAST4 suggest a role in transcription and/or splicing. If these interactions occur *in vivo* MAST4 would join a group of activity-dependent protein that have already been shown to play a role in the nucleus, such as AIDA-1 and zif268. However, an effect on elongation rate during transcription would reveal a novel point of regulation following synaptic activity. This would reinforce the observation that changes in the transcriptome of neurons is a necessary part of its response to synaptic activity.

Appendix A

The expression of MAST4 transcript has been investigated using in situ hybridisation. However, to fully characterise MAST4 expression immunohistochemistry is required. At the beginning of this study there was not an antibody available to study MAST4 protein expression. Therefore, a region of the C-domain of MAST4 was expressed and used as an antigen to raise antisera against MAST4. An outline of this part of the study is illustrated schematically in Figure A1 below.

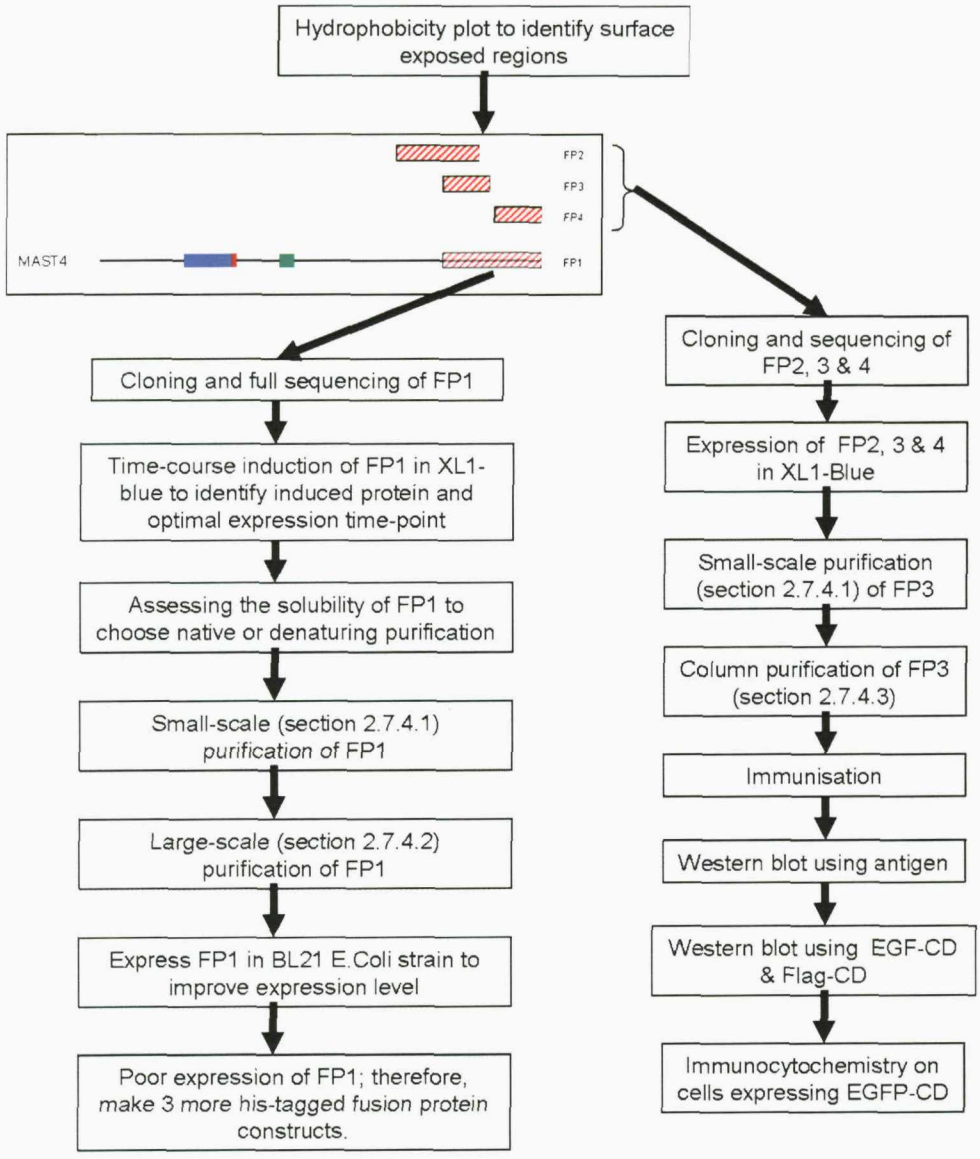

Figure A1. Expression of His-tagged fusion protein for use as antigens to raise antisera against MAST4. Initially, a 65kDa region of the C-terminus of MAST4 was expressed as a his-tag fusion protein; however, due to poor expression levels 3 more constructs were made. Construct 'FP3' expressed well enough to be purified for use as an antigen to raise antisera against MAST4.

As shown in Figure A1, a 64kDa region of the C-domain of MAST4, termed FP1, was initially cloned in-frame in to the vector pQE-30. This allows this region of MAST4 to be expressed as a His-tagged fusion protein (6X histidine residues at the N-terminus), which can therefore be purified using NiNTA resin (Qiagen; section 2.7.4).

This region of MAST4 expressed poorly in XL1-blue E.Coli, which lead to an inability to purify sufficient quantities for an immunisation protocol (Figure A1). Therefore, 3 more regions of the C-domain were chosen to be expressed as his-tagged fusion proteins (Figure A1). One of these, FP3, expressed at high enough levels to be purified and used as an antigen to raise antisera against MAST4. The immunisation protocol involved the inoculation of two rabbits (Eurogentec) and is described in section 2.8.

Pre-immune, small and large bleeds were received from Eurogenetec and an initial characterisation of the antisera conducted. The antigen used to raise antisera was run through an SDS-PAGE gel and transferred onto nitrocellulose. This was probed using the antisera and bands of the expected size were detected (data not shown). Subsequently, Flag-CD (see Chapter 2) was used to transfect HEK293 cells and a homogenate collected for use in western blotting. This homogenate was separated using SDS-PAGE electrophoresis and the proteins transferred onto nitrocellulose. The blot was probed using the antisera and a Flag specific monoclonal antibody. The results for this western blot are shown in Figure A2.

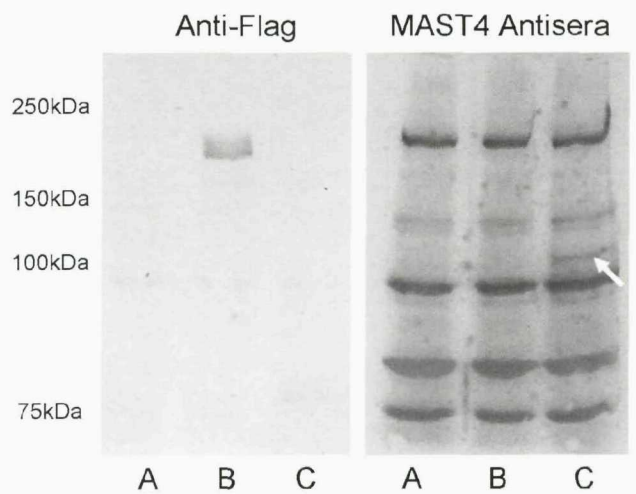

Figure A2. Western blot using a homogenate from a Flag-CD transfection and antisera raised against MAST4. Two 7.5% SDS-PAGE gels were loaded with a homogenate from untransfected HEK293 cells (A), Flag-MAST1 transfected HEK293 cells (B), and Flag-CD transfected HEK93 cells (C). Following immobilisation of protein onto nitrocellulose, each blot was probed with an anti-Flag monoclonal antibody (1:500) and crude antisera for MAST (1:500). A specific band using the Flag-CD homogenate was detected using the antisera (white arrow)

The western blot illustrated in Figure A2 shows that a specific band at about 110kDa can be seen only with the homogenate from the Flag-CD transfection. The flag antibody did not detect this band or one of the expected size (140kDa) on this western blot, which suggests that the C-domain is being cleaved about 30kDa from the N-terminal end (i.e. where the Flag epitope is fused to the C-domain). Interestingly, when a western blot is performed using EGFP-CD and probed using a GFP specific antibody (Figure 6.1) a 80kDa band can be seen. EGFP is 27kDa in size, therefore, this implies that the C-domain is being cleaved about 50kDa from the N-terminal end. Due to differences in gel resolving strength and estimation of protein size, the results for described above suggest that the C-domain of MAST4 is being cleaved ≈40kDa +/- 10kDa from the N-terminal end prior to, or during, the extraction process. This possibility is illustrated in Figure A3 below.

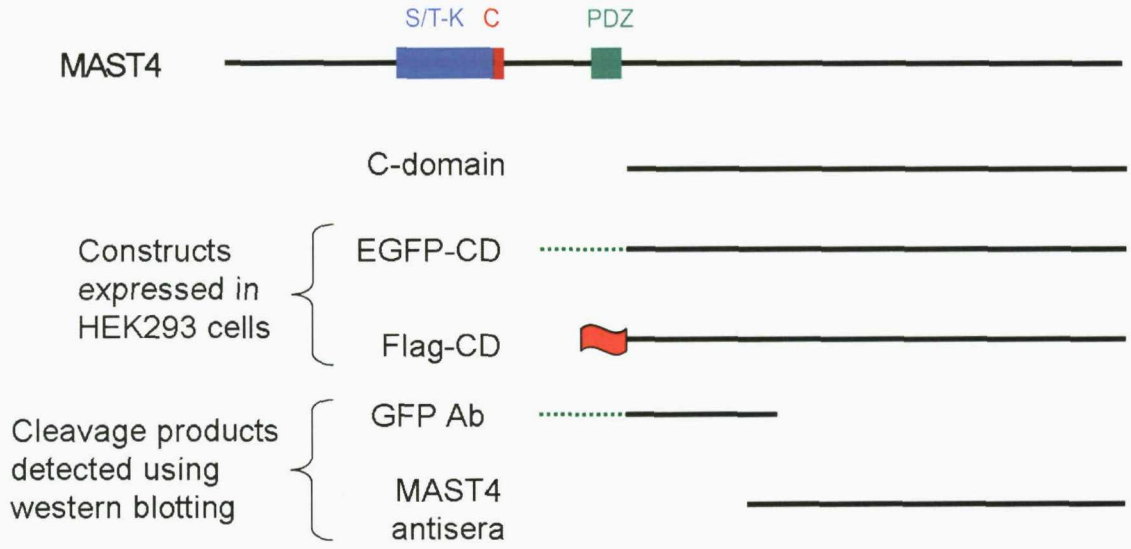

Figure A3. C-domain constructs expressed in HEK293 cells and possible cleavage products detected using western blotting. From top to bottom, full-length MAST4 is illustrated compared to the isolated C-domain. The C-domain was expressed as a GFP- and Flag-tagged fusion protein in HEK293 cells. Western blotting using homogenates from transfected cells revealed a ≈50kDa protein using a GFP-specific antibody and ≈110kDa protein using a MAST4 antisera. These may represent two cleavage products from the C-domain of MAST4.

This cleavage may represent a functionally important proteolytic processing of MAST4 or simply an artefact of the expression of this region of MAST4 within HEK293 cells. If the former scenario is true then this cleavage may allow MAST4 to localise to one compartment of the cell (e.g. the synapse in neurons) and signal to other regions (e.g. the nucleus) following, for example, synaptic activity.

To assess the antisera raised against MAST4 further is was decided to perform immunocytochemistry on HEK293 cells transfected with EGFP-CD. This would therefore allow the GFP signal from this construct to be co-localised to another fluorescent signal produced by immunocytochemistry (section 2.5) using the MAST4 antisera. As a control, this experiment was repeated using a pre-immunisation antisera. The result for this experiment is illustrated in Figure A4 & A5 below.

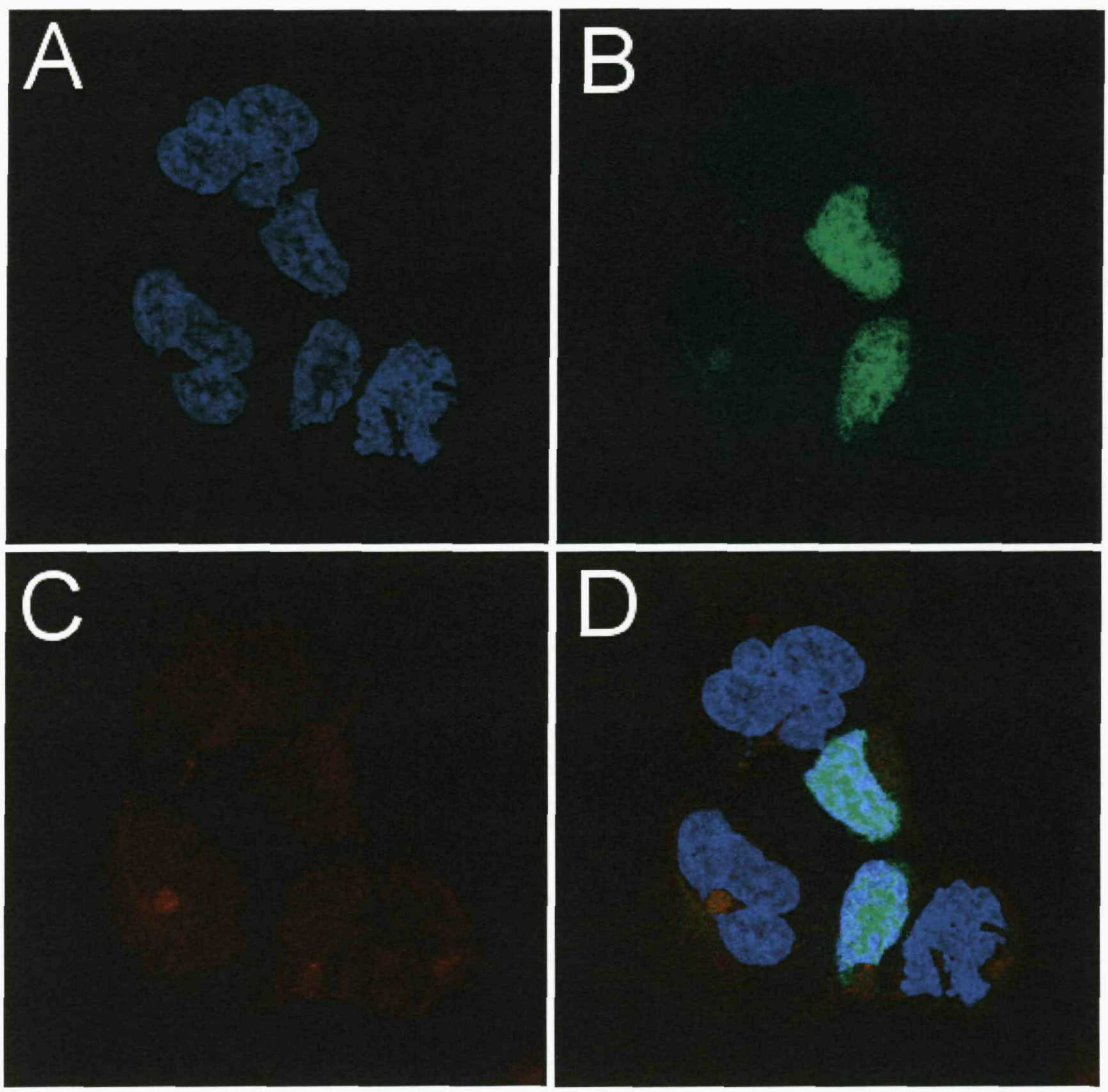

Figure A4. Immunocytochemistry on HEK293 cells expression EGFP-CD using the pre-immunisation antisera. HEK293 cells were transfected with EGFP-CD, fixed with 4% PFA, and probed using 1:500 dilution of the pre-immunisation antisera (see section 2.5 for full method). (A) fluorescent derived from DAPI staining: excitation = 359nm & filter 400-550 band pass. (B) Fluorescence derived from GFP: excitation = 488 & filter = 500-600 band pass. (C) fluorescent derived from an Alexa 633 specific settings: Excitation = 633 & filter 648-680 band pass. (D) overlay of fluorescence from A-C. Images were collected sequentially. The pre-immune sera does not reveal the nuclear staining observed via GFP fluorescence.

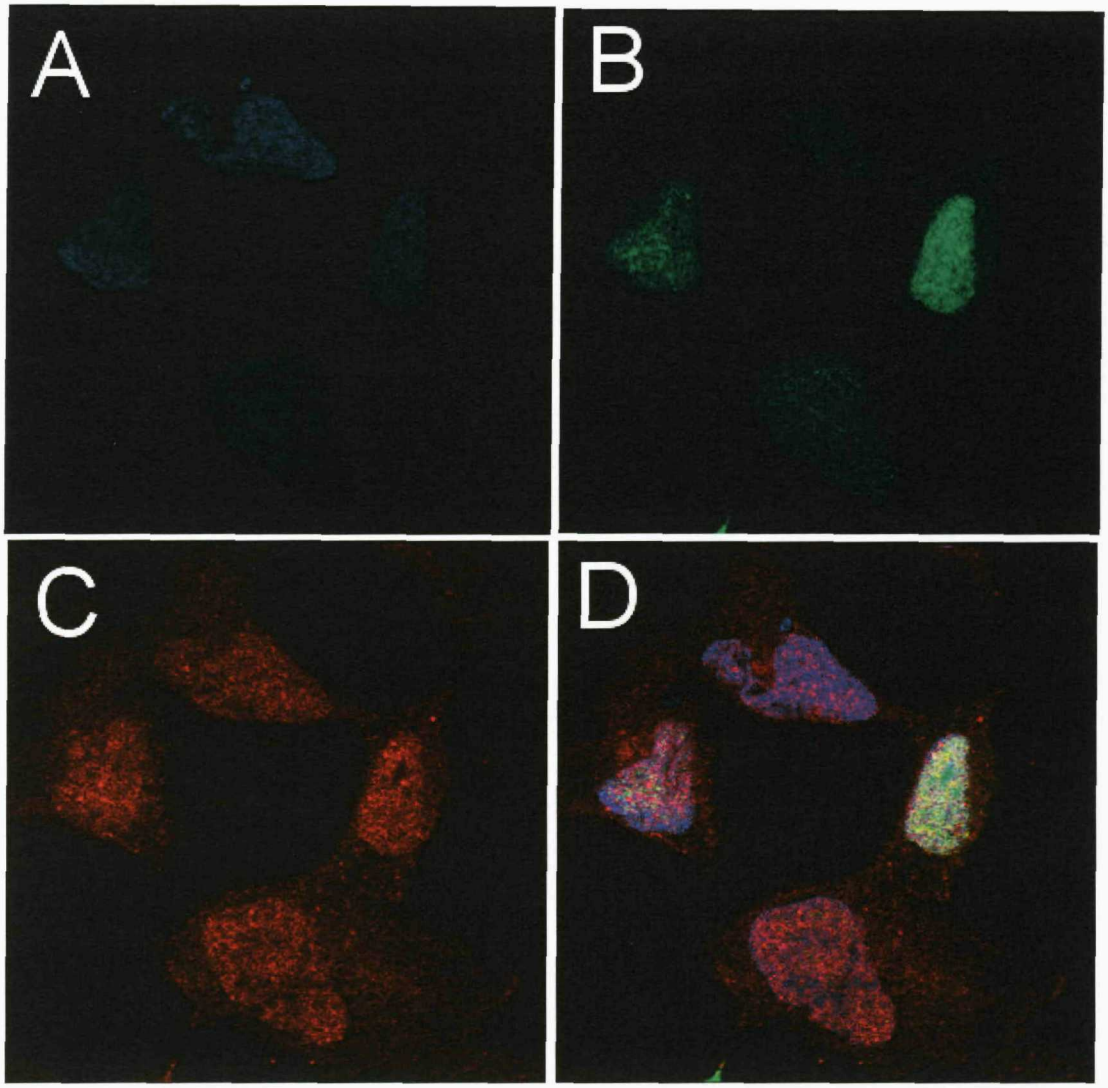

Figure A5. Immunocytochemistry on HEK293 cells expression EGFP-CD using antisera raised against MAST4. HEK293 cells were transfected with EGFP-CD, fixed with 4% PFA, and probed using 1:500 dilution of the antisera raised against MAST4 and a secondary antibody conjugated to Alexa 633 (see section 2.5 for full method). (A) fluorescent derived from DAPI staining: excitation = 359nm & filter 400-550 band pass. (B) Fluorescence derived from GFP: excitation = 488 & filter = 500-600 band pass. (C) fluorescent derived from an Alexa 633 specific settings: Excitation = 633 & filter 648-680 band pass. (D) overlay of fluorescence from A-C. Images were collected sequentially. Antisera raised against MAST4 is able to label the EGFP-CD

Figures A4 and A5 shows that the antisera raised against MAST4 can detect the EGFP-CD construct, which includes the region encompassed by the antigen used for immunisation (Figure A1). As can be seen in Figure A5, the GFP signal is localised to the nucleus, which is also the site of the strongest fluorescence seen using the antisera. Figure A5 also shows evidence of background staining of the rest of the HEK293 cell. This, again, is evidence that the antisera needs to be purified.

The images shown in Figures A4 & A5 are representative of multiple examples evident for the single transfection which these images are derived from.

The antisera raised against MAST4 does appear able to detect this protein; however, it needs to be purified as it generates a large background as can be seen in Figure A2. Following purification, this antisera could potentially be used to perform some of the experiments described in Chapter 7 (e.g. immunohistochemistry and/or immunoprecipitation of MAST4 and any interacting proteins).

Reference List

Adey NB, Huang L, Ormonde PA, Baumgard ML, Pero R, Byreddy DV, Tavtigian SV, Bartel PL, 2000. Threonine phosphorylation of the MMAC1/PTEN PDZ binding domain both inhibits and stimulates PDZ binding. Cancer Res. 60: 35-37.

Ahn AH, Kunkel LM, 1995. Syntrophin binds to an alternatively spliced exon of dystrophin. J. Cell Biol. 128: 363-371.

Alarcon JM, Malleret G, Touzani K, Vronskaya S, Ishii S, Kandel ER, Barco A, 2004. Chromatin acetylation, memory, and LTP are impaired in CBP+/- mice: a model for the cognitive deficit in Rubinstein-Taybi syndrome and its amelioration. Neuron 42: 947-959.

Alvarez-Buylla A, Lim DA, 2004. For the long run: maintaining germinal niches in the adult brain. Neuron 41: 683-686.

Balda MS, Garrett MD, Matter K, 2003. The ZO-1-associated Y-box factor ZONAB regulates epithelial cell proliferation and cell density. J. Cell Biol. 160: 423-432.

Balda MS, Matter K, 2000. The tight junction protein ZO-1 and an interacting transcription factor regulate ErbB-2 expression. EMBO J. 19: 2024-2033.

Baranes D, Lederfein D, Huang YY, Chen M, Bailey CH, Kandel ER, 1998. Tissue plasminogen activator contributes to the late phase of LTP and to synaptic growth in the hippocampal mossy fiber pathway. Neuron 21: 813-825.

Baxter HC, Liu WG, Forster JL, Aitken A, Fraser JR, 2002. Immunolocalisation of 14-3-3 isoforms in normal and scrapie-infected murine brain. Neuroscience 109: 5-14.

Benson DL, 1997. Dendritic compartmentation of NMDA receptor mRNA in cultured hippocampal neurons. Neuroreport 8: 823-828.

Berger SL, 2007. The complex language of chromatin regulation during transcription. Nature 447: 407-412.

Bergles DE, Roberts JD, Somogyi P, Jahr CE, 2000. Glutamatergic synapses on oligodendrocyte precursor cells in the hippocampus. Nature 405: 187-191.

Beullens M, Bollen M, 2002. The protein phosphatase-1 regulator NIPP1 is also a splicing factor involved in a late step of spliceosome assembly. J. Biol. Chem. 277: 19855-19860.

Blanquet PR, 2000. Casein kinase 2 as a potentially important enzyme in the nervous system. Prog. Neurobiol. 60: 211-246.

Bliss TV, Collingridge GL, Morris RG, 2003. Introduction. Long-term potentiation and structure of the issue. Philos. Trans. R. Soc. Lond B Biol. Sci. 358: 607-611.

Bliss TV, Lomo T, 1973. Long-lasting potentiation of synaptic transmission in the dentate area of the anaesthetized rabbit following stimulation of the perforant path. J. Physiol 232: 331-356.

Boeckers TM, Winter C, Smalla KH, Kreutz MR, Bockmann J, Seidenbecher C, Garner CC, Gundelfinger ED, 1999. Proline-rich synapse-associated proteins ProSAP1 and ProSAP2 interact with synaptic proteins of the SAPAP/GKAP family. Biochem. Biophys. Res. Commun. 264: 247-252.

Bottai D, Guzowski JF, Schwarz MK, Kang SH, Xiao B, Lanahan A, Worley PF, Seeburg PH, 2002. Synaptic activity-induced conversion of intronic to exonic sequence in Homer 1 immediate early gene expression. J. Neurosci. 22: 167-175.

Bourtchuladze R, Frenguelli B, Blendy J, Cioffi D, Schutz G, Silva AJ, 1994. Deficient long-term memory in mice with a targeted mutation of the cAMP-responsive element-binding protein. Cell 79: 59-68.

Bradshaw KD, Emptage NJ, Bliss TV, 2003. A role for dendritic protein synthesis in hippocampal late LTP. Eur. J. Neurosci. 18: 3150-3152.

Brakeman PR, Lanahan AA, O'Brien R, Roche K, Barnes CA, Huganir RL, Worley PF, 1997. Homer: a protein that selectively binds metabotropic glutamate receptors. Nature 386: 284-288.

Bregman DB, Hirsch AH, Rubin CS, 1991. Molecular characterization of bovine brain P75, a high affinity binding protein for the regulatory subunit of cAMP-dependent protein kinase II beta. J. Biol. Chem. 266: 7207-7213.

Brunet A, Kanai F, Stehn J, Xu J, Sarbassova D, Frangioni JV, Dalal SN, DeCaprio JA, Greenberg ME, Yaffe MB, 2002. 14-3-3 transits to the nucleus and participates in dynamic nucleocytoplasmic transport. J. Cell Biol. 156: 817-828.

Burgin KE, Waxham MN, Rickling S, Westgate SA, Mobley WC, Kelly PT, 1990. In situ hybridization histochemistry of Ca2+/calmodulin-dependent protein kinase in developing rat brain. J. Neurosci. 10: 1788-1798.

Cameron HA, McEwen BS, Gould E, 1995. Regulation of adult neurogenesis by excitatory input and NMDA receptor activation in the dentate gyrus. J. Neurosci. 15: 4687-4692.

Campbell NA, Reece JB, 2004. Biology. Benjamin Cummings.

Carr DW, Stofko-Hahn RE, Fraser ID, Cone RD, Scott JD, 1992. Localization of the cAMP-dependent protein kinase to the postsynaptic densities by A-kinase anchoring proteins. Characterization of AKAP 79. J. Biol. Chem. 267: 16816-16823.

Carrion AM, Link WA, Ledo F, Mellstrom B, Naranjo JR, 1999. DREAM is a Ca2+-regulated transcriptional repressor. Nature 398: 80-84.

Ceulemans H, Bollen M, 2004. Functional diversity of protein phosphatase-1, a cellular economizer and reset button. Physiol Rev. 84: 1-39.

Chamberlain J, 1999. The dynamics of dystroglycan. Nat. Genet. 23: 256-258.

Chambers CB, Peng Y, Nguyen H, Gaiano N, Fishell G, Nye JS, 2001. Spatiotemporal selectivity of response to Notch1 signals in mammalian forebrain precursors. Development 128: 689-702.

Chawla S, Vanhoutte P, Arnold FJ, Huang CL, Bading H, 2003. Neuronal activity-dependent nucleocytoplasmic shuttling of HDAC4 and HDAC5. J. Neurochem. 85: 151-159.

Chowdhury S, Shepherd JD, Okuno H, Lyford G, Petralia RS, Plath N, Kuhl D, Huganir RL, Worley PF, 2006. Arc/Arg3.1 interacts with the endocytic machinery to regulate AMPA receptor trafficking. Neuron 52: 445-459.

Christopherson KS, Sweeney NT, Craven SE, Kang R, El-Husseini A, Bredt DS, 2003. Lipid- and protein-mediated multimerization of PSD-95: implications for receptor clustering and assembly of synaptic protein networks. J. Cell Sci. 116: 3213-3219.

Coghlan VM, Perrino BA, Howard M, Langeberg LK, Hicks JB, Gallatin WM, Scott JD, 1995. Association of protein kinase A and protein phosphatase 2B with a common anchoring protein. Science 267: 108-111.

Cole AJ, Saffen DW, Baraban JM, Worley PF, 1989. Rapid increase of an immediate early gene messenger RNA in hippocampal neurons by synaptic NMDA receptor activation. Nature 340: 474-476.

Colledge M, Dean RA, Scott GK, Langeberg LK, Huganir RL, Scott JD, 2000. Targeting of PKA to glutamate receptors through a MAGUK-AKAP complex. Neuron 27: 107-119.

Colledge M, Snyder EM, Crozier RA, Soderling JA, Jin Y, Langeberg LK, Lu H, Bear MF, Scott JD, 2003. Ubiquitination regulates PSD-95 degradation and AMPA receptor surface expression. Neuron 40: 595-607.

Costa RM, Drew C, Silva AJ, 2005. Notch to remember. Trends Neurosci. 28: 429-435.

Costa RM, Honjo T, Silva AJ, 2003. Learning and memory deficits in Notch mutant mice. Curr. Biol. 13: 1348-1354.

Coutinho V, Knopfel T, 2002. Metabotropic glutamate receptors: electrical and chemical signaling properties. Neuroscientist. 8: 551-561.

Cracco JB, Serrano P, Moskowitz SI, Bergold PJ, Sacktor TC, 2005. Protein synthesis-dependent LTP in isolated dendrites of CA1 pyramidal cells. Hippocampus 15: 551-556.

Crawford BD, Hess JL, 2006. MLL core components give the green light to histone methylation. ACS Chem. Biol. 1: 495-498.

Cuadrado A, Navarro-Yubero C, Furneaux H, Kinter J, Sonderegger P, Munoz A, 2002. HuD binds to three AU-rich sequences in the 3'-UTR of neuroserpin mRNA and

promotes the accumulation of neuroserpin mRNA and protein. Nucleic Acids Res. 30: 2202-2211.

Darling DL, Yingling J, Wynshaw-Boris A, 2005. Role of 14-3-3 proteins in eukaryotic signaling and development. Curr. Top. Dev. Biol. 68: 281-315.

Deisseroth K, Bito H, Tsien RW, 1996. Signaling from synapse to nucleus: postsynaptic CREB phosphorylation during multiple forms of hippocampal synaptic plasticity. Neuron 16: 89-101.

Deisseroth K, Heist EK, Tsien RW, 1998. Translocation of calmodulin to the nucleus supports CREB phosphorylation in hippocampal neurons. Nature 392: 198-202.

Deisseroth K, Mermelstein PG, Xia H, Tsien RW, 2003. Signaling from synapse to nucleus: the logic behind the mechanisms. Curr. Opin. Neurobiol. 13: 354-365.

Deisseroth K, Singla S, Toda H, Monje M, Palmer TD, Malenka RC, 2004. Excitation-neurogenesis coupling in adult neural stem/progenitor cells. Neuron 42: 535-552.

Dolmetsch RE, Pajvani U, Fife K, Spotts JM, Greenberg ME, 2001. Signaling to the nucleus by an L-type calcium channel-calmodulin complex through the MAP kinase pathway. Science 294: 333-339.

Doyle DA, Lee A, Lewis J, Kim E, Sheng M, MacKinnon R, 1996. Crystal structures of a complexed and peptide-free membrane protein-binding domain: molecular basis of peptide recognition by PDZ. Cell 85: 1067-1076.

Dragunow M, Robertson HA, 1987. Kindling stimulation induces c-fos protein(s) in granule cells of the rat dentate gyrus. Nature 329: 441-442.

Ehlers MD, 2003. Activity level controls postsynaptic composition and signaling via the ubiquitin-proteasome system. Nat. Neurosci. 6: 231-242.

Ehrengruber MU, Kato A, Inokuchi K, Hennou S, 2004. Homer/Vesl proteins and their roles in CNS neurons. Mol. Neurobiol. 29: 213-227.

Eissenberg JC, Ma J, Gerber MA, Christensen A, Kennison JA, Shilatifard A, 2002. dELL is an essential RNA polymerase II elongation factor with a general role in development. Proc. Natl. Acad. Sci. U. S. A 99: 9894-9899.

Esteban JA, Shi SH, Wilson C, Nuriya M, Huganir RL, Malinow R, 2003. PKA phosphorylation of AMPA receptor subunits controls synaptic trafficking underlying plasticity. Nat. Neurosci. 6: 136-143.

Estojak J, Brent R, Golemis EA, 1995. Correlation of two-hybrid affinity data with in vitro measurements. Mol. Cell Biol. 15: 5820-5829.

Ferreira A, Chin LS, Li L, Lanier LM, Kosik KS, Greengard P, 1998. Distinct roles of synapsin I and synapsin II during neuronal development. Mol. Med. 4: 22-28.

Fields RD, 2005. Myelination: an overlooked mechanism of synaptic plasticity? Neuroscientist. 11: 528-531.

Fields S, Song O, 1989. A novel genetic system to detect protein-protein interactions. Nature 340: 245-246.

Fischer M, Kaech S, Knutti D, Matus A, 1998. Rapid actin-based plasticity in dendritic spines. Neuron 20: 847-854.

French PJ, O'Connor V, Jones MW, Davis S, Errington ML, Voss K, Truchet B, Wotjak C, Stean T, Doyere V, Maroun M, Laroche S, Bliss TV, 2001a. Subfield-specific immediate early gene expression associated with hippocampal long-term potentiation in vivo. Eur. J. Neurosci. 13: 968-976.

French PJ, O'Connor V, Voss K, Stean T, Hunt SP, Bliss TV, 2001b. Seizure-induced gene expression in area CA1 of the mouse hippocampus. Eur. J. Neurosci. 14: 2037-2041.

Fukazawa Y, Saitoh Y, Ozawa F, Ohta Y, Mizuno K, Inokuchi K, 2003. Hippocampal LTP is accompanied by enhanced F-actin content within the dendritic spine that is essential for late LTP maintenance in vivo. Neuron 38: 447-460.

Fukuchi M, Tabuchi A, Tsuda M, 2004. Activity-dependent transcriptional activation and mRNA stabilization for cumulative expression of pituitary adenylate cyclase-activating polypeptide mRNA controlled by calcium and cAMP signals in neurons. J. Biol. Chem. 279: 47856-47865.

Gallo V, Zhou JM, McBain CJ, Wright P, Knutson PL, Armstrong RC, 1996. Oligodendrocyte progenitor cell proliferation and lineage progression are regulated by glutamate receptor-mediated K+ channel block. J. Neurosci. 16: 2659-2670.

Genin A, French P, Doyere V, Davis S, Errington ML, Maroun M, Stean T, Truchet B, Webber M, Wills T, Richter-Levin G, Sanger G, Hunt SP, Mallet J, Laroche S, Bliss TV, O'Connor V, 2003. LTP but not seizure is associated with up-regulation of AKAP-150. Eur. J. Neurosci. 17: 331-340.

Gericke A, Munson M, Ross AH, 2006. Regulation of the PTEN phosphatase. Gene 374: 1-9.

Ginty DD, Kornhauser JM, Thompson MA, Bading H, Mayo KE, Takahashi JS, Greenberg ME, 1993. Regulation of CREB phosphorylation in the suprachiasmatic nucleus by light and a circadian clock. Science 260: 238-241.

Goldman S, 2003. Glia as neural progenitor cells. Trends Neurosci. 26: 590-596.

Gonzalez-Mariscal L, Betanzos A, vila-Flores A, 2000. MAGUK proteins: structure and role in the tight junction. Semin. Cell Dev. Biol. 11: 315-324.

Gottardi CJ, Arpin M, Fanning AS, Louvard D, 1996. The junction-associated protein, zonula occludens-1, localizes to the nucleus before the maturation and during the remodeling of cell-cell contacts. Proc. Natl. Acad. Sci. U. S. A 93: 10779-10784.

Gould E, Beylin A, Tanapat P, Reeves A, Shors TJ, 1999. Learning enhances adult neurogenesis in the hippocampal formation. Nat. Neurosci. 2: 260-265.

Graef IA, Mermelstein PG, Stankunas K, Neilson JR, Deisseroth K, Tsien RW, Crabtree GR, 1999. L-type calcium channels and GSK-3 regulate the activity of NF-ATc4 in hippocampal neurons. Nature 401: 703-708.

Guan Z, Giustetto M, Lomvardas S, Kim JH, Miniaci MC, Schwartz JH, Thanos D, Kandel ER, 2002. Integration of long-term-memory-related synaptic plasticity involves bidirectional regulation of gene expression and chromatin structure. Cell 111: 483-493.

Hardingham GE, Arnold FJ, Bading H, 2001. A calcium microdomain near NMDA receptors: on switch for ERK-dependent synapse-to-nucleus communication. Nat. Neurosci. 4: 565-566.

Hastings NB, Gould E, 1999. Rapid extension of axons into the CA3 region by adult-generated granule cells. J. Comp Neurol. 413: 146-154.

Hillier BJ, Christopherson KS, Prehoda KE, Bredt DS, Lim WA, 1999. Unexpected modes of PDZ domain scaffolding revealed by structure of nNOS-syntrophin complex. Science 284: 812-815.

Hsueh YP, 2006. The role of the MAGUK protein CASK in neural development and synaptic function. Curr. Med. Chem. 13: 1915-1927.

Hsueh YP, Sheng M, 1999. Requirement of N-terminal cysteines of PSD-95 for PSD-95 multimerization and ternary complex formation, but not for binding to potassium channel Kv1.4. J. Biol. Chem. 274: 532-536.

Hsueh YP, Wang TF, Yang FC, Sheng M, 2000. Nuclear translocation and transcription regulation by the membrane-associated guanylate kinase CASK/LIN-2. Nature 404: 298-302.

Hu D, Mayeda A, Trembley JH, Lahti JM, Kidd VJ, 2003. CDK11 complexes promote pre-mRNA splicing. J. Biol. Chem. 278: 8623-8629.

Huang Y, Lu W, Ali DW, Pelkey KA, Pitcher GM, Lu YM, Aoto H, Roder JC, Sasaki T, Salter MW, MacDonald JF, 2001. CAKbeta/Pyk2 kinase is a signaling link for induction of long-term potentiation in CA1 hippocampus. Neuron 29: 485-496.

Huang YY, Bach ME, Lipp HP, Zhuo M, Wolfer DP, Hawkins RD, Schoonjans L, Kandel ER, Godfraind JM, Mulligan R, Collen D, Carmeliet P, 1996. Mice lacking the gene encoding tissue-type plasminogen activator show a selective interference with late-phase long-term potentiation in both Schaffer collateral and mossy fiber pathways. Proc. Natl. Acad. Sci. U. S. A 93: 8699-8704.

Hughes PE, Alexi T, Walton M, Williams CE, Dragunow M, Clark RG, Gluckman PD, 1999. Activity and injury-dependent expression of inducible transcription factors, growth factors and apoptosis-related genes within the central nervous system. Prog. Neurobiol. 57: 421-450.

Huynh DP, Scoles DR, Nguyen D, Pulst SM, 2003. The autosomal recessive juvenile Parkinson disease gene product, parkin, interacts with and ubiquitinates synaptotagmin XI. Hum. Mol. Genet. 12: 2587-2597.

Ishibashi T, Dakin KA, Stevens B, Lee PR, Kozlov SV, Stewart CL, Fields RD, 2006. Astrocytes promote myelination in response to electrical impulses. Neuron 49: 823-832.

Jagiello I, Van EA, Vulsteke V, Beullens M, Boudrez A, Keppens S, Stalmans W, Bollen M, 2000. Nuclear and subnuclear targeting sequences of the protein phosphatase-1 regulator NIPP1. J. Cell Sci. 113 Pt 21: 3761-3768.

James AB, Conway AM, Thiel G, Morris BJ, 2004. Egr-1 modulation of synapsin I expression: permissive effect of forskolin via cAMP. Cell Signal. 16: 1355-1362.

Jordan BA, Fernholz BD, Khatri L, Ziff EB, 2007. Activity-dependent AIDA-1 nuclear signaling regulates nucleolar numbers and protein synthesis in neurons. Nat. Neurosci. 10: 427-435.

Kang H, Schuman EM, 1996. A requirement for local protein synthesis in neurotrophin-induced hippocampal synaptic plasticity. Science 273: 1402-1406.

Kang H, Sun LD, Atkins CM, Soderling TR, Wilson MA, Tonegawa S, 2001. An important role of neural activity-dependent CaMKIV signaling in the consolidation of long-term memory. Cell 106: 771-783.

Kapuscinski J, 1995. DAPI: a DNA-specific fluorescent probe. Biotech. Histochem. 70: 220-233.

Karin M, Hunter T, 1995. Transcriptional control by protein phosphorylation: signal transmission from the cell surface to the nucleus. Curr. Biol. 5: 747-757.

Kato A, Ozawa F, Saitoh Y, Fukazawa Y, Sugiyama H, Inokuchi K, 1998. Novel members of the Vesl/Homer family of PDZ proteins that bind metabotropic glutamate receptors. J. Biol. Chem. 273: 23969-23975.

Kato A, Ozawa F, Saitoh Y, Hirai K, Inokuchi K, 1997. vesl, a gene encoding VASP/Ena family related protein, is upregulated during seizure, long-term potentiation and synaptogenesis. FEBS Lett. 412: 183-189.

Kauselmann G, Weiler M, Wulff P, Jessberger S, Konietzko U, Scafidi J, Staubli U, Bereiter-Hahn J, Strebhardt K, Kuhl D, 1999. The polo-like protein kinases Fnk and Snk associate with a Ca(2+)- and integrin-binding protein and are regulated dynamically with synaptic plasticity. EMBO J. 18: 5528-5539.

Kemp JM, Powell TP, 1971. The structure of the caudate nucleus of the cat: light and electron microscopy. Philos. Trans. R. Soc. Lond B Biol. Sci. 262: 383-401.

Kempermann G, Kuhn HG, Gage FH, 1997. More hippocampal neurons in adult mice living in an enriched environment. Nature 386: 493-495.

Kim CH, Braud S, Isaac JT, Roche KW, 2005. Protein kinase C phosphorylation of the metabotropic glutamate receptor mGluR5 on Serine 839 regulates Ca2+ oscillations. J. Biol. Chem. 280: 25409-25415.

Kim E, Magen A, Ast G, 2007. Different levels of alternative splicing among eukaryotes. Nucleic Acids Res. 35: 125-131.

Kim E, Naisbitt S, Hsueh YP, Rao A, Rothschild A, Craig AM, Sheng M, 1997. GKAP, a novel synaptic protein that interacts with the guanylate kinase-like domain of the PSD-95/SAP90 family of channel clustering molecules. J. Cell Biol. 136: 669-678.

Kim E, Niethammer M, Rothschild A, Jan YN, Sheng M, 1995. Clustering of Shaker-type K+ channels by interaction with a family of membrane-associated guanylate kinases. Nature 378: 85-88.

Kim E, Sheng M, 2004. PDZ domain proteins of synapses. Nat. Rev. Neurosci. 5: 771-781.

Kim JJ, Jung MW, 2006. Neural circuits and mechanisms involved in Pavlovian fear conditioning: a critical review. Neurosci. Biobehav. Rev. 30: 188-202.

Klann E, Antion MD, Banko JL, Hou L, 2004. Synaptic plasticity and translation initiation. Learn. Mem. 11: 365-372.

Klauck TM, Faux MC, Labudda K, Langeberg LK, Jaken S, Scott JD, 1996. Coordination of three signaling enzymes by AKAP79, a mammalian scaffold protein. Science 271: 1589-1592.

Konietzko U, Kauselmann G, Scafidi J, Staubli U, Mikkers H, Berns A, Schweizer M, Waltereit R, Kuhl D, 1999. Pim kinase expression is induced by LTP stimulation and required for the consolidation of enduring LTP. EMBO J. 18: 3359-3369.

Kopec CD, Li B, Wei W, Boehm J, Malinow R, 2006. Glutamate receptor exocytosis and spine enlargement during chemically induced long-term potentiation. J. Neurosci. 26: 2000-2009.

Kornau HC, Schenker LT, Kennedy MB, Seeburg PH, 1995. Domain interaction between NMDA receptor subunits and the postsynaptic density protein PSD-95. Science 269: 1737-1740.

Kornblihtt AR, 2006. Chromatin, transcript elongation and alternative splicing. Nat. Struct. Mol. Biol. 13: 5-7.

Korzus E, Rosenfeld MG, Mayford M, 2004. CBP histone acetyltransferase activity is a critical component of memory consolidation. Neuron 42: 961-972.

Krogan NJ, Dover J, Wood A, Schneider J, Heidt J, Boateng MA, Dean K, Ryan OW, Golshani A, Johnston M, Greenblatt JF, Shilatifard A, 2003. The Paf1 complex is required for histone H3 methylation by COMPASS and Dot1p: linking transcriptional elongation to histone methylation. Mol. Cell 11: 721-729.

Krucker T, Siggins GR, Halpain S, 2000. Dynamic actin filaments are required for stable long-term potentiation (LTP) in area CA1 of the hippocampus. Proc. Natl. Acad. Sci. U. S. A 97: 6856-6861.

Kubo T, Hata K, Yamaguchi A, Yamashita T, 2007. Rho-ROCK inhibitors as emerging strategies to promote nerve regeneration. Curr. Pharm. Des 13: 2493-2499.

Kukley M, Capetillo-Zarate E, Dietrich D, 2007. Vesicular glutamate release from axons in white matter. Nat. Neurosci. 10: 311-320.

Kvissel AK, Orstavik S, Eikvar S, Brede G, Jahnsen T, Collas P, Akusjarvi G, Skalhegg BS, 2007. Involvement of the catalytic subunit of protein kinase A and of HA95 in pre-mRNA splicing. Exp. Cell Res. 313: 2795-2809.

Lamond AI, Spector DL, 2003. Nuclear speckles: a model for nuclear organelles. Nat. Rev. Mol. Cell Biol. 4: 605-612.

Lamprecht R, LeDoux J, 2004. Structural plasticity and memory. Nat. Rev. Neurosci. 5: 45-54.

Lein ES, Hawrylycz MJ, Ao N, Ayres M, Bensinger A, Bernard A, Boe AF, Boguski MS, Brockway KS, Byrnes EJ, Chen L, Chen L, Chen TM, Chin MC, Chong J, Crook BE, Czaplinska A, Dang CN, Datta S, Dee NR, Desaki AL, Desta T, Diep E, Dolbeare TA, Donelan MJ, Dong HW, Dougherty JG, Duncan BJ, Ebbert AJ, Eichele G, Estin LK, Faber C, Facer BA, Fields R, Fischer SR, Fliss TP, Frensley C, Gates SN, Glattfelder KJ, Halverson KR, Hart MR, Hohmann JG, Howell MP, Jeung DP, Johnson RA, Karr PT, Kawal R, Kidney JM, Knapik RH, Kuan CL, Lake JH, Laramee AR, Larsen KD, Lau C, Lemon TA, Liang AJ, Liu Y, Luong LT, Michaels J, Morgan JJ, Morgan RJ, Mortrud MT, Mosqueda NF, Ng LL, Ng R, Orta GJ, Overly CC, Pak TH, Parry SE, Pathak SD, Pearson OC, Puchalski RB, Riley ZL, Rockett HR, Rowland SA, Royall JJ, Ruiz MJ, Sarno NR, Schaffnit K, Shapovalova NV, Sivisay T, Slaughterbeck CR, Smith SC, Smith KA, Smith BI, Sodt AJ, Stewart NN, Stumpf KR, Sunkin SM, Sutram M, Tam A, Teemer CD, Thaller C, Thompson CL, Varnam LR, Visel A, Whitlock RM, Wohnoutka PE, Wolkey CK, Wong VY, Wood M, Yaylaoglu MB, Young RC, Youngstrom BL, Yuan XF, Zhang B, Zwingman TA, Jones AR, 2007. Genome-wide atlas of gene expression in the adult mouse brain. Nature 445: 168-176.

Levenson JM, O'Riordan KJ, Brown KD, Trinh MA, Molfese DL, Sweatt JD, 2004. Regulation of histone acetylation during memory formation in the hippocampus. J. Biol. Chem. 279: 40545-40559.

Li L, Chin LS, Shupliakov O, Brodin L, Sihra TS, Hvalby O, Jensen V, Zheng D, McNamara JO, Greengard P, ., 1995. Impairment of synaptic vesicle clustering and of synaptic transmission, and increased seizure propensity, in synapsin I-deficient mice. Proc. Natl. Acad. Sci. U. S. A 92: 9235-9239.

Li Y, Fanning AS, Anderson JM, Lavie A, 2005. Structure of the conserved cytoplasmic C-terminal domain of occludin: identification of the ZO-1 binding surface. J. Mol. Biol. 352: 151-164.

Li Z, Okamoto K, Hayashi Y, Sheng M, 2004. The importance of dendritic mitochondria in the morphogenesis and plasticity of spines and synapses. Cell 119: 873-887.

Lie DC, Song H, Colamarino SA, Ming GL, Gage FH, 2004. Neurogenesis in the adult brain: new strategies for central nervous system diseases. Annu. Rev. Pharmacol. Toxicol. 44: 399-421.

Lin SC, Bergles DE, 2004. Synaptic signaling between GABAergic interneurons and oligodendrocyte precursor cells in the hippocampus. Nat. Neurosci. 7: 24-32.

Link W, Konietzko U, Kauselmann G, Krug M, Schwanke B, Frey U, Kuhl D, 1995. Somatodendritic expression of an immediate early gene is regulated by synaptic activity. Proc. Natl. Acad. Sci. U. S. A 92: 5734-5738.

Lipscombe D, 2005. Neuronal proteins custom designed by alternative splicing. Curr. Opin. Neurobiol. 15: 358-363.

Lipscombe D, Madison DV, Poenie M, Reuter H, Tsien RW, Tsien RY, 1988. Imaging of cytosolic Ca2+ transients arising from Ca2+ stores and Ca2+ channels in sympathetic neurons. Neuron 1: 355-365.

Loyer P, Trembley JH, Lahti JM, Kidd VJ, 1998. The RNP protein, RNPS1, associates with specific isoforms of the p34cdc2-related PITSLRE protein kinase in vivo. J. Cell Sci. 111 (Pt 11): 1495-1506.

Lu X, Wyszynski M, Sheng M, Baudry M, 2001. Proteolysis of glutamate receptor-interacting protein by calpain in rat brain: implications for synaptic plasticity. J. Neurochem. 77: 1553-1560.

Lumeng C, Phelps S, Crawford GE, Walden PD, Barald K, Chamberlain JS, 1999. Interactions between beta 2-syntrophin and a family of microtubule-associated serine/threonine kinases. Nat. Neurosci. 2: 611-617.

Lunyak VV, Burgess R, Prefontaine GG, Nelson C, Sze SH, Chenoweth J, Schwartz P, Pevzner PA, Glass C, Mandel G, Rosenfeld MG, 2002. Corepressor-dependent silencing of chromosomal regions encoding neuronal genes. Science 298: 1747-1752.

Lyford GL, Yamagata K, Kaufmann WE, Barnes CA, Sanders LK, Copeland NG, Gilbert DJ, Jenkins NA, Lanahan AA, Worley PF, 1995. Arc, a growth factor and activity-regulated gene, encodes a novel cytoskeleton-associated protein that is enriched in neuronal dendrites. Neuron 14: 433-445.

Lynch G, Baudry M, 1984. The biochemistry of memory: a new and specific hypothesis. Science 224: 1057-1063.

Maisel M, Herr A, Milosevic J, Hermann A, Habisch HJ, Schwarz S, Kirsch M, Antoniadis G, Brenner R, Hallmeyer-Elgner S, Lerche H, Schwarz J, Storch A, 2007. Transcription profiling of adult and fetal human neuroprogenitors identifies divergent paths to maintain the neuroprogenitor cell state. Stem Cells.

Malenka RC, Bear MF, 2004. LTP and LTD: an embarrassment of riches. Neuron 44: 5-21.

Malenka RC, Nicoll RA, 1999. Long-term potentiation--a decade of progress? Science 285: 1870-1874.

Malinow R, Malenka RC, 2002. AMPA receptor trafficking and synaptic plasticity. Annu. Rev. Neurosci. 25: 103-126.

Malter JS, 2001. Regulation of mRNA stability in the nervous system and beyond. J. Neurosci. Res. 66: 311-316.

Manning G, Whyte DB, Martinez R, Hunter T, Sudarsanam S, 2002. The protein kinase complement of the human genome. Science 298: 1912-1934.

Maple J, Moller SG, 2007. Yeast two-hybrid screening. Methods Mol. Biol. 362: 207-223.

Martin S, Nishimune A, Mellor JR, Henley JM, 2007. SUMOylation regulates kainate-receptor-mediated synaptic transmission. Nature 447: 321-325.

Martin SJ, Clark RE, 2007. The rodent hippocampus and spatial memory: from synapses to systems. Cell Mol. Life Sci. 64: 401-431.

Matsuzaki M, 2007. Factors critical for the plasticity of dendritic spines and memory storage. Neurosci. Res. 57: 1-9.

Matsuzaki M, Honkura N, Ellis-Davies GC, Kasai H, 2004. Structural basis of long-term potentiation in single dendritic spines. Nature 429: 761-766.

McKee AE, Neretti N, Carvalho LE, Meyer CA, Fox EA, Brodsky AS, Silver PA, 2007. Exon expression profiling reveals stimulus-mediated exon use in neural cells. Genome Biol. 8: R159.

McKinney RA, Capogna M, Durr R, Gahwiler BH, Thompson SM, 1999. Miniature synaptic events maintain dendritic spines via AMPA receptor activation. Nat. Neurosci. 2: 44-49.

Mercer A, Ronnholm H, Holmberg J, Lundh H, Heidrich J, Zachrisson O, Ossoinak A, Frisen J, Patrone C, 2004. PACAP promotes neural stem cell proliferation in adult mouse brain. J. Neurosci. Res. 76: 205-215.

Mermelstein PG, Deisseroth K, Dasgupta N, Isaksen AL, Tsien RW, 2001. Calmodulin priming: nuclear translocation of a calmodulin complex and the memory of prior neuronal activity. Proc. Natl. Acad. Sci. U. S. A 98: 15342-15347.

Miller CA, Sweatt JD, 2007. Covalent modification of DNA regulates memory formation. Neuron 53: 857-869.

Miller S, Yasuda M, Coats JK, Jones Y, Martone ME, Mayford M, 2002. Disruption of dendritic translation of CaMKIIalpha impairs stabilization of synaptic plasticity and memory consolidation. Neuron 36: 507-519.

Miller T, Williams K, Johnstone RW, Shilatifard A, 2000. Identification, cloning, expression, and biochemical characterization of the testis-specific RNA polymerase II elongation factor ELL3. J. Biol. Chem. 275: 32052-32056.

Ming GL, Song H, 2005. Adult neurogenesis in the mammalian central nervous system. Annu. Rev. Neurosci. 28: 223-250.

Miranda E, Lomas DA, 2006. Neuroserpin: a serpin to think about. Cell Mol. Life Sci. 63: 709-722.

Misteli T, Caceres JF, Clement JQ, Krainer AR, Wilkinson MF, Spector DL, 1998. Serine phosphorylation of SR proteins is required for their recruitment to sites of transcription in vivo. J. Cell Biol. 143: 297-307.

Misteli T, Caceres JF, Spector DL, 1997. The dynamics of a pre-mRNA splicing factor in living cells. Nature 387: 523-527.

Morgan JI, Cohen DR, Hempstead JL, Curran T, 1987. Mapping patterns of c-fos expression in the central nervous system after seizure. Science 237: 192-197.

Mori H, Manabe T, Watanabe M, Satoh Y, Suzuki N, Toki S, Nakamura K, Yagi T, Kushiya E, Takahashi T, Inoue Y, Sakimura K, Mishina M, 1998. Role of the carboxy-terminal region of the GluR epsilon2 subunit in synaptic localization of the NMDA receptor channel. Neuron 21: 571-580.

Mu Y, Otsuka T, Horton AC, Scott DB, Ehlers MD, 2003. Activity-dependent mRNA splicing controls ER export and synaptic delivery of NMDA receptors. Neuron 40: 581-594.

Nacher J, Varea E, Miguel Blasco-Ibanez J, Gomez-Climent MA, Castillo-Gomez E, Crespo C, Martinez-Guijarro FJ, McEwen BS, 2007. N-methyl-d-aspartate receptor expression during adult neurogenesis in the rat dentate gyrus. Neuroscience 144: 855-864.

Naisbitt S, Kim E, Tu JC, Xiao B, Sala C, Valtschanoff J, Weinberg RJ, Worley PF, Sheng M, 1999. Shank, a novel family of postsynaptic density proteins that binds to the NMDA receptor/PSD-95/GKAP complex and cortactin. Neuron 23: 569-582.

Ng HH, Dole S, Struhl K, 2003. The Rtf1 component of the Paf1 transcriptional elongation complex is required for ubiquitination of histone H2B. J. Biol. Chem. 278: 33625-33628.

Nicolay DJ, Doucette JR, Nazarali AJ, 2007. Transcriptional control of oligodendrogenesis. Glia 55: 1287-1299.

Nicole O, Docagne F, Ali C, Margaill I, Carmeliet P, MacKenzie ET, Vivien D, Buisson A, 2001. The proteolytic activity of tissue-plasminogen activator enhances NMDA receptor-mediated signaling. Nat. Med. 7: 59-64.

Noguchi J, Matsuzaki M, Ellis-Davies GC, Kasai H, 2005. Spine-neck geometry determines NMDA receptor-dependent Ca2+ signaling in dendrites. Neuron 46: 609-622.

Okamoto K, Nagai T, Miyawaki A, Hayashi Y, 2004. Rapid and persistent modulation of actin dynamics regulates postsynaptic reorganization underlying bidirectional plasticity. Nat. Neurosci. 7: 1104-1112.

Osawa M, Tong KI, Lilliehook C, Wasco W, Buxbaum JD, Cheng HY, Penninger JM, Ikura M, Ames JB, 2001. Calcium-regulated DNA binding and oligomerization of the neuronal calcium-sensing protein, calsenilin/DREAM/KChIP3. J. Biol. Chem. 276: 41005-41013.

Ostroff LE, Fiala JC, Allwardt B, Harris KM, 2002. Polyribosomes redistribute from dendritic shafts into spines with enlarged synapses during LTP in developing rat hippocampal slices. Neuron 35: 535-545.

Otmakhov N, Tao-Cheng JH, Carpenter S, Asrican B, Dosemeci A, Reese TS, Lisman J, 2004. Persistent accumulation of calcium/calmodulin-dependent protein kinase II in dendritic spines after induction of NMDA receptor-dependent chemical long-term potentiation. J. Neurosci. 24: 9324-9331.

Ouyang Y, Rosenstein A, Kreiman G, Schuman EM, Kennedy MB, 1999. Tetanic stimulation leads to increased accumulation of Ca(2+)/calmodulin-dependent protein kinase II via dendritic protein synthesis in hippocampal neurons. J. Neurosci. 19: 7823-7833.

Pak DT, Sheng M, 2003. Targeted protein degradation and synapse remodeling by an inducible protein kinase. Science 302: 1368-1373.

Parent JM, Yu TW, Leibowitz RT, Geschwind DH, Sloviter RS, Lowenstein DH, 1997. Dentate granule cell neurogenesis is increased by seizures and contributes to aberrant network reorganization in the adult rat hippocampus. J. Neurosci. 17: 3727-3738.

Paxinos G, Watson C, 2007. The Rat Brain in Stereotaxic Coordinates. Elsevier Academic Press, San Diego.

Pegan S, Tan J, Huang A, Slesinger PA, Riek R, Choe S, 2007. NMR studies of interactions between C-terminal tail of Kir2.1 channel and PDZ1,2 domains of PSD95. Biochemistry 46: 5315-5322.

Peters MF, Adams ME, Froehner SC, 1997. Differential association of syntrophin pairs with the dystrophin complex. J. Cell Biol. 138: 81-93.

Petersen JD, Chen X, Vinade L, Dosemeci A, Lisman JE, Reese TS, 2003. Distribution of postsynaptic density (PSD)-95 and Ca2+/calmodulin-dependent protein kinase II at the PSD. J. Neurosci. 23: 11270-11278.

Peterson FC, Penkert RR, Volkman BF, Prehoda KE, 2004. Cdc42 regulates the Par-6 PDZ domain through an allosteric CRIB-PDZ transition. Mol. Cell 13: 665-676.

Phatnani HP, Greenleaf AL, 2006. Phosphorylation and functions of the RNA polymerase II CTD. Genes Dev. 20: 2922-2936.

Plath N, Ohana O, Dammermann B, Errington ML, Schmitz D, Gross C, Mao X, Engelsberg A, Mahlke C, Welzl H, Kobalz U, Stawrakakis A, Fernandez E, Waltereit R, Bick-Sander A, Therstappen E, Cooke SF, Blanquet V, Wurst W, Salmen B, Bosl MR, Lipp HP, Grant SG, Bliss TV, Wolfer DP, Kuhl D, 2006. Arc/Arg3.1 is essential for the consolidation of synaptic plasticity and memories. Neuron 52: 437-444.

Ploski JE, Newton SS, Duman RS, 2006. Electroconvulsive seizure-induced gene expression profile of the hippocampus dentate gyrus granule cell layer. J. Neurochem. 99: 1122-1132.

Qian Z, Gilbert ME, Colicos MA, Kandel ER, Kuhl D, 1993. Tissue-plasminogen activator is induced as an immediate-early gene during seizure, kindling and long-term potentiation. Nature 361: 453-457.

Rao A, Steward O, 1991. Evidence that protein constituents of postsynaptic membrane specializations are locally synthesized: analysis of proteins synthesized within synaptosomes. J. Neurosci. 11: 2881-2895.

Regan MR, Huang YH, Kim YS, Dykes-Hoberg MI, Jin L, Watkins AM, Bergles DE, Rothstein JD, 2007. Variations in promoter activity reveal a differential expression and physiology of glutamate transporters by glia in the developing and mature CNS. J. Neurosci. 27: 6607-6619.

Richardson CL, Tate WP, Mason SE, Lawlor PA, Dragunow M, Abraham WC, 1992. Correlation between the induction of an immediate early gene, zif/268, and long-term potentiation in the dentate gyrus. Brain Res. 580: 147-154.

Roche KW, Standley S, McCallum J, Dune LC, Ehlers MD, Wenthold RJ, 2001. Molecular determinants of NMDA receptor internalization. Nat. Neurosci. 4: 794-802.

Rook MS, Lu M, Kosik KS, 2000. CaMKIIalpha 3' untranslated region-directed mRNA translocation in living neurons: visualization by GFP linkage. J. Neurosci. 20: 6385-6393.

Rumbaugh G, Sia GM, Garner CC, Huganir RL, 2003. Synapse-associated protein-97 isoform-specific regulation of surface AMPA receptors and synaptic function in cultured neurons. J. Neurosci. 23: 4567-4576.

Sacco-Bubulya P, Spector DL, 2002. Disassembly of interchromatin granule clusters alters the coordination of transcription and pre-mRNA splicing. J. Cell Biol. 156: 425-436.

Saffen DW, Cole AJ, Worley PF, Christy BA, Ryder K, Baraban JM, 1988. Convulsant-induced increase in transcription factor messenger RNAs in rat brain. Proc. Natl. Acad. Sci. U. S. A 85: 7795-7799.

Sala C, Futai K, Yamamoto K, Worley PF, Hayashi Y, Sheng M, 2003. Inhibition of dendritic spine morphogenesis and synaptic transmission by activity-inducible protein Homer1a. J. Neurosci. 23: 6327-6337.

Sala C, Piech V, Wilson NR, Passafaro M, Liu G, Sheng M, 2001. Regulation of dendritic spine morphology and synaptic function by Shank and Homer. Neuron 31: 115-130.

Seabold GK, Burette A, Lim IA, Weinberg RJ, Hell JW, 2003. Interaction of the tyrosine kinase Pyk2 with the N-methyl-D-aspartate receptor complex via the Src homology 3 domains of PSD-95 and SAP102. J. Biol. Chem. 278: 15040-15048.

Shepherd JD, Rumbaugh G, Wu J, Chowdhury S, Plath N, Kuhl D, Huganir RL, Worley PF, 2006. Arc/Arg3.1 mediates homeostatic synaptic scaling of AMPA receptors. Neuron 52: 475-484.

Shilatifard A, Conaway RC, Conaway JW, 2003. The RNA polymerase II elongation complex. Annu. Rev. Biochem. 72: 693-715.

Shilatifard A, Duan DR, Haque D, Florence C, Schubach WH, Conaway JW, Conaway RC, 1997. ELL2, a new member of an ELL family of RNA polymerase II elongation factors. Proc. Natl. Acad. Sci. U. S. A 94: 3639-3643.

Shilatifard A, Lane WS, Jackson KW, Conaway RC, Conaway JW, 1996. An RNA polymerase II elongation factor encoded by the human ELL gene. Science 271: 1873-1876.

Sims RJ, III, Belotserkovskaya R, Reinberg D, 2004. Elongation by RNA polymerase II: the short and long of it. Genes Dev. 18: 2437-2468.

Smith FD, Langeberg LK, Scott JD, 2006. The where's and when's of kinase anchoring. Trends Biochem. Sci. 31: 316-323.

Sng JC, Taniura H, Yoneda Y, 2004. A tale of early response genes. Biol. Pharm. Bull. 27: 606-612.

Sng JC, Taniura H, Yoneda Y, 2006. Histone modifications in kainate-induced status epilepticus. Eur. J. Neurosci. 23: 1269-1282.

Songyang Z, Fanning AS, Fu C, Xu J, Marfatia SM, Chishti AH, Crompton A, Chan AC, Anderson JM, Cantley LC, 1997. Recognition of unique carboxyl-terminal motifs by distinct PDZ domains. Science 275: 73-77.

Staudinger J, Lu J, Olson EN, 1997. Specific interaction of the PDZ domain protein PICK1 with the COOH terminus of protein kinase C-alpha. J. Biol. Chem. 272: 32019-32024.

Stegmuller J, Werner H, Nave KA, Trotter J, 2003. The proteoglycan NG2 is complexed with alpha-amino-3-hydroxy-5-methyl-4-isoxazolepropionic acid (AMPA) receptors by the PDZ glutamate receptor interaction protein (GRIP) in glial progenitor cells. Implications for glial-neuronal signaling. J. Biol. Chem. 278: 3590-3598.

Steigerwald F, Schulz TW, Schenker LT, Kennedy MB, Seeburg PH, Kohr G, 2000. C-Terminal truncation of NR2A subunits impairs synaptic but not extrasynaptic localization of NMDA receptors. J. Neurosci. 20: 4573-4581.

Stevens B, Fields RD, 2000. Response of Schwann cells to action potentials in development. Science 287: 2267-2271.

Stevens B, Porta S, Haak LL, Gallo V, Fields RD, 2002. Adenosine: a neuron-glial transmitter promoting myelination in the CNS in response to action potentials. Neuron 36: 855-868.

Steward O, Levy WB, 1982. Preferential localization of polyribosomes under the base of dendritic spines in granule cells of the dentate gyrus. J. Neurosci. 2: 284-291.

Steward O, Wallace CS, Lyford GL, Worley PF, 1998. Synaptic activation causes the mRNA for the IEG Arc to localize selectively near activated postsynaptic sites on dendrites. Neuron 21: 741-751.

Steward O, Worley PF, 2001. Selective targeting of newly synthesized Arc mRNA to active synapses requires NMDA receptor activation. Neuron 30: 227-240.

Sudhof TC, 2004. The synaptic vesicle cycle. Annu. Rev. Neurosci. 27: 509-547.

Sun J, Tadokoro S, Imanaka T, Murakami SD, Nakamura M, Kashiwada K, Ko J, Nishida W, Sobue K, 1998. Isolation of PSD-Zip45, a novel Homer/vesl family protein containing leucine zipper motifs, from rat brain. FEBS Lett. 437: 304-308.

Tada T, Sheng M, 2006. Molecular mechanisms of dendritic spine morphogenesis. Curr. Opin. Neurobiol. 16: 95-101.

Takahashi Y, 2003. The 14-3-3 proteins: gene, gene expression, and function. Neurochem. Res. 28: 1265-1273.

Takemura NU, 2005. Evidence for neurogenesis within the white matter beneath the temporal neocortex of the adult rat brain. Neuroscience 134: 121-132.

Tamaskovic R, Bichsel SJ, Hemmings BA, 2003. NDR family of AGC kinases--essential regulators of the cell cycle and morphogenesis. FEBS Lett. 546: 73-80.

Tate P, Lee M, Tweedie S, Skarnes WC, Bickmore WA, 1998. Capturing novel mouse genes encoding chromosomal and other nuclear proteins. J. Cell Sci. 111 (Pt 17): 2575-2585.

Tavalin SJ, Colledge M, Hell JW, Langeberg LK, Huganir RL, Scott JD, 2002. Regulation of GluR1 by the A-kinase anchoring protein 79 (AKAP79) signaling complex shares properties with long-term depression. J. Neurosci. 22: 3044-3051.

Testa CM, Standaert DG, Young AB, Penney JB, Jr., 1994. Metabotropic glutamate receptor mRNA expression in the basal ganglia of the rat. J. Neurosci. 14: 3005-3018.

Thirman MJ, Levitan DA, Kobayashi H, Simon MC, Rowley JD, 1994. Cloning of ELL, a gene that fuses to MLL in a t(11;19)(q23;p13.1) in acute myeloid leukemia. Proc. Natl. Acad. Sci. U. S. A 91: 12110-12114.

Thomas U, 2002. Modulation of synaptic signalling complexes by Homer proteins. J. Neurochem. 81: 407-413.

Thompson KR, Otis KO, Chen DY, Zhao Y, O'Dell TJ, Martin KC, 2004. Synapse to nucleus signaling during long-term synaptic plasticity; a role for the classical active nuclear import pathway. Neuron 44: 997-1009.

Trembley JH, Hu D, Hsu LC, Yeung CY, Slaughter C, Lahti JM, Kidd VJ, 2002. PITSLRE p110 protein kinases associate with transcription complexes and affect their activity. J. Biol. Chem. 277: 2589-2596.

Trembley JH, Hu D, Slaughter CA, Lahti JM, Kidd VJ, 2003. Casein kinase 2 interacts with cyclin-dependent kinase 11 (CDK11) in vivo and phosphorylates both the RNA polymerase II carboxyl-terminal domain and CDK11 in vitro. J. Biol. Chem. 278: 2265-2270.

Trinkle-Mulcahy L, Ajuh P, Prescott A, Claverie-Martin F, Cohen S, Lamond AI, Cohen P, 1999. Nuclear organisation of NIPP1, a regulatory subunit of protein phosphatase 1 that associates with pre-mRNA splicing factors. J. Cell Sci. 112 (Pt 2): 157-168.

Tu JC, Xiao B, Naisbitt S, Yuan JP, Petralia RS, Brakeman P, Doan A, Aakalu VK, Lanahan AA, Sheng M, Worley PF, 1999. Coupling of mGluR/Homer and PSD-95 complexes by the Shank family of postsynaptic density proteins. Neuron 23: 583-592.

Turrigiano GG, Nelson SB, 2004. Homeostatic plasticity in the developing nervous system. Nat. Rev. Neurosci. 5: 97-107.

Upton N, Blackburn TP, Campbell CA, Cooper D, Evans ML, Herdon HJ, King PD, Ray AM, Stean TO, Chan WN, Evans JM, Thompson M, 1997. Profile of SB-204269, a mechanistically novel anticonvulsant drug, in rat models of focal and generalized epileptic seizures. Br. J. Pharmacol. 121: 1679-1686.

Valiente M, ndres-Pons A, Gomar B, Torres J, Gil A, Tapparel C, Antonarakis SE, Pulido R, 2005. Binding of PTEN to specific PDZ domains contributes to PTEN protein stability and phosphorylation by microtubule-associated serine/threonine kinases. J. Biol. Chem. 280: 28936-28943.

Valtschanoff JG, Weinberg RJ, 2001. Laminar organization of the NMDA receptor complex within the postsynaptic density. J. Neurosci. 21: 1211-1217.

van Ham M, Hendriks W, 2003. PDZ domains-glue and guide. Mol. Biol. Rep. 30: 69-82.

van Praag H, Schinder AF, Christie BR, Toni N, Palmer TD, Gage FH, 2002. Functional neurogenesis in the adult hippocampus. Nature 415: 1030-1034.

Vickers CA, Dickson KS, Wyllie DJ, 2005. Induction and maintenance of late-phase long-term potentiation in isolated dendrites of rat hippocampal CA1 pyramidal neurones. J. Physiol 568: 803-813.

von Poser C, Ichtchenko K, Shao X, Rizo J, Sudhof TC, 1997. The evolutionary pressure to inactivate. A subclass of synaptotagmins with an amino acid substitution that abolishes Ca2+ binding. J. Biol. Chem. 272: 14314-14319.

Walden PD, Cowan NJ, 1993. A novel 205-kilodalton testis-specific serine/threonine protein kinase associated with microtubules of the spermatid manchette. Mol. Cell Biol. 13: 7625-7635.

Walden PD, Millette CF, 1996. Increased activity associated with the MAST205 protein kinase complex during mammalian spermiogenesis. Biol. Reprod. 55: 1039-1044.

Wei F, Qiu CS, Liauw J, Robinson DA, Ho N, Chatila T, Zhuo M, 2002. Calcium calmodulin-dependent protein kinase IV is required for fear memory. Nat. Neurosci. 5: 573-579.

Weick JP, Groth RD, Isaksen AL, Mermelstein PG, 2003. Interactions with PDZ proteins are required for L-type calcium channels to activate cAMP response element-binding protein-dependent gene expression. J. Neurosci. 23: 3446-3456.

Wells DG, Dong X, Quinlan EM, Huang YS, Bear MF, Richter JD, Fallon JR, 2001. A role for the cytoplasmic polyadenylation element in NMDA receptor-regulated mRNA translation in neurons. J. Neurosci. 21: 9541-9548.

Wisden W, Errington ML, Williams S, Dunnett SB, Waters C, Hitchcock D, Evan G, Bliss TV, Hunt SP, 1990. Differential expression of immediate early genes in the hippocampus and spinal cord. Neuron 4: 603-614.

Wong W, Scott JD, 2004. AKAP signalling complexes: focal points in space and time. Nat. Rev. Mol. Cell Biol. 5: 959-970.

Wood A, Schneider J, Dover J, Johnston M, Shilatifard A, 2003. The Paf1 complex is essential for histone monoubiquitination by the Rad6-Bre1 complex, which signals for histone methylation by COMPASS and Dot1p. J. Biol. Chem. 278: 34739-34742.

Wu GY, Deisseroth K, Tsien RW, 2001. Activity-dependent CREB phosphorylation: convergence of a fast, sensitive calmodulin kinase pathway and a slow, less sensitive mitogen-activated protein kinase pathway. Proc. Natl. Acad. Sci. U. S. A 98: 2808-2813.

Wu L, Wells D, Tay J, Mendis D, Abbott MA, Barnitt A, Quinlan E, Heynen A, Fallon JR, Richter JD, 1998. CPEB-mediated cytoplasmic polyadenylation and the regulation of experience-dependent translation of alpha-CaMKII mRNA at synapses. Neuron 21: 1129-1139.

Xiao B, Tu JC, Petralia RS, Yuan JP, Doan A, Breder CD, Ruggiero A, Lanahan AA, Wenthold RJ, Worley PF, 1998. Homer regulates the association of group 1 metabotropic glutamate receptors with multivalent complexes of homer-related, synaptic proteins. Neuron 21: 707-716.

Xiong H, Li H, Chen Y, Zhao J, Unkeless JC, 2004. Interaction of TRAF6 with MAST205 regulates NF-kappaB activation and MAST205 stability. J. Biol. Chem. 279: 43675-43683.

Xu Y, Tamamaki N, Noda T, Kimura K, Itokazu Y, Matsumoto N, Dezawa M, Ide C, 2005. Neurogenesis in the ependymal layer of the adult rat 3rd ventricle. Exp. Neurol. 192: 251-264.

Yano R, Yap CC, Yamazaki Y, Muto Y, Kishida H, Okada D, Hashikawa T, 2003. Sast124, a novel splice variant of syntrophin-associated serine/threonine kinase